NASA/TM–2018-219027/ Vol. 7

PACE Technical Report Series, Volume 7

Ivona Cetinić, Charles R. McClain, and P. Jeremy Werdell, Editors

Ocean Color Instrument (OCI) Concept Design Studies

Ziauddin Ahmad, Robert Arnone, Michael J. Behrenfeld, Brian Cairns, Ivona Cetinić, Robert E. Eplee, Bryan Franz, David Haffner, Amir Ibrahim, Antonio Mannino, Lachlan I. W. McKinna, Gerhard Meister, Aimee Neeley, Nima Pahlevan, Frederick S. Patt, Wayne Robinson, Sergio R. Signorini, Ryan Vandermeulen, Toby Westberry, and Jeremy Werdell

National Aeronautics and
Space Administration

Goddard Space Flight Center
Greenbelt, Maryland 20771

December 2018

NASA STI Program ... in Profile

Since its founding, NASA has been dedicated to the advancement of aeronautics and space science. The NASA scientific and technical information (STI) program plays a key part in helping NASA maintain this important role.

The NASA STI program operates under the auspices of the Agency Chief Information Officer. It collects, organizes, provides for archiving, and disseminates NASA's STI. The NASA STI program provides access to the NASA Aeronautics and Space Database and its public interface, the NASA Technical Report Server, thus providing one of the largest collections of aeronautical and space science STI in the world. Results are published in both non-NASA channels and by NASA in the NASA STI Report Series, which includes the following report types:

- TECHNICAL PUBLICATION. Reports of completed research or a major significant phase of research that present the results of NASA Programs and include extensive data or theoretical analysis. Includes compilations of significant scientific and technical data and information deemed to be of continuing reference value. NASA counterpart of peer-reviewed formal professional papers but has less stringent limitations on manuscript length and extent of graphic presentations.
- TECHNICAL MEMORANDUM. Scientific and technical findings that are preliminary or of specialized interest, e.g., quick release reports, working papers, and bibliographies that contain minimal annotation. Does not contain extensive analysis.
- CONTRACTOR REPORT. Scientific and technical findings by NASA-sponsored contractors and grantees.
- CONFERENCE PUBLICATION. Collected papers from scientific and technical conferences, symposia, seminars, or other meetings sponsored or co-sponsored by NASA.
- SPECIAL PUBLICATION. Scientific, technical, or historical information from NASA programs, projects, and missions, often concerned with subjects having substantial public interest.
- TECHNICAL TRANSLATION. English-language translations of foreign scientific and technical material pertinent to NASA's mission.

Specialized services also include organizing and publishing research results, distributing specialized research announcements and feeds, providing help desk and personal search support, and enabling data exchange services. For more information about the NASA STI program, see the following:

- Access the NASA STI program home page at http://www.sti.nasa.gov
- E-mail your question via the Internet to help@sti.nasa.gov
- Phone the NASA STI Information Desk at 757-864-9658
- Write to:
  NASA STI Information Desk
  Mail Stop 148
  NASA's Langley Research Center
  Hampton, VA 23681-2199

NASA/TM–2018-219027/ Vol. 7

PACE Technical Report Series, Volume 7

Editors:

Ivona Cetinić
GESTAR/Universities Space Research Association, Columbia, Maryland
Charles R. McClain
Science Applications International Corporation, Reston, Virginia
P. Jeremy Werdell
NASA Goddard Space Flight Center, Greenbelt, Maryland

Ocean Color Instrument (OCI) Concept Design Studies

Ziauddin Ahmad
Science Applications International Corporation, Reston, VA
Robert Arnone
University of Southern Mississippi, Hattiesburg, MS
Michael J. Behrenfeld
Oregon State University, Corvallis, OR
Brian Cairns
NASA Goddard Institute for Space Studies, New York, NY
Ivona Cetinić
GESTAR/Universities Space Research Association, Columbia, MD
Robert E. Eplee
Science Applications International Corporation, Reston, VA
Bryan Franz
NASA Goddard Space Flight Center, Greenbelt, MD
David Haffner
NASA Goddard Space Flight Center, Greenbelt, MD
Amir Ibrahim
Science Systems and Applications Inc, Lanham, MD
Antonio Mannino
NASA Goddard Space Flight Center, Greenbelt, MD
Lachlan I. W. McKinna
Go2Q Pty Ltd, Buderim, Australia
Gerhard Meister
NASA Goddard Space Flight Center, Greenbelt, MD
Aimee Neeley
Science Systems and Applications Inc, Lanham, MD
Nima Pahlevan
Science Systems and Applications Inc, Lanham, MD
Frederick S. Patt
Science Applications International Corporation, Reston, VA
Wayne Robinson
Science Applications International Corporation, Reston, VA
Sergio R. Signorini
Science Applications International Corporation, Reston, VA
Ryan Vandermeulen
Science Systems and Applications Inc, Lanham, MD
Toby Westberry
Oregon State University, Corvallis, OR
Jeremy Werdell
NASA Goddard Space Flight Center, Greenbelt, MD

National Aeronautics and
Space Administration

Goddard Space Flight Center
Greenbelt, Maryland 20771

December 2018

Level of Review: This material has been technically reviewed by technical management.

Available from

NASA STI Program
Mail Stop 148
NASA's Langley Research Center
Hampton, VA 23681-2199

National Technical Information Service
5285 Port Royal Road
Springfield, VA 22161
703-605-6000

Available in electronic form at http://

INTRODUCTION

Introduction to Volume 7: Ocean Color Instrument (OCI) Concept Design Studies

The Plankton, Aerosol, Cloud, ocean Ecosystem (PACE; https://pace.gsfc.nasa.gov) mission represents NASA's next great investment in satellite ocean color and the combined study of Earth's ocean-atmosphere system. At its core, PACE builds upon NASA's multi-decadal legacies of the Coastal Zone Color Scanner (1978-1986), Sea-viewing Wide Field-of-view Sensor (SeaWiFS; 1997-2010), Moderate Resolution Imaging Spectroradiometers (MODIS) onboard Terra (1999-present) and Aqua (2002-present), and Visible Infrared Imaging Spectroradiometer (VIIRS) onboard Suomi NPP (2012-present) and JPSS-1 (2017-present; to be renamed NOAA-20). The ongoing, combined climate data record from these instruments changed the way we view our planet and – to this day – offers an unparalleled opportunity to expand our senses into space, compress time, and measure life itself.

This volume presents PACE Project scientific studies related to formulation and concept design of the ocean color instrument (OCI) – namely, those studies that guided and influenced the design of the preliminary OCI concept during the mission's Pre-phase A (2014-2016; pre-formulation: define a viable and affordable concept) and Phase A (2016-2017; concept and technology development). During Pre-Phase A and Phase A (as well as within Phase B at the time of this writing), the OCI systems engineering and Project Science teams worked hand-in-hand to iteratively achieve an instrument concept that satisfied all mission science objectives under its cost cap. Both teams executed numerous trade studies under an atmosphere of healthy tension, with gives-and-takes that we believe resulted in an advanced radiometer system that will advance both ocean color and atmospheric science, while filling scientific and technological gaps in the fleet of satellite instruments expected to fly in the 2022-2025 timeframe. Much work remains to be done, but hopefully this volume provides the user community insight into the conception and preliminary implementation of PACE's OCI.

Thanks to the Project Science and OCI systems engineering teams for meeting several times a week over many years and hearing each other out. Not every gathering was pleasant, but we're all better for it.

P. J. Werdell
PACE Project Scientist
March 2018

Contents

Chapter 1

Extended UV capability on OCI for Ozone retrieval

Antonio Mannino, NASA Goddard Space Flight Center, Greenbelt, Maryland [1]

David Haffner, NASA Goddard Space Flight Center, Greenbelt, Maryland

Wayne Robinson, Science Applications International Corporation, Reston, Virginia

Ziauddin Ahmad, Science Applications International Corporation, Reston, Virginia

1.1. Introduction

Extending OCI hyperspectral radiance measurements in the ultraviolet to 320 nm on the blue spectrograph enables quantitation of atmospheric total column ozone (O_3) for use in ocean color atmospheric correction algorithms. The strong absorption by atmospheric ozone below 340 nm enables the quantification of total column ozone. Other applications are possible but were not investigated due to their exploratory nature and lower priority.

The first step in the atmospheric correction processing, which converts top-of-the-atmosphere radiances to water-leaving radiances, is removal of the absorbance by atmospheric trace gases such as water vapor, oxygen, ozone and nitrogen dioxide. Details of the atmospheric correction process currently used by the Ocean Biology Processing Group (OBPG) and will be employed for PACE with appropriate modifications, are described by *Mobley et al.* [2016].

Atmospheric ozone absorbs within the visible to near-infrared spectrum between ~450 nm and 800 nm and most appreciably between 530 nm and 650 nm, a spectral region critical for maintaining NASA's chlorophyll-*a* climate data record and for PACE algorithms planned to characterize phytoplankton community composition and other ocean color products.

While satellite-based observations will likely be available during PACE's mission lifetime, the difference in acquisition time with PACE, the coarseness in their spatial resolution, and differences in viewing geometries will introduce significant levels of uncertainties in PACE ocean color data products.

1.2. Justification for Ozone Measurement Capability on OCI

A relatively modest error in total ozone concentrations can result in significant impacts to normalized ocean water-leaving radiances (*nLw*). For example, a sensitivity analysis demonstrated that a 20 Dobson Unit (DU; 1 DU equals 2.69×10^{16} molecules cm^{-2}) increase in ozone would result in nearly 12% increase in *nLw* at 667 nm and 5% at *nLw* at 551 nm, whereas a small decrease in *nLw* would occur for the lower blue wavelengths (Fig. 1.1). This is because of ozone correction, which removes the effect of ozone from the observed radiances at the top-of-atmosphere (TOA). The correction follows the Beer's Law, and

[1] Cite as: Mannino, A., D. Haffner, W. Robinson, and Z. Ahmad (2018), Extended UV capability on OCI for Ozone retrieval, in *PACE Technical Report Series, Volume 7: Ocean Color Instrument (OCI) Concept Design Studies (NASA/TM-2018 – 2018-219027/ Vol. 7)*, edited by I. Cetinić, C. R. McClain and P. J. Werdell, NASA Goddard Space Flight Space Center Greenbelt, MD.

over/under estimates the TOA radiance if a higher/lower value of ozone is assumed. In other words, in case of higher ozone value, the excess radiance would result in a higher *nLw* for the spectral range where ozone attenuates light transmittance through the atmosphere (<360 nm and between ~420 and 870 nm). Furthermore, the effect on *nLw* would be greater at higher satellite view angles and solar zenith angles. The small decrease in *nLw* for the shorter blue bands can be attributed to other components of the atmospheric correction process.

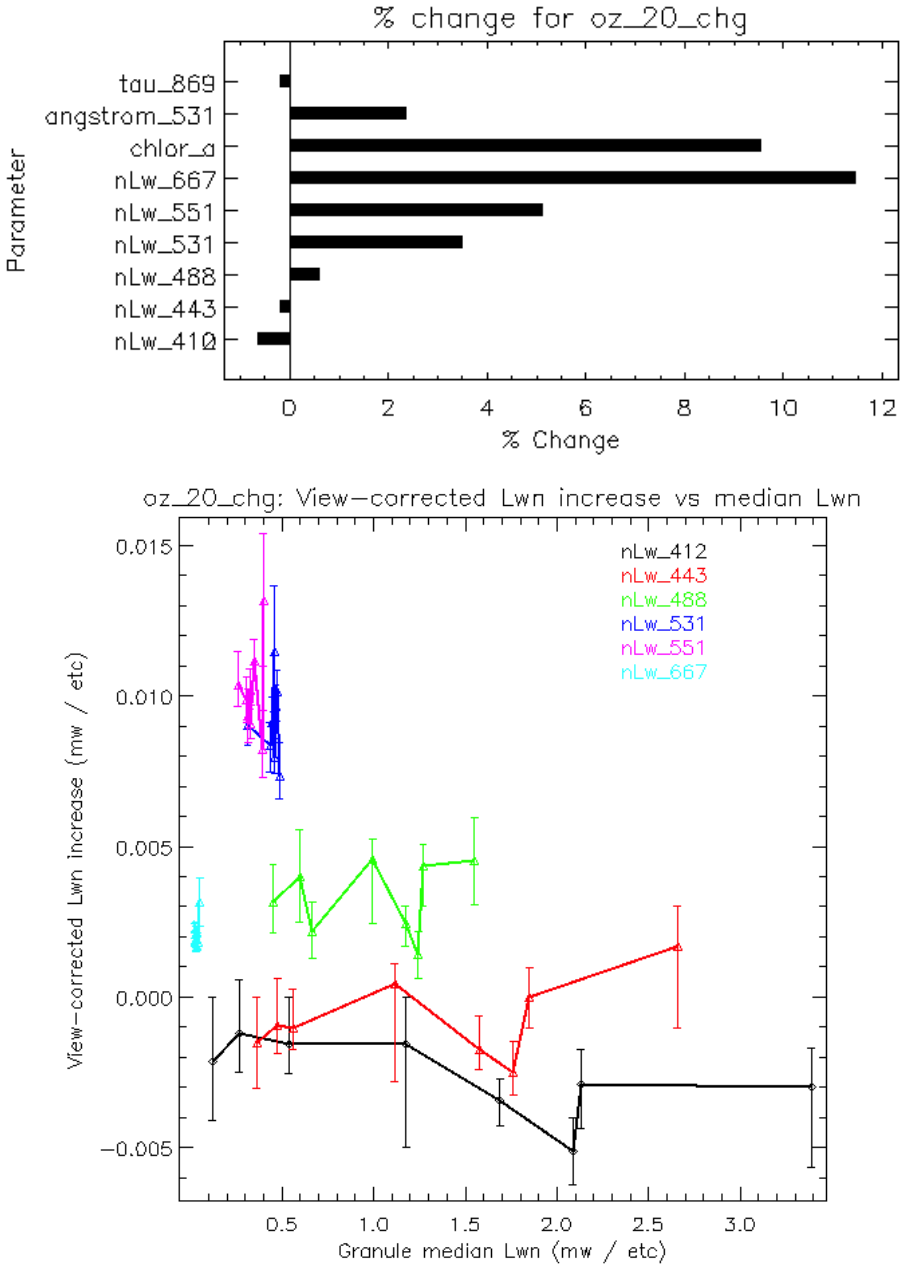

Figure 1.1. Sensitivity of ocean color products including water-leaving radiances (nLw)to changes in total column ozone concentrations as a (a) percent change and (b) absolute change in nLw from a 20 DU increase. Analysis was performed using 8 MODIS-Aqua granules representing different water types. The granules were processed using standard OBPG processing except for the use of a constant ozone across the scenes of 300 DU ozone and were then processed a second time with an ozone value of 320 DU, giving a 20 DU change as the only difference.

To reduce some of the uncertainty introduced by ozone concentration time and space variability, the OBPG recently transitioned to using atmospheric total column ozone fields from the Ozone Monitoring Instrument (OMI) on Aura with the TOAST product (NOAA/NESDIS Total Ozone from Analysis of Stratospheric and Tropospheric) serving as an alternate if data gaps of greater than 1 day are present in the OMI data. The OMI products currently in use are the L3 0.25° x 0.25° daily product. The latest TOAST ozone product is a global daily 1° x 1° dataset and combines retrievals of ozone from the Solar Backscatter Ultraviolet Version 2 (SBUV/2) and the Cross-track Infrared Sounder (CrIS) instruments. These products are relatively coarse spatially and available at a frequency of 1-2 days if all conditions are optimal.

PACE could rely on total column ozone data products from the Ozone Monitoring Profiler Suite (OMPS) on the Joint Polar Satellite System (JPSS) missions and potentially TROPOMI on Sentinel 5p and 5, ESA follow-on instruments to OMI. However, both OMPS and TROPOMI have a 1330 equator crossing time compared to PACE's planned 1300 crossing time. The unique flight path of each mission will lead to greater mismatch in time between ozone and OCI ocean color than suggested by the equator crossing times as well as significant difference in viewing and solar geometry conditions. Furthermore, OMPS and TROPOMI will produce global ozone products at 17x17km and 7x7km, respectively. Indeed, published studies from field campaigns demonstrate that total column ozone concentrations vary substantially through the course of each day [e.g. *Aculinin*, 2006; *Ancellet and Ravetta*, 2005; *Johnson et al.*, 1990; *Kouvarakis et al.*, 2002; *Lubin and Frederick*, 1990; *Mount et al.*, 1987; *Nair et al.*, 2011; *Oltmans*, 1981; *Tzortziou et al.*, 2012] and across horizontal space [e.g. *Ancellet and Ravetta*, 2005]. Therefore, the capability to retrieve total column ozone from OCI will contribute to PACE meeting and exceeding its data quality requirements.

1.3. Approach to Measuring Atmospheric Total Column Ozone on OCI

The goal is to retrieve total column ozone from OCI to within 3 to 6 DU for the purposes of ocean color atmospheric correction. The heritage ozone algorithms from the Total Ozone Monitoring Instrument (TOMS) requires three narrow UV bands centered at 317.5 nm, 340 nm and 388 nm with a 1 nm bandwidth. The 317.5 nm band is sensitive to ozone while the other UV bands are insensitive. Preliminary analysis by P. K. Bhartia, NASA GSFC (pers. comm.) indicated that a 5 nm spectral bandwidth/resolution should suffice for quantifying ozone with a center wavelength of 317.5 nm. The main concern for such a large bandwidth is the red shift effect, where the effective center wavelength shifts to the red. Such a red shift was detected at 317.5 nm but was fairly minor. P. K. Bhartia pointed out the importance of minimizing straylight and out-of-band response for the 5 nm bands on OCI.

One of the challenges identified by the OCI systems engineering team for extending OCI further into the UV for ozone measurements was the reflectance throughput of the enhanced silver coatings under consideration for OCI's mirrors and other optical surfaces. The OCI team conducted irradiation exposure experiments in 2015 on four enhanced silver mirror coatings and identified three of these mirror coatings as possible candidates for use on OCI [*Heaney et al.*, 2015]. The ZeCoat 425-7R coating yielded the highest reflectance throughput below 340 nm (Fig. 1.2). However, the performance of ZeCoat was slightly lower in the red-NIR (~1.5% reflectance throughput reduction at 665 nm) and SWIR spectrum (~1% reflectance throughput reduction at 1640 nm) than the Quantum Silver coating (Fig. 1.3). The reduction in reflectance from the ZeCoat would result in a total throughput loss of ~5% at 665 nm and ~3.7% at 1640 nm. The other major technological concern is the quantum efficiency (QE) of the "blue" CCD detector below 340 nm.

The OCI systems team determined that the OCI spectral range could not be extended to enable measurements for a band at 317.5 nm. Hence, PACE project science consulted the ozone retrieval experts at NASA GSFC (P.K. Bhartia, J. Gleason, D. Haffner, C. Seftor, R.D. McPeters, J. Hermann) on whether total column ozone could be quantified at UV wavelengths centered above 320 nm. Haffner conducted an analysis with OMPS data for 5 nm bands (full-width half max; FWHM) centered at 317.5, 322, and 325 nm along with ozone insensitive bands centered at 340 and 380 nm using version 9 of the TOMS ozone algorithm (Haffner et al. 2015) and compared with the standard version 8 algorithm (V8) that employs 1 nm FWHM for the 317.5 nm ozone band [*Bhartia and Wellemeyer*, 2002; *Wellemeyer et al.*, 2004]. Because the OMPS nadir mapper does not provide spectral data beyond 380.5 nm, the 374 nm band (5 nm FWHM) was applied rather than the 380 nm band.

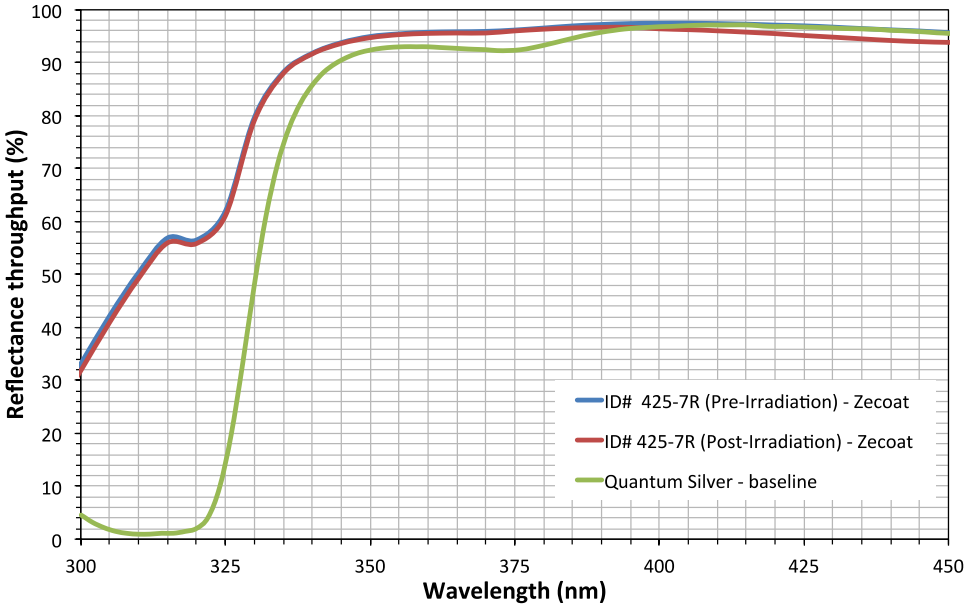

Figure 1.2. Reflectance throughput of two candidate mirror surface coatings on OCI.

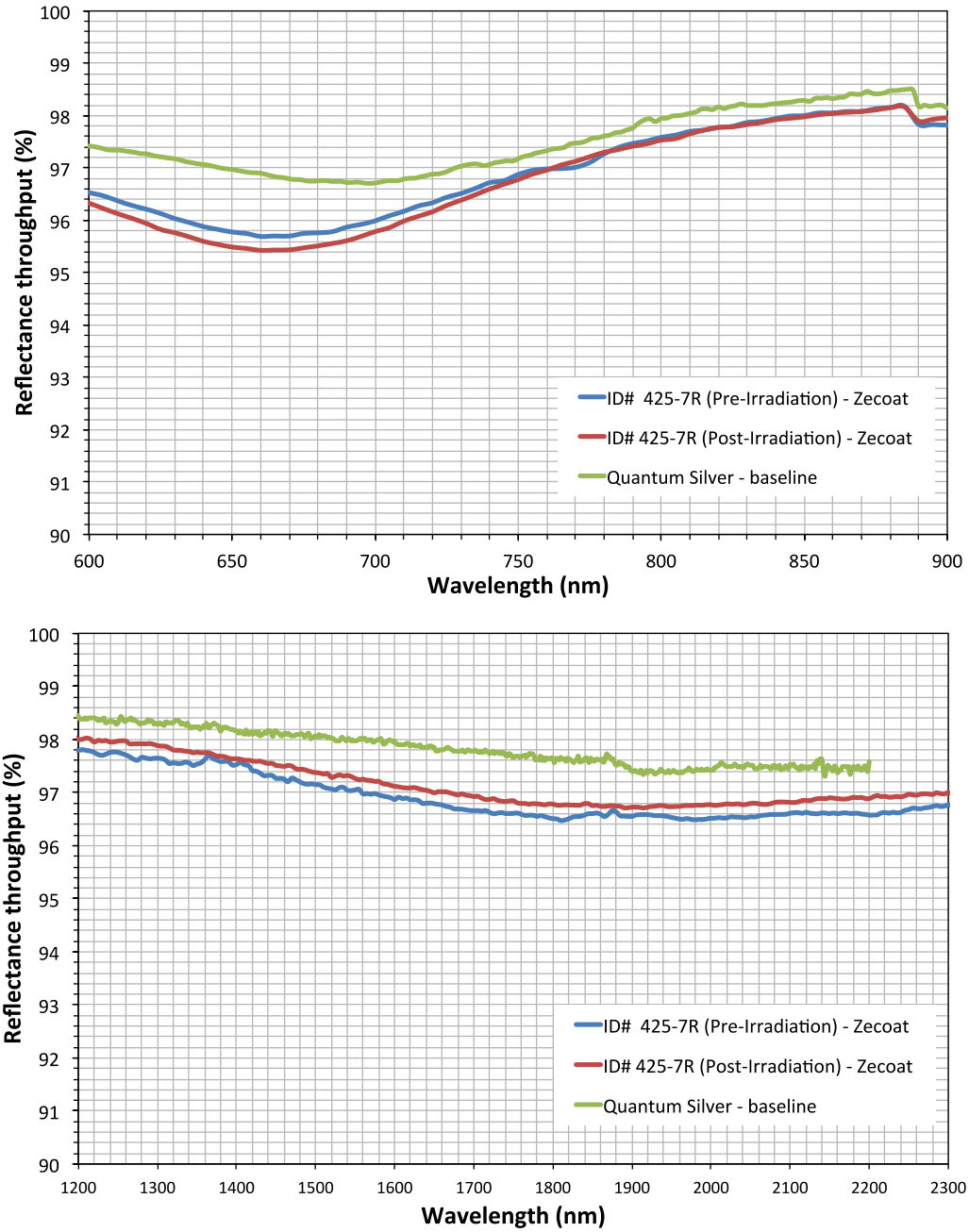

Figure 1.3. Reflectance throughput of two candidate mirror surface coatings on OCI for the (a) red-NIR spectral region and (b) short-wave infrared spectral region.

From Haffner, "The measured [OMPS] radiances and irradiance were smoothed and then normalized to I/F [backscattered radiance/solar flux] for the retrieval. For the tables, I made a standard OMPS instrument table at 1 nm resolution and then converted the Sun-normalized radiance tables to Earthshine radiances using a reference solar flux [solar spectral irradiance], and then smoothed those radiances. I smoothed the reference solar [spectrum] at 5 nm as well, and then re-normalized to I/F for use in the retrieval. I did not apply any soft-calibration adjustments to the 5 nm smoothed results. I expect calibration error is responsible for some of the bias you see between the smoothed retrievals at different

wavelengths. I think the important take home message is that 5 nm bandpass measurements can be used to retrieve total ozone for OCI well."

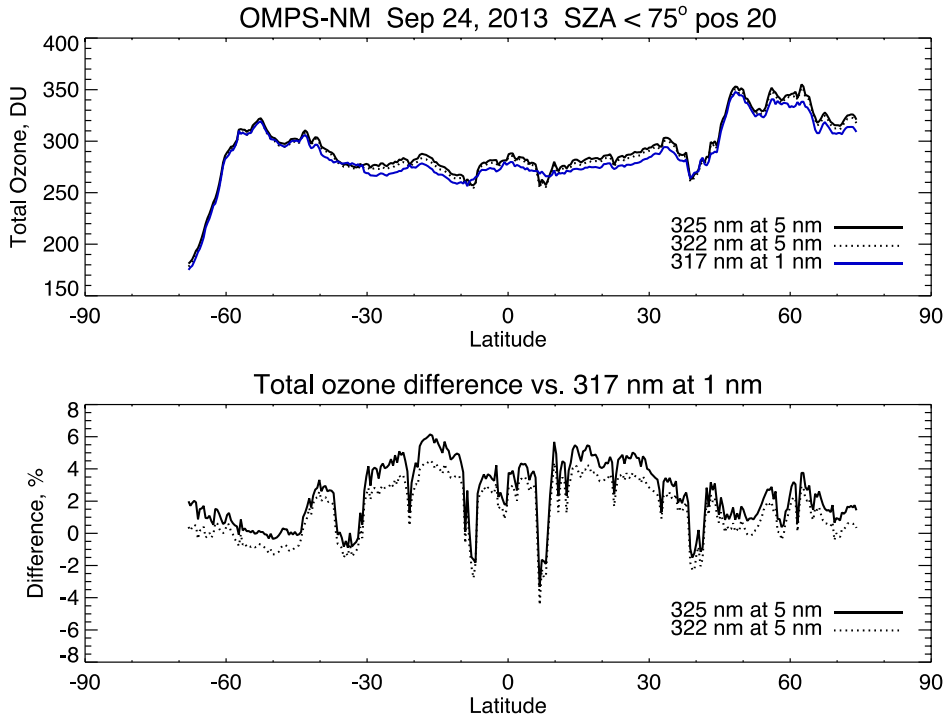

Figure 1.4. Total ozone retrieval from the OMPS nadir mapper for September 24, 2013 comparing (a) global total ozone concentration and (b) difference in ozone between the V9 algorithm with 5 nm bandwidths centered at 322 and 325 nm and the heritage V8 algorithm with 1 nm bandwidths centered at 317.5 nm. Source: David Haffner, NASA GSFC/SSAI/Code 614.

The results demonstrate that the ozone retrievals from the V9 algorithm with 5 nm bandwidths centered at 322 and 325 nm yield equivalent results as the heritage V8 algorithm with 1 nm bandwidths (Fig. 1.4). The differences in total ozone between the 317.5 nm V8 retrieval and from 322 nm and 325 nm are within ±4% and ±6%, respectively (Fig. 1.4b). The V9 analysis was not corrected for uncertainty introduced by clouds. The anti-correlation between reflectivity at 340 nm and the differences between the V9 and V8 algorithms are associated with cloud error. Retrieval of atmospheric sulfur dioxide (SO_2) could be accomplished with a band centered at 322 nm to resolve anomalous ozone concentrations in the presence of elevated SO_2 such as would occur from volcanic activity.

1.4. Conclusions

Extending the UV spectral range on OCI to obtain measurements for bands centered at ~322 nm and ~325 nm enables coincident and simultaneous retrieval of total ozone concentration, which will substantially reduce uncertainties in ocean color products compared to utilization of ozone data products from JPSS OMPS or Sentinel 5 TROPOMI satellite missions. By achieving the ozone concentration retrieval goal of 3 to 6 DU, the extended spectral capability in the UV contributes to meeting PACE and OCI ocean color product requirements.

Chapter 2

Requirements for the Measurement of Chlorophyll Fluorescence

Michael J. Behrenfeld, Oregon State University, Corvallis, Oregon[2]

Toby Westberry, Oregon State University, Corvallis, Oregon

Bryan Franz, NASA Goddard Space Flight Center, Greenbelt, Maryland

2.1. Introduction

The entire global biomass of marine phytoplankton is produced and consumed on average every 2 to 6 days [*Behrenfeld and Falkowski*, 1997a]. This phenomenal turnover rate is the consequence of a tight coupling between phytoplankton growth rates and rates of loss to zooplankton grazers, viruses, and other processes [*Behrenfeld*, 2010; *Behrenfeld and Boss*, 2014; *Behrenfeld et al.*, 2013; *Behrenfeld et al.*, 2017]. Accordingly, temporal changes in phytoplankton biomass observed by a satellite ocean color sensor, such as PACE, represent only a small fraction of the temporal changes in ocean net primary production (NPP) occurring at the same time [*Behrenfeld and Boss*, 2014]. In other words, satellite ocean color measurements do not detect the rapid transfer rate from NPP to other trophic levels, but only the small net difference between division and loss rates [*Behrenfeld and Boss*, 2018; *Behrenfeld et al.*, 2017]. Understanding phytoplankton biomass dynamics, ecosystem predator-prey relationships, and biogeochemical cycles of organic carbon in the ocean thus requires accurate estimates of NPP from satellite observables. PACE observations will permit far more accurate estimates of global ocean NPP than heritage sensors because of its ability to (1) better discriminate absorption by phytoplankton pigments and colored dissolved organic matter (cDOM), (2) characterize the full spectral distribution of phytoplankton absorption coefficients (a_{ph}), and (3) determine the magnitude and spectral characteristics of phytoplankton fluorescence.

Satellite-based assessments of ocean NPP have traditionally been based on chlorophyll concentration alone [*Antoine et al.*, 1996; *Behrenfeld and Falkowski*, 1997a; *Behrenfeld and Falkowski*, 1997b; *Morel*, 1991; *Platt et al.*, 1991; *Platt and Sathyendranath*, 1988]. More recently, the advent of ocean color spectral inversion algorithms [*Garver and Siegel*, 1997; *Lee et al.*, 2002; *Maritorena et al.*, 2002; *Siegel et al.*, 2002; *Werdell et al.*, 2013] has provided not one, but two pieces of information on phytoplankton populations: carbon and chlorophyll concentration [*Behrenfeld et al.*, 2005; *Westberry et al.*, 2008]. The significance of this development is that it provides a measure of phytoplankton biomass (C_{phyto}) [*Graff et al.*, 2015] and information of physiological variability through the chlorophyll:carbon ratio (*Chl:C*). One of the largest sources of uncertainty in NPP estimates has been uncharacterized changes in assimilation efficiencies (carbon fixed per unit chlorophyll) (Behrenfeld & Falkowski 1997b). The ability to now retrieve information on *Chl:C* provides an observable directly tied to variability in assimilation efficiencies. However, to achieve the desired accuracies in NPP additional information is needed and this is where simultaneous retrievals of phytoplankton fluorescence becomes essential. To understand this

[2] Cite as: Behrenfeld, M. J., T. Westberry, and B. Franz (2018), Requirements for the Measurement of Chlorophyll Fluorescence, in *PACE Technical Report Series, Volume 7: Ocean Color Instrument (OCI) Concept Design Studies (NASA/TM-2018 – 2018-219027/ Vol. 7)*, edited by I. Cetinić, C. R. McClain and P. J. Werdell, NASA Goddard Space Flight Space Center Greenbelt, MD.

need, it is necessary here to briefly digress into some details on phytoplankton physiology. Understanding these details not only clarifies the need for accurate fluorescence retrievals by PACE but also creates a foundation for defining measurement requirements.

As is the case with all oxygenic photoautotrophs, the photosynthetic membranes of phytoplankton contain two primary types of pigmented complexes, termed photosystems I and II. Each type of complex has a 'core' set of pigment-proteins and a 'peripheral' set of pigment proteins (i.e., 'antennae complexes'). In eukaryotic algae, both types of pigment-proteins are imbedded in the thylakoid membrane, whereas in prokaryotic cells the antennae complexes (called 'phycobilisomes') are located outside of the membrane (the relevance of this to PACE is explained below). Both photosystem I and photosystem II emit fluorescence in situ. However, the contribution of photosystem I is typically small compared to photosystem II under low light conditions. Another difference between photosystems is that a large fraction of the sunlight energy absorbed by photosystem II under high light conditions is dissipated as heat in a process call 'non-photochemical quenching' (NPQ), which causes the fluorescence signal measured by PACE to be small under its near-noon observing conditions than it would be without NPQ. The fluorescence of photosystem I is not quenched under high light, but instead increases linearly with increasing incident sunlight. Again, the relevance of NPQ to the PACE mission is explained below. A final key attribute of phytoplankton fluorescence is that the quantum yield of fluorescence (i.e., fluoresced energy per unit of pigment-absorbed light energy) varies with the growth conditions of the phytoplankton. Characterizing this variability in quantum yields is a primary target objective for the PACE fluorescence retrievals.

Phytoplankton possess a variety of photosynthetically active pigments, but only chlorophyll-a is found in the photosystem cores. The other types of pigments are all located in the peripheral antennae and they function to efficiently absorb light at wavelengths less effectively absorbed by chlorophyll-a. This energy is then passed on to chlorophyll-a as the energy migrates from the peripheral antennae to the core. Essentially, the pigment supercomplex of the photosystems acts as an 'energy funnel'. When this energy arrives at the core, it can be used for photochemistry (i.e., photosynthesis), dissipated as heat, or lost as fluorescence. For photosystem II, this fluorescence is centered at 685 nm, whereas for photosystem I it is centered around 710 nm (but note that the spectral distribution of PSI fluorescence overlaps with that of PSII). The correct approach for calculating the quantum yield of fluorescence is as the ratio of fluorescence from chlorophyll-a divided by the light absorbed by all photosynthetic pigments. For heritage ocean color sensors (MODIS, MERIS), quantum yields have essentially been calculated as fluorescence per unit chlorophyll [e.g. *Behrenfeld et al.*, 2009; *Huot et al.*, 2005]. The high spectral resolution of the PACE instrument will allow fluorescence to be more properly divided by the full spectrum of light absorption.

With this background information, we can now return to the issue of phytoplankton physiology. PACE will provide global assessments of phytoplankton absorption to carbon ratios (a_{ph}*:C*), rather than simply *Chl:C*. A primary driver of variability in a_{ph}:C is phytoplankton growth rate, with the former changing in direct proportion to the latter [*Halsey and Jones*, 2015; *Halsey et al.*, 2010; *Laws and Bannister*, 1980]. For example, a 2-fold change in growth rate is paralleled by a 2-fold change in a_{ph}:C. The reason for this direct relationship is that the light-harvesting capacity of the photosystems is finely tuned to match the cellular demands for photosynthetic products (ATP, NADPH) [*Halsey and Jones*, 2015; *Halsey et al.*, 2010; 2014; *Halsey et al.*, 2013]. Thus, a doubling in growth rate requires a doubling in photosynthesis, and thus a doubling in light harvesting (i.e., a_{ph}). And, this is the key. If no other factors than growth rate (μ) influenced a_{ph}:C, than variability in this ratio could be used to accurately quantify μ

and thus NPP (i.e., NPP = μC_{phyto}). Unfortunately, other properties of the environment also cause changes in a_{ph}:C.

Across the global ocean, the value of a_{ph}:C retrieved from ocean color data first and foremost reflects a balancing point between nutrient-dependent growth rate and the light available in the surface mixed layer (I_g). In phytoplankton, a_{ph}:C increases with decreasing light (a response referred to as 'photoacclimation') for a given growth rate [*Behrenfeld et al.*, 2016; *Geider*, 1987]. Thus, to use a_{ph}:C data to estimate μ, a correction must be made for variations in I_g. This correction is achieved using an empirical photoacclimation response curve (based on laboratory and field data and theory)[*Behrenfeld et al.*, 2016], remote sensing retrievals of incident light and diffuse attenuation coefficients, and data-assimilating model estimates of mixing depth. Thus, an approach is in-hand for the photoacclimation correction. What remains to be accounted for are other factors influencing a_{ph}:C variability. This is where fluorescence retrievals become crucial.

On the time scale of physiological acclimations (i.e., days), phytoplankton in the surface ocean mixed layer generally exist under the condition of steady-state growth. In other words, they are physiologically acclimated to their growth conditions. Under steady-state macronutrient limitation (nitrogen or phosphate), fluorescence quantum yields are relatively invariant with growth rate [*Behrenfeld et al.*, 2006]. The same is true when phytoplankton are iron limited in the absence of excess macronutrients [*Behrenfeld et al.*, 2006; *Schrader et al.*, 2011]. However, across more the 30% of the ocean's surface, mixed layer phytoplankton exist under the condition of limiting iron and replete macronutrients (a condition referred to as High Nitrogen, Low Chlorophyll (HNLC)) [*Boyd et al.*, 2007]. In HNLC waters, phytoplankton respond in a very unique way to their growth environment. Specifically, they produce far more pigment than is needed to support their photosynthesis [*Behrenfeld and Milligan*, 2013; *Behrenfeld et al.*, 2006; *Macey et al.*, 2014; *Schrader et al.*, 2011]. Furthermore, this excess pigment is not energetically connected to the photosystems. What this means is that another correction is necessary for deriving μ (thus NPP) from a_{ph}:C in HNLC waters. Fortunately, the energetically disconnected pigment-protein complexes also emit fluorescence and this signal can be detected in satellite-retrieved fluorescence quantum yields [*Behrenfeld et al.*, 2009; *Westberry et al.*, 2013]. Thus, accurate fluorescence retrievals by the PACE sensor are of fundamental importance for identifying different nutrient-limited growth conditions, characterizing how these conditions change over time, and accurately quantifying NPP and carbon cycling [*Westberry and Behrenfeld*, 2014].

The unique response of phytoplankton to HNLC conditions is not the only factor governing fluorescence quantum yields. Another contributor is changes in photosystem ratios (PSII:PSI). This ratio is also influenced by iron stress (whether in the presence or absence of excess micronutrients) and by the ratio of prokaryotic:eukaryotic cells in a given population (i.e., prokaryotes naturally have a much lower PSII:PSI ratio than eukaryotes) [*Behrenfeld and Milligan*, 2013]. As noted above, fluorescence emission spectra differ between PSII and PSI. Thus, as the PSI contribution increases, the fluorescence emission spectrum broadens on the red-side of the PSII emission peak (i.e., 685 nm). The super-spectral sampling capabilities of the PACE sensor (i.e., 5-nm resolution with sampling capabilities down to 0.625 nm) will provide the first opportunity ever to detect this PSI effect. The potential for PSI to influence the retrieved fluorescence spectra is due to the fact that PACE measurements are collected near noon when PSII fluorescence is highly quenched. Specifically, the NPQ response is so large that PSI fluorescence (which is not quenched) can become a significant fraction of total fluorescence emission, particularly in iron-stressed or prokaryote-dominated populations.

A final factor that can also influence fluorescence quantum yields is again related to the contribution of prokaryotes to total phytoplankton biomass. As noted above, eukaryotic phytoplankton have membrane

imbedded peripheral antennae. In these cells, energy transfer to the photosystem cores is so efficient that essentially all fluorescence comes from the core chlorophyll molecules. In prokaryotes, on the other hand, the phycobilisome complexes outside the membrane have a somewhat lower energy transfer efficiency to the core antennae and this inefficiency results in fluorescence emission from the phycobilisomes. This additional fluorescence emission is referred to as spillover and it can contaminate the chlorophyll-a fluorescence signal (thus resulting in an apparently enhanced fluorescence quantum yield *Suggett et al.* [2009]). The phycobilisome fluorescence spectrum, however, is blue-shifted relative to chlorophyll-a, causing the overall fluorescence spectrum to broaden at the shorter wavelengths. Again, the super-spectral sampling capabilities of the PACE sensor will provide the first opportunity ever to detect this potential phycobilisome signal and thus the means to account for prokaryotic contributions and improve interpretations of PACE fluorescence data.

To summarize this introductory section, advances in ocean color data analysis have provided a path for greatly improving estimates of ocean productivity and carbon cycling. This path begins with the assessment of phytoplankton carbon and phytoplankton cellular pigmentation. With the spectral resolution provided by PACE, this latter physiological property is significantly improved over traditional *Chl:C* data to now be quantified as spectrally-resolved a_{ph}*:C*. The a_{ph}*:C* signal contains a direct dependence on phytoplankton growth rate and NPP, but multiple other governing influences must first be accounted for. These additional factors are linked, as described above, to the magnitude and spectral features of fluorescence. Thus, accurate characterization of fluorescence is not a stand-alone science product for PACE, but an integral objective for meeting the mission's goals of improved understanding of ocean ecosystems and biogeochemistry.

2.2. Remotely Sensed Fluorescence

Fluorescence emission is typically characterized by a Gaussian function with a peak at 685 nm and full-width at half maximum (FWHM) of 25 nm [*Gordon*, 1979]. Strong absorption in the relevant spectral region (~660-700 nm for PSII fluorescence) by seawater and to a lesser extent by chlorophyll itself can confound the measurement of fluorescence *in situ*. Additional absorption by molecular oxygen in the atmosphere (specifically, O_2-B) places further constraints on fluorescence measurements from satellite. Resultant water leaving radiances in the chlorophyll fluorescence region are extremely small and sensor design characteristics strongly impact the accuracy of fluorescence retrievals. Therefore, determination of sufficient sensor requirements is of critical importance.

Here, we use a combination of underwater radiative transfer simulations and analysis of previous satellite (MODIS-Aqua) chlorophyll fluorescence measurements to assess expected water leaving radiances attributable to fluorescence and associated target uncertainties.

Paired simulations of the underwater light field were carried out with and without fluorescence using the Hydrolight (v5.1) underwater radiative transfer model [*Mobley*, 1994]. This allows estimation of the bulk water leaving radiance and/or isolation of the fluorescent component from elastically backscattered radiance under a variety of atmospheric and oceanic conditions. The range of various input properties used in the simulations were not meant to be exhaustive, but rather to provide a baseline representative of the global open ocean. HydroLight employs an idealized semi-empirical sky radiance model following *Harrison and Coombes* [1988] with the following inputs: Solar zenith angle = 30°, atmospheric pressure = 29.92 in Hg, relative humidity = 80%, visibility = 15km, ozone concentration = 300 DU, and "typical" marine aerosols. Transfer across the atmosphere-ocean interface is governed by the Cox-Munk wind-speed wave-slope statistics [*Cox and Munk*, 1954], temperature and salinity-dependent Fresnel reflectances, and Monte Carlo ray tracing as described in *Mobley* [1994]. The in-water bio-optical model

is taken from *Morel and Maritorena* [2001], which is itself a compendium of past work. Briefly, absorption is specified by three components: pure sea-water [*Pope and Fry*, 1997], pigmented particles [*Bricaud et al.*, 1998], and colored dissolved material. Scattering is described by only two components: pure seawater [*Morel*, 1974; *Smith and Baker*, 1981] and pigmented particles [*Morel et al.*, 2002]. However, the particle phase function is a combination of small- and large-particle phase functions with the fraction of each defined by the chlorophyll concentration [*Morel et al.*, 2002]. Other attributes held constant in all simulations were a cloud-free atmosphere, constant surface wind speed of 5 m/s, and an infinitely deep water column. Further details about sky radiance and in-water bio-optical models can be found in the HydroLight Technical Documentation [*Mobley and Sundman*, 2012].

Inelastic radiance sources were limited to fluorescence from chlorophyll (i.e., no CDOM fluorescence or Raman scattering [see *McKinna et al.*, 2016; *Westberry et al.*, 2013 for global significance of Raman scattering] and the quantum yield of chlorophyll fluorescence was fixed at 2% (=0.02 mol photons fluoresced per mol photons absorbed). This value is slightly higher than the global average reported for MODIS fluorescence data [*Behrenfeld et al.*, 2009], but is a reasonable starting point and may still reside within the uncertainty around the MODIS global mean. Estimates of bulk water leaving radiance, $L_w(\lambda)$, and the fluorescence contribution to water leaving radiance (ΔL_w) for a wide range of chlorophyll concentrations (0.04-4.00 mg m^{-3}) are shown in Figure 2.1. The quantity ΔL_w is calculated as the difference between simulated $L_w(\lambda)$ with and without fluorescence included and is comparable to the MODIS fluorescence line height (FLH) product when evaluated at 678nm (MODIS Band 14).

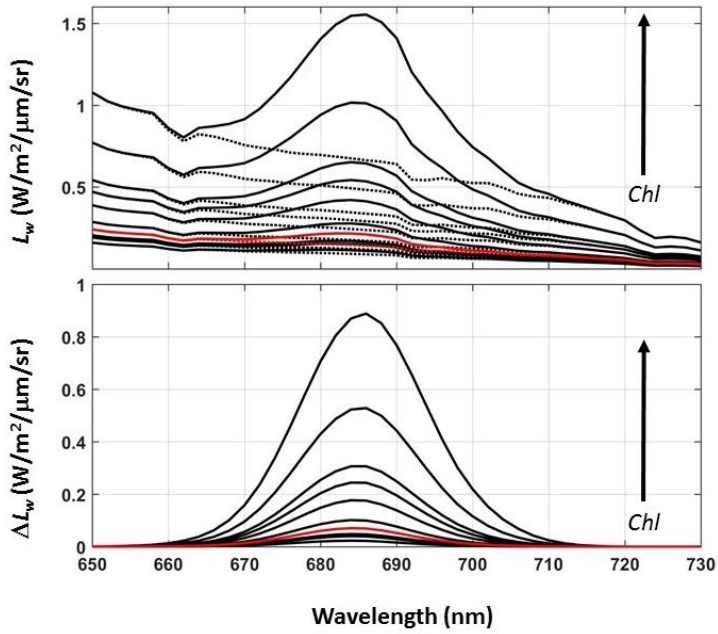

Figure 2.1. HydroLight simulation results showing chlorophyll fluorescence effects on water leaving radiance, Lw(λ). (Top) Lw(λ) for a range of Chl concentrations (0.04, 0.08, 0.1, 0.16, 0.25, 0.5, 0.75, 1.0, 2.0, 4.0 mg m-3). Chl increases from lower to upper spectra and red lines are results for global mean Chl of 0.16 mg m^{-3}. Results are shown with fluorescence included (solid lines) and without (dotted lines). (Bottom) Fluorescence contribution to water leaving radiance (ΔLw(λ)), calculated as the difference between paired HydroLight runs with and without fluorescence. This quantity is comparable to the MODIS FLH product, but represents the "line height" spectrally, instead of only at the central wavelength. Values for both properties at the peak wavelength (685nm) are given in Table 2.1.

Here, we report ΔL_w at 685 nm to better capture the peak of fluorescence emission. When *Chl* is set equal to the global median value of 0.16 mg m^{-3}, we find that $\Delta L_w(685)$ is nearly identical to median global MODIS fluorescence line height (FLH) ~5e-02 W m^{-2} μm^{-1} sr^{-1}. $\Delta L_w(685)$ from higher *Chl* (2-4 mg m^{-3}) are near the 95th percentile of global MODIS FLH measurements in shallow, productive environments and outside both the baseline and threshold ranges identified in the PACE Mission Science Definition Team Report [Table A-1, PACE Science Definition *Team*, 2018]. These simulation results provide a quantitative means to estimate uncertainty requirements in the fluorescence spectral region. For each *Chl* concentration, Table 2.1 also provides the uncertainty required in $L_w(685)$ to achieve a target uncertainty of 10% in $\Delta L_w(685)$. This σ_{Lw} is derived by assuming the uncertainty in $L_w(685)$ is the same with as without the fluorescence contribution, and thus $\sigma_{Lw} = 0.10\ \Delta L_w(685) / 2^{0.5}$. Again using the global mean *Chl* of 0.16 mg m^{-3} as a point of reference, we can expect $\Delta L_w(685)$ = 0.0697 W m^{-2} μm^{-1} sr^{-1}, which can be estimated to within 10% if the uncertainty (σ_{Lw}) in $L_w(685)$ is less than 4.93e-03 W m^{-2} μm^{-1} sr^{-1}.

Table 2.1. Simulated water leaving radiances (Lw), fluorescence contribution to water leaving radiance (ΔLw), and associated 10% target uncertainty in both water leaving radiance and reflectance (σ_{Lw} and $\sigma_{\rho w}$, respectively). All values are reported at wavelength of peak fluorescence emission (685nm). Chlorophyll concentration of 0.16 mg/m3 (shaded gray) is representative of global median Chl.

Chl (mg/m^3)	$L_w(685)$ (W/m^2/μm/sr)	$\Delta L_w(685)$ (W/m^2/μm/sr)	σ_{Lw} (W/m^2/μm/sr)	$\sigma_{\rho w}$ (unitless)
0.04	0.1134	0.0224	1.58e-03	3.32e-06
0.08	0.1512	0.0395	2.79e-03	5.85e-06
0.10	0.1679	0.0474	3.35e-03	7.02e-06
0.16	0.2139	0.0697	4.93e-03	1.03e-05
0.25	0.2745	0.1003	7.09e-03	1.49e-05
0.50	0.4171	0.1761	1.25e-02	2.61e-05
0.75	0.5388	0.2439	1.73e-02	3.61e-05
1.00	0.6480	0.3065	2.12e-02	4.54e-05
2.00	1.0134	0.5257	3.72e-02	7.79e-05
4.00	1.5488	0.8795	6.22e-02	1.30e-04

2.3. PACE Mission Requirement

Table 2.1 provides the target uncertainties in $L_w(685)$ needed to achieve the PACE mission science goal of measuring the magnitude of chlorophyll fluorescence to within 10% at the spectral location of peak signal (685 nm). To support mission development, this science goal must be translated to a radiometric performance requirement on the OCI sensor. PACE science requirements on ocean color uncertainties have been previously defined in terms of reflectance, so the σ_{Lw} of Table 2.1 have been translated to reflectance units as $\sigma_{\rho w} = (\pi/\langle F_0 \rangle)\sigma_{Lw}$, where $\langle F_0 \rangle$ is the mean extraterrestrial solar irradiance in W m^{-2} μm^{-1} at 685 nm. For the typical open ocean case with chlorophyll concentration of 0.16 mg m^{-3} and target uncertainty in fluorescence signal of 10%, Table 2.1 shows that we require an uncertainty in water-leaving reflectance at 685 nm of 1.03e-5. This is very small, and notably well below the current baseline

water-leaving reflectance uncertainty requirements for the fluorescence spectral region of $3e^{-4}$ [*Franz and Karaköylü*, 2018]. A significant mitigating factor, however, is that the fluorescence signal is measured relative to the signal in nearby spectral bands (i.e., a band difference). If we assume that systematic errors, modeling errors, and propagation errors are spectrally correlated, as can be expected due to the nature of the atmospheric correction algorithm [*Franz and Karaköylü*, 2016], then uncertainty in $\sigma_{\rho w}$ can be assumed to be driven exclusively by the instrument noise in the individual bands surrounding the fluorescence spectral region. Table 2.2 shows estimated $\sigma_{\rho w}$ at 670-nm (proxy for the fluorescence spectral regime) as a function of signal-to-noise ratio (SNR) at the typical at-sensor radiance over oceans (L_{typ}, [*Franz and Karaköylü*, 2018]). This analysis is based on Monte-Carlo simulations as described in [*Franz and Karaköylü*, 2018], but with no contribution of noise in the near infrared channels (which would otherwise contribute to spectrally correlated noise in the fluorescence region, [*Franz and Karaköylü*, 2016]. The numbers quoted are the 50^{th} percentile of the global distribution of derived uncertainties, to be consistent with the median open-ocean $\sigma_{\rho w}$ requirements described above. The last column of Table 2.2 shows the uncertainty that could be achieved by spatial averaging, wherein the native resolution (nominally 1-km x 1-km) is reduced to 4-km x 4-km through binning. Comparing with Table 2.1 and extrapolating/interpolating to the $\sigma_{\rho w}$ requirement of $1.03e^{-5}$, these results suggest that, the science goal of measuring chlorophyll fluorescence in the open ocean to within 10% can be achieved at nominal spatial resolution if the SNR of OCI exceeds 1570, or at reduced spatial resolution if the SNR of OCI at L_{typ} exceeds 1115.

Table 2.2. Uncertainty in water-leaving reflectance ($\sigma_{\rho w}$) at 670-nm as a function of Signal to Noise Ratio (SNR) at typical at-sensor radiance over ocean (Ltyp). Results are derived from Monte-Carlo simulations. Results are presented for both nominal resolution (1-km x 1-km) and reduced resolution (4-km x 4-km).

SNR	**$\sigma_{\rho w}$ (1-km x 1-km)**	**$\sigma_{\rho w}$ (4-km x 4-km)**
572	6.28e-5	1.57e-5
979	5.03e-5	1.26e-5
1351	2.51e-5	6.27e-6

These OCI SNR performance requirements are challenging to meet, while also satisfying other driving requirements such as the capability to make radiometric measurements over the full dynamic range of earth observations, from the darkest oceans to the brightest clouds, without digital saturation. Initial OCI noise modeling showed a best SNR estimate (without margin) of less than 950, which is insufficient to meet the PACE science goal of measuring chlorophyll fluorescence in the open ocean to within 10% (e.g., SNR of 1115 is needed to meet the requirement at 4-km x 4-m km spatial resolution).

One approach to increase OCI SNR performance is to increase the gains on the detector amplifiers, but this will result in digital saturation for the brightest observed radiances. To enhance OCI radiometric performance and meet the science goals for measuring chlorophyll fluorescence, the requirement to avoid digital saturation was relaxed, but only for a limited spectral range that encompasses the fluorescence region (nominally 650-720nm). This decision has two major impacts: 1) cloud science will be limited in the fluorescence region, and 2) the maximum observed brightness in this spectral region will not be known for purposes of estimating straylight errors. The first impact is readily mitigated by the fact that cloud science algorithms do not traditionally use this spectral range. The second impact is mitigated by the availability of adjacent spectral regions that do not saturate over the brightest signals, and thus can be used to model the peak brightness observed in the fluorescence region. It should be noted that this enhanced SNR performance was accomplished by increasing the gain on the detector electronics. This is a

hardware solution that ensures maximum benefit in noise reduction as a function of L_{max}, but the amount that the gain can be increased is limited. With this implementation, recent model estimates on OCI radiometric performance show SNR in the fluorescence spectral region of 1351 at L_{typ} (as in Table 2.2). This suggests that the PACE science goal of measuring chlorophyll fluorescence in the open ocean to within 10% can be achieved (with margin) at the reduced spatial resolution of 4-km x 4-km. Note that the 10% goal may be achievable at the nominal 1-km x 1-km spatial resolution for moderate to higher chlorophyll levels (higher L_w(685) signal levels, Table 2.1) that are more typical of coastal environments and more productive ocean regions, where the higher resolution is of value in resolving natural variability.

Chapter 3

Estimating coastal ocean feature sizes for optimal remote sensing of coastal waters

Nima Pahlevan, Science Systems and Applications Inc, Lanham, MD[8]

Sergio R. Signorini, Science Applications International Corporation, Reston, Virginia

Ivona Cetinić, GESTAR/Universities Space Research Association, Columbia, Maryland

Executive Summary

This chapter aims at recommendations for optimal spatial-sample distance for capturing in-water bio-optical and geochemical features in coastal waters. To do so, Landsat-derived products as well as LiDAR/field data over coastal shelf waters were analyzed and evaluated for spatial variability. The analyses of Landsat data products indicated average feature sizes on the order of 150-200m. The LiDAR/field data collected in relatively clear coastal shelf waters pointed to larger feature sizes, i.e., ~ 1 km, on average. It is concluded that to enable un-aliased sampling of features in coastal areas, the ground sampling distance (GSD) should ideally be at least 75-100 m. It should further be emphasized that to avoid land and/or cloud adjacency effects, i.e., to increase number of valid observations/pixels, in nearshore coastal waters smaller GSDs are highly recommended.

3.1. Introduction

Many existing ocean color missions spatially sample global bodies of water at nominal 1 km, which does not capture small-scale biological and oceanography features in nearshore and estuarine coastal waters. Ideally, ocean color missions are desired to sample the global bodies of water with smaller footprints (pixels), however, the design constraints, including frequency of revisit, signal-to-noise ratio (SNR), and available bandwidths for data downlink, limit the instrument-science trade space. It is, thus, critical to identify an optimal spatial sampling size to expand the utility of climate-quality ocean color products into coastal areas, such as harbors, bays, lagoons, etc. Therefore, the question is: what is the optimal GSD that enables capturing various features in near-shore environments? The answer is, however, not trivial and requires extensive analyses of various coastal systems. The biological/oceanography features vary in scales from tens of meters to many kilometers depending on the forcing physical, biological, and environmental factors. Among all the driving factors are river discharge, tidal currents, upwelling, convergence, advection, thermal bar formation in mid-latitude lakes, wind speed, air temperature, phytoplankton processes, including grazing and viral infections. Ongoing human activities, including transportation, tourism, and waste outfalls further triggers harmful ecosystem impacts endangering aquatic resources and economy. In addition to the physical size of in-water features that provides hints on optimal sampling size of a remote sensor, adjacency effects [*Frouin et al.*, 2009] further restricts the use of ocean color products near coastlines. This impact also largely limits the number of valid observations at the proximity of sea ice in climate-sensitive Polar Regions [*Feng and Hu*, 2016]. *Meister and McClain* [2010] analyzed MODIS pre-

[3] Cite as: Pahlevan, N., S. R. Signorini, and I. Cetinić (2018), Estimating coastal ocean feature sizes for optimal remote sensing of coastal waters, in *PACE Technical Report Series, Volume 7: Ocean Color Instrument (OCI) Concept Design Studies (NASA/TM-2018 – 2018-219027/ Vol. 7)*, edited by I. Cetinić, C. R. McClain and P. J. Werdell, NASA Goddard Space Flight Space Center Greenbelt, MD.

launch Line Spread Functions (LSF) and concluded that a window size of 5x7 pixels is required to minimize the impact of straylight due to nearby clouds or land objects. This results in high-fidelity products while inducing loss of invaluable observations over open ocean and coastal/inland waters.

Furthermore, high-quality 4 km or 9 km Level-3 ocean color products do not adequately resolve horizontal features in near-shore regions. *Bissett et al.* [2004] applied a statistical technique to airborne image data to estimate optimal GSD in a well-mixed region and found the scale of variability to be on the order of 100m. *Aurin et al.* [2013] used a similar approach on MODIS 250 m products in four major river deltas and suggested a ~500 m resolution as an optimal GSD in coastal waters. On the other hand, *Kutser* [2004] suggests that the horizontal variability during algal bloom events is significant and that a full characterization requires spatial sampling on the order of 10s of meters. *Mackas* [1984] showed that the spatial variability of plankton community across bathymetric contours is larger than that along the contour lines and that a finer spatial sampling regime is needed to map community composition than for biomass distribution. *Blackwell et al.* [2008] studied the critical scale of variability within coastal waters of Monterey Bay (California), San Luis Obispo Bay (California), and New Jersey shelf. Using the Autonomous Underwater Vehicle (AUV) measurements with ~2 m sampling frequency, they revealed that the scale of variability varies within 50-190 m depending on vertical distributions of biomass in their study sites. *Washburn et al.* [1998] performed a similar analysis with a different observational scheme in subarctic North Atlantic region. With coarse undulating frequency AUV observations (1.1 km), they found 550 m to be the scale of variability in the open waters. However, these in situ-based analyses are representative of limited temporal and geographical extents.

In this study, we used three different techniques to evaluate scales of variability from which an optimal GSD in diverse coastal systems is proposed. We utilize Landsat-derived 30 m ocean color products along with in situ observations made during NASA's Ship-Aircraft Bio-Optical Research (SABOR), and several others field campaigns.

3.2. Data and Methods

Geo-statistical analysis has long been used to determine the scale of variability using discrete set of measurements of a variable of interest (e.g., soil moisture) in the spatial domain. The sparse measurements are then used to construct empirical spatial functions, one of which used most frequency is variogram [*Rahman et al.*, 2003], which explicitly describe the correlation between a quantity measured at discrete data points as a function of distance between them. Spatial autocorrelation and/or autocovariance functions, multifractal and spectral analyses are among the other techniques for estimating the characteristics of spatial variability. The following sections elaborate on the methods applied in each section. In section 3.2.1, we will describe how we utilized Landsat-derived R_{rs} and section 3.2.2 explains airborne and field data and how we used for the spatial analyses.

3.1.1. Analysis Using OLI Products

The high-quality OLI ocean color products at nominal 30m footprints are the basis of the image analysis. Since there are several possible methods to investigate the optimal GSD, we followed two slightly different approaches. The first method follows the same technique proposed by *Bissett et al.* [2004] and utilized in *Aurin et al.* [2013]. They examined spatial variability along transects drawn near-perpendicular to coastlines to capture the maximum gradient in bio-optical properties. While the former applied the procedure to a limited set of high-resolution (2 to 20 m) airborne imagery, the latter evaluated the scale of variability for more than 2000 MODIS images at 250 m nominal pixel size. We refer to this approach as the transect method. For the second approach, we examine the spatial representativeness of each OLI pixel against

locally defined windows of variable size through pixel aggregation. We refer to this method as scene-wide method.

The OLI onboard Landsat-8 has been shown to considerably outperform previous generation of Landsat sensors when studying aquatic systems [*Gerace et al.*, 2013; *Pahlevan and Schott*, 2013]. This is because of its improved SNR, the 12-bit radiometric resolution, and the addition of the new 443 nm channel [*Pahlevan et al.*, 2014; *Vanhellemont and Ruddick*, 2014]. The OLI Level-1 data products (TOA reflectance) were obtained from the USGS web portal (http://glovis.usgs.gov/). In order to provide 30 m OC products, the OLI data were processed using the SeaDAS package [*Franz et al.*, 2015]. According to the recommendations in *Franz et al.* [2015], we used the NIR-SWIR (865 nm-2201 nm) band combination for the atmospheric corrections (AC) followed by the iterations on the NIR channel to account for non-zero reflectance [*Bailey et al.*, 2010] in the NIR. This strategy was chosen to allow for smoother ocean color products. At this point, the OLI-derived R_{rs} products (at 443, 482,561, 655, and 1601nm) are generated and supplied to the spatial-analysis process as described below. The retrieval of secondary products, including chlorophyll-a ([*Chla*],[*O'Reilly et al.*, 1998]), diffuse attenuation of downwelling irradiance at 490nm (K_d(490),[*Mueller*, 2000]), and particulate backscattering at 655nm (b_{bp}(655), [*Lee et al.*, 2012] will be derived later in paper from the simulated coarse-resolution R_{rs} products [*Lee et al.*, 2012].

3.1.1.1. Transect Method

Here, the spatial variability along two different transects in two different coastal systems, i.e., Chesapeake Bay and Exmouth Gulf, is examined (Fig. 3.1).

3.3. Study Sites

Chesapeake Bay is a large estuary located in the USA's mid-Atlantic coastal region. The Bay is almost 300 km long, with a relatively deep (20 to 30 m) and narrow (1 to 4 km) central channel confined by a sill at its seaward end [*Kemp et al.*, 2005]. River flow (average of 2300 m^3 s^{-1}) drives the estuarine circulation, characterized by a lower-layer counter-flow that creates relatively long residence times (90 to 180 days) for freshwater and nutrients [*Pritchard*, 1956; 1967]. The distribution of [*Chla*] in highly productive Chesapeake Bay has strong seasonal and spatial patterns, clearly observed by ocean color satellites and confirmed by in situ observations. Positioning of the [*Chla*] maximum was generally downstream of the turbidity maximum, coinciding with increased light penetration, and the development of stratification. We selected Chesapeake Bay for one of our analyses because of the complex nature of its physical and biological dynamics, relatively high phytoplankton productivity and terrestrial organic matter inputs, as well as its optical characteristics (turbid waters scenario).

In contrast, we selected Exmouth Gulf as a typical example of a region characterized by less optically complex waters (clearer waters scenario) and geometry. Exmouth Gulf is an inlet of the Indian Ocean in Western Australia, between North West Cape and the mainland. It is 90 km long north to south and 48 km across the mouth and has a maximum depth of 22 m. The Gulf is considered to be an arid zone estuary with no rivers discharging into it. Most of the rainfall occurs in summer due to occasional storms and tropical cyclones. Consequently, the terrestrial input of freshwater and nutrients into the Gulf is insignificant during the most of the year and the Gulf is considered to be relatively unproductive [*Ayukai and Miller*, 1998]. In the Gulf, [*Chla*] concentrations typically range from 0.2 to 0.3 mg m^{-3}. The low phytoplankton biomass and production in the Gulf are seemingly related to the aridity of the region and hence the small terrestrial runoff of nutrients [*Ayukai and Miller*, 1998].

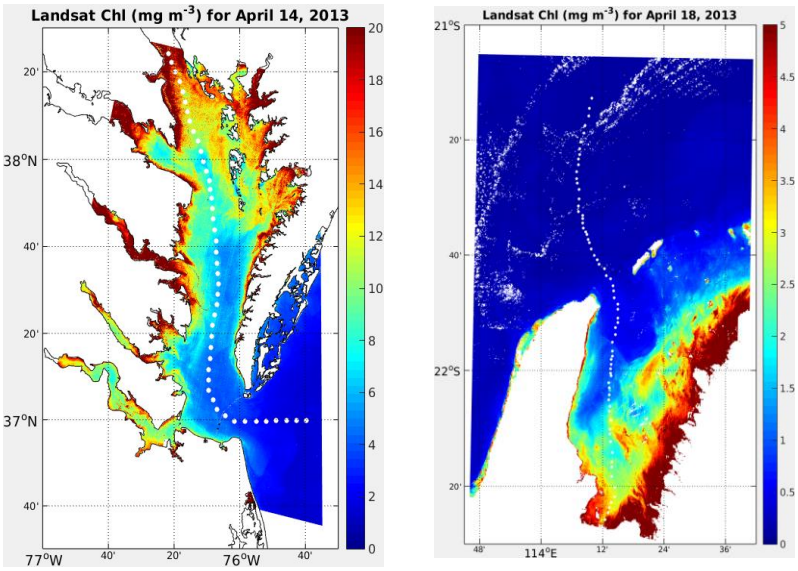

Figure 3.4. The Landsat-derived chlorophyll-a [Chla] products obtained from two images acquired on April 14 and 18th 2013 over Chesapeake Bay (left) and Exmouth Gulf. Shown on the products are the transect along which the analyses were carried out.

3.3.1.1.1. Spatial Analysis

The spatial variability along the transects is tested at virtual stations (along a transect) where coefficient of variability (CV) is computed for progressively expanding window size, i.e., 2×2, 3×3, 4×4, …. The parameter CV is compared against the overall noise (N_t) computed for each array. The parameter CV^m for each band λ (dropped for brevity) is calculated as follows

$$CV^m = {\sigma_{R_{rs}}}^m / {\tilde{R}_{rs}}^m \quad \text{(Eq 3.1)}$$

where ${\sigma_{R_{rs}}}^m$ and ${\tilde{R}_{rs}}^m$ are the standard deviation and median value within an $m \times m$ array, respectively. For an $m \times m$ array, if $CV^m > N_t$, the scale of variability (SV) is calculated as: $SV = (\overline{m, m-1})$. The overall noise is partitioned into two major components, i.e., photon noise (N_p) and noise due to atmospheric correction (N_{ACO}), both of which are expressed in units of remote sensing reflectance (R_{rs}). The quantity (R_{rs}) is defined as the ratio of water-leaving radiance and total downwelling irradiance just above water and plays a central role in deriving biogeochemical properties of upper water column. The photon noise (N_p) propagated to R_{rs} products is calculated as below

$$N_s = (a + bL_t)^{0.5} \qquad [W/(m^2 sr \mu m)] \quad \text{(Eq 3.2)}$$

$$SNR = L_t / N_s \quad \text{(Eq 3.3)}$$

$$N_{L_t} = L_t / SNR \;\; [W/(m^2 sr \mu m)] \quad \text{(Eq 3.4)}$$

$$N_p = N_{L_t} R_{rs} / L_w \qquad [1/sr] \quad \text{(Eq 3.5)}$$

where a and b are OLI pre-launch noise parameters establishing a linear relationship between noise (N_s) and top-of-atmosphere (TOA) radiance. The SNR is the signal-to-noise ratio, and L_w is the water-leaving radiance. The uncertainty (noise) in the atmospheric correction process [*Gordon and Wang*, 1994] is calculated as below

$$N_{ACO} = N_{L_t}(2201)\, L_a/L_a(2201) \qquad [W/(m^2 sr \mu m)] \qquad \text{(Eq. 3.6)}$$

where $L_a = L_t - L_r$ is the spectral aerosol radiance, and $L_a(2201)$ and $N_{L_t}(2201)$ are the aerosol radiance and noise at $\lambda = 2201nm$, respectively [*Wang and Shi*, 2007]. Note that, here, we assume the Rayleigh radiance (L_r) and the Rayleigh-aerosol components are noise free. The radiance noise then (N_{L_a}) is converted into units of $[1/sr]$ in a similar fashion as in Eq. 3.5. The overall noise N_t is then estimated as

$$N_t = \left({N_p}^2 + {N_{ACO}}^2\right)^{0.5} \qquad [1/sr] \qquad \text{(Eq. 3.7)}$$

Note that, in regions with turbid atmosphere, the overall noise is dominated by the N_{L_a} component.

3.3.1.2. Scene-Wide Method

Recognizing that Chesapeake Bay and Exmouth Gulf do not represent all bio-physical in-water features, globally distributed OLI scenes (Fig. 3.1) across various coastal environments ranging from extremely turbid waters to moderately turbid were selected as candidate areas. In addition, we will implement a slightly different procedure to identify scale of variability within these scenes.

3.3.1.2.1. Study Sites

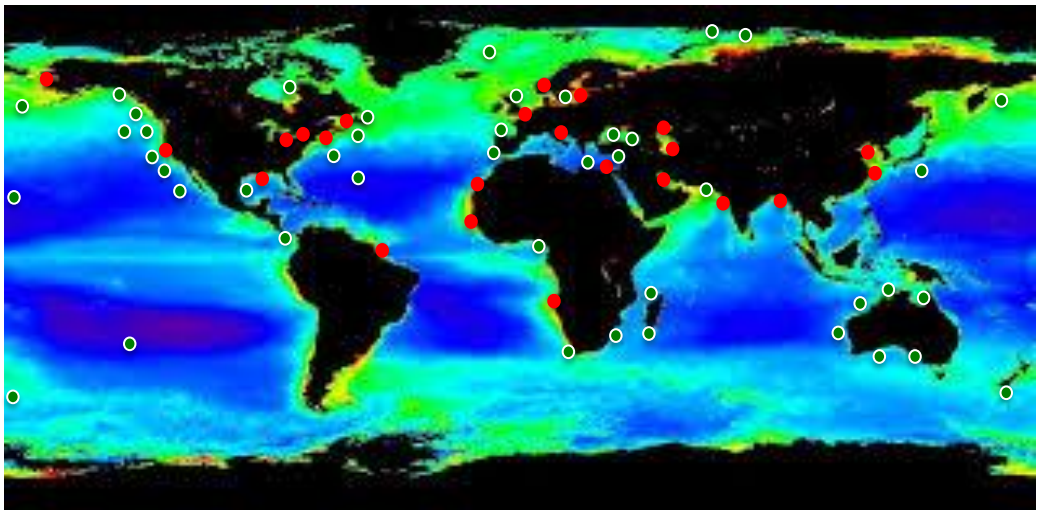

Figure 3.5. Site locations where Landsat/OLI data were processed to measure the scale of variability in coastal waters.

In order to capture various environmental conditions, 56 cloud-free OLI scenes distributed globally across different inland/coastal ecosystems were utilized. These scenes (denoted by red circles) represent varieties of turbidity and trophic status with [*Chla*] ranging from 1.5 to 22 mg m^{-3}. The most turbid waters include the scenes over the Amazon River basin, Mississippi River, Bay of Bengal, and Yangtze River basin. Note that in some cases multiple OLI scenes are employed in a geographic area. The breadth of biological/physical conditions encountered within these scenes will allow for a robust analysis of the

optimal ground sampling to remotely measure in-water biogeochemical properties. While the scale of variability was estimated using the OLI-derived products over the marked coastal/inland waters, the OLI product noise was calculated using OLI scenes over clear coastal/oceanic waters (green circles).

3.3.1.2.2. Spatial Analysis

In this section, we characterize the optimal sampling distance by evaluating spatial representativeness at selected OLI pixels (Fig. 3.3). To reduce computation time, every 30 OLI pixels along the rows and columns is evaluated for spatial uniformity. This evaluation is performed by calculating normalized difference between a center pixel ($R_{rs}(i,j)$) and the mean R_{rs} ($\bar{R}_{rs}$) computed over a varying array size of m centered at (i,j):

$$\delta^m = \left(R_{rs}(i,j) - \bar{R}_{rs}{}^m\right)/\tilde{R}_{rs}{}^m) \quad m = 3,5,7,\ldots \qquad \text{(Eq 3.8)}$$

where $\bar{R}_{rs}{}^m$ and $\tilde{R}_{rs}{}^m$ are the mean and median values, respectively. In other words, at each window size, we simulate the footprint of a virtual sensor with a larger instantaneous field of view (IFOV) and compare against the $30\,m \times 30\,m$ center pixel. Similar to previous section, the parameter δ^m is compared against the overall noise (N_t). However, the noise due to the atmospheric correction (N_{ACO}) is computed in a different fashion than in Eq. 6. In this section, we estimate this noise component using the recorded OLI products over oligotrophic waters where [*Chla*] < 0.1 mg m^{-3} [*Hu et al.*, 2012]. The noise is estimated by computing the standard deviation of the R_{rs} products (σ) over 3×3-element arrays across 85 OLI scenes. As a result, the instrument striping/banding is also incorporated in the product noise estimation. For different water types, the noise in the visible bands ($\sigma_{R_{rs}(\lambda<700nm)}$) is estimated as a function of noise $R_{rs}(1609)$, i.e., $\sigma_{R_{rs}(1609)}$. For an ideal sensor (with no striping) and a perfect atmospheric correction procedure, $\sigma_{R_{rs}(1609)}$ is expected to equal zero across all water types. As an example, Fig. 3.4 illustrates the relationship found for $\sigma_{R_{rs}(443)}$ and $\sigma_{R_{rs}(1609)}$. Similar linear relationships were obtained for the other visible channels. With the known noise models, $N_{ACO}(\lambda < 700nm)$ for each $m \times m$ array under investigation is determined. The overall noise (N_t) is then calculated as in Eq. 3.7 and compared against δ^m per array. The scale of variability (SV) is then specified when $\delta^m > N_t$. Note that SV obtained in this fashion is an odd multiplication of OLI pixel size (30m).

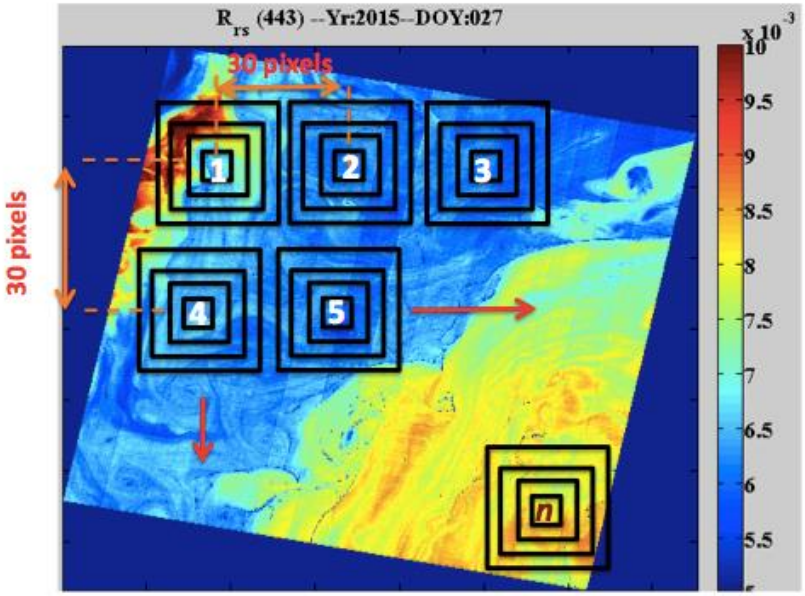

Fig. 3.6. The schematic outline of how the scene-wide method has been implemented for one example of OLI-derived $R_{rs}(443)$ product. Within each window, $\boldsymbol{\delta^m}$ and $\boldsymbol{N_t}$ are computed. The imagery was collected on Jan 27th 2015 over Atlantic Ocean.

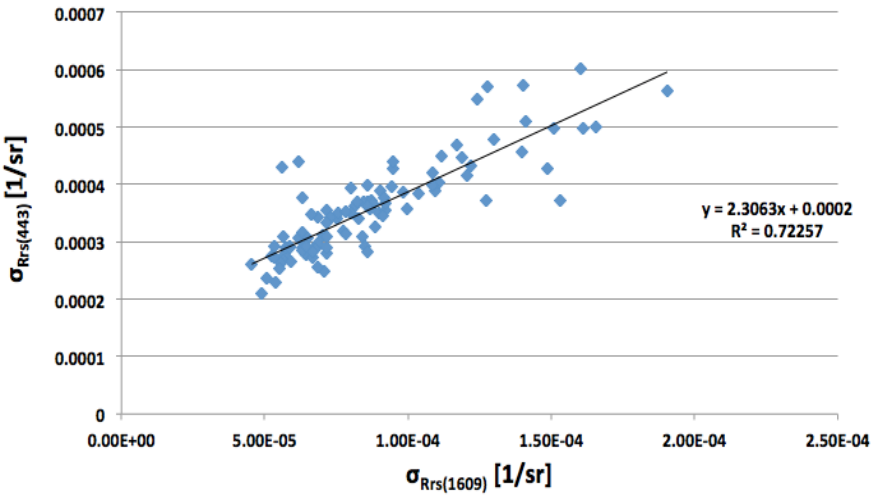

Fig. 3.7. The relationship between noise in $R_{rs}(1609)$ and $R_{rs}(443)$ found for 85 OLI scenes in oligotrophic waters. This relationship is used to estimate noise in Rrs(443) over various eutrophic/turbidity conditions.

3.3.2. LiDAR- and Field-based Approach

3.3.2.1. Collection Method and Study Sites

Several different temporally and spatially continuous datasets were used in this analysis. Aircraft-based High Spectral Resolution LiDAR (HSRL) measurements were collected during NASA's Ship-Aircraft Bio-Optical Research (SABOR) campaign in June 2014, in the areas of Gulf of Maine, along the East Coast of USA and across the Gulf Stream to Bermuda. Details on HSRL technique can be found in in *Hair et al.* [2015]. In short, depth resolved vertical profiles resulting from each laser shot, were averaged every half a second, resulting with ~50 m horizontal resolution (variable depending on the aircraft velocity). Although LiDAR profiles were resolving up to 3 optical depths, only the top 5 m data was used in this study. The particulate backscattering coefficient, b_{bp} (532 nm, 180°) was calculated as described in [*Hair et al.*, 2015; *Hair et al.*, 2008; *Moses et al.*, 2016]. The HSRL based b_{bp} dataset was subdivided based on the geographical location (e.g. Gulf of Maine vs. Gulf Stream) and encountered b_{bp} range.

In situ data were collected by optical instruments deployed aboard an undulating vehicle ("Dolphin", see *Twardowski et al.* [2007b] and *Miller et al.* [2003]), in Ligurian Sea (October 2008), Hudson river plume (May and November 2007, July 2008 and July 2009) and around Hawaii (March 2007). The platform was undulating within the top 10-20 m, however, only data from the top 7 m were used for this analysis. The instrument package contained Seabird's CTD and a variable number of optical instruments, dependent on the campaign; here, we only use particle absorption data originating from two in situ spectrophotometers (WETLabs ac-9/ac-S), and $b_{bp}(\lambda)$, data originating from WETLab's BB3 backscattering meter. Particulate absorption was calculated as a difference between the 0.2 μm filtered absorption and non-filtered absorption measurements (as measured by two parallel deployed ac type instruments). Particulate backscattering was calculated following the previously described methodology (e.g. *Twardowski et al.* [2007a]). Data was collected with 1 Hz frequency, depending on the velocity of the vehicle, resulting horizontal resolution was ~1 m. Similar to the method described for HSRL dataset, these in situ datasets were subdivided based on the geo-location and encountered data range.

3.3.2.2. Spatial Analysis

Based on the geographical location, and accoutered range of the collected parameters, each of the sub-datasets were assigned to specific water type (oligotrophic/open ocean, or eutrophic/costal ocean), and specific ocean basin (Atlantic, Pacific and Mediterranean). Prior to further analysis, each sub-dataset was first median filtered (7-point median filter, modified Matlab code *medfilt1.m*) to remove spikes and similar outliers. Sub-datasets were then divided, based on the along-track distance, in 50 m cells (pixels), where a mean value of all data within the cell was assigned as a nominal value of that specific "pixel". The semi-variance (γ) of two optical values (z(x) and z(x+h)) at a certain separation distance (h) was expressed as [*Rahman et al.*, 2003]:

$$\gamma(h) = \frac{1}{2}[z(x) - z(x+h)]^2 \qquad \text{(Eq. 3.9)}$$

Within each of the sub-datasets, there will be a number (n) of such paired observations, and total semivairance (Γ), for specific separation distance (h) will then be

$$\Gamma(h) = \frac{1}{2n}\sum_{i=1}^{n}[z(x_i) - z(x_i+h)]^2 \qquad \text{(Eq 3.10)}$$

When calculated across the whole transect and across different separation distances (50 m – 3000 m), and displayed as a function of the increasing separation distances, the resulting semi-variance (semi-variogram) is a good measure of the spatial variability in targeted parameters.

A simple logarithmic function was fitted though the semi-variogram data points and the resulting curve was normalized to 0-1 range. For each of those curves, sill (point in which semi-variogram curve flattens) was determined visually. Following the sampling theorems (described by *Rahman et al.* [2003], and references within), we define the ground critical sampling distance, for any given dataset, as a value smaller than or equal to the spatial distance on which the sill is reached.

3.4. Results

According to the analyses implemented, we present the results in three separate sections describing the two image-based approaches and the LiDAR-/field-based method.

3.4.1. Transect-based Analysis

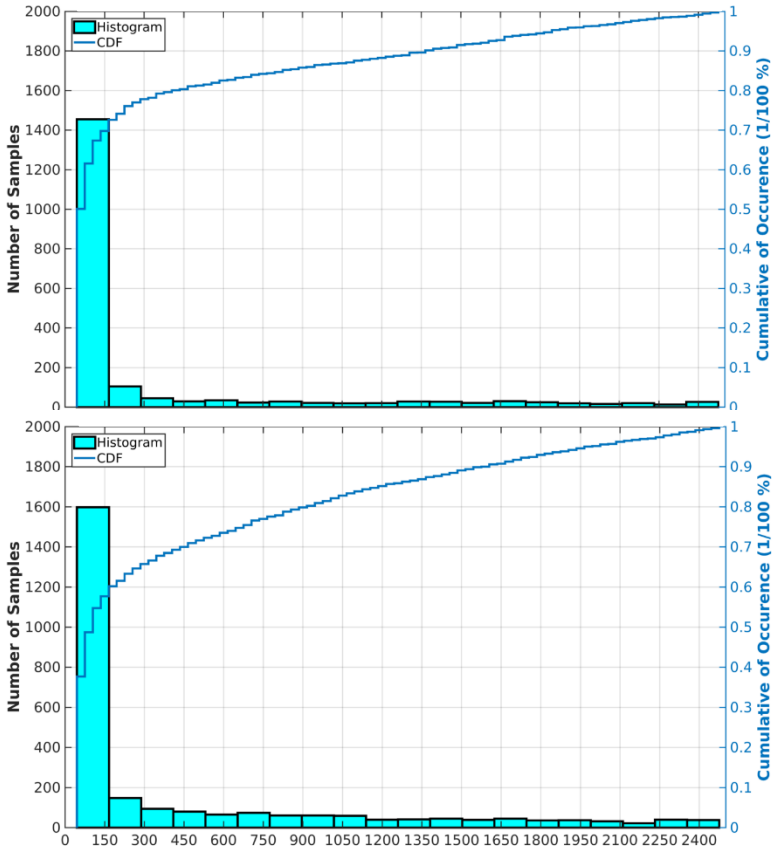

Figure 3.8. Histograms and cumulative distributions associated with the critical spatial distance generated through analyzing products like [Chla], $R_{rs}(655)$,$a_t(443)$, and $b_{bp}(561)$. The upper and lower panels show the results of the spatial analyses in Chesapeake Bay and Exmouth Gulf.

The histograms and the cumulative distribution of critical distances (CDs) are shown in Fig. 3.5. The statistics provided are average values for multiple products, including [Chla], $b_{bp}(560)$, and R_{rs} in the blue and red regions. The results for both sites clearly indicate that most of the spatial variability (~70th percentile) occurs within the range of < 150 m for Chesapeake Bay and < 450 m for the Exmouth Gulf. It is also worthwhile noting that there is only minimal spatial information gained for sampling sizes > 500 m for the Chesapeake Bay.

This conclusion, however, cannot be made for the Exmouth Gulf as the cumulative histogram steadily increases by increasing the sample size, i.e., the number of samples remains sizable even at distances as great as 2.4 km. The analysis performed here for these two distinct regions reveals striking differences between the more stringent spatial resolution requirements for turbid waters of estuarine systems and those of clearer waters of coastal regions.

3.4.2. Scene-wide Analysis

In order to provide insights on variations of critical distance for all the regions, all of the pixels processed (>10e^6) are combined and analyzed. The OLI coastal scenes include areas with [*Chla*] ranging from 0.05 to 80 mg m^{-3}. To isolate the analysis to coastal areas, in this section, we decided to examine the areas with [*Chla*] > 0.5 mg m^{-3}. Fig. 3.6 illustrates the histograms of CDs obtained from OLI-derived products. The x-axes are binned at multiples of 30 m to represent increments of OLI inherent pixel size, whereas y-axes are labeled at different scales to show the percent of the pixels within each bin (left y-axis) as well as the full range for the cumulative distribution (right y-axis).

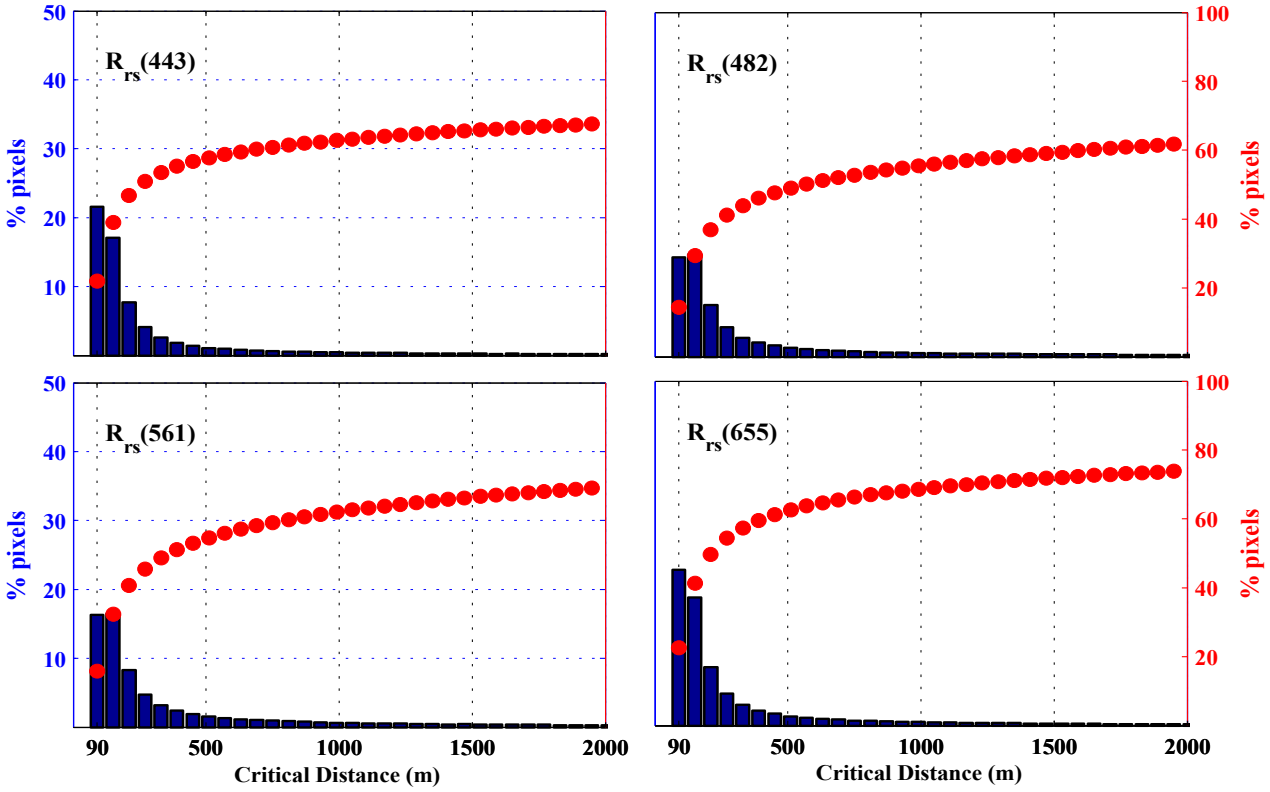

Figure 3.9. Average histogram and cumulative distributions derived from scene-wide analyses of Landsat products. It is revealed that most spatial variablity can be found in scales < 150m. There is, however, not much information beyond 500m.

A large portion of total OLI pixels (20-40 %) fall within the range of 90 to 120 m suggesting that, as expected, there is a large spatial variability in eutrophic/turbid waters (median [*Chla*] ~ 3.8 mg m^{-3}). This is not, however, always true as we found larger CDs associated with a large-scale river plumes or near-shore environments, which commonly represent spatially well-mixed, uniform water masses. The cumulative distributions indicate that for $R_{rs}(443)$ and $R_{rs}(655)$ more than 50% of the pixels fall below 150m. The CDs found for $R_{rs}(482)$ and $R_{rs}(561)$ were found to be at 330 m and 210 m, respectively. The remaining half of the OLI pixels are rather uniformly distributed from 500 to 2500 m. This indicates that the information content does not change by changing the sampling size.

3.4.3. LiDAR- and Field-based Data Analysis

The airborne and in situ data allow for an independent analysis of critical sampling distances. Fig. 3.7 illustrates the semivariograms for all the sample transects provided separately for oligotrophic and eutrophic coastal waters, regardless of the origin of the data (airborne or in situ) or type of optical parameter measured. While the mean critical distances were found to be ~1500 m and ~983 m for the two water types (open ocean vs. coastal ocean), the minimum distances are estimated to be ~ 950m and 171 m, respectively.

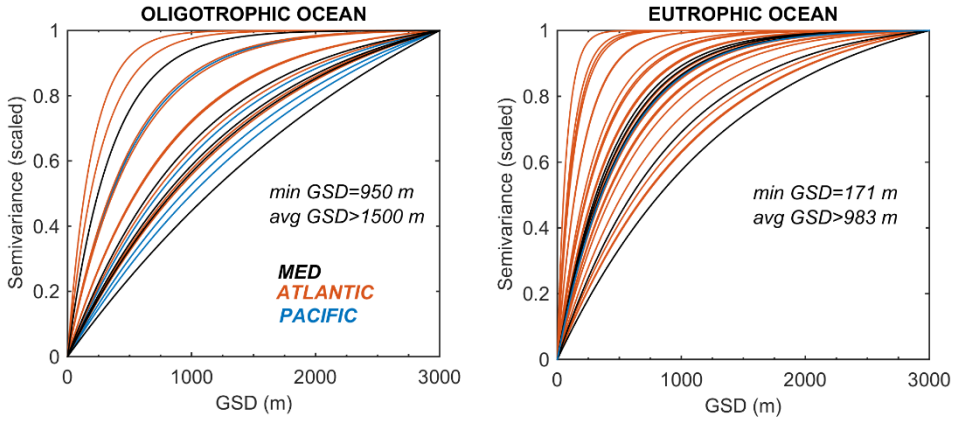

Figure 3.10. Semivariamce as a function of increasing sampling size, for open (oligotrophic) ocean on left panel and coastal, eutrophic ocean on right panel. Lines are color-coded based on the data origin.

3.5. Discussion

Overall, the results associated with analyzing LiDAR and in situ data were not consistent with results obtained from analyzing Landsat data products. While minimal CD encountered in airborne/in situ dataset were similar to the median value encountered with satellite imagery, the majority of the semi-variograms indicated with in situ analysis point to the larger average CS. Observed differences may be attributed to the limited availability of airborne and in situ data, and the fact that these data do not represent the diversity of optical regimes captured with Landsat imagery. The minority of the data, that originates from the highly complex waters (Hudson River Plume), show smaller CS than the rest of the dataset with the smallest CS of 171 m, encountered in the Hudson River Plume. On the other hand, the analyses of Landsat-derived R_{rs} may also skew toward smaller spatial distances. This is because even though the images were processed using median spatial filters, the noise does not fully get removed and residual noise may impact our analyses. That said, the noise impacts are more pronounced in the clearer waters and areas identified with high backscattering are less affected by noise in these products.

In general, the critical spatial distance varies for various coastal and ocean systems. What we presented in this document are the results of examining in-water spatial variability in various systems. The critical distance was found to vary between 150-200m in coastal turbid waters. According to the Nyquist sampling theorem to enable full reconstructions of natural features, the observation frequency must be at least twice the desired frequency. This means that satellite sensors should be designed with GSD of 75-150m to capture in-water spatial variabilities in coastal areas. Note that for the open sea/ocean waters, however, the semi-variograms presented here do account for the Nyquist sampling frequency. It should be emphasized that the GSDs proposed in this study assumes no adjacency effects from surrounding land or clouds. To increase the number of valid observations, the spatial-sampling size has to be even smaller.

Chapter 4

Project Science Analyses Supporting the Addition of a PACE OCI 1038 nm Band

Amir Ibrahim, Science Systems and Applications Inc, Lanham, Maryland[4]

Lachlan I. W. McKinna, Go2Q Pty Ltd, Buderim, Australia

Executive Summary

This work documents the Plankton, Aerosol, Cloud, ocean Ecosystem (PACE) project science and engineering team analyses for adding a new SWIR channel, 1038 nm, for the Ocean Color Instrument (OCI). The 1038 nm channel is to complement OCI's current SWIR suite of bands 940, 1250, 1378, 1615, 2130, and 2260 nm bands [*Cairns and Ibrahim*, 2018]. During Phase A of the mission, it was decided that an additional band at 1038 was desirable and could be accommodated, so the 1038 nm channel was made a baseline requirement of the OCI SWIR suite of bands. The 1038 nm channel provides the following benefits:

1. Improves ocean color atmospheric correction, thus reducing uncertainties in threshold and baseline science data products;
2. Allows the retrieval of the concentration of total suspended matter at very high concentrations, a highly desirable derived science product; and,
3. Offers significant risk reduction. in case the red spectrograph fails. This band (in combination with 1250, 1615, & 2260 nm) allows the retrieval of spectral water-leaving reflectances that meet threshold requirements. Without this band, in this scenario, threshold requirements on water-leaving reflectances cannot be met.

4.1. Introduction

For ocean color remote sensing, the sensor-observed top-of-atmosphere (TOA) radiance (signal) can be broadly treated as the combination of water-leaving and atmospheric radiances. Effective removal of the atmospheric contribution, known as atmospheric correction (AC), is crucial for accurately deriving spectral water-leaving radiances.

Traditionally, near-infrared channels (NIR; 700 – 1000 nm) are used for AC because the water-leaving radiance at these wavelengths is considered negligible [*Knaeps et al.*, 2012]. Specifically, NIR channels are used to quantify the radiance contribution due to aerosols, which is then subtracted from the TOA radiance.

However, for waters with moderate concentrations of scattering particles (e.g. phytoplankton or mineral sediments), the assumption of negligible water-leaving NIR signal is often invalid [*Bailey et al.*, 2010; *Gordon and Wang*, 1994; *Pahlevan et al.*, 2017]. To address this concern, short-wave infrared

[4] Cite as: Ibrahim, A., and L. I. W. McKinna (2018), Project Science Analyses Supporting the Addition of a PACE OCI 1038 nm Band, in *PACE Technical Report Series, Volume 7: Ocean Color Instrument (OCI) Concept Design Studies (NASA/TM-2018 – 2018-219027/ Vol. 7),* edited by I. Cetinić, C. R. McClain and P. J. Werdell, NASA Goddard Space Flight Space Center Greenbelt, MD.

(SWIR) channels have been used in place of NIR channels during AC [*Wang and Shi*, 2007; *Wang et al.*, 2009]. At wavelengths above ~925 nm, absorption of light by water molecules is substantial, as shown in Fig. 4.1. Thus, SWIR channels can be advantageous for AC as the oceanic water-leaving radiance signal is truly negligible in that spectral region [*Ahmad et al.*, 2010; *Gordon and Wang*, 1994]. While successful AC been previously accomplished using bands >1200 nm from MODIS, extrapolating aerosol information from this (longer) spectral region to the (shorter) visible region can introduce AC errors [*Wang and Shi*, 2007; *Wang et al.*, 2009; *Werdell et al.*, 2010]. Therefore, to enhance ocean color AC, a conveniently situated, shorter SWIR channel with appropriate bandwidth and signal-to-noise (SNR) is desirable. For this purpose, we seek a spectral region where atmospheric transmittance is maximized (atmospheric window). The desired SWIR channel should have the following characteristics:

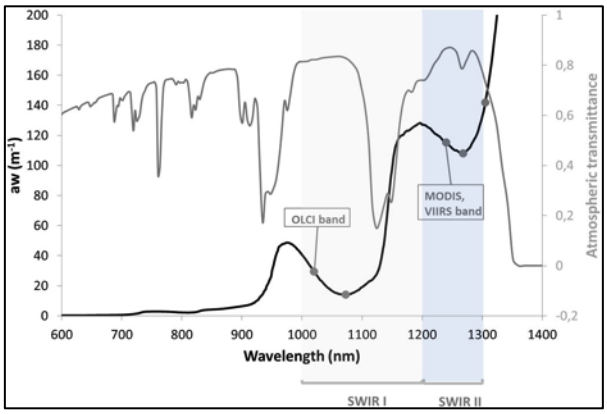

Figure 4.1. Atmospheric transmittance showing atmospheric windows in the 600 – 1400 nm range (grey line). The absorption coefficient of seawater is also plotted (solid black line).Modified after Knaeps et al.[2012]

- Have broad spectral bandwidth to maximize SNR;
- Be sensitive to aerosol optical properties; and,
- Have negligible ocean radiance.

A channel centered on 1038 nm satisfies these characteristics as it is ideally centered on a wide atmospheric transmittance window (see Fig. 4.2). Additionally, a 1038 nm channel has:

- Negligible water-leaving radiance in moderately turbid waters (total suspended matter (TSM) < 35 mg L^{-1}); and,
- More sensitivity to the aerosol optical properties relative to longer wavelengths in the SWIR range.

As an added benefit, a 1038 nm channel will be sensitive to extremely turbid waters where the TSM concentrations exceeds 35 mg L^{-1}. Typically, the water-leaving signal due to TSM is absorbed completely by water molecules. However, a local minimum in water absorption occurs in the vicinity of 1038 nm (as shown in Fig. 4.1) meaning that a strong radiance signal due extreme TSM scattering can be discerned using this channel. Ultimately, the water-leaving radiance at 1038 nm is directly proportional to extreme TSM and, as such, 1038 nm can be used to derive concentrations of TSM [*Knaeps et al.*, 2012]. Note that longer SWIR bands will be used for AC in these extremely turbid waters. This additional information provided by the 1038 nm band will facilitate better turbidity detection and, therefore, further improve the AC process for optically complex coastal waters. A list of ocean color applications is shown below:

- Potential to explore new methods for quantifying extreme turbidity;
- Potential to explore new methods for observing floating algae/vegetation; and,
- Improved flagging and/or characterization of extremely turbid water.

4.2. AC Band Characteristics

Ocean color AC exploits several "atmospheric windows" where the almost complete atmospheric transmittance occurs and water-leaving radiances are considered near-zero. Atmospheric windows are thus treated as sensitive only to aerosol optical properties. Four windows are centered at 750, 870, 1038, and 1240 nm, as shown in Fig. 4.2. For aerosol characterization in AC, at least two windows are needed [*Gordon and Wang*, 1994]. Contemporary AC methods use the ratio of two window channels to determine the aerosol optical properties. This information is then extrapolated into the shortwave channels (400 – 700 nm). NASA's heritage AC approach typically uses windows 1 and 2 (750 and 870 nm). Ocean color AC is sensitive to the spacing between window channels, which can impact the determination of the aerosol properties [*Gordon and Wang*, 1994]. For example, the spectral ratio between close together window channels 1 (750 nm) and 2 (870 nm) is more sensitive to measurement uncertainties [*Pahlevan et al.*, 2017]. However, window channels spaced further apart, for example window 1 (750 nm) and 3 (1038 nm), are less sensitive to measurement uncertainties for AC assuming, similar SNR on both bands [*Pahlevan et al.*, 2017].

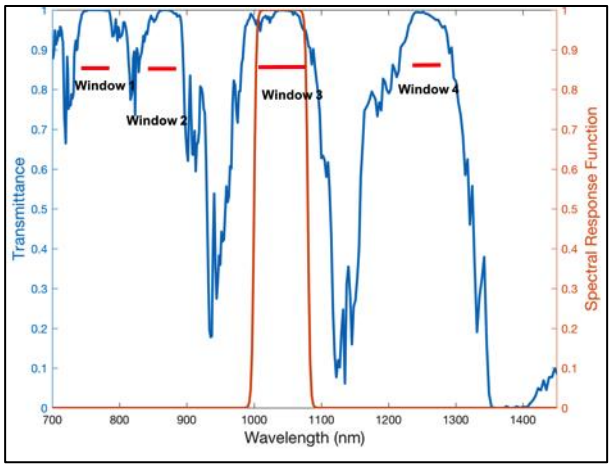

Figure 4.2. The atmospheric gases transmittance from 700 to 1500 nm showing 4 window regions for the AC. The figure also shows the optimal spectral response function of the 1038nm channel for AC.

4.3. AC Case Study

To demonstrate the feasibility of the AC using the 1038 nm band, we present results of a case study. Spectral normalized water-leaving radiances (L_{wn}) derived from NASA's Airborne Visible/Infrared Imaging Spectrometer (AVIRIS), were compared with in-situ AERONET-OC "truth" measurements collected at the WaveCIS (Coastal Studies Instrument) site located in the Gulf of Mexico. AVIRIS data was processed using a hyperspectral version of NASA's standard ocean color AC [*Ahmad et al.*, 2010; *Bailey et al.*, 2010; *Gordon and Wang*, 1994; *Ibrahim et al.*, 2018].

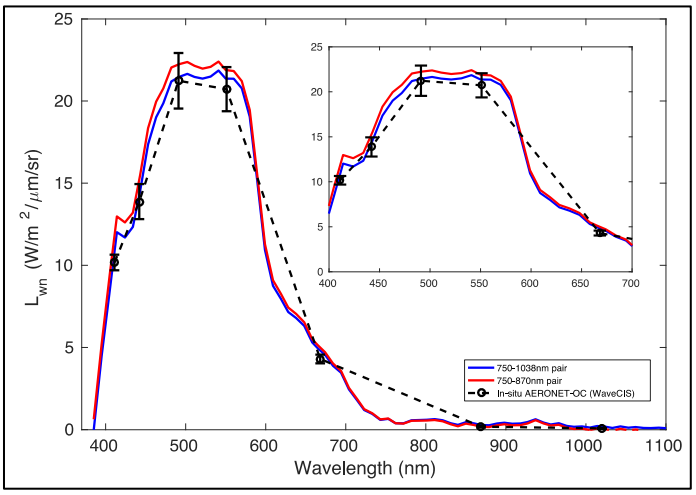

Figure 4.3. AVIRIS and AERONET-OC in-situ match-ups of the water-leaving radiance, L_{wn}, using the 750-870nm pair and the 750-1038nm pair for AC.

Two AC band configurations were performed: AC1 and AC2. AC1 used windows 1 and 2 (750 and 870 nm), and AC2 used windows 1 and 3 (750 and 1038 nm). In Fig. 4.3, AC2 showed the retrieval of L_{wn} in the shortwave spectral region (370 – 1100 nm) with an inset figure of spectral range (400 – 700 nm) relative to AC1 and in-situ AERONET-OC measurements. Fig. 4.3 indicates that the AC is feasible using the 1038 nm, and both retrievals of AC1 and AC2 are within the in-situ measurements uncertainty. We note

that accurate determination of L_{wn} in the shortwave region is critical for reducing uncertainties in derived biogeochemical data products such as chlorophyll pigment concentration. A detailed description of the uncertainity analysis of the AC is discussed in section V.

NASA's standard ocean color AC typically uses NIR channels centered on/near windows 1 and 2 (750 and 870 nm). This brief study demonstrates that by using the 750 and 1038 nm channel pair the AC is feasible.

4.3.1. Current SWIR Approaches: OLCI

The Ocean and Land Color Instrument (OLCI) onboard ESA's Sentinel-3 mission has a 1020 nm channel. An example OLCI image captured over Belgian/Dutch coastline is shown in Fig. 4.4. A true-color image shows regions of highly turbid water parallel to the coast. While the corresponding false-color image at 1020 nm channel shows variability in the TOA radiance at 1020 nm due to the variability in TSM.

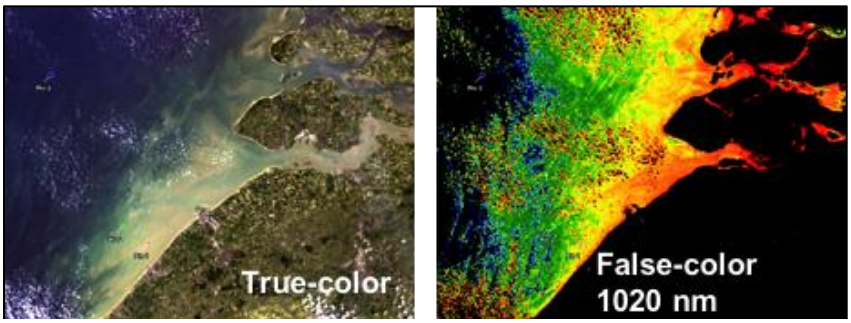

Figure 4.4. True-color image and false-color image at 1020nm from OLCI's TOA measurements over coastal regions.

The OLCI 1020 nm channel has shown promise for both AC and ocean color applications [*Knaeps et al.*, 2015; *Ruddick and Vanhellemont*, 2015]. For example, [*Knaeps et al.*, 2015] demonstrated the ability to detect and estimate TSM concentration under extremely turbid conditions (> 35 mg L^{-1}). While Ruddick et al. [*Ruddick and Vanhellemont*, 2015] used radiative transfer simulations to demonstrate the potential benefit of the 1020 nm channel for atmospheric correction over moderately turbid water.

4.3.2. Risk Mitigation for the OCI

An uncertainty analysis has been conducted using the Monte Carlo (MC) approach, where the TOA radiances were perpetuated within the noise uncertainty of the expected OCI measurement noise [*Franz and Karaköylü*, 2016]. The signal-to-noise (SNR) ratio on the SWIR channels were adjusted several times to better understand the engineering constraints of adding a new channel in the SWIR suite. Due to limited number of fiber optics connection (an inherent engineering design limitation) on the SWIR spectrograph, the addition of 1038 nm band was only possible with a decreased SNR performance on the other SWIR channels. By collaborating with the OCI engineering team, we were able to reach a set of band configurations (i.e., band centers, bandwidths, and SNR) that allows for optimal performance of the instrument. The analyses were mainly conducted using Vector Radiative Transfer (VRT) simulations to estimate the typical TOA radiance (of which a typical SNR is calculated for the 1038 nm band), band centers, and band widths as shown in Fig. 4.5.

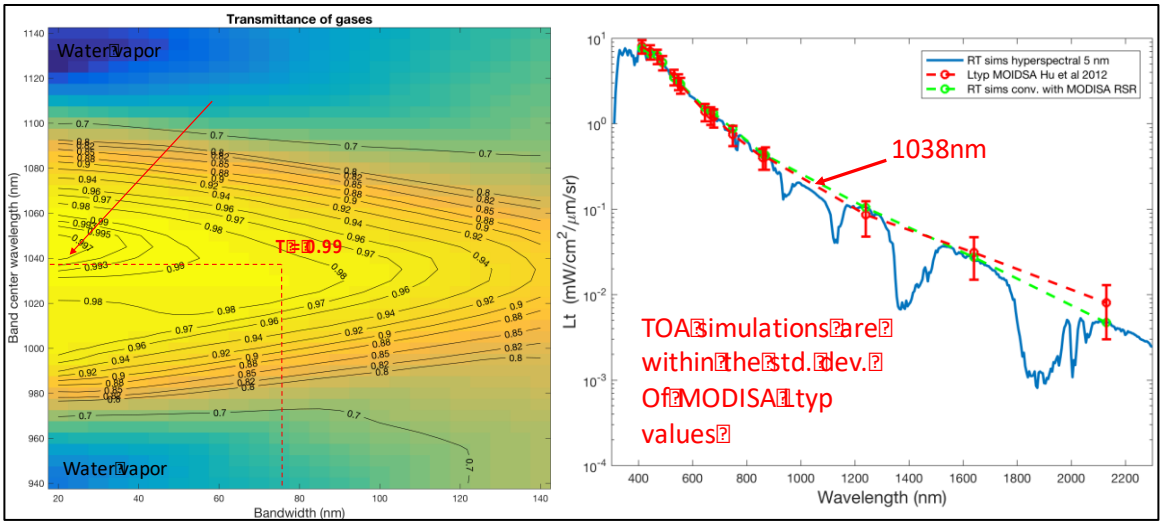

Figure 4.5. The left-hand side figure shows the gas transmittance for various 1038 nm band configurations. The right-hand side figure shows the typical TOA radiance calculated using VRT simulations.

The 1038 nm band center and width was selected to maximize the atmospheric transmittance and avoid major absorption features by the water vapor at wavelengths < 1000 nm and > 1080 nm. The typical hyperspectral TOA radiances, Ltyp, were calculated using VRT simulations that included absorbing gases for a set of geometric and atmospheric conditions as detailed in *Hu et al.* [2012] where the simulated TOA radiance was similar within the standard deviation of typical MODIS-Aqua observations. The Ltyp at 1038 nm band is estimated to be 2 mW cm^{-2} μm^{-1} sr^{-1}.

With the best estimate band configurations, a MC analysis was conducted for a wide range of optical properties of aerosols (i.e., varying aerosol optical depth and models). A modified version of the heritage (operational) AC algorithm was then used to derive the ocean remote sensing reflectance ($R_{rs}(\lambda)$ or $\rho_w(\lambda)$) for 1000 iterations. The modification allows for a multi-band atmospheric correction method where a combination of the NIR and SWIR bands can be used. The multi-band AC minimizes a cost function as follows:

$$\chi^2(model) = \sqrt{\frac{\sum_{\lambda=b0}^{bn}(\rho_a^{obs}(\lambda) - \rho_a^{mdl}(\lambda))^2}{nbands}}, \qquad \text{(Eq 4.1)}$$

where the $\rho_a^{obs}(\lambda)$ is the observed TOA radiance after correcting for surface Rayleigh scattering, $\rho_a^{mdl}(\lambda)$ is the aerosol model reflectance at TOA, and $nbands$ is the number of bands. The algorithm computes the χ^2 for every pre-computed aerosol model, where the final aerosol reflectance, necessary for the AC, is weighted by the χ^2 values.

We tested the AC process for 4 scenarios and optimal band configurations (shown in Table 4.1) with and without the 1038 nm band. The analysis tested the following scenarios:

Scenario 1. AC with NIR&SWIR with 1038 nm (i.e., 750, 870, 1038, 1250, 1615, and 2130 nm).

Scenario 2. AC with NIR&SWIR without 1038 nm (i.e., 750, 870, 1250, 1615, and 2130 nm).

Scenario 3. AC with SWIR only without 1038 nm (i.e., 1250, 1615, and 2130 nm).

Scenario 4. AC with SWIR only with 1038 nm (i.e., 1038, 1250, 1615, and 2130 nm).

Table 4.1. SNR configuration (0% margins) for the MC AC analysis for 4 chosen scenarios.

	SNR (λ)					
	750 nm	870 nm	1038 nm	1250 nm	1615 nm	2130 nm
Scenario 1	600	600	303	230	157	62
Scenario 2	600	600		256	176	62
Scenario 3				256	176	62
Scenario 4			303	230	157	62

Scenarios 1 and 2 test the potential of adding the 1038 nm channel for the AC in the case of normally operating OCI NIR and SWIR channels according to the threshold requirements of the instrument. Scenarios 3 and 4 test the impact of the 1038 nm channel on the AC in the case of a failing red spectrograph (NIR) channels. Figure 4.6 shows the uncertainty in the water reflectance, ρ_w, for the aforementioned scenarios using the modified AC algorithm to accommodate the multi-band correction schemes.

The threshold AC model error allocation of the ρ_w retrieval is 0.5×10^{-3} throughout the visible spectrum (400 – 700 nm). In scenarios 1 and 2, the retrieval accuracy well exceeds the requirements, i.e., the uncertainty is well below the requirement. The addition of the 1038 nm band does not provide a significant gain in the case of normally operating NIR and SWIR bands. However, a failure in the NIR bands and without having the 1038 nm band (scenario 3), the uncertainty in the retrieval will not meet the requirements. With a failure of the two NIR bands, utilizing the 1038 nm band allows the AC to meet the requirements (scenario 4). This is a significant advantage to the mission since it allows for a risk reduction to the OCI instrument, e.g. loss of the NIR focal plane.

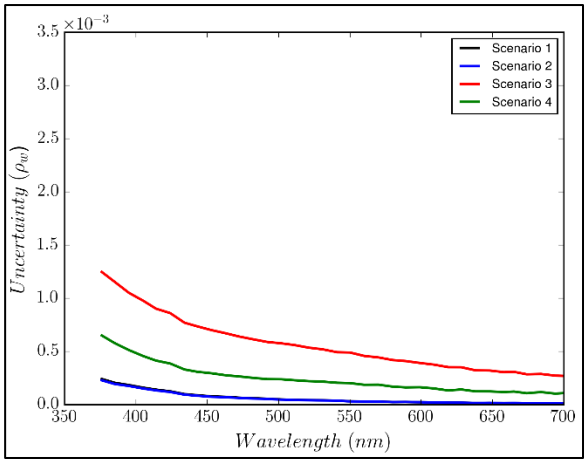

Figure 4.6. The retrieval uncertainty of the water reflectance, ρ_w, using the multi-band AC for the 4 cases (note that the line depicting scenario 1 is hidden behind blue line depicting scenario 2).

4.4. Conclusions

The analysis provided here defined the benefits and requirements for the 1038 nm band. The 1038n m band allows for risk mitigation of the OCI instrument operations in the case of red spectrograph failure, while it also provides a science application in coastal waters. The wide band (75 nm) improved the signal-to-noise at the detector level, in which case the threshold requirements of the AC can be met.

Chapter 5

Analysis of PACE OCI SWIR Bands

Brian Cairns, NASA Goddard Institute for Space Studies, New York, New York[5]

Amir Ibrahim, Science Systems and Applications Inc, Lanham, Maryland

Executive Summary

The Phytoplankton, Aerosol, Cloud, ocean Ecosystem (PACE) Ocean Color Instrument (OCI) is required to have a set of shortwave infrared (SWIR) bands. The exact spectral locations of these bands and their widths is determined by both heritage from previous and ongoing missions and the need to provide the required scientific performance while also allowing the required signal-to-noise ratios to be achieved. Spectral transmission calculations based on the HITRAN database [Rothman et al., 2013] together with a model for the water vapor continuum have been used to assess band performance in terms of the effects on them of water vapor and well mixed gases. The spectral band model and a simplified transmission model that is used to summarize spectral band performance is presented here together with results. The results have been used to specify the spectral band centers, widths, and filter shapes given in the conclusions to this document.

5.1. Introduction

OCI will have spectrometers to make measurements in the ultra-violet, visible and near infrared spectral domain, but in the SWIR spectral domain, the measurements will be made in discrete spectral bands on or near 940, 1240, 1370, 1640, 2130, and 2250 per PACE mission level-1 requirements. It is therefore necessary to specify the spectral locations and widths of those bands. In Fig. 5.1, the effect of absorption by gases in the atmosphere is shown to demonstrate why care must be taken in the selection of spectral band parameters.

While such a figure has interesting information about the spectral locations of different gaseous absorption features, in the selection of spectral band parameters some simplified performance metrics are required that allow for an objective assessment of what the best parameters are. In the next section the analysis methods that are used in providing that objective assessment are introduced.

[5] Cite as: Cairns, B., and A. Ibrahim (2018), Analysis of PACE OCI SWIR Bands, in *PACE Technical Report Series, Volume 7: Ocean Color Instrument (OCI) Concept Design Studies (NASA/TM-2018 – 2018-219027/ Vol. 7)*, edited by I. Cetinić, C. R. McClain and P. J. Werdell, NASA Goddard Space Flight Space Center Greenbelt, MD.

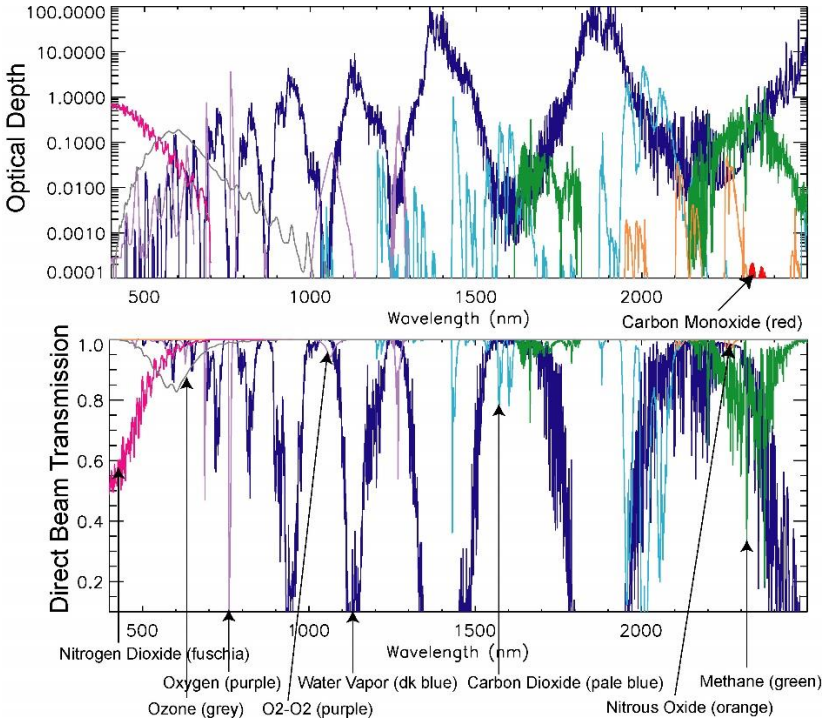

Figure. 5.1. Spectral optical depths and direct solar beam transmission (for an airmass of three) as a result of absorption by different gases. Concentrations are for a US standard atmosphere except for nitrogen dioxide (fuchsia) which has been increased by a factor of 10 for display purposes.

5.2. Analysis methods

5.2.1. Spectral Band Shape

The OCI SWIR bands will be defined by discrete filters and we therefore need to have a model for the spectral response of the filter. The model needs to allow for the center of the band, the width of the band, and the shape of the band (how steeply it cuts off outside the central transmissive domain) to be varied and to have a functional form that is a reasonable representation of actual filter spectral responses. A filter response that is used for this purpose by systems engineers in industry (e.g. Raytheon SBRS, Ball, Lockheed Martin) is a modified Lorentzian filter with the form

$$r(\lambda) = \frac{1}{1+\left|\frac{2(\lambda-\lambda_0)}{FWHM}\right|^{\kappa}} \qquad \text{(Eq. 5.1)}$$

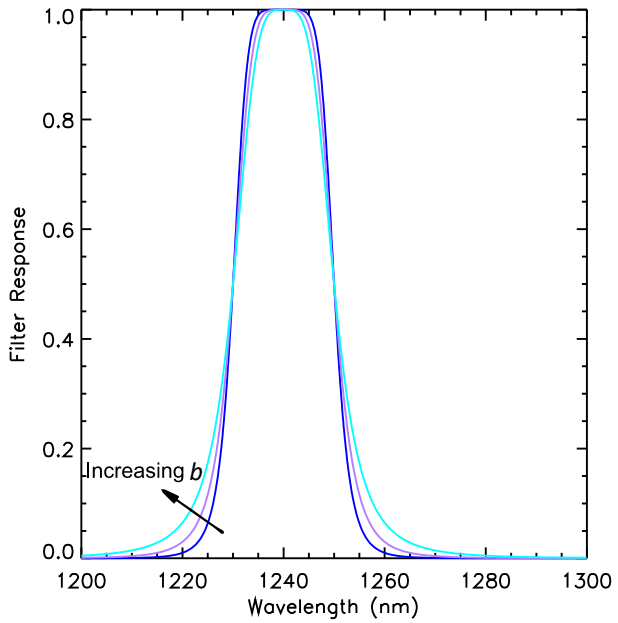

Figure 5.2. Shape of filter response for values of b of 2, 2.5 and 3.3 shown in blue, mauve and turquoise respectively with band center of 1240 nm and FWHM of 20 nm.

where FWHM is the full width at half maximum, λ_0 is the band center wavelength and κ is an exponent that allows the band shape to be changed. Generally a filter specification of shape will use the Full Width at 1% (FW1P), rather than the exponent κ. Moreover the FW1P is usually specified as being a multiple of the FWHM Eq.(2). The exponent κ and the factor b multiplying the FWHM are related by the formula $\kappa=\ln(99)/\ln(b)$. For filter radiometers such as MODIS and VIIRS the range of b is between 1.5 and 3.3, because filter designs with cutoffs of this type are robust and readily manufactured. In the set of tables that are appendices to this document, values of b of 2, 2.5 and 3.3 are used to evaluate the effect of band pass shape on filter performance. The small variation in filter shape corresponding to the different exponents is shown in Fig. 5.2.

$$FW1P = b \times FWHM. \qquad \text{(Eq. 5.2)}$$

For spectral bands that are nominally in atmospheric windows where there is little gaseous absorption, such as 1240, 1640, 2130 and 2250 nm band centers, it is desirable to select band location, width and shape to minimize the effects of gaseous absorption. There are two different types of absorption that are of concern for SWIR bands. One is well mixed greenhouse gases (WMGHG), e.g., CO_2, CH_4, O_2, CO, N_2O and the other is water vapor, a greenhouse gas that is not well mixed.

5.2.2. Well Mixed Greenhouse Gases

For well mixed greenhouse gases (for bands of the width of interest for OCI) the amount and profile of gaseous absorption is well known and the total column variations in these gases are dominated by variations in concentrations in the free troposphere and stratosphere that have long mixing length scales. Absorption by these gases can therefore be accurately corrected using global mean values, or, if better accuracy is required, climatologies from chemical transport models.

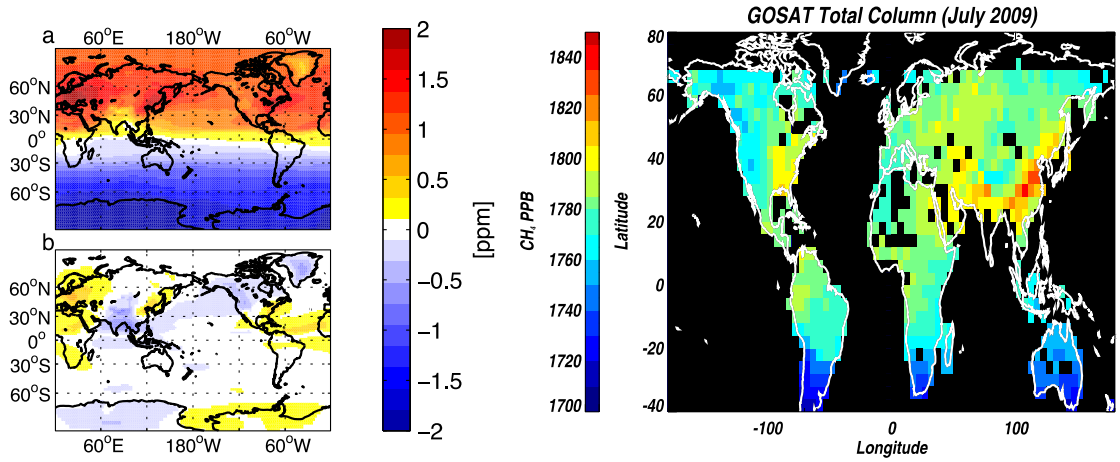

Figure 5.3. Left panels is modified Fig.3 of Keppel-Aleks et al. [2011]. It shows (a) August column mean mixing ratio of CO_2 fossil with global mean removed. Because the bulk of emissions occurs in the north, mixing ratio of CO_2 fossil is 2 ppm higher in the Northern Hemisphere than in the Southern Hemisphere. (b) Deviation of August column mean mixing ratio of CO_2 fossil from the zonal mean at each latitude. Contrasts between emission regions (e.g., eastern United States, Europe, and China) and upwind regions are less than 1 ppm. Right panel is Fig. 2 of Worden et al. [2015]. It shows total column methane (CH_4) retrieved by Greenhouse gases Observing SATellite – Thermal And Near-infrared for carbon Observation mission.

Well mixed greenhouse gas contamination is evaluated by calculating two pass transmission for a total air-mass of 3 (e.g. vertical view and 60° solar zenith) for a standard atmosphere containing no water vapor. This is tabulated in a companion spreadsheet as $TnoH_2O$. As this transmission is easy to correct it is primarily of concern as a signal loss issue. This being the case we regard transmission losses as minimal (<6%) or acceptable (< 13%, light green) in evaluating whether a particular set of filter parameters provide adequate performance with regard to well mixed greenhouse gases. Obviously, if a band can be made 20% wider at the expense of a 10% transmission loss that might be regarded as an acceptable trade since the SNR would be increased. Given the expected transmission in the OCI SWIR bands and the indicated variability of these two well mixed greenhouse gases (CO_2 and CH_4), which are the primary WMGHG absorbers for the OCI SWIR bands, we find that using global mean values of the concentrations of these two gases to calculate absorption would lead to maximum errors of less than 0.1% and 0.5% respectively.

5.2.3. Water Vapor Absorption

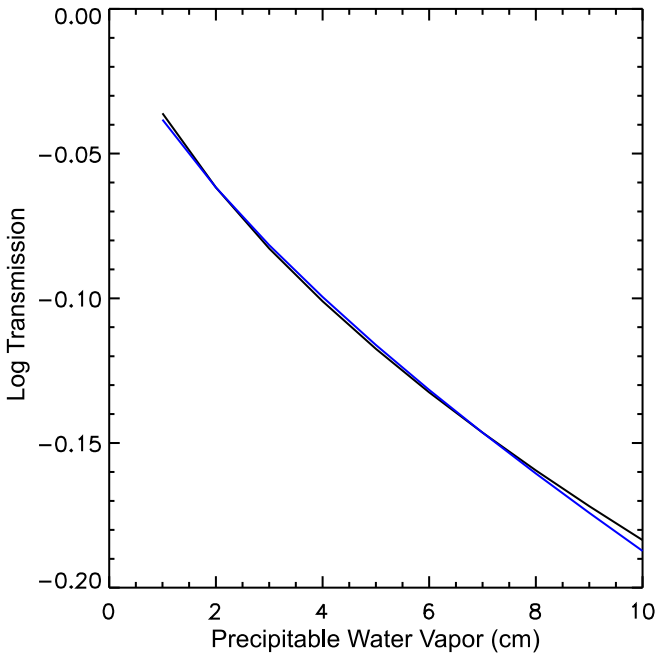

Figure 5.4. Correlated k-distribution (derived from HITRAN 2008) calculation of transmission (black) as a function of column water vapor and model fit (blue) for a spectral band with λ_0=2130 nm, $\Delta\lambda$=50 nm and b=2.0.

Water vapor absorption is more of a problem to atmospherically correct in the OCI SWIR bands than WMGHG since you do not a priori know how much is there, nor what its vertical profile is. Estimates for water vapor amount from 940 nm and 820 nm can be made, but the accuracy with which the other SWIR bands can be corrected is affected by and depends on the different amounts of scattering at the shorter wavelengths compared to the longer wavelengths that need to be corrected. Thus, keeping water vapor contamination low is highly desirable and also minimizes the required accuracy on the water vapor estimate. It is possible to model the two-pass transmission for water vapor using an equation of the form

$$transmission(w) = e^{-\alpha(mw)^{\beta}}. \qquad \text{(Eq. 5.3)}$$

where *w* is the total column water vapor amount in precipitable cm, *m* is the air-mass and α and β are calculated based on a fit of this transmission function to line by line calculations of transmission over a range of 1-10 precipitable cm of water vapor. In essence, α is a measure of the strength of the water vapor absorption and β is a measure of how complicated it is to correct for that absorption. If β is unity, then this model for transmission reduces to Beer's law and the effects of absorption are captured by the absorption optical depth. The greater the deviation from unity the more sophisticated the model of correction needs to be since two or more absorption coefficients are then required to capture the effects of absorption.

Since the strength of water vapor absorption is represented by α ideally you would keep its value as low as possible. The actual value will depend on the particular window under evaluation since extension of water vapor absorption into the windows increases at longer wavelengths meaning that there is necessarily more water vapor contamination in the longest wavelength bands. In Table 5.1, the values highlighted as good (dark green) and acceptable (light green) for each band in the companion spreadsheet are given. The rationale for these values is that in the 2200 nm window the total correction for water

vapor is ~5-10% and in the other windows it is ~1-2%. Complexity of correction affects accuracy with which you can reasonably expect to correct the effects of water vapor so ideally β is greater than 0.9 so it can be corrected using a two-coefficient model for absorption, or at least greater than 0.8 so that a two or three absorption coefficient model is sufficient.

Table 5.1. Boundaries used in companion spreadsheets to identify spectral band performance that is good (dark green) or acceptable (light green) for window bands.

	α		**β**		**TnoH2O**	
Wavelength	Good	Acceptable	Good	Acceptable	Good	Acceptable
2250	0.005	0.01	0.9	0.8	0.94	0.87
2130	0.005	0.01	0.9	0.8	0.94	0.87
1640	0.001	0.002	0.9	0.8	0.94	0.87
1240	0.002	0.005	0.9	0.8	0.94	0.87

5.2.4. Absorption by Clouds

In addition to ensuring that window bands at 1240, 1640, 2130 and 2250 are only minimally contaminated by gaseous absorption, it is important that they are spectrally located such that they can be used to estimate cloud particle sizes. The absorption cross-section, C_{abs}, has the following proportional dependence for weakly absorbing particles (as is the case for liquid and solid water in the solar spectrum) viz.,

$$C_{abs} \sim \frac{V n_i}{\lambda} \qquad \text{(Eq. 5.4)}$$

where V is the volume, n_i is the imaginary index and λ is the wavelength, while the extinction cross-section, C_{ext} has the dependence

$$C_{ext} \sim A \qquad \text{(Eq. 5.5)}$$

where A is the average projected cross-sectional area. The single-scattering co-albedo (1 – single scattering albedo, ϖ) for cloud particles, which is proportional to the fraction of light absorbed in each collision of light with a particle, is therefore proportional to

$$1 - \varpi = \frac{C_{abs}}{C_{ext}} \sim \frac{r_{eff} n_i}{\lambda} \qquad \text{(Eq. 5.6)}$$

where r_{eff} is the effective particle size (ratio of the mean of r^3 to the mean of r^2). The appropriate quantity to evaluate whether spectral bands will perform similarly to existing MODIS and VIIRS bands in terms of particle size retrievals is, therefore, the ratio of imaginary index to wavelength and these values are tabulated in the companion spreadsheets.

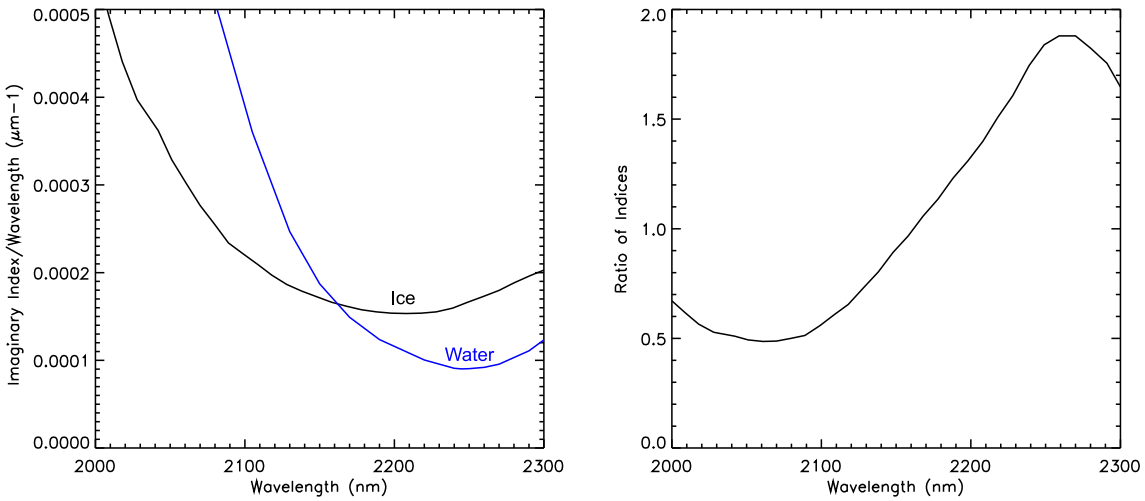

Figure 5.5. Spectral variation of the ratio of imaginary index to wavelength (left) and the ratio of water to ice imaginary index (right).

In Fig. 5.5, the variation of this quantity is shown as a function of wavelength for ice and water. The significant difference in ice and water absorption between 2130 and 2250 nm is the reason that OCI is expected to provide better phase discrimination for ice and water clouds.

5.2.5. Spectral Bands Located in Water Vapor Absorption Bands

The purpose of the 940 nm band is to estimate water vapor column amount and it therefore needs to be located where it is sensitive to the presence of water vapor, but not so sensitive that it is only of use at very low water vapor amounts. A total column precipitable amount of water vapor of three centimeters is common in the summer hemispheres and is representative of much of the sub-tropics. The table for the 940 nm band is therefore the two-pass transmission for a total air mass of 3 and a precipitable amount of water vapor of 3 cm. Transmission values of 0.2-0.3 are highlighted in green since the reduction in transmission caused by the water vapor is substantial, but there is still enough light left to detect a signal if there are sufficient aerosols, or Sun glint present to provide scattered light. The middle table for α has values greater than 0.3 highlighted indicating sufficient water vapor absorption to provide a signal. The bottom table for β has values less than 0.6 highlighted such that the rate of decrease in log transmission with water vapor amount is less than linear, providing some skill in estimating water vapor amount at higher water vapor amounts.

The purpose of the 1370 nm band is to detect cirrus clouds and it therefore needs to be well isolated from the lower atmosphere. The top table for the spreadsheets associated with this band are therefore calculated for a column of water vapor of 1 cm and air mass of 3, being representative of a moderately dry atmosphere. Transmission values of less than 0.001 (dark green) demonstrate extremely good suppression of signals from the lower atmosphere and those less than 0.002 (light green) would still allow a cirrus cloud to be detected in the presence of typical low level clouds. Values of α greater than 3.4 are highlighted (dark green) since they are indicative of strong absorption as are values greater than 3.0 (light green), but the transmission is probably a better measure of the quality of a given set of band parameters to achieve the purpose of cirrus detection. The values of β are not a useful measure of performance for this band.

5.3. Results

The results of the calculations described above are given in a companion tables (see 5.5 - Appendix) where the performance of the different spectral bands is captured for varying center wavelengths, band widths and passband shapes.

5.4. Conclusions

In terms of the specification of filter parameters the calculations described above and the results from the companion spreadsheet lead to the following parameters in Table 5.2 being selected for the OCI spectral bands.

*Table 5.2. Recommended spectral band parameters for SWIR OCI bands based on analysis of atmospheric and cloud particle absorption; * FW1P = b x FWHM*

Center (nm)	*FWHM (nm)*	*b**
2260	75	2
2130	50	2.1
1615	75	2
1378	15	2
1250	30	2
940	45	2

5.5. Appendix – tables with transmission, α and β values for the targeted SWIR bands

Table 5.3. Transmission (TnoH2O) values for 2000-2300 nm, with b of 2.0 comparison run.

tnoh2o:	40	45	50	55	60	65	70	75	80	85	90
2000	0.4801843	0.4949844	0.5081876	0.5193794	0.5284413	0.5359923	0.541382	0.5462195	0.5503851	0.5540445	0.557257
2005	0.4214955	0.4593367	0.4906682	0.514937	0.5332817	0.5463247	0.554503	0.5591342	0.5620763	0.56323	0.5636894
2010	0.3861231	0.4367931	0.4774089	0.5084245	0.5315572	0.5477804	0.5575015	0.5633264	0.5660037	0.5664693	0.5665115
2015	0.3830298	0.4288157	0.4673918	0.4979852	0.5209144	0.5376047	0.5489344	0.5557188	0.5602117	0.5626684	0.56415
2020	0.4214163	0.4437713	0.4662273	0.4867067	0.5039114	0.5181898	0.5295447	0.5387393	0.5462256	0.5526623	0.5572806
2025	0.4850709	0.4807054	0.4798817	0.4830379	0.4895931	0.4986753	0.5092592	0.5195756	0.5301186	0.5393382	0.5483018
2030	0.5439748	0.5202474	0.5029862	0.4927067	0.4892568	0.4913566	0.4979395	0.507096	0.5180576	0.5294167	0.5409112
2035	0.5857319	0.5541252	0.5311677	0.5149526	0.5056297	0.5016848	0.5029007	0.5082783	0.5169653	0.5282131	0.5395144
2040	0.6135084	0.5858194	0.5632882	0.5453032	0.5334088	0.5264019	0.5239259	0.5252848	0.5306216	0.5380631	0.5477293
2045	0.6246117	0.6075335	0.591682	0.578012	0.567538	0.5606059	0.5564041	0.5551596	0.5567777	0.5605052	0.5666268
2050	0.6137812	0.6133413	0.6110319	0.6074104	0.6026059	0.5983828	0.5947932	0.5922206	0.5914851	0.592095	0.5943818
2055	0.5959149	0.6111492	0.622359	0.6291885	0.632268	0.6328559	0.6320261	0.630244	0.6286595	0.6277862	0.6274431
2060	0.5862536	0.6103741	0.6295145	0.6432209	0.653377	0.6594913	0.6628023	0.6640975	0.6638615	0.6627815	0.6617267
2065	0.5916885	0.6157622	0.6369828	0.6541112	0.6685084	0.6787872	0.6866084	0.6911727	0.6937176	0.6939421	0.6935033
2070	0.6192436	0.6351418	0.6523085	0.6683645	0.683035	0.694939	0.7047939	0.7119509	0.716588	0.7196317	0.7204142
2075	0.6689829	0.6745712	0.682662	0.6924551	0.7025691	0.7124667	0.721759	0.7292962	0.7352558	0.7395007	0.7421691
2080	0.7256472	0.7251531	0.7256396	0.7275793	0.7308884	0.7357165	0.7416577	0.747187	0.7526014	0.7568127	0.7603378
2085	0.7833164	0.7768979	0.7722098	0.7685469	0.7666346	0.7659527	0.7669397	0.7690623	0.7717357	0.7748842	0.7774729
2090	0.8385059	0.8278068	0.8187378	0.8110218	0.8053725	0.8008251	0.7978902	0.7958437	0.7951843	0.7953632	0.7960143
2095	0.8835596	0.8730494	0.8625928	0.8527583	0.8442638	0.8368957	0.8305513	0.8257985	0.8219114	0.8190433	0.817203
2100	0.9156852	0.9079233	0.8991436	0.8898864	0.8805557	0.8718336	0.8637354	0.8565389	0.8503134	0.8450174	0.8406569
2105	0.9394004	0.9333324	0.9266435	0.9193001	0.9110239	0.9026551	0.8939323	0.8858402	0.8782035	0.8713003	0.8650214
2110	0.957745	0.9528115	0.9472977	0.9412769	0.9345356	0.9272831	0.9194581	0.9115431	0.9035696	0.8958902	0.8887458
2115	0.9705215	0.9670463	0.9627237	0.9577045	0.9521273	0.9459994	0.9394743	0.9323595	0.9250633	0.9176801	0.9103683
2120	0.9785413	0.9762751	0.973187	0.9692916	0.964842	0.9598031	0.9542323	0.9483616	0.9420626	0.9355768	0.9288243
2125	0.9836202	0.9817958	0.9795102	0.9766481	0.9733263	0.9694534	0.9651305	0.9602612	0.9551161	0.9495432	0.9437539
2130	0.9869584	0.9851199	0.9831917	0.9810632	0.9785779	0.9757443	0.9724382	0.9687324	0.9646721	0.9601607	0.9553686
2135	0.9887953	0.9871409	0.9854537	0.9837267	0.9817634	0.9796675	0.9772455	0.9744778	0.9714279	0.967941	0.9640747
2140	0.9894134	0.9880502	0.9866689	0.9852387	0.9837509	0.9821304	0.9804051	0.9782836	0.9760256	0.9733571	0.9702958
2145	0.988829	0.987949	0.9870288	0.985921	0.9849495	0.983754	0.9824014	0.9807928	0.9790487	0.9769284	0.9744425
2150	0.9874102	0.9871223	0.9867467	0.9861829	0.9855418	0.9847102	0.9836579	0.9823038	0.9808139	0.9790095	0.9768532
2155	0.9856452	0.9859124	0.9860281	0.9860259	0.9855452	0.9849362	0.9840384	0.9827802	0.981391	0.9797297	0.9777935
2160	0.9839926	0.9846374	0.9850546	0.9852442	0.9848581	0.9842449	0.9831889	0.9820216	0.9806998	0.979154	0.977604
2165	0.9829412	0.9835443	0.9838203	0.9835739	0.9831034	0.9822114	0.9813303	0.9800482	0.9789116	0.9779155	0.9767567
2170	0.9825345	0.9823902	0.981812	0.9807051	0.9798961	0.9788567	0.9780407	0.9774936	0.9770091	0.9762766	0.9755903
2175	0.9813688	0.9798014	0.9780542	0.9766048	0.9758696	0.9754013	0.9754745	0.9751643	0.9749747	0.974492	0.9741057
2180	0.9769456	0.9745914	0.973179	0.9729819	0.9728137	0.9730228	0.9730247	0.9731855	0.9728655	0.9727032	0.9721389
2185	0.9704871	0.9700412	0.9702126	0.9712167	0.9711283	0.9714497	0.9712217	0.9711481	0.9708292	0.9703053	0.9695873
2190	0.9677221	0.9686702	0.9692473	0.9698395	0.969716	0.969825	0.9691663	0.9686795	0.9680558	0.9673128	0.966446
2195	0.9671865	0.9679561	0.968113	0.9677182	0.9677006	0.9674574	0.9662486	0.9655975	0.9647856	0.9637831	0.962753
2200	0.9654309	0.9659225	0.9657698	0.9649825	0.9647284	0.9640599	0.9632007	0.9618413	0.9608915	0.9597731	0.9585345
2205	0.9618178	0.9622282	0.9619785	0.9612255	0.9606339	0.9596446	0.958562	0.9573873	0.956154	0.955071	0.9537748
2210	0.9565244	0.9567283	0.9565573	0.9563088	0.9553672	0.9542502	0.9536026	0.9521546	0.9510921	0.9497148	0.9484264
2215	0.9507823	0.9502653	0.9500281	0.9500467	0.9490272	0.9477417	0.9471484	0.9460274	0.9450195	0.9437186	0.9424612
2220	0.9483055	0.9455782	0.9439563	0.9429152	0.9419487	0.9404857	0.9400839	0.9389967	0.9378273	0.9370527	0.9359375
2225	0.9455973	0.9423199	0.9393638	0.9365683	0.935002	0.9330907	0.9321987	0.9313639	0.9306273	0.9296954	0.929024
2230	0.9378969	0.9360061	0.9336851	0.9305403	0.9284619	0.9262226	0.9253064	0.9238036	0.923358	0.9224533	0.9219655
2235	0.9268299	0.9257551	0.9245909	0.9228991	0.9211674	0.9194928	0.9176511	0.916807	0.9161822	0.9155564	0.9150305
2240	0.9140881	0.9136554	0.9134998	0.9131749	0.9125053	0.9119365	0.9117402	0.9100204	0.909476	0.9089611	0.9083626
2245	0.9011313	0.9016972	0.9024169	0.9026014	0.9030625	0.9035106	0.9031203	0.9027566	0.9026617	0.9022214	0.901761
2250	0.8898997	0.8907875	0.8919355	0.8928293	0.8936059	0.8948034	0.894993	0.894803	0.8951548	0.8949425	0.8948069
2255	0.879917	0.8809802	0.8823418	0.8836351	0.8845098	0.8860384	0.8865762	0.8863102	0.886991	0.8871898	0.8873432
2260	0.8705134	0.8723276	0.8737378	0.8750997	0.8757276	0.8772036	0.8761211	0.8775335	0.8783532	0.878949	0.8796827
2265	0.8628234	0.8643363	0.8654153	0.8663435	0.8668787	0.8683386	0.8690934	0.8689392	0.8699266	0.8712514	0.8723162
2270	0.8557294	0.8563322	0.8567535	0.856804	0.8579479	0.859448	0.858685	0.8611757	0.8629866	0.8641037	0.8654779
2275	0.8482441	0.8477467	0.8478079	0.8487613	0.8498391	0.8519631	0.854181	0.854565	0.8563752	0.8575181	0.8590779
2280	0.8402585	0.8399469	0.8404695	0.8425872	0.8439302	0.8462875	0.8472327	0.8487058	0.850068	0.851808	0.8531038
2285	0.8339346	0.8352311	0.8368402	0.8387604	0.839979	0.8412207	0.8424801	0.8432781	0.8451173	0.8465064	0.8477131
2290	0.8319648	0.8341076	0.8352419	0.8353739	0.8361235	0.8364444	0.8383075	0.8388627	0.8403047	0.8416227	0.84282
2295	0.8321244	0.8318673	0.8314758	0.8311189	0.8326272	0.8332689	0.8336886	0.8356276	0.8367774	0.8374781	0.8380858
2300	0.8260536	0.8264682	0.8278352	0.8295197	0.8307672	0.8310723	0.8331067	0.8326126	0.8330423	0.8332108	0.8333091

Table 5.4. α for 2000-2300 nm with b of 2.0 comparison run

alpha:	40	45	50	55	60	65	70	75	80	85	90
2000	0.1482253	0.1520783	0.1566179	0.1611435	0.1670107	0.1737644	0.1822891	0.1909362	0.2017582	0.2110648	0.2214807
2005	0.1309017	0.132953	0.1358576	0.1389718	0.1430379	0.1482437	0.1533988	0.1603426	0.167669	0.176967	0.1856974
2010	0.1146625	0.1160284	0.1182078	0.1207473	0.1233407	0.1272808	0.1320181	0.1361788	0.1427029	0.1490059	0.1564597
2015	0.0995575	0.1005836	0.1023186	0.104692	0.1067294	0.1096564	0.1129543	0.1166975	0.1220481	0.1272828	0.1330054
2020	0.0855212	0.0869271	0.0884573	0.0898064	0.0923171	0.0949102	0.0977159	0.1007332	0.1045672	0.1094604	0.1141338
2025	0.0722887	0.0740017	0.0758636	0.0775524	0.0798329	0.0825866	0.0856632	0.0874572	0.0913498	0.0948225	0.0987338
2030	0.0617051	0.0627316	0.064583	0.0669188	0.0691382	0.072126	0.0734744	0.0762648	0.0794944	0.0826218	0.085917
2035	0.0525658	0.054543	0.0562207	0.0580234	0.0600928	0.0630778	0.0648021	0.0665741	0.0694644	0.0720661	0.0750692
2040	0.0446162	0.0470151	0.0491498	0.0509393	0.0526728	0.0551591	0.0561646	0.058174	0.0608451	0.0631625	0.0658017
2045	0.0392019	0.0407662	0.0425226	0.0444957	0.0460731	0.0482888	0.0492553	0.0510269	0.0533179	0.0555749	0.0578577
2050	0.0347069	0.035937	0.037259	0.0389119	0.0402514	0.0422202	0.0436521	0.044936	0.0471665	0.0490054	0.0511164
2055	0.0317611	0.0324161	0.0332876	0.0343543	0.0355393	0.037034	0.038411	0.0397284	0.0416372	0.0434635	0.0454504
2060	0.0296747	0.0300231	0.0304441	0.0310852	0.0319468	0.033115	0.0346284	0.0355511	0.0372659	0.0389474	0.0406676
2065	0.027954	0.0279353	0.0282651	0.0287807	0.0294958	0.030206	0.0315644	0.0323917	0.0340705	0.0351963	0.0366218
2070	0.027017	0.0267493	0.0269264	0.0272427	0.0280221	0.0282875	0.0293699	0.0300167	0.0311006	0.0321672	0.0332701
2075	0.0260339	0.0264008	0.0266307	0.0266969	0.0271421	0.0270069	0.0278343	0.0281793	0.0289188	0.0297214	0.0306166
2080	0.0252504	0.0260615	0.0262751	0.026364	0.0263695	0.0260909	0.026436	0.0267956	0.0273443	0.0278814	0.028556
2085	0.0248408	0.0249702	0.0250598	0.0256247	0.0253904	0.0253604	0.0256612	0.0257934	0.0260679	0.0265227	0.0269282
2090	0.0236996	0.023605	0.0237471	0.0243089	0.024386	0.0247689	0.0249716	0.0249166	0.0252801	0.0253405	0.0255596
2095	0.0225496	0.022778	0.0229721	0.0231255	0.023526	0.0241759	0.0237221	0.0238892	0.0239604	0.0241248	0.0243317
2100	0.0222515	0.0225106	0.022599	0.0224774	0.0227157	0.0232718	0.0229319	0.0226862	0.022789	0.0229504	0.0232398
2105	0.022803	0.0225195	0.0221887	0.0218729	0.0217013	0.0222097	0.021331	0.0215173	0.0218785	0.0219694	0.0223779
2110	0.0230783	0.0222204	0.0214386	0.0211289	0.0206091	0.0208838	0.0205914	0.0206395	0.0209405	0.0215593	0.0218629
2115	0.0217076	0.0210211	0.0203525	0.0201553	0.019772	0.0198648	0.0199014	0.0202603	0.0208073	0.0211636	0.0217028
2120	0.0188741	0.0189207	0.0189694	0.0190009	0.0194086	0.0195042	0.0201381	0.0203877	0.0208853	0.0213841	0.0218327
2125	0.0165698	0.0170583	0.0178184	0.0186294	0.0194166	0.0196907	0.020488	0.0208036	0.0212694	0.0217287	0.0221877
2130	0.0161437	0.017071	**0.0179301**	0.0190348	0.0196093	0.0198566	0.0210208	0.0212643	0.0218525	0.0222381	0.0227026
2135	0.0173747	0.0181824	0.0188381	0.0197016	0.0201193	0.0203256	0.0211509	0.0217037	0.0223703	0.0228563	0.0233428
2140	0.0182292	0.0191036	0.0198426	0.0201831	0.0209337	0.0211456	0.0221017	0.0223136	0.0232766	0.0235527	0.0240984
2145	0.0187778	0.019884	0.020598	0.0207559	0.0218144	0.0221408	0.022703	0.0232972	0.0239244	0.024519	0.0249419
2150	0.0199837	0.0206423	0.0212881	0.022087	0.0228978	0.0235743	0.024382	0.0245836	0.0250367	0.0255297	0.0257931
2155	0.0222862	0.0224295	0.0229395	0.0241791	0.0245092	0.0254706	0.0258116	0.0258639	0.0265005	0.0265106	0.0265326
2160	0.0258735	0.0257675	0.0260341	0.0268801	0.0266883	0.0273567	0.0268464	0.0269551	0.0272474	0.0272654	0.0270487
2165	0.0304084	0.0302651	0.0298488	0.0293731	0.0290548	0.0291174	0.0290034	0.0279098	0.0279341	0.0276216	0.0273062
2170	0.0342182	0.0338552	0.0330245	0.0315228	0.031331	0.0309449	0.0292478	0.0287764	0.028418	0.0278581	0.0273438
2175	0.0363729	0.0357205	0.0350801	0.0337936	0.0331205	0.032327	0.0313653	0.0294548	0.0288742	0.0280417	0.0272489
2180	0.0378796	0.0369711	0.0360636	0.0353311	0.0338054	0.0327188	0.0309164	0.0297566	0.0292398	0.027979	0.0270765
2185	0.0380884	0.0370885	0.0359486	0.0354027	0.0334663	0.0323759	0.0312261	0.029521	0.0286508	0.0277744	0.0267714
2190	0.037814	0.0362243	0.0348912	0.0337591	0.0324117	0.0313062	0.0303171	0.0287416	0.0279911	0.0272081	0.026246
2195	0.0367561	0.0349359	0.0335102	0.0315977	0.0308913	0.0296943	0.0285663	0.0275445	0.0272364	0.0261889	0.0254351
2200	0.0341019	0.032743	0.0315526	0.0298599	0.0291129	0.0279391	0.0276923	0.0260873	0.0257609	0.0250377	0.024377
2205	0.0291481	0.0290031	0.0285718	0.0276526	0.0269615	0.026071	0.024981	0.0244742	0.024214	0.0236649	0.02313
2210	0.0243958	0.0243971	0.0245492	0.0246382	0.0241889	0.0236791	0.0239435	0.0226849	0.022556	0.0221811	0.0217418
2215	0.0198483	0.0201225	0.0204835	0.0209433	0.0208695	0.0207162	0.0206664	0.0205792	0.0206428	0.0204215	0.0202218
2220	0.0151396	0.0158984	0.0166056	0.0170307	0.0174898	0.0175875	0.0183148	0.0181287	0.0185365	0.0185506	0.0185148
2225	0.0110558	0.0119597	0.0128556	0.0133866	0.0142156	0.0145477	0.015265	0.0155183	0.0160552	0.0163955	0.0166007
2230	0.0081366	0.0088139	0.0096293	0.0102755	0.0111555	0.0117756	0.0124428	0.0129481	0.0136209	0.0141979	0.014553
2235	0.0059188	0.006515	0.0071769	0.0078056	0.008527	0.0093043	0.0100635	0.0105353	0.011422	0.0119087	0.0125016
2240	0.0043192	0.0047905	0.0053419	0.0058693	0.0064954	0.0072565	0.0077015	0.0084095	0.0092256	0.0099121	0.0105728
2245	0.0032792	0.0036192	0.0040291	0.0045035	0.0049719	0.0056446	0.0062518	0.0066893	0.0074341	0.0081565	0.0088821
2250	0.0026585	0.0028698	**0.0031626**	0.0035532	0.0039059	0.0044327	0.0048288	0.00541	0.006118	0.0068039	0.0075462
2255	0.0023186	0.0024667	0.002661	0.0029179	0.0032294	0.0036369	0.0041287	0.0045603	0.0052013	0.0058927	0.0066487
2260	0.0021174	0.0022414	0.0024054	0.0026038	0.0028856	0.0032195	0.0036388	0.0041338	0.0047633	0.0054506	0.0062334
2265	0.0020342	0.002161	0.0023236	0.0025204	0.0028235	0.0031593	0.0036079	0.0041343	0.0047881	0.0055076	0.0063256
2270	0.0020613	0.0022109	0.0024226	0.0026922	0.0030516	0.0034627	0.0039986	0.0045715	0.0052871	0.0060635	0.0069484
2275	0.0022447	0.0024761	0.0027851	0.0031773	0.0036288	0.0041549	0.0047719	0.0054717	0.0062855	0.0071582	0.0081223
2280	0.0026966	0.0030781	0.003526	0.0040456	0.0046288	0.0052983	0.0060956	0.0069023	0.0078475	0.0088332	0.0098335
2285	0.003617	0.0041297	0.0047188	0.0053972	0.0061636	0.0070236	0.0079811	0.0089285	0.0099042	0.0109509	0.01202
2290	0.005056	0.0057281	0.0065162	0.0074271	0.0084193	0.0094613	0.0104842	0.0114825	0.0124589	0.0135105	0.0146522
2295	0.0071835	0.0081481	0.0092311	0.0103939	0.0114477	0.0124275	0.0134179	0.0144116	0.0155377	0.0165506	0.0178283
2300	0.010556	0.0118877	0.0129892	0.0139875	0.0148421	0.01564	0.016587	0.017809	0.0189438	0.0202787	0.0216846

Table 5.5. β for 2000-2300 nm with b of 2.0 comparison run.

beta:	40	45	50	55	60	65	70	75	80	85	90
2000	0.5901687	0.5837101	0.5746247	0.5649489	0.5530948	0.5392932	0.5243916	0.5088753	0.4923584	0.477152	0.4622342
2005	0.5952418	0.5894441	0.5818728	0.5735741	0.564244	0.5520054	0.5419293	0.5278023	0.5145568	0.4994337	0.4851099
2010	0.5977944	0.5930105	0.586441	0.57922	0.5725619	0.5620971	0.5525233	0.5437582	0.5322079	0.5201041	0.5070918
2015	0.6001362	0.5961828	0.5910415	0.5852368	0.5801982	0.5720751	0.5672311	0.5578423	0.5477245	0.5383149	0.5272974
2020	0.6031896	0.5999256	0.5966723	0.5938597	0.588433	0.5820739	0.576735	0.5711489	0.5641491	0.5548445	0.5455846
2025	0.6121795	0.6083563	0.6048	0.6021484	0.5981585	0.5929796	0.5886299	0.5844252	0.5776206	0.5703042	0.5619933
2030	0.6234959	0.6209049	0.6175696	0.6137834	0.6102986	0.6051916	0.6033255	0.5975407	0.5908825	0.5842983	0.5767665
2035	0.6371734	0.6343989	0.6320862	0.6287746	0.6248283	0.618573	0.6147563	0.6108155	0.6043975	0.597806	0.590225
2040	0.6544275	0.6508321	0.6473818	0.6431806	0.639509	0.6329475	0.6306196	0.6240374	0.6168516	0.610047	0.602676
2045	0.6703959	0.6679032	0.6641256	0.6579323	0.6539743	0.6468159	0.6428352	0.6367516	0.6290956	0.621828	0.6145774
2050	0.6885783	0.6842856	0.6793836	0.672676	0.667415	0.6597903	0.6542289	0.6485466	0.6407584	0.6335613	0.6260735
2055	0.7028745	0.6973996	0.6916126	0.6861101	0.6790536	0.6716868	0.6650612	0.6595879	0.6514962	0.6443993	0.6370012
2060	0.711433	0.7061046	0.7006124	0.6955301	0.6886232	0.6818009	0.674014	0.6692113	0.661158	0.6544755	0.6472445
2065	0.7166678	0.712406	0.7068961	0.7013995	0.6951941	0.6901739	0.6813745	0.6771347	0.669134	0.6633664	0.6569067
2070	0.7169297	0.7136353	0.709047	0.7042959	0.6981384	0.6956576	0.688203	0.6835274	0.6771654	0.67165	0.665915
2075	0.7133226	0.709056	0.7053731	0.7023274	0.6984115	0.6984496	0.6912715	0.6886699	0.6838383	0.6787485	0.6735612
2080	0.7065685	0.7022007	0.7003237	0.6984237	0.6976525	0.6991926	0.6957174	0.692294	0.6881487	0.6841788	0.6795485
2085	0.6963155	0.697238	0.697928	0.6956497	0.6971472	0.6979924	0.6949239	0.6937598	0.6907587	0.6870428	0.6836099
2090	0.6883981	0.6929294	0.6956698	0.6952149	0.6959376	0.6944609	0.6934501	0.69306	0.6901583	0.6883864	0.6860527
2095	0.6845213	0.6880099	0.6910629	0.6932209	0.6922752	0.6885763	0.6922058	0.6912265	0.6899614	0.6892148	0.68746
2100	0.6819201	0.6830496	0.6847397	0.6867491	0.6862198	0.682762	0.6863047	0.6891509	0.6893041	0.6888909	0.6881142
2105	0.6753119	0.6760097	0.677869	0.679232	0.6811045	0.6780083	0.6869894	0.6870947	0.6871849	0.6884127	0.6880298
2110	0.6665667	0.6691225	0.6729509	0.6737096	0.6784188	0.6772198	0.6820394	0.6852687	0.6865087	0.6858248	0.6867894
2115	0.6657093	0.6681665	0.6721944	0.6729807	0.677465	0.6787145	0.6832643	0.6835088	0.6838036	0.6846662	0.6843864
2120	0.6768108	0.6753766	0.6764313	0.6777591	0.6779599	0.6809454	0.6798339	0.6815789	0.6815237	0.6814232	0.6809465
2125	0.6883447	0.6862187	0.6846742	0.6825308	0.6805525	0.6825891	0.6797239	0.6792937	0.6790861	0.6777202	0.6766869
2130	0.6913915	0.6907482	**0.6897773**	0.6849343	0.6834798	0.6847592	0.6772493	0.6768644	0.6745321	0.6735842	0.6722792
2135	0.6889158	0.6898679	0.6892431	0.6844438	0.6827536	0.683571	0.6773944	0.6744674	0.671143	0.6696738	0.6680663
2140	0.6878071	0.6855116	0.6832672	0.6822838	0.6780656	0.6786211	0.6727488	0.6713083	0.6674031	0.6660115	0.6639901
2145	0.68608	0.6791785	0.676551	0.6773928	0.6721441	0.6725379	0.6686999	0.6663904	0.663795	0.6619091	0.6600584
2150	0.6829776	0.67688	0.6732645	0.6691365	0.6659	0.664321	0.6611368	0.6601399	0.6589637	0.657364	0.656462
2155	0.6767484	0.6732057	0.6688426	0.6609202	0.6593047	0.6555167	0.6532331	0.6546679	0.653032	0.6529773	0.6534935
2160	0.6673868	0.6639451	0.6599218	0.6536501	0.6532703	0.6495368	0.6522139	0.6512259	0.6500531	0.6505723	0.651534
2165	0.6567513	0.653156	0.6512856	0.6495557	0.6490123	0.6461406	0.6454815	0.6498653	0.6491135	0.6499512	0.650603
2170	0.6461712	0.6457171	0.6460708	0.648154	0.6464486	0.6439456	0.6503956	0.6497202	0.6491516	0.6498877	0.6506771
2175	0.6349599	0.6387647	0.6414046	0.6446912	0.6445845	0.6435887	0.6456468	0.6499411	0.6490744	0.6502988	0.6513593
2180	0.6284685	0.6327467	0.6365254	0.6395316	0.6426482	0.643813	0.6479667	0.650079	0.6488864	0.6510842	0.6519087
2185	0.6289904	0.6311184	0.6340896	0.6353282	0.6404228	0.6423395	0.645974	0.6496621	0.649765	0.6506655	0.6520307
2190	0.6306184	0.6327802	0.6347016	0.6355585	0.639294	0.6418175	0.6422782	0.6485513	0.649028	0.6496006	0.6514561
2195	0.6313172	0.6338702	0.6358792	0.6387866	0.6398626	0.6426244	0.6454602	0.6474338	0.6469093	0.6491365	0.6505525
2200	0.6344251	0.636099	0.6375673	0.6406288	0.640827	0.6429626	0.6405694	0.6469263	0.6459744	0.6478759	0.6497103
2205	0.6450617	0.6428033	0.6414033	0.6428574	0.6420997	0.6433549	0.6471794	0.6474526	0.6463402	0.6481944	0.6496724
2210	0.6564181	0.6528801	0.6493023	0.6466905	0.6461006	0.6466386	0.6436597	0.6493006	0.6483847	0.6491594	0.6509318
2215	0.6692131	0.6648042	0.6604563	0.6548576	0.6546357	0.6538671	0.65359	0.6537578	0.6519974	0.6528459	0.6536646
2220	0.688305	0.6814283	0.6753386	0.6713548	0.6672858	0.6658495	0.6607507	0.6620346	0.6583818	0.6580406	0.6586456
2225	0.7152914	0.7056972	0.696756	0.6924807	0.6844248	0.6824759	0.675283	0.6744962	0.6699113	0.667984	0.6667145
2230	0.7449976	0.7354206	0.7247697	0.7176376	0.7073299	0.7023573	0.6953642	0.6912063	0.6849672	0.6803682	0.6785029
2235	0.7814777	0.769015	0.7570583	0.7467952	0.7363669	0.7267027	0.7164901	0.7126482	0.7031276	0.6989875	0.6943173
2240	0.8211429	0.8085484	0.7941622	0.781208	0.7691683	0.7559977	0.7489782	0.7391516	0.7278834	0.7204981	0.714112
2245	0.858363	0.8464086	0.8327761	0.8181598	0.8056953	0.7892126	0.7760098	0.7696319	0.7566379	0.7465338	0.7375478
2250	0.8937148	0.8830811	**0.8699812**	0.8553154	0.8425249	0.825565	0.8162894	0.8018473	0.786428	0.7743266	0.7627785
2255	0.9227633	0.9134287	0.9026425	0.8901784	0.8761308	0.8601937	0.8428865	0.8320405	0.815377	0.8002816	0.7861427
2260	0.9477009	0.9387439	0.9282153	0.9165558	0.9022914	0.8872532	0.8719963	0.8548316	0.8363851	0.8195327	0.8028332
2265	0.9649605	0.9560713	0.9455302	0.9335384	0.9174889	0.9018939	0.8832347	0.8652464	0.8454	0.8268794	0.8086855
2270	0.9746203	0.9647084	0.9518563	0.9367861	0.9190146	0.9013354	0.8805218	0.8612305	0.840473	0.8214355	0.8025767
2275	0.9736311	0.9606112	0.9444371	0.9258518	0.9062476	0.8865576	0.8653865	0.8444937	0.824228	0.8050548	0.7870503
2280	0.9599335	0.9421799	0.9230626	0.902651	0.8816734	0.8608505	0.8383436	0.8188864	0.7993963	0.7820385	0.766958
2285	0.9328655	0.913096	0.8923466	0.8703951	0.8489096	0.8281203	0.8075045	0.7896109	0.7741847	0.7599039	0.7467955
2290	0.8984192	0.8773485	0.8553395	0.8327242	0.8115845	0.7930229	0.7760479	0.7628242	0.7514967	0.7397891	0.728446
2295	0.8591315	0.8358582	0.8134485	0.7927388	0.7765604	0.7642478	0.7522845	0.7417461	0.730786	0.7219923	0.7112821
2300	0.812461	0.7899084	0.7740676	0.7614539	0.7520567	0.7445473	0.7349074	0.7242159	0.7149481	0.7046383	0.6948074

Table 5.6. Transmission (TnoH2O) for 2000-2300 nm, with b of 2.5 comparison run.

tnoh2o:	40	45	50	55	60	65	70	75	80	85	90
2000	0.4867998	0.5007295	0.51288	0.5232162	0.5318184	0.5394005	0.5453958	0.5511988	0.5567085	0.5619413	0.566848
2005	0.4336401	0.4671384	0.4942238	0.5150485	0.5310977	0.5431558	0.5516298	0.5576047	0.5627301	0.5666121	0.5700663
2010	0.4013031	0.4455192	0.4805904	0.5071984	0.5272932	0.5420166	0.551753	0.5589379	0.5640624	0.5676596	0.5711255
2015	0.400934	0.4404815	0.4732473	0.4992022	0.5190654	0.5342412	0.5453949	0.5531961	0.5595605	0.5644659	0.5687159
2020	0.4352719	0.4563468	0.4762286	0.4939964	0.5091401	0.5221503	0.5329269	0.5421087	0.5501163	0.5574874	0.563456
2025	0.4889292	0.4884338	0.4909958	0.4962119	0.5033625	0.5119534	0.521471	0.5306922	0.5402687	0.5489016	0.5576077
2030	0.5416329	0.5241449	0.5129494	0.5074489	0.5070138	0.5104023	0.5169243	0.5251029	0.5346013	0.5443589	0.5543389
2035	0.5818756	0.556236	0.538508	0.5270178	0.5217882	0.5209481	0.5239079	0.5297045	0.5376512	0.5473387	0.5567614
2040	0.6069868	0.5836307	0.566012	0.5530188	0.5456108	0.5423059	0.5425415	0.545517	0.5513608	0.5583707	0.5668666
2045	0.6165481	0.6025651	0.5906387	0.5810406	0.5743931	0.5708246	0.5695494	0.570601	0.5738656	0.5785147	0.5848107
2050	0.6106122	0.6099969	0.6083187	0.6061544	0.6034972	0.601843	0.6010257	0.6011394	0.6027831	0.6053443	0.6090054
2055	0.598556	0.6110677	0.6201298	0.62592	0.6291889	0.6310165	0.6321269	0.6327034	0.6335939	0.6350731	0.6368152
2060	0.5927952	0.6135039	0.6297406	0.6412303	0.6499743	0.6556041	0.6593018	0.6617413	0.6632349	0.664224	0.6653681
2065	0.6019396	0.623125	0.6413278	0.6555758	0.6674252	0.6757978	0.6824333	0.6866795	0.689708	0.6911063	0.6923024
2070	0.6307186	0.6456137	0.660448	0.673629	0.6853648	0.694664	0.7023752	0.7080615	0.711965	0.7149608	0.7163556
2075	0.6756762	0.6827057	0.6909212	0.6996183	0.7078102	0.7154232	0.7224154	0.7278959	0.7322345	0.7353949	0.7375674
2080	0.7279254	0.7285329	0.7303441	0.7331636	0.7364935	0.7404538	0.7448982	0.748628	0.752198	0.7547757	0.7570053
2085	0.7825309	0.7771968	0.7735789	0.7710528	0.7700679	0.7698513	0.7706612	0.7719564	0.7733842	0.7750379	0.7761527
2090	0.8341129	0.8248582	0.8171421	0.8106108	0.805979	0.8023165	0.799936	0.7980852	0.7971269	0.7965778	0.7962064
2095	0.8767546	0.8669658	0.8576493	0.8490549	0.8417771	0.8354917	0.830065	0.8259748	0.8224978	0.8197098	0.8175958
2100	0.9090752	0.9006498	0.8919286	0.8832885	0.8749079	0.8672752	0.8602424	0.8540272	0.8486283	0.8439462	0.8399487
2105	0.9337536	0.9266391	0.9191235	0.9114076	0.9032695	0.8954853	0.8876386	0.8805149	0.8738968	0.8679041	0.862383
2110	0.9525273	0.9466639	0.9402522	0.9334459	0.9262072	0.9188529	0.9113049	0.9039842	0.8968386	0.8900783	0.8838398
2115	0.9658872	0.961391	0.956153	0.9503058	0.9440575	0.9374595	0.9306917	0.9236576	0.9167251	0.9099396	0.9033664
2120	0.9748291	0.9714671	0.9673695	0.962572	0.9573662	0.9516977	0.9456382	0.9394521	0.9330811	0.9267445	0.9203351
2125	0.9808082	0.9780527	0.9747965	0.970984	0.9667701	0.9621043	0.9570953	0.9516782	0.9461331	0.9403329	0.9345084
2130	0.9847559	0.9822884	0.979572	0.9765679	0.9731458	0.9694041	0.9652696	0.9608169	0.9561267	0.9510972	0.9459472
2135	0.9870236	0.9848828	0.9826031	0.9801704	0.9773942	0.9744099	0.9710886	0.9674457	0.963564	0.9593555	0.9548815
2140	0.9879342	0.9862092	0.9843693	0.9823522	0.9801895	0.9777782	0.9751766	0.9721486	0.968963	0.9654419	0.961619
2145	0.9876906	0.986478	0.9851391	0.9835151	0.9819247	0.9800134	0.9778441	0.9753882	0.9727541	0.9697585	0.9664761
2150	0.9865992	0.9859586	0.9851482	0.9840723	0.9828326	0.9813157	0.9795442	0.9774339	0.9751671	0.9726033	0.9697253
2155	0.985096	0.984972	0.9846112	0.9840683	0.9829925	0.9817367	0.9802369	0.9783788	0.9763931	0.9741389	0.9715893
2160	0.9836038	0.9837976	0.9836827	0.9833351	0.9824023	0.9812807	0.9798133	0.9782309	0.9764763	0.9744332	0.9722912
2165	0.9824979	0.9826071	0.9823816	0.9817287	0.9809301	0.9797931	0.978668	0.9770707	0.9755028	0.9739271	0.9720961
2170	0.9816657	0.9812012	0.9804452	0.9793024	0.9784914	0.9773561	0.9762477	0.9752035	0.9741087	0.9726901	0.9712661
2175	0.9801204	0.9787778	0.9774135	0.976182	0.9753784	0.9745691	0.9740524	0.9730871	0.9722158	0.9710445	0.9699578
2180	0.9765163	0.9747838	0.9735403	0.9730708	0.9724331	0.9720829	0.9714624	0.9709978	0.9700968	0.9693386	0.9681916
2185	0.9713787	0.9706677	0.970346	0.9707779	0.9702036	0.9700646	0.9693968	0.968851	0.9680939	0.9671063	0.9659177
2190	0.9679409	0.9683489	0.9685161	0.9687614	0.9683412	0.9681516	0.9671817	0.9663793	0.9654407	0.964337	0.9630893
2195	0.9664734	0.9669738	0.9669238	0.9663464	0.9661108	0.9656667	0.9642769	0.963357	0.962292	0.9610195	0.9596884
2200	0.964455	0.9647419	0.9644004	0.9634497	0.9630226	0.9622234	0.9611398	0.9596607	0.9585082	0.9571833	0.9557173
2205	0.9607936	0.9609406	0.9605076	0.959618	0.9588828	0.9577718	0.9565797	0.9552338	0.9538582	0.9526229	0.9511785
2210	0.9558147	0.9556649	0.9552369	0.9547824	0.9536421	0.9523677	0.9515706	0.9500399	0.9488797	0.9474351	0.9460669
2215	0.9510531	0.9499929	0.9492378	0.9488205	0.9475198	0.9460406	0.945304	0.9440798	0.9430209	0.941692	0.9403952
2220	0.9478828	0.9454351	0.9436699	0.9422843	0.940984	0.9392899	0.9386959	0.9374717	0.9362534	0.9354113	0.9342363
2225	0.9436368	0.9409065	0.9384771	0.9360116	0.9344793	0.9325179	0.9314463	0.9304952	0.9296088	0.9285539	0.9277451
2230	0.9359776	0.933983	0.9319595	0.9293694	0.9277703	0.9258258	0.9250455	0.9234768	0.9228758	0.9217989	0.9211255
2235	0.9256303	0.9243989	0.9231945	0.9216567	0.92019	0.9187644	0.9172339	0.9165246	0.9159132	0.9152011	0.9145373
2240	0.9137566	0.9132727	0.9129375	0.9124301	0.9116571	0.9110327	0.9109684	0.9094493	0.9090199	0.9085677	0.9079978
2245	0.9015468	0.9019285	0.9024031	0.9023677	0.9026178	0.9028293	0.9023917	0.9020386	0.9019993	0.9016828	0.9013781
2250	0.8905376	0.8913385	0.8923178	0.8930156	0.893559	0.8944573	0.8945257	0.8942707	0.8946093	0.8945144	0.8945321
2255	0.8806092	0.8816962	0.8829272	0.8840091	0.8847262	0.8860497	0.8864927	0.8862571	0.8869545	0.8872116	0.887444
2260	0.8712603	0.8729011	0.8742192	0.8754647	0.8761736	0.8776857	0.8767149	0.8781646	0.8790061	0.8795751	0.8802702
2265	0.8632878	0.8647701	0.8658937	0.866924	0.8677391	0.8694252	0.8703147	0.8702379	0.8711667	0.8723667	0.8732592
2270	0.8561417	0.8568662	0.8576286	0.8580586	0.8594877	0.8611373	0.8604905	0.8628028	0.8644667	0.865403	0.8666138
2275	0.8490165	0.8490654	0.8495814	0.8507616	0.8518924	0.8538412	0.8558505	0.8561357	0.8578327	0.8589132	0.8604068
2280	0.8417014	0.8420259	0.8427779	0.8446984	0.8457735	0.8478455	0.8487808	0.8502786	0.8516364	0.8533813	0.8546339
2285	0.8357154	0.8369134	0.8382544	0.8399598	0.8412427	0.8426757	0.8441239	0.8451117	0.8468614	0.8481728	0.8493051
2290	0.8326574	0.8342412	0.8354763	0.8361673	0.8374981	0.8381565	0.8400928	0.8406343	0.8419448	0.8431919	0.8444115
2295	0.8312432	0.8319511	0.8324571	0.8325588	0.8340347	0.8345588	0.8349332	0.8368504	0.8380404	0.8389577	0.8398498
2300	0.8272337	0.8279847	0.8290357	0.8303148	0.8312134	0.8314213	0.8335477	0.8334282	0.8342588	0.8348987	0.8354775

Table 5.7. α for 2000-2300 nm, with b of 2.5 comparison run.

alpha:	40	45	50	55	60	65	70	75	80	85	90
2000	0.1527101	0.1578064	0.1637934	0.1698128	0.177053	0.1849032	0.1941598	0.2030418	0.2138198	0.2229271	0.2330075
2005	0.1340308	0.1374695	0.141722	0.1461981	0.151591	0.1580324	0.164309	0.1721622	0.1800219	0.189574	0.1983203
2010	0.1174021	0.1196049	0.1228669	0.1267272	0.1305516	0.1356974	0.1416313	0.1469717	0.1544085	0.1614103	0.1693164
2015	0.1018323	0.1037373	0.1063603	0.1096481	0.1127917	0.1168678	0.1214264	0.1262653	0.1326359	0.1387767	0.1452637
2020	0.0873047	0.089438	0.0918506	0.0940638	0.0975617	0.1011833	0.1049767	0.1090494	0.113886	0.1197532	0.125339
2025	0.0744857	0.0764634	0.0789101	0.0812925	0.0843885	0.0879781	0.0918148	0.094621	0.0994517	0.1038834	0.1087306
2030	0.0637381	0.0655156	0.0677566	0.0703964	0.0731126	0.0766932	0.0788637	0.0823949	0.086498	0.090549	0.0947715
2035	0.0540916	0.0564529	0.0587312	0.0610851	0.0636287	0.067131	0.0694784	0.0719593	0.0756243	0.0790698	0.0829271
2040	0.0463032	0.0487004	0.0510768	0.0533454	0.0556659	0.0587791	0.0603608	0.0630141	0.066392	0.0694077	0.0728078
2045	0.040567	0.0424736	0.0445068	0.0467306	0.048725	0.051425	0.0530166	0.055362	0.0582582	0.0611808	0.0641398
2050	0.0360527	0.0375405	0.0391637	0.0410897	0.0428038	0.0451199	0.0470058	0.048829	0.0516209	0.0540447	0.056743
2055	0.0328175	0.0338345	0.0350328	0.0364356	0.0379673	0.0398073	0.0415734	0.0433068	0.0456535	0.0479473	0.0504586
2060	0.0304148	0.0310936	0.0319219	0.0329877	0.034213	0.0356699	0.0375446	0.0388078	0.0408713	0.0429491	0.045137
2065	0.0287606	0.029	0.0295892	0.0303972	0.0314325	0.0324031	0.0340909	0.0352573	0.0372913	0.0388383	0.0406922
2070	0.0275821	0.0276536	0.0280648	0.0285752	0.0295366	0.0300526	0.0314785	0.0325096	0.0339814	0.0354561	0.0370003
2075	0.0263375	0.0268102	0.0272083	0.0275311	0.0282504	0.0284429	0.0296335	0.0303643	0.0314979	0.0326878	0.0339828
2080	0.0253613	0.0260854	0.0264529	0.0268331	0.0271934	0.0272592	0.0279609	0.0286616	0.029569	0.0304666	0.0315387
2085	0.0248729	0.0251581	0.0253855	0.026074	0.0260518	0.0262471	0.0268321	0.027269	0.0278905	0.0287258	0.0295491
2090	0.0240047	0.0240286	0.0242173	0.024794	0.0249392	0.025442	0.0258256	0.0260406	0.0267635	0.027235	0.0278802
2095	0.0228811	0.0231261	0.0233335	0.02351	0.0239679	0.0247308	0.0244987	0.0248836	0.0253067	0.0258416	0.0264474
2100	0.0224679	0.0226745	0.0227624	0.022724	0.0231011	0.0238396	0.0237335	0.0237468	0.0241598	0.024631	0.0252222
2105	0.0227409	0.0225098	0.0222929	0.0221668	0.0222095	0.0229363	0.0223288	0.0227053	0.0232983	0.0236148	0.0242332
2110	0.0227071	0.022134	0.0216469	0.021601	0.0213283	0.0218068	0.0216884	0.0218871	0.0223437	0.0230981	0.0235514
2115	0.0214062	0.0210064	0.0206493	0.0207043	0.020577	0.0208346	0.0209876	0.0214223	0.0220739	0.0225353	0.0231943
2120	0.0191924	0.0192649	0.0194201	0.0195675	0.0200891	0.0202848	0.020996	0.0213331	0.0219386	0.0225576	0.0231302
2125	0.0174112	0.0179068	0.0185243	0.0192071	0.0199152	0.020227	0.0210837	0.0215193	0.022115	0.0227033	0.0232919
2130	0.0168806	0.017753	**0.0185501**	0.0196025	0.0201204	0.0203449	0.021542	0.0218512	0.0225415	0.023031	0.0236103
2135	0.0176111	0.0185064	0.0192652	0.0201917	0.0206567	0.0208674	0.0217092	0.022293	0.0229753	0.0235086	0.0240419
2140	0.0184816	0.0193476	0.0201157	0.0205696	0.0214105	0.0216979	0.0227054	0.0228977	0.0237997	0.0240463	0.0245682
2145	0.0191438	0.0201694	0.0209203	0.0211724	0.0222531	0.0226127	0.0231479	0.0236936	0.0242656	0.0247938	0.025176
2150	0.0205546	0.0212784	0.0219017	0.0225906	0.0232877	0.0238365	0.0245163	0.0246526	0.0250759	0.0255389	0.0258049
2155	0.0229737	0.0231594	0.0235909	0.0246202	0.0247428	0.0254727	0.0257189	0.0256818	0.0262911	0.0263139	0.0263653
2160	0.0262896	0.0261368	0.0262656	0.0269639	0.0266647	0.0272082	0.0266673	0.0266739	0.0269359	0.0269584	0.0267871
2165	0.0299919	0.029825	0.0294804	0.0290726	0.0288015	0.0288578	0.0286793	0.0275887	0.0275995	0.0273043	0.0270456
2170	0.0332894	0.0329637	0.0322518	0.0308519	0.0307237	0.0304146	0.0287902	0.0283753	0.028069	0.0275811	0.0271433
2175	0.035721	0.0348685	0.0340465	0.0327308	0.0321179	0.0314661	0.0306404	0.0289175	0.0284677	0.0277747	0.0271042
2180	0.036991	0.0359285	0.0349483	0.0341573	0.0326821	0.0316949	0.0300623	0.0290752	0.0287114	0.0276408	0.026913
2185	0.0372567	0.0361107	0.034926	0.0343321	0.0324598	0.0313868	0.0303352	0.0287746	0.0280546	0.0273496	0.026537
2190	0.0370195	0.0354871	0.0341166	0.0329386	0.0315604	0.0304647	0.0295075	0.0280437	0.0273854	0.0267398	0.0259463
2195	0.0358971	0.0341404	0.0327738	0.0309336	0.0302215	0.0290484	0.0279402	0.0269728	0.0267146	0.0257686	0.0251403
2200	0.0330516	0.0318241	0.0307451	0.0291767	0.0285125	0.0274134	0.0271913	0.0256523	0.0253548	0.0247067	0.0241455
2205	0.0286761	0.0283025	0.0278132	0.026958	0.0263478	0.0255492	0.0245539	0.0241155	0.0239047	0.0234346	0.0229969
2210	0.0243104	0.0242282	0.0242038	0.0241784	0.0236663	0.0231722	0.0234841	0.0223469	0.0223045	0.022022	0.0217001
2215	0.0198731	0.0201338	0.0204537	0.0208335	0.0206512	0.0204248	0.0203664	0.0203128	0.0204518	0.0203341	0.0202526
2220	0.015425	0.0161036	0.0167475	0.0171403	0.0175476	0.0176106	0.0182734	0.0180673	0.018502	0.0185759	0.0186504
2225	0.0115958	0.0124316	0.0132549	0.013718	0.0145013	0.0148372	0.0154899	0.0157288	0.0162646	0.0166435	0.0169264
2230	0.0086846	0.0094306	0.0102441	0.0108534	0.0116934	0.0123025	0.0129182	0.0134296	0.0141107	0.0147251	0.0151479
2235	0.006438	0.0071056	0.007844	0.0085307	0.0092668	0.0100497	0.0108297	0.0112885	0.0122036	0.012744	0.0134093
2240	0.0047979	0.0053642	0.0060036	0.0066357	0.0073261	0.0081604	0.008646	0.0094189	0.0103015	0.0110602	0.0118112
2245	0.0036993	0.004142	0.0046675	0.005256	0.0058402	0.006633	0.0073704	0.0078992	0.0087641	0.0096052	0.0104501
2250	0.0030166	0.003348	**0.003766**	0.0042781	0.0047894	0.0054796	0.006022	0.0067684	0.0076499	0.0085035	0.0094131
2255	0.0026118	0.0028799	0.0032212	0.0036306	0.0041225	0.0047258	0.005413	0.0060386	0.0068994	0.0077949	0.0087629
2260	0.0023907	0.002634	0.0029444	0.0033138	0.003796	0.004353	0.0049928	0.0057161	0.006594	0.0075206	0.0085468
2265	0.0023158	0.0025677	0.0028879	0.0032694	0.0037782	0.0043456	0.0050272	0.0058107	0.0067268	0.0077163	0.0088004
2270	0.0023943	0.0026831	0.003057	0.0035173	0.0040816	0.0047202	0.0055115	0.0063413	0.0073305	0.0083841	0.0095711
2275	0.0026575	0.003039	0.0035144	0.0040957	0.0047554	0.0055037	0.0063653	0.0073406	0.0084206	0.0095763	0.0108522
2280	0.0032111	0.0037385	0.0043551	0.005071	0.0058741	0.0067609	0.0078086	0.0088539	0.0100536	0.0113145	0.0126435
2285	0.0042187	0.0049046	0.0056792	0.0065596	0.007526	0.0085714	0.0097389	0.0109232	0.0121681	0.0135252	0.0149479
2290	0.0057931	0.0066524	0.0076119	0.0086829	0.0098179	0.0110147	0.0122631	0.0135491	0.0148538	0.0162732	0.0177936
2295	0.0080882	0.0091777	0.0103306	0.0115876	0.0127942	0.0140162	0.0153636	0.0166934	0.0181705	0.0195557	0.0211898
2300	0.0114337	0.0127294	0.0139117	0.0151595	0.016331	0.0175025	0.0187853	0.0203713	0.0218254	0.0234595	0.0252012

Table 5.8. β for 2000-2300 nm, with b of 2.5 comparison run.

beta:	40	45	50	55	60	65	70	75	80	85	90
2000	0.5800316	0.5709267	0.5594895	0.5477163	0.5341778	0.5194537	0.5044439	0.4894207	0.473913	0.4597477	0.4459682
2005	0.5868282	0.5785866	0.5686758	0.5582094	0.5469069	0.5332651	0.5218574	0.507163	0.4938923	0.4793507	0.4658018
2010	0.5905781	0.5840164	0.5755091	0.5659865	0.5571558	0.5448579	0.5334883	0.5230348	0.5106061	0.4980024	0.4850014
2015	0.5941146	0.5885794	0.5816489	0.5739033	0.5664697	0.5561779	0.5488106	0.5375714	0.5258498	0.5151474	0.5032683
2020	0.5992692	0.5940245	0.5884883	0.5836411	0.5759507	0.5672494	0.5595548	0.5514645	0.5422493	0.5311909	0.5204408
2025	0.6076493	0.6029746	0.5977799	0.5931547	0.5866548	0.5789939	0.5722898	0.5651147	0.5560892	0.5466262	0.5365346
2030	0.6188433	0.6147557	0.6100888	0.6048331	0.5990787	0.5917782	0.5869141	0.5788343	0.5698477	0.5610256	0.5515414
2035	0.6327858	0.6284839	0.6240598	0.6188596	0.6131454	0.6050556	0.5989469	0.5925025	0.5839332	0.5751083	0.5655692
2040	0.6487292	0.6442709	0.639204	0.6330692	0.6273717	0.6189746	0.6144949	0.6059858	0.5968165	0.5881008	0.5787939
2045	0.6649018	0.6603633	0.6548824	0.6473299	0.6415506	0.6329263	0.6266813	0.6188987	0.6096261	0.6005025	0.5914025
2050	0.6819195	0.6760201	0.669628	0.6617154	0.6547999	0.6459888	0.6386917	0.6309695	0.6215758	0.6125727	0.6033883
2055	0.6961966	0.6893614	0.6821087	0.6750768	0.666604	0.6578308	0.6495669	0.6422896	0.6326342	0.6238623	0.6147498
2060	0.705721	0.698945	0.6918248	0.6848531	0.6764195	0.6683846	0.6590069	0.6524342	0.6429431	0.6346311	0.6256029
2065	0.7107322	0.7052062	0.6985076	0.6916701	0.6839752	0.6776121	0.6674945	0.6613211	0.6518426	0.6439842	0.635664
2070	0.7119086	0.7071214	0.7014259	0.6955169	0.6885545	0.6845063	0.6754026	0.6687318	0.6604659	0.652953	0.6450397
2075	0.7099715	0.7049615	0.7003912	0.6959082	0.6906081	0.6885821	0.6796525	0.6746867	0.667748	0.6605942	0.6533657
2080	0.7046756	0.7004029	0.6975247	0.6939961	0.6910112	0.6902521	0.6846551	0.679149	0.6729549	0.6670213	0.6603659
2085	0.6956416	0.6953066	0.6948835	0.6913483	0.6911187	0.6900579	0.6852571	0.6819891	0.6771445	0.671401	0.6658377
2090	0.6879703	0.6907176	0.692189	0.6906433	0.6902946	0.6876088	0.6852965	0.6832823	0.6784894	0.6745036	0.6699049
2095	0.6843305	0.6866488	0.6884653	0.6895621	0.6877531	0.6832642	0.6852887	0.6829836	0.6797037	0.6767125	0.6726235
2100	0.6812226	0.6822709	0.6838344	0.6852331	0.6838017	0.6792091	0.6810564	0.6819307	0.6799385	0.677205	0.6742632
2105	0.6755722	0.6766381	0.6785091	0.6791732	0.6799233	0.6754577	0.682077	0.6805429	0.6785375	0.6775148	0.6751366
2110	0.6692607	0.6713263	0.6742005	0.6739495	0.6771932	0.6747149	0.6778988	0.6792533	0.6785164	0.6760649	0.6750523
2115	0.6689993	0.6706265	0.6734797	0.6733696	0.6762012	0.6760574	0.6790665	0.6780134	0.6767521	0.675928	0.6741047
2120	0.6767846	0.6761515	0.6771054	0.6777583	0.6768162	0.6783401	0.6761971	0.676771	0.6755238	0.6740918	0.6723545
2125	0.6851143	0.6834649	0.6826386	0.6807299	0.6787215	0.6799193	0.67663	0.6753859	0.6742193	0.6719906	0.6699682
2130	0.6879864	0.6869176	**0.6857406**	0.6811048	0.680023	0.6815816	0.6742858	0.6737206	0.6709285	0.6693906	0.6671982
2135	0.6865634	0.6861152	0.6848912	0.6802869	0.6788903	0.6801269	0.6743627	0.6714631	0.6681919	0.6663335	0.6642448
2140	0.6856183	0.6831747	0.6808438	0.6792773	0.674966	0.6753327	0.6694421	0.6682114	0.6646748	0.663397	0.661254
2145	0.6850118	0.6789145	0.6757642	0.675466	0.6699182	0.6699134	0.6661792	0.6641231	0.6617632	0.660022	0.6581724
2150	0.6807459	0.6749206	0.6714198	0.6677125	0.6646707	0.6633417	0.6604692	0.6595745	0.6581915	0.6563951	0.6552081
2155	0.6733082	0.6698629	0.666409	0.6599989	0.6593037	0.6562589	0.6539875	0.6553523	0.6532582	0.6527262	0.6527004
2160	0.6648942	0.6622038	0.659214	0.6538603	0.6541275	0.6507598	0.6533411	0.6523783	0.6507407	0.6506923	0.6509328
2165	0.656145	0.6534523	0.6518852	0.6503212	0.6497512	0.646989	0.6464164	0.6506664	0.6496314	0.6500031	0.6499925
2170	0.6461243	0.6456903	0.6461948	0.648499	0.6468353	0.6443817	0.6506416	0.6498607	0.6491466	0.6494775	0.649819
2175	0.6359864	0.6390671	0.6414284	0.6446025	0.6445022	0.6434199	0.6454653	0.6495072	0.648403	0.649249	0.6499192
2180	0.6305746	0.6344032	0.6374232	0.6398521	0.6425437	0.643356	0.6473246	0.6491873	0.647861	0.6496782	0.6500473
2185	0.6304379	0.6329314	0.6355653	0.6364132	0.6407743	0.6423481	0.6453501	0.6486549	0.6484572	0.6489799	0.6499667
2190	0.6311709	0.6334535	0.6356999	0.6366395	0.6401898	0.6423233	0.6423752	0.6480019	0.6480786	0.6482109	0.6496163
2195	0.6321208	0.6345738	0.6364914	0.6393909	0.6405194	0.6432028	0.6459399	0.6475253	0.6466019	0.6483777	0.6491515
2200	0.6360646	0.6372432	0.6384337	0.6413482	0.6414774	0.6437272	0.6413354	0.6475154	0.6463974	0.6477386	0.6489093
2205	0.6448762	0.6435781	0.6427013	0.6443268	0.6435158	0.6447273	0.6483212	0.6484304	0.6471298	0.6484759	0.6492082
2210	0.6552877	0.6525234	0.6500025	0.6479723	0.6480543	0.6487041	0.6455501	0.6507404	0.6493403	0.6496727	0.6505919
2215	0.6679057	0.6638257	0.6600485	0.6551562	0.6556936	0.6555166	0.6553637	0.6553616	0.6531929	0.6533558	0.6534123
2220	0.6855391	0.6793773	0.6739008	0.6702394	0.6668635	0.6659341	0.6613303	0.6628308	0.6591088	0.6583821	0.6581347
2225	0.708897	0.7005637	0.6928033	0.6893628	0.6820838	0.6802361	0.6739848	0.6734944	0.6690984	0.666923	0.665074
2230	0.7365358	0.7265748	0.7168427	0.7107632	0.7016524	0.6970667	0.6912702	0.6874298	0.6815615	0.6769087	0.6744961
2235	0.769633	0.7572126	0.7451934	0.735225	0.7257809	0.717149	0.7077713	0.7047088	0.6957862	0.6914135	0.6863555
2240	0.8050847	0.7915098	0.7773155	0.7641293	0.7530192	0.7406664	0.7343132	0.724911	0.7143186	0.7069893	0.700305
2245	0.8407747	0.8263233	0.8108135	0.7953825	0.782562	0.7666912	0.7534829	0.7470146	0.7345183	0.7245864	0.7155464
2250	0.8745486	0.8597307	**0.8434865**	0.8272408	0.8117083	0.7939053	0.7835479	0.7690521	0.7540638	0.7419872	0.7304647
2255	0.9038078	0.8888204	0.872368	0.8557885	0.8377757	0.8191392	0.8009643	0.7883373	0.7714963	0.7568523	0.7430021
2260	0.9271561	0.9117693	0.8946891	0.8768258	0.8573238	0.8378252	0.8200718	0.8018224	0.783161	0.7667068	0.7508805
2265	0.942628	0.9262947	0.908123	0.8888506	0.8677147	0.8472828	0.82669	0.8071342	0.7874688	0.7694398	0.7524902
2270	0.9486023	0.9308736	0.9109147	0.8893085	0.867282	0.8460317	0.8235382	0.8034624	0.7832688	0.7650776	0.7468936
2275	0.9441255	0.9240232	0.9022171	0.8791943	0.8564042	0.83485	0.8130479	0.7917811	0.7724723	0.7541164	0.7363489
2280	0.9288042	0.906189	0.8832099	0.8598811	0.8369283	0.8156658	0.7933123	0.7743522	0.7558061	0.7389674	0.7231914
2285	0.9035579	0.8800327	0.856889	0.8335086	0.8117667	0.7918429	0.771877	0.7540678	0.738198	0.7231669	0.7088853
2290	0.8717923	0.8484867	0.8259974	0.8039674	0.783964	0.7662641	0.7487702	0.733902	0.7207481	0.7071248	0.6942499
2295	0.8360781	0.8134675	0.7930434	0.7735914	0.7573318	0.7434516	0.7285467	0.7158602	0.7031512	0.6922888	0.6803792
2300	0.7975631	0.7778403	0.7623568	0.7476205	0.7354597	0.7247013	0.7129381	0.700178	0.6894234	0.6782538	0.6673571

Table 5.9. Transmission (TnoH2O) for 2000-2300 nm, with b of 3.3 comparison run.

tnoh2o:	40	45	50	55	60	65	70	75	80	85	90
2000	0.4970434	0.5104911	0.522273	0.5325671	0.5415264	0.5498651	0.557067	0.5642641	0.5713491	0.5782075	0.5847133
2005	0.4496742	0.4786516	0.5020526	0.5204009	0.5352553	0.5473403	0.556915	0.5647488	0.5722346	0.5787372	0.5848503
2010	0.4216039	0.4587496	0.4883551	0.5112474	0.5293587	0.5436772	0.5543392	0.563423	0.5711449	0.5777085	0.5842037
2015	0.4234119	0.4566997	0.4841676	0.5062817	0.523982	0.5384611	0.5500934	0.5593443	0.5677759	0.5751282	0.5819616
2020	0.4536404	0.4732847	0.491192	0.5070946	0.520941	0.5333079	0.5440503	0.5537204	0.562675	0.5712541	0.5786829
2025	0.498972	0.5022188	0.507673	0.5146767	0.5226198	0.531322	0.5405429	0.5494478	0.5587274	0.5672909	0.5760789
2030	0.5451493	0.5346215	0.5293425	0.5282105	0.5305299	0.535274	0.5420793	0.5498196	0.5584962	0.5673018	0.5763555
2035	0.5818605	0.5639149	0.5526437	0.5463498	0.5449771	0.5466971	0.5509595	0.5570657	0.5645301	0.5731769	0.5813912
2040	0.6038283	0.5868456	0.5753069	0.5677726	0.5648154	0.5648667	0.5673649	0.5715755	0.5777469	0.5844336	0.5920934
2045	0.611648	0.6020257	0.5949117	0.5899938	0.5875328	0.5874305	0.5889511	0.5920084	0.5965543	0.6018252	0.6081719
2050	0.6090394	0.6095696	0.6097769	0.6100699	0.6102319	0.6114361	0.6133876	0.6159357	0.6195682	0.623657	0.6283299
2055	0.602456	0.6130192	0.6210522	0.6268862	0.6311414	0.6346602	0.6378742	0.6407288	0.6438454	0.647317	0.6507457
2060	0.601431	0.6185946	0.6321847	0.6420445	0.6501104	0.6559668	0.6605911	0.6644669	0.6677355	0.6706264	0.6736495
2065	0.6145402	0.6322395	0.6471993	0.6587632	0.6685957	0.6757909	0.6819685	0.6864907	0.6903697	0.6930721	0.6958013
2070	0.6438646	0.6570854	0.6693645	0.6797951	0.6889566	0.6962141	0.7024414	0.7073392	0.7111081	0.7144757	0.7167086
2075	0.6847709	0.692084	0.6995989	0.7068467	0.7131765	0.718868	0.7241136	0.7282091	0.731634	0.734363	0.7365716
2080	0.7322095	0.7336533	0.7359968	0.7388419	0.7416362	0.7445981	0.7477727	0.7502309	0.7526389	0.7543387	0.7560003
2085	0.7820484	0.7780615	0.7755325	0.7738085	0.7731953	0.7729583	0.7733518	0.7739125	0.7744983	0.7752633	0.7756355
2090	0.82879	0.8212202	0.8150164	0.8097349	0.8060243	0.8029884	0.8008604	0.7989976	0.7977533	0.7967403	0.7958347
2095	0.8681448	0.8593874	0.8513979	0.844138	0.8381001	0.8328547	0.8282432	0.8246584	0.8214755	0.8187584	0.816543
2100	0.899546	0.8909956	0.8827286	0.8749269	0.8676022	0.8610758	0.8550841	0.8497767	0.8451155	0.8409799	0.8373415
2105	0.9243102	0.9164532	0.9085988	0.9009784	0.8933194	0.8863021	0.8794051	0.8732371	0.8675727	0.8624177	0.8575976
2110	0.9433416	0.9364859	0.929355	0.9221332	0.9148378	0.9077699	0.9007776	0.8941905	0.8879098	0.8820338	0.8766438
2115	0.9573563	0.9516284	0.94542	0.9388464	0.9321944	0.9254741	0.9188325	0.91218	0.9058216	0.899738	0.8939342
2120	0.9673761	0.9626243	0.9573469	0.9515854	0.9456915	0.939572	0.933292	0.9271038	0.9209638	0.9150227	0.909129
2125	0.9745035	0.9704175	0.9659085	0.9609849	0.9558283	0.950424	0.9448681	0.9391176	0.9334345	0.9276925	0.9220986
2130	0.979418	0.9758123	0.9719153	0.9677715	0.963254	0.9585553	0.9536235	0.9485453	0.9434158	0.938114	0.9328852
2135	0.9824875	0.9793523	0.9760055	0.972473	0.9685943	0.9645563	0.9602757	0.9557905	0.9512077	0.9464747	0.941642
2140	0.9840398	0.9814337	0.9786274	0.9755648	0.9723505	0.968872	0.9652306	0.9612474	0.9571916	0.9529601	0.9485771
2145	0.9843924	0.9823495	0.9800906	0.9774772	0.9748585	0.9718936	0.9686781	0.9652369	0.9616823	0.9578617	0.9539047
2150	0.9838547	0.9823714	0.9806464	0.9786003	0.9763602	0.9738106	0.9710535	0.9679825	0.9648102	0.9614171	0.9578136
2155	0.9827967	0.9818043	0.980522	0.9790294	0.9769931	0.9747598	0.9723521	0.9696228	0.9667971	0.9637554	0.9604639
2160	0.9816113	0.9809176	0.9798971	0.9786697	0.976854	0.9748729	0.9726341	0.9702488	0.9677181	0.9649072	0.9620043
2165	0.9805822	0.9798637	0.9788501	0.9774759	0.9759594	0.9741299	0.9722847	0.9699601	0.9676282	0.9652339	0.9625944
2170	0.9795762	0.9785265	0.9772819	0.9756669	0.9743336	0.9726022	0.9707943	0.9689217	0.9669792	0.964701	0.9624088
2175	0.9779993	0.9764974	0.9749753	0.9734069	0.9720862	0.9705911	0.9692176	0.9673717	0.9656122	0.9635628	0.9616072
2180	0.9751326	0.9734602	0.971966	0.9709203	0.9695645	0.9683929	0.9668992	0.9655365	0.9638079	0.9622173	0.9602928
2185	0.9710637	0.9698953	0.9688833	0.9684924	0.967156	0.9662359	0.9648236	0.9635028	0.9620321	0.9603505	0.9584961
2190	0.9673256	0.9669504	0.966391	0.9659584	0.9649296	0.9641343	0.9625545	0.9611833	0.9596851	0.9580037	0.9561946
2195	0.9648443	0.9647946	0.9642375	0.9632221	0.9625101	0.9616221	0.959821	0.9583986	0.9568719	0.9551411	0.9533477
2200	0.9623978	0.9622694	0.9615215	0.9602212	0.9594112	0.9582788	0.9567533	0.9549807	0.9534467	0.9517612	0.949923
2205	0.9587578	0.9584512	0.9576321	0.9564145	0.9553545	0.9539661	0.9525067	0.9508357	0.9491777	0.9476426	0.945911
2210	0.9543343	0.9535897	0.952693	0.951834	0.9503594	0.9488077	0.9477133	0.9459718	0.9445747	0.9429221	0.941335
2215	0.9502992	0.9486854	0.9473794	0.9464142	0.944742	0.9429679	0.9419479	0.9404915	0.9392285	0.9377319	0.936255
2220	0.9464515	0.9440807	0.9421694	0.9404639	0.9388461	0.9368982	0.9360281	0.9345581	0.9331649	0.9321212	0.9307671
2225	0.9411294	0.9387053	0.936573	0.9342841	0.9327263	0.9307039	0.929433	0.9283316	0.9272349	0.9260051	0.9249918
2230	0.9335051	0.9315134	0.9297078	0.9274462	0.9260697	0.9242624	0.9235262	0.9218911	0.921138	0.9199007	0.9190422
2235	0.9238824	0.9225386	0.9213285	0.9199132	0.9185961	0.9172698	0.9158992	0.91522	0.9145676	0.9137678	0.912984
2240	0.9129911	0.9124029	0.9118817	0.9112604	0.9104167	0.909721	0.909707	0.9082828	0.9078594	0.9074012	0.9068235
2245	0.9017606	0.9019229	0.9020888	0.9018556	0.9018779	0.9018956	0.9014512	0.9011013	0.9010689	0.9007841	0.9005365
2250	0.8912387	0.8918636	0.8925642	0.8930495	0.8933555	0.894011	0.8940228	0.8937582	0.8940706	0.8940423	0.8941141
2255	0.8815225	0.8825272	0.8835676	0.8844468	0.8850262	0.8861705	0.8865463	0.8863587	0.8870443	0.8873255	0.8875944
2260	0.8723616	0.87387	0.8750892	0.8761932	0.8769667	0.8784506	0.8775779	0.8790063	0.8798319	0.8803758	0.8810676
2265	0.8643301	0.8658249	0.8670415	0.8681209	0.8691298	0.8708936	0.8718209	0.8718207	0.872701	0.8738402	0.8746619
2270	0.8573729	0.8582898	0.8593501	0.8600314	0.8616073	0.863306	0.8627934	0.8649697	0.8665413	0.8673936	0.8685137
2275	0.8506774	0.8512291	0.8521305	0.8534503	0.8546287	0.8564566	0.8583416	0.8586502	0.8602536	0.8612907	0.8627294
2280	0.8439434	0.8447788	0.8457736	0.847618	0.8486317	0.8505347	0.8515139	0.8530059	0.854322	0.856082	0.8573649
2285	0.838187	0.839439	0.8407596	0.8424129	0.8437828	0.8453047	0.8468643	0.8480526	0.8498145	0.8512025	0.8524323
2290	0.8342515	0.8357172	0.8371236	0.8381528	0.8398423	0.8407988	0.8429167	0.843702	0.8451224	0.846508	0.8479111
2295	0.8316326	0.8329491	0.8340651	0.8346684	0.8363383	0.837077	0.8377064	0.8398355	0.8412304	0.8424878	0.843748
2300	0.8284992	0.8297087	0.830842	0.8321766	0.8330879	0.8335095	0.8359098	0.8363037	0.8375998	0.8387617	0.8398652

Table 5.10. α for 2000-2300 nm, with b of 3.3 comparison run.

alpha:	40	45	50	55	60	65	70	75	80	85	90
2000	0.1620361	0.1688974	0.1765834	0.1841538	0.1926514	0.2013908	0.2112488	0.2202777	0.2309253	0.2397669	0.2493733
2005	0.1414166	0.1467622	0.1528155	0.1590298	0.1658887	0.1735522	0.1808421	0.189421	0.1976759	0.2073484	0.2160131
2010	0.1239027	0.1276986	0.1325885	0.1381419	0.1434623	0.1499582	0.1571446	0.1635754	0.1717556	0.1792982	0.1874951
2015	0.107383	0.1108341	0.1149844	0.1197272	0.1243867	0.1298699	0.1357992	0.1418033	0.1491619	0.1561072	0.1632119
2020	0.0923136	0.0957021	0.0994926	0.1030542	0.107964	0.112973	0.1180486	0.1233502	0.1292742	0.136122	0.1425409
2025	0.0794431	0.0824108	0.085943	0.0894553	0.0937769	0.0986172	0.103554	0.1076451	0.1136056	0.1191068	0.124916
2030	0.0681369	0.0710563	0.0743236	0.0779021	0.0816275	0.0862752	0.0896105	0.0942152	0.0994071	0.1045545	0.1098329
2035	0.058091	0.0612483	0.0644544	0.0677842	0.0712789	0.0757606	0.0791575	0.0827195	0.0874568	0.0919758	0.0968763
2040	0.0500321	0.0530089	0.0561074	0.0592468	0.0624884	0.0665808	0.0691609	0.0728557	0.0772946	0.0813188	0.085715
2045	0.0438621	0.0464294	0.0491813	0.0521038	0.054962	0.0585243	0.0611265	0.0643843	0.0682209	0.0721379	0.0760823
2050	0.0390875	0.0412244	0.0435392	0.0461043	0.0486236	0.051692	0.0544286	0.0571373	0.0608293	0.0641669	0.067782
2055	0.0354172	0.0371305	0.0390231	0.0411347	0.0433772	0.0459153	0.0484647	0.0509982	0.0541734	0.0572796	0.0606524
2060	0.0326591	0.0339628	0.0354835	0.0372635	0.0391742	0.0412792	0.043895	0.0458935	0.0486855	0.0515519	0.0545758
2065	0.0307517	0.0315965	0.0327928	0.034223	0.0358883	0.0374577	0.0398399	0.0417264	0.044475	0.0467965	0.049427
2070	0.0291811	0.0298333	0.0308034	0.0318869	0.0334147	0.0345267	0.0366408	0.0383642	0.0405493	0.0427804	0.0451083
2075	0.0275547	0.0284228	0.0293099	0.0302099	0.0315164	0.0323344	0.0342069	0.0356447	0.0375082	0.0394391	0.0414873
2080	0.026294	0.0272575	0.0280584	0.0289833	0.0299502	0.0306417	0.032024	0.0333957	0.0350207	0.036626	0.0384539
2085	0.0256061	0.0262277	0.0268677	0.0279626	0.0284931	0.0292275	0.0304326	0.0314711	0.0327879	0.0343234	0.0358937
2090	0.0248223	0.0251784	0.0256876	0.0265713	0.0271479	0.0281156	0.0289988	0.0297995	0.0311828	0.0323576	0.0337234
2095	0.0237525	0.0241949	0.0246444	0.0251221	0.0259512	0.0271535	0.0274521	0.0283243	0.0293955	0.0305676	0.0318622
2100	0.0231636	0.0235323	0.0238725	0.0241743	0.0249373	0.0261312	0.0264829	0.0270222	0.02803	0.0290929	0.0302854
2105	0.0231125	0.0231617	0.0232843	0.0235691	0.0240391	0.0252113	0.0250983	0.0258986	0.0270005	0.0278392	0.0289837
2110	0.0227749	0.0226513	0.0226278	0.0230268	0.0232095	0.0241156	0.0243846	0.0249747	0.0258619	0.0270472	0.0279691
2115	0.0215903	0.0215986	0.021683	0.0221206	0.0224231	0.0230578	0.0235494	0.0242995	0.025324	0.0261696	0.0272467
2120	0.019961	0.020219	0.0206038	0.0209938	0.0217853	0.0222774	0.0232695	0.023898	0.024851	0.0258241	0.0267991
2125	0.0185752	0.019179	0.0198455	0.0206209	0.0214354	0.0219553	0.0230255	0.0237514	0.0246628	0.0256094	0.0265851
2130	0.0179719	0.0188957	**0.0197381**	0.0208735	0.0214923	0.0218843	0.0232925	0.0238327	0.0248062	0.0256142	0.0265496
2135	0.0182959	0.0192843	0.0201799	0.0212517	0.021888	0.0222632	0.0232926	0.0240897	0.0249988	0.0258122	0.0266539
2140	0.0190293	0.0199746	0.0208608	0.0214955	0.0224851	0.0229453	0.0241377	0.0244979	0.0255703	0.0260718	0.026867
2145	0.0198356	0.020844	0.0216615	0.0220419	0.0231963	0.0236834	0.0243462	0.0250282	0.0257847	0.0265125	0.0271603
2150	0.0213228	0.0221031	0.0227403	0.0234034	0.0241044	0.0246638	0.025401	0.0256665	0.026271	0.0269453	0.0274982
2155	0.0237414	0.0239591	0.0243474	0.0252574	0.0253427	0.026015	0.0263402	0.0264114	0.027189	0.0274712	0.0278339
2160	0.0266206	0.0264706	0.0265604	0.0271971	0.0269204	0.0274748	0.0270796	0.0272128	0.02768	0.0279742	0.0281298
2165	0.0294515	0.0293293	0.0290807	0.0287901	0.0286615	0.0288693	0.0288229	0.0279928	0.0282467	0.0282558	0.0283507
2170	0.032171	0.0318762	0.0313178	0.0301239	0.0301846	0.0301326	0.0287783	0.0286382	0.0286455	0.0285071	0.0284651
2175	0.0345105	0.0336221	0.0328285	0.0316503	0.0312377	0.0308807	0.0303458	0.0290245	0.028946	0.0286667	0.0284356
2180	0.0356811	0.0345262	0.0335768	0.032889	0.031653	0.0309471	0.0296839	0.0290749	0.0291047	0.0284928	0.0282355
2185	0.0359173	0.0347467	0.0336177	0.0331167	0.0314778	0.0306443	0.0299182	0.0287588	0.0284404	0.0281758	0.0278536
2190	0.0357209	0.0342838	0.0330179	0.0319661	0.0307563	0.0298695	0.0291894	0.0281015	0.0278141	0.0276014	0.0272883
2195	0.0345576	0.0329628	0.0317455	0.0301175	0.0295827	0.0286331	0.027795	0.0271608	0.0272455	0.0267291	0.0265566
2200	0.0317564	0.0306365	0.0297302	0.0284012	0.0279637	0.02713	0.0271612	0.025972	0.0260228	0.025778	0.0256764
2205	0.0279324	0.0274712	0.027011	0.0263167	0.0258954	0.0253545	0.0246648	0.0245555	0.0246957	0.0246456	0.0246664
2210	0.0240021	0.0238859	0.0238222	0.0238522	0.0234508	0.0231414	0.0236872	0.0229185	0.0232384	0.0233773	0.0235275
2215	0.0199087	0.0201434	0.0204547	0.0208762	0.0207705	0.0206918	0.0208616	0.0210938	0.0215849	0.0218822	0.0222703
2220	0.0158589	0.0164794	0.0171071	0.0175422	0.0180303	0.0182539	0.0190789	0.019146	0.0199122	0.0203811	0.0209231
2225	0.0123602	0.0131771	0.0139918	0.0144827	0.0153556	0.0158701	0.0166805	0.0171712	0.0180195	0.0187887	0.0195633
2230	0.0095805	0.0104124	0.0112903	0.0119675	0.0129178	0.0137045	0.0144854	0.0152686	0.0162663	0.017271	0.0184566
2235	0.0074005	0.0081977	0.0090723	0.009911	0.0108046	0.0117945	0.0128201	0.0135346	0.0147897	0.0159605	0.0170215
2240	0.0057666	0.0065117	0.0073393	0.008197	0.0090923	0.01019	0.0109376	0.0120534	0.0134954	0.0145777	0.0157421
2245	0.0046372	0.0052998	0.0060614	0.0069068	0.0077748	0.0088882	0.0099947	0.0109496	0.0121837	0.0135009	0.0148648
2250	0.0039094	0.0044948	**0.0051892**	0.0059827	0.0068529	0.0079306	0.0088644	0.0100581	0.0114289	0.0128116	0.0142926
2255	0.0034705	0.0040086	0.0046596	0.0053992	0.0062821	0.0073439	0.0084897	0.0096039	0.0110209	0.0124839	0.014075
2260	0.0032445	0.0037718	0.0044039	0.0051545	0.0060802	0.0071271	0.0082773	0.0095354	0.0110185	0.012565	0.0142598
2265	0.0032035	0.0037564	0.0044359	0.0052426	0.0061973	0.0072803	0.0084894	0.0098736	0.0114195	0.0130884	0.0148849
2270	0.0033772	0.003999	0.0047471	0.0056445	0.0066673	0.0078321	0.0092154	0.0106441	0.012296	0.014059	0.0159815
2275	0.0037821	0.004508	0.0053689	0.0063889	0.0075311	0.0088024	0.0102429	0.0118845	0.0136544	0.015552	0.0175819
2280	0.0045054	0.0053781	0.0063924	0.0075467	0.0088543	0.0102655	0.0119485	0.0136334	0.0155462	0.0175689	0.0197149
2285	0.0056796	0.0067376	0.0079137	0.0092428	0.010709	0.012271	0.0140656	0.0159316	0.0179204	0.0200806	0.0223898
2290	0.0074448	0.008682	0.0100348	0.0115613	0.013168	0.0148911	0.0167994	0.0188062	0.0208897	0.0231861	0.0256259
2295	0.0099292	0.0113527	0.0128649	0.0145709	0.0162824	0.0180908	0.020191	0.022265	0.0245752	0.0268612	0.0294489
2300	0.0133097	0.0148914	0.0164748	0.0182733	0.0201095	0.021909	0.0239065	0.0263165	0.0286432	0.0311595	0.0338867

Table 5.11. β for 2000-2300 nm, with b of 3.3 comparison run.

beta:	40	45	50	55	60	65	70	75	80	85	90
2000	0.5609697	0.5486332	0.5347809	0.521219	0.5066472	0.4916978	0.4770209	0.4627911	0.448501	0.4355352	0.4231023
2005	0.5692897	0.5579225	0.545403	0.5326703	0.5197257	0.5052238	0.4931193	0.4785714	0.4657279	0.4521481	0.4396226
2010	0.5747228	0.5651996	0.5539861	0.5418792	0.5308767	0.5171217	0.5044648	0.4930323	0.4805011	0.4680311	0.4556053
2015	0.5800534	0.571426	0.5615838	0.5511962	0.5410258	0.5286381	0.5191541	0.5065845	0.4940422	0.4828695	0.4709824
2020	0.5868561	0.5784747	0.5696917	0.561742	0.5511808	0.5398874	0.5298538	0.5196875	0.5089935	0.4970544	0.4857779
2025	0.595255	0.5877088	0.5795133	0.5718156	0.5622178	0.551684	0.5425636	0.5326594	0.5219627	0.5110558	0.5000099
2030	0.6060923	0.5989833	0.5912457	0.5831155	0.5743112	0.5642406	0.5561755	0.5457554	0.5349631	0.5244895	0.5137084
2035	0.6194668	0.612104	0.6044521	0.59609	0.5874992	0.5770259	0.5680385	0.5588651	0.5483752	0.5377892	0.5268694
2040	0.6342239	0.6268062	0.6187091	0.6094864	0.600931	0.5901942	0.5826153	0.5717788	0.5606843	0.5501817	0.5394639
2045	0.6498951	0.6420032	0.6332909	0.6231958	0.6143957	0.6035758	0.5941647	0.5842277	0.5731903	0.5622534	0.5515063
2050	0.6659723	0.6568246	0.6472974	0.6370232	0.627114	0.616169	0.6062518	0.5960057	0.5847699	0.5738419	0.5629709
2055	0.6801201	0.6701512	0.6599119	0.64996	0.6388565	0.6277816	0.6169361	0.6070799	0.5953977	0.5847734	0.5739202
2060	0.6904275	0.6806209	0.6702701	0.6601809	0.6490401	0.6385427	0.626739	0.6173151	0.6059039	0.5954099	0.5843272
2065	0.6964207	0.6876053	0.6777622	0.667843	0.6574103	0.6483123	0.6358294	0.6265944	0.6151134	0.6047028	0.5942584
2070	0.6991106	0.6911593	0.6823621	0.6732655	0.6635485	0.6562259	0.6443887	0.6347716	0.6239671	0.6138327	0.6034771
2075	0.6993962	0.6917649	0.6841416	0.6761966	0.6676883	0.6619626	0.6501409	0.6417027	0.6318437	0.6218107	0.6119558
2080	0.6961332	0.6897926	0.6838555	0.6768726	0.6701184	0.665346	0.6561987	0.6473512	0.6379687	0.6290575	0.6194758
2085	0.6893274	0.6860689	0.6822687	0.6758024	0.6714974	0.6667069	0.6584451	0.651795	0.6434683	0.6346896	0.6259538
2090	0.6829318	0.6821926	0.6802636	0.6758191	0.671872	0.6659311	0.6604682	0.654826	0.6467721	0.6392077	0.6311944
2095	0.679666	0.6792682	0.6782003	0.6761795	0.6712899	0.6639517	0.6619729	0.6566085	0.6495665	0.6430624	0.6353664
2100	0.6771478	0.6764075	0.6755481	0.6740715	0.6697376	0.6621949	0.6605256	0.6573948	0.6515392	0.645051	0.6384818
2105	0.6732745	0.6727368	0.6724386	0.6702299	0.6678093	0.6604378	0.6624386	0.6575618	0.651877	0.6468263	0.6408029
2110	0.6696188	0.6695616	0.6697372	0.6667075	0.6662338	0.6605462	0.6600463	0.6576822	0.653219	0.6474188	0.6425019
2115	0.6699551	0.6695024	0.6695195	0.6668058	0.6659938	0.6624684	0.6620371	0.6579238	0.6534021	0.6489782	0.6436929
2120	0.6746712	0.6730446	0.6721489	0.6705717	0.6671013	0.6653569	0.6606274	0.6582897	0.6539658	0.6495227	0.6444167
2125	0.6800578	0.6775172	0.6757169	0.6723146	0.6688505	0.6675512	0.6624294	0.6586734	0.6548892	0.6497852	0.6446747
2130	0.6822384	0.6798816	**0.6776461**	0.67208	0.6698403	0.6695698	0.6611161	0.6585327	0.6536969	0.649537	0.6445225
2135	0.6817524	0.6797039	0.6772273	0.6716945	0.6691818	0.6689975	0.6621395	0.6577138	0.6527113	0.6485252	0.6438959
2140	0.6816168	0.6782652	0.6749741	0.6719466	0.6668132	0.6657375	0.6587005	0.6559593	0.6509753	0.6473753	0.6428331
2145	0.6815448	0.6756485	0.671662	0.6698968	0.663532	0.6620894	0.6570123	0.6535698	0.6494397	0.6457379	0.6414446
2150	0.6774479	0.6715372	0.66774	0.6636472	0.6597995	0.6575444	0.6535193	0.650995	0.6476499	0.6437215	0.6399224
2155	0.6698345	0.6663285	0.6630383	0.6571125	0.655892	0.6522948	0.6487734	0.6484605	0.6445085	0.6414733	0.6385682
2160	0.6625178	0.6601869	0.6574878	0.6523265	0.6520458	0.6479844	0.6490334	0.646424	0.642737	0.6401274	0.6375042
2165	0.6554345	0.6530645	0.6515332	0.6496825	0.6482963	0.6445534	0.6428072	0.6449354	0.6418806	0.6396722	0.6367906
2170	0.6464307	0.6457808	0.6458761	0.6477408	0.6452721	0.6417158	0.6464286	0.6439297	0.6411598	0.6389779	0.6363423
2175	0.6374237	0.6396949	0.6412816	0.6436867	0.6427057	0.6403939	0.6411921	0.643286	0.6401079	0.638402	0.6360682
2180	0.6328556	0.6360206	0.6380732	0.6393611	0.6408844	0.6403165	0.6426669	0.6426503	0.6392326	0.6383635	0.6357734
2185	0.632317	0.6345437	0.6365843	0.6364063	0.6396002	0.6397424	0.6409269	0.6420141	0.6396071	0.6374238	0.6352651
2190	0.6323284	0.634459	0.6362943	0.6366247	0.6391461	0.6400195	0.6383893	0.641517	0.6391841	0.63647	0.6345754
2195	0.6334063	0.6355742	0.6371213	0.6393937	0.6394331	0.6409524	0.6419401	0.6412101	0.6378271	0.6364551	0.6337723
2200	0.6377478	0.6387837	0.6394574	0.6415997	0.6406644	0.6416007	0.6376192	0.6413541	0.6375621	0.6356676	0.6330562
2205	0.6453876	0.6445754	0.6437901	0.644822	0.6432335	0.6430214	0.6445652	0.6421532	0.6380603	0.6358344	0.6325856
2210	0.6546943	0.6525212	0.6504626	0.6480693	0.6475192	0.6468826	0.6419143	0.6439984	0.6395196	0.6360912	0.6326962
2215	0.6664248	0.6628293	0.6593207	0.6541696	0.653989	0.652477	0.6500233	0.647238	0.641829	0.6380111	0.6335898
2220	0.6817329	0.6762823	0.6710533	0.666989	0.6627688	0.6601751	0.6538824	0.652171	0.6452434	0.6403347	0.6353192
2225	0.7010022	0.6934713	0.686235	0.682463	0.6743892	0.6703318	0.6623775	0.6587434	0.6510181	0.6446273	0.6373652
2230	0.7241751	0.7142099	0.7047079	0.6982521	0.6884248	0.6816089	0.6739962	0.6668031	0.6576055	0.6488245	0.6354939
2235	0.7505296	0.7381043	0.7259353	0.7152735	0.7047017	0.6940658	0.6825023	0.6759987	0.664107	0.6500986	0.6420262
2240	0.7785087	0.7636244	0.7487845	0.7342129	0.7219507	0.7078105	0.6983657	0.6856564	0.6676104	0.6588562	0.6493229
2245	0.8069991	0.7894294	0.7718174	0.7545227	0.7393256	0.721777	0.70581	0.6929424	0.6795712	0.6660301	0.6529613
2250	0.8336632	0.8134708	**0.793365**	0.7747262	0.7551395	0.7348258	0.720376	0.7030927	0.6858817	0.670512	0.6556627
2255	0.8561996	0.8339862	0.8117793	0.79084	0.7689704	0.7459546	0.7256969	0.7090179	0.6900657	0.673291	0.6570383
2260	0.8735251	0.8497074	0.8262398	0.8018715	0.7768999	0.7531708	0.7322437	0.7121211	0.6919188	0.6739306	0.6566272
2265	0.8845236	0.858906	0.8324147	0.805362	0.7804899	0.7559456	0.7335788	0.7119308	0.6914035	0.6722178	0.6542854
2270	0.8858566	0.8581367	0.8310052	0.8035229	0.7784604	0.7539833	0.7297379	0.7084467	0.6875872	0.6683977	0.650132
2275	0.8791955	0.8511823	0.8238487	0.7969119	0.7713352	0.7477456	0.7246653	0.7018853	0.6816415	0.662211	0.6443416
2280	0.8657178	0.8381502	0.8110077	0.785112	0.7598937	0.7372519	0.7134048	0.6929137	0.6730449	0.6546568	0.637233
2285	0.846752	0.8194261	0.7938524	0.7687035	0.7452815	0.7242674	0.7023087	0.6822897	0.6638509	0.6464708	0.6295111
2290	0.8232515	0.7975616	0.7736845	0.7499433	0.7288042	0.7094733	0.689102	0.6709701	0.6544874	0.6374339	0.6215423
2295	0.7967165	0.7733028	0.7519816	0.7307059	0.7120109	0.6950798	0.6760393	0.6598824	0.6436402	0.6288137	0.6135945
2300	0.7689539	0.7486641	0.7308915	0.7125113	0.6954283	0.6814575	0.6660494	0.649596	0.6347902	0.6203553	0.6059631

Table 5.12. Indices 2000-2300 nm. IW/λ – Index Water/Wavelength, II/λ – Index Ice/Wavelength

λ (nm)	IW/λ	II/λ	λ (nm)	IW/λ	II/λ	λ (nm)	IW/λ	II/λ	λ (nm)	IW/λ	II/λ	λ (nm)	IW/λ	II/λ	λ (nm)	IW/λ	II/λ
2000	0.0005505	0.00082	2056	0.0003149	0.000643	2112	0.0002049	0.0003286	2168	0.0001617	0.0001529	2224	0.0001546	0.0000985	2280	0.0001883	0.0001032
2001	0.0005441	0.0008178	2057	0.0003122	0.0006382	2113	0.0002036	0.000324	2169	0.0001613	0.000151	2225	0.0001548	0.000098	2281	0.0001891	0.000104
2002	0.0005377	0.0008155	2058	0.0003094	0.0006335	2114	0.0002023	0.0003195	2170	0.0001609	0.0001491	2226	0.0001549	0.0000975	2282	0.0001898	0.0001048
2003	0.0005313	0.0008133	2059	0.0003066	0.0006287	2115	0.000201	0.0003149	2171	0.0001605	0.0001478	2227	0.0001551	0.0000971	2283	0.0001906	0.0001055
2004	0.0005249	0.000811	2060	0.0003039	0.000624	2116	0.0001997	0.0003104	2172	0.0001601	0.0001465	2228	0.0001552	0.0000966	2284	0.0001913	0.0001063
2005	0.0005185	0.0008088	2061	0.0003011	0.0006192	2117	0.0001985	0.0003058	2173	0.0001597	0.0001453	2229	0.0001556	0.0000961	2285	0.0001921	0.000107
2006	0.0005122	0.0008066	2062	0.0002984	0.0006145	2118	0.0001972	0.0003013	2174	0.0001593	0.000144	2230	0.000156	0.0000956	2286	0.0001929	0.0001078
2007	0.0005058	0.0008043	2063	0.0002957	0.0006086	2119	0.0001961	0.0002967	2175	0.0001589	0.0001427	2231	0.0001564	0.0000952	2287	0.0001936	0.0001086
2008	0.0004994	0.0008021	2064	0.0002929	0.0006027	2120	0.000195	0.0002922	2176	0.0001585	0.0001414	2232	0.0001568	0.0000947	2288	0.0001944	0.0001093
2009	0.000493	0.0007999	2065	0.0002902	0.0005968	2121	0.000194	0.0002876	2177	0.0001581	0.0001402	2233	0.0001572	0.0000942	2289	0.0001952	0.0001101
2010	0.0004871	0.0007976	2066	0.0002875	0.000591	2122	0.0001929	0.0002831	2178	0.0001577	0.0001389	2234	0.0001575	0.0000938	2290	0.0001959	0.0001108
2011	0.0004813	0.0007954	2067	0.0002848	0.0005851	2123	0.0001919	0.0002785	2179	0.0001574	0.0001376	2235	0.0001579	0.0000933	2291	0.0001967	0.0001121
2012	0.0004755	0.0007931	2068	0.000282	0.0005792	2124	0.0001908	0.000274	2180	0.0001572	0.0001363	2236	0.0001583	0.0000928	2292	0.0001974	0.0001133
2013	0.0004696	0.0007909	2069	0.0002793	0.0005733	2125	0.0001897	0.0002694	2181	0.0001569	0.0001351	2237	0.0001587	0.0000924	2293	0.0001981	0.0001146
2014	0.0004638	0.0007887	2070	0.0002766	0.0005675	2126	0.0001887	0.0002649	2182	0.0001567	0.0001338	2238	0.0001591	0.0000919	2294	0.0001988	0.0001158
2015	0.000458	0.0007864	2071	0.0002744	0.0005616	2127	0.0001876	0.0002604	2183	0.0001564	0.0001325	2239	0.0001595	0.0000914	2295	0.0001995	0.0001171
2016	0.0004521	0.0007842	2072	0.0002722	0.0005557	2128	0.0001866	0.0002558	2184	0.0001562	0.0001312	2240	0.0001602	0.0000909	2296	0.0002002	0.0001183
2017	0.0004463	0.000782	2073	0.00027	0.0005498	2129	0.0001858	0.0002513	2185	0.0001559	0.00013	2241	0.0001608	0.0000908	2297	0.0002009	0.0001196
2018	0.0004404	0.0007797	2074	0.0002677	0.000544	2130	0.000185	0.0002467	2186	0.0001557	0.0001287	2242	0.0001615	0.0000907	2298	0.0002016	0.0001208
2019	0.0004361	0.0007775	2075	0.0002655	0.0005381	2131	0.0001843	0.0002437	2187	0.0001554	0.0001274	2243	0.0001622	0.0000905	2299	0.0002023	0.0001221
2020	0.0004317	0.0007752	2076	0.0002633	0.0005322	2132	0.0001835	0.0002408	2188	0.0001552	0.0001262	2244	0.0001629	0.0000904	2300	0.000203	0.0001233
2021	0.0004274	0.0007723	2077	0.0002611	0.0005264	2133	0.0001828	0.0002378	2189	0.000155	0.0001249	2245	0.0001635	0.0000902			
2022	0.000423	0.0007694	2078	0.0002589	0.0005205	2134	0.000182	0.0002348	2190	0.0001549	0.0001236	2246	0.0001642	0.0000903			
2023	0.0004187	0.0007665	2079	0.0002567	0.0005146	2135	0.0001812	0.0002318	2191	0.0001547	0.0001228	2247	0.0001649	0.0000903			
2024	0.0004143	0.0007636	2080	0.0002545	0.0005087	2136	0.0001805	0.0002289	2192	0.0001546	0.0001221	2248	0.0001656	0.0000904			
2025	0.00041	0.0007607	2081	0.0002522	0.0005029	2137	0.0001797	0.0002259	2193	0.0001544	0.0001213	2249	0.0001663	0.0000904			
2026	0.0004056	0.0007578	2082	0.0002499	0.000497	2138	0.000179	0.0002229	2194	0.0001543	0.0001205	2250	0.0001669	0.0000904			
2027	0.0004013	0.000755	2083	0.0002476	0.0004911	2139	0.0001783	0.0002199	2195	0.0001542	0.0001197	2251	0.0001675	0.0000906			
2028	0.0003969	0.0007521	2084	0.0002453	0.0004852	2140	0.0001777	0.000217	2196	0.000154	0.000119	2252	0.0001681	0.0000907			
2029	0.0003944	0.0007492	2085	0.000243	0.0004792	2141	0.000177	0.000214	2197	0.0001539	0.0001182	2253	0.0001688	0.0000909			
2030	0.000392	0.0007463	2086	0.0002407	0.0004733	2142	0.0001764	0.000211	2198	0.0001537	0.0001174	2254	0.0001694	0.000091			
2031	0.0003895	0.0007434	2087	0.0002384	0.0004673	2143	0.0001757	0.000208	2199	0.0001537	0.0001166	2255	0.00017	0.0000912			
2032	0.000387	0.0007405	2088	0.0002361	0.0004614	2144	0.0001751	0.0002051	2200	0.0001537	0.0001159	2256	0.0001707	0.0000913			
2033	0.0003845	0.0007376	2089	0.0002338	0.0004555	2145	0.0001744	0.0002021	2201	0.0001536	0.0001151	2257	0.0001713	0.0000915			
2034	0.000382	0.0007347	2090	0.0002325	0.0004495	2146	0.0001738	0.0001991	2202	0.0001536	0.0001143	2258	0.0001719	0.0000916			
2035	0.0003795	0.0007318	2091	0.0002313	0.0004436	2147	0.0001731	0.0001961	2203	0.0001536	0.0001135	2259	0.0001726	0.0000918			
2036	0.000377	0.0007289	2092	0.00023	0.0004376	2148	0.0001725	0.0001932	2204	0.0001535	0.0001128	2260	0.0001732	0.0000919			
2037	0.0003745	0.000726	2093	0.0002288	0.0004317	2149	0.0001719	0.0001902	2205	0.0001535	0.000112	2261	0.0001739	0.0000923			
2038	0.000372	0.0007231	2094	0.0002275	0.0004257	2150	0.0001712	0.0001872	2206	0.0001535	0.0001112	2262	0.0001745	0.0000927			
2039	0.0003695	0.0007202	2095	0.0002262	0.0004198	2151	0.0001706	0.0001853	2207	0.0001534	0.0001104	2263	0.0001752	0.0000931			
2040	0.000367	0.0007173	2096	0.000225	0.0004139	2152	0.00017	0.0001834	2208	0.0001534	0.0001097	2264	0.0001758	0.0000934			
2041	0.0003645	0.0007144	2097	0.0002237	0.0004079	2153	0.0001694	0.0001815	2209	0.0001534	0.0001089	2265	0.0001765	0.0000938			
2042	0.000362	0.0007096	2098	0.0002225	0.000402	2154	0.0001687	0.0001796	2210	0.0001535	0.0001081	2266	0.0001772	0.0000942			
2043	0.0003583	0.0007048	2099	0.0002212	0.000396	2155	0.0001681	0.0001777	2211	0.0001535	0.0001073	2267	0.0001778	0.0000945			
2044	0.0003546	0.0007001	2100	0.00022	0.0003901	2156	0.0001675	0.0001758	2212	0.0001535	0.0001066	2268	0.0001785	0.0000949			
2045	0.0003509	0.0006953	2101	0.0002187	0.0003842	2157	0.0001668	0.0001739	2213	0.0001536	0.0001058	2269	0.0001791	0.0000953			
2046	0.0003472	0.0006906	2102	0.0002175	0.0003782	2158	0.0001662	0.000172	2214	0.0001536	0.000105	2270	0.0001798	0.0000956			
2047	0.0003435	0.0006858	2103	0.0002162	0.0003723	2159	0.0001658	0.0001701	2215	0.0001536	0.0001042	2271	0.0001806	0.0000964			
2048	0.0003398	0.0006811	2104	0.000215	0.0003663	2160	0.0001653	0.0001681	2216	0.0001537	0.0001035	2272	0.0001815	0.0000972			
2049	0.0003361	0.0006763	2105	0.0002137	0.0003604	2161	0.0001649	0.0001662	2217	0.0001537	0.0001027	2273	0.0001823	0.0000979			
2050	0.0003324	0.0006715	2106	0.0002125	0.0003558	2162	0.0001644	0.0001643	2218	0.0001537	0.0001019	2274	0.0001832	0.0000987			
2051	0.0003287	0.0006668	2107	0.0002113	0.0003513	2163	0.000164	0.0001624	2219	0.0001539	0.0001011	2275	0.000184	0.0000994			
2052	0.000326	0.000662	2108	0.00021	0.0003467	2164	0.0001635	0.0001605	2220	0.000154	0.0001004	2276	0.0001849	0.0001002			
2053	0.0003232	0.0006573	2109	0.0002088	0.0003422	2165	0.0001631	0.0001586	2221	0.0001542	0.0000999	2277	0.0001857	0.000101			
2054	0.0003204	0.0006525	2110	0.0002075	0.0003376	2166	0.0001626	0.0001567	2222	0.0001543	0.0000994	2278	0.0001866	0.0001017			
2055	0.0003177	0.0006478	2111	0.0002062	0.0003331	2167	0.0001622	0.0001548	2223	0.0001545	0.0000989	2279	0.0001874	0.0001025			

Table 5.13. Transmission (TnoH2O) for 1550-1700 nm, with b of 2.0 comparison run.

tnoh2o:	15	20	25	30	35	40	45	50	55	60	65	70	75	80	85	90
1550	0.9970189	0.9951362	0.9932867	0.990771	0.9873462	0.9833767	0.979627	0.9766594	0.9746274	0.9734722	0.972901	0.9728034	0.9729077	0.9730743	0.973242	0.9732144
1555	0.9991934	0.9968227	0.9917743	0.9848002	0.9780694	0.9731088	0.9700146	0.9685114	0.9680683	0.9683578	0.9688529	0.9695063	0.9699717	0.9704074	0.9704115	0.9703535
1560	0.9947718	0.985121	0.9752711	0.9687263	0.9649991	0.9632145	0.9628546	0.963441	0.9643733	0.9654424	0.9662175	0.9668952	0.9670762	0.9670746	0.9671135	0.9670511
1565	0.9604837	0.9539702	0.9524495	0.9528399	0.9546763	0.9569679	0.9593771	0.9613264	0.9626628	0.9634112	0.9636445	0.9636618	0.9635072	0.9634115	0.9633995	0.9635643
1570	0.9207814	0.9282412	0.9357188	0.9431325	0.949492	0.9542691	0.9575463	0.9594367	0.9602409	0.9601781	0.9598163	0.9596034	0.9593429	0.9596245	0.9599137	0.9604834
1575	0.8931249	0.9140567	0.9294066	0.9401014	0.9472694	0.9517438	0.9539961	0.9548464	0.9548845	0.9547427	0.9547372	0.9549063	0.9553907	0.9560978	0.9571974	0.9582491
1580	0.9181168	0.9230146	0.9312827	0.9387269	0.943288	0.9454551	0.9462883	0.9468225	0.9474297	0.9483746	0.9496518	0.9509847	0.9523823	0.9540502	0.9554467	0.9568394
1585	0.9563699	0.9510646	0.9448329	0.9392091	0.9360815	0.9354999	0.9364815	0.938345	0.9405841	0.9431572	0.9458429	0.9481608	0.9504354	0.9525947	0.954302	0.955855
1590	0.9835539	0.9662017	0.9500327	0.939209	0.932991	0.9305944	0.931115	0.9336284	0.936839	0.940401	0.9437957	0.9467328	0.9491761	0.9513327	0.9533474	0.9548514
1595	0.9609964	0.9513828	0.9448715	0.9391808	0.9354869	0.9338837	0.9340618	0.9356004	0.937902	0.9406529	0.9435069	0.9460263	0.9482827	0.9505788	0.9520851	0.9536191
1600	0.9238909	0.9292944	0.9337743	0.937587	0.9400515	0.9412585	0.9418672	0.9423431	0.9429966	0.9438411	0.9450136	0.9465755	0.9479153	0.9494506	0.9509296	0.9522973
1605	0.8934448	0.9122621	0.9265178	0.9364819	0.9430079	0.9468265	0.9485682	0.9490483	0.9488308	0.9484365	0.9480625	0.9482728	0.9485383	0.9492668	0.9503111	0.9513373
1610	0.9116529	0.9178297	0.9274798	0.9366304	0.9436066	0.9483624	0.9511396	0.9524164	0.9524967	0.9520299	0.9511787	0.9507294	0.9501923	0.9504389	0.9506253	0.9512581
1615	0.9458393	0.9445471	0.9430922	0.9433026	0.9454994	0.9482924	0.9506736	0.9522721	0.9529943	0.9532571	0.9530756	0.9526585	0.9522138	0.9519243	0.9519879	0.9522179
1620	0.9775378	0.9687088	0.9618563	0.9568546	0.9531477	0.9511895	0.950717	0.9512204	0.9520784	0.9528349	0.9536385	0.9537493	0.9538177	0.9538727	0.9537953	0.9538103
1625	0.9877124	0.9825533	0.9755294	0.9682127	0.9618762	0.9573484	0.9543497	0.9528637	0.9527893	0.9529533	0.9540733	0.9543579	0.9547684	0.9552614	0.9552971	0.955429
1630	0.9835082	0.9804906	0.9765375	0.9723075	0.9677509	0.9636108	0.9602064	0.9577395	0.9563341	0.9553692	0.9556356	0.9551625	0.9556097	0.9558759	0.956517	0.9568243
1635	0.9708763	0.9704711	0.9703026	0.9698405	0.9688737	0.9674722	0.9655243	0.9633501	0.9610391	0.9594808	0.9586933	0.9577613	0.9573357	0.9576901	0.9578583	0.9582354
1640	0.9591812	0.9612563	0.9634851	0.963677	0.9676324	0.9682977	0.96786	0.9666109	0.9647489	0.9634306	0.9624467	0.9609117	0.9603864	0.9601533	0.9598756	0.9600765
1645	0.9512798	0.9562643	0.9605764	0.9637975	0.9657022	0.9664079	0.9667652	0.9668224	0.9667718	0.9663079	0.9658672	0.9651059	0.9640497	0.9632466	0.9628486	0.9625186
1650	0.9574032	0.9594943	0.960995	0.9615113	0.9621253	0.9632943	0.9649736	0.9663444	0.9676585	0.9679517	0.9679394	0.9676108	0.9672062	0.9666572	0.9659323	0.9652817
1655	0.96779	0.9633933	0.95978	0.959481	0.960912	0.9630274	0.9648465	0.9663959	0.9679272	0.9686419	0.9687905	0.9693934	0.9692476	0.9688528	0.9684522	0.9678235
1660	0.9632955	0.9619579	0.9627841	0.9636452	0.9643782	0.9653507	0.9661758	0.9671151	0.9679595	0.9689955	0.9691329	0.9701427	0.9702747	0.9703437	0.9701216	0.9697255
1665	0.9638696	0.9678749	0.9690327	0.9690515	0.9688668	0.9686059	0.968649	0.9687687	0.9689353	0.9696401	0.9695724	0.9702766	0.9707482	0.9710251	0.9710383	0.9709349
1670	0.964169	0.9691175	0.9716318	0.9725043	0.9725011	0.9719446	0.9715694	0.9711339	0.9709783	0.9708688	0.9705625	0.9713432	0.9711726	0.971258	0.9716603	0.9717108
1675	0.9802336	0.9739466	0.9726483	0.9734724	0.9742582	0.9742879	0.9739753	0.9734036	0.9729919	0.9724396	0.972011	0.9717202	0.9719427	0.9722227	0.9721933	0.972392
1680	0.9834875	0.9823445	0.9795368	0.9769722	0.9758112	0.9754894	0.9751584	0.9747474	0.9744268	0.9739432	0.9736537	0.9735956	0.9731619	0.9732091	0.9731565	0.9732114
1685	0.982478	0.9825762	0.9821907	0.981057	0.9791602	0.9773361	0.9762242	0.9756289	0.9753509	0.9752578	0.9751381	0.9747002	0.9745827	0.9743522	0.9743058	0.9742531
1690	0.9818608	0.9819336	0.9814066	0.980774	0.9799659	0.9790328	0.9781819	0.9774165	0.9769037	0.9766545	0.9765682	0.9761743	0.9759019	0.9758093	0.9756299	0.9754934
1695	0.9811714	0.9799086	0.9791323	0.9791611	0.9794375	0.9797142	0.9796755	0.9793059	0.978862	0.978218	0.9779497	0.9775041	0.9771382	0.9769977	0.9769716	0.9768617
1700	0.9772059	0.9772658	0.9780647	0.97901	0.9797071	0.9801175	0.9802033	0.9800599	0.9797955	0.9794579	0.9792438	0.9786305	0.9785191	0.9785055	0.9783635	0.978308

Table 5.14. α for 1550-1700 nm, with b of 2.0 comparison run.

alpha:	15	20	25	30	35	40	45	50	55	60	65	70	75	80	85	90
1550	0.0027913	0.003007	0.0033864	0.0039426	0.0047476	0.0058228	0.0071934	0.0088505	0.0108211	0.0131214	0.0156852	0.0188201	0.0221212	0.0258718	0.0300721	0.0346574
1555	0.0017795	0.0021012	0.0024055	0.0026883	0.0031056	0.0036751	0.0044934	0.0055808	0.0069298	0.0085764	0.0104436	0.0127613	0.0153145	0.0183024	0.0215558	0.0251879
1560	0.0016453	0.0016512	0.0017031	0.0018666	0.0021363	0.0024933	0.0029842	0.003653	0.0045088	0.0056323	0.0069418	0.008606	0.0104814	0.0127036	0.01521	0.0180573
1565	0.0013524	0.00129	0.0013356	0.0014279	0.0015867	0.0018261	0.0021547	0.0025781	0.0031291	0.0038376	0.004709	0.005865	0.0071744	0.0087785	0.0106283	0.0128065
1570	0.0010846	0.001133	0.0011669	0.0012396	0.0013586	0.0015124	0.0017172	0.0019804	0.0023361	0.0027703	0.0033449	0.0040407	0.0049851	0.006096	0.0074474	0.0090451
1575	0.0007838	0.0009617	0.0011137	0.0012151	0.001304	0.0013992	0.0015093	0.0016532	0.0018597	0.0021236	0.0024986	0.002971	0.003574	0.0043212	0.0052647	0.0064273
1580	0.000979	0.0010332	0.001118	0.0012138	0.0012934	0.0013408	0.0013908	0.0014548	0.0015601	0.0017255	0.001968	0.0022377	0.0026752	0.0031854	0.0038385	0.0046551
1585	0.0012926	0.0012996	0.0012918	0.0012699	0.0012513	0.0012542	0.0012785	0.0013126	0.0013725	0.0014796	0.0016341	0.0018299	0.0021051	0.0024402	0.0029047	0.0034822
1590	0.0016679	0.0015365	0.0014016	0.0012965	0.0012228	0.0011986	0.0011939	0.0012097	0.0012491	0.0013196	0.0014161	0.0015381	0.0017459	0.001981	0.0023071	0.0027252
1595	0.0016116	0.0014873	0.0013733	0.0012867	0.0012232	0.001188	0.0011608	0.0011495	0.0011749	0.0012084	0.0012712	0.0013709	0.0015259	0.0016982	0.0019436	0.0022558
1600	0.0012992	0.0012924	0.0012728	0.0012467	0.0012135	0.0011704	0.0011385	0.0011128	0.001136	0.0011448	0.0011912	0.0012822	0.0014074	0.0015412	0.0017409	0.001988
1605	0.0009234	0.0010667	0.00113	0.0011417	0.0011319	0.0011059	0.0010922	0.0010837	0.0011087	0.0011317	0.0011789	0.001253	0.0013729	0.0014918	0.0016605	0.0018656
1610	0.0008201	0.0008634	0.0008952	0.0009387	0.0009774	0.0010052	0.0010346	0.0010664	0.001104	0.0011607	0.0012259	0.0013193	0.0014114	0.0015233	0.0016743	0.0018534
1615	0.0008209	0.0007409	0.0007231	0.0007626	0.00084	0.0009149	0.0009955	0.0010679	0.0011336	0.0012198	0.0013124	0.0013809	0.0015115	0.001621	0.0017604	0.0019269
1620	0.0006617	0.0006608	0.0007023	0.0007585	0.0008282	0.0009089	0.0010039	0.0011039	0.0012031	0.0013152	0.0014389	0.0015489	0.0016589	0.001772	0.0019115	0.0020661
1625	0.0005328	0.0006895	0.0007771	0.000855	0.000927	0.001013	0.0011088	0.0012199	0.0013437	0.0014627	0.0015942	0.0016847	0.0018387	0.0019624	0.0020963	0.0022588
1630	0.0007106	0.0008013	0.0009072	0.0010037	0.0010974	0.0012173	0.001331	0.0014452	0.001566	0.0016748	0.0017865	0.0019193	0.0020457	0.0021736	0.0023259	0.0025067
1635	0.0011242	0.0011073	0.0011773	0.0012743	0.0014005	0.0015287	0.0016446	0.0017424	0.0018342	0.0019386	0.0020157	0.0021508	0.0022931	0.0024384	0.0026161	0.002832
1640	0.0015612	0.0015985	0.001689	0.0017798	0.0018596	0.0019266	0.0020043	0.0020756	0.0021521	0.0022405	0.0023005	0.0024681	0.0026098	0.0027942	0.0030099	0.0032753
1645	0.0021604	0.0023058	0.0023434	0.0023493	0.0023701	0.0023899	0.0024076	0.0024388	0.0025107	0.0025862	0.0026635	0.0028468	0.0030389	0.0032675	0.0035604	0.0038876
1650	0.0029973	0.0029042	0.0029201	0.0029073	0.0028683	0.0028434	0.0028283	0.0028469	0.002918	0.0030223	0.003159	0.0033839	0.0036367	0.0039468	0.0043093	0.0047178
1655	0.0037086	0.0036316	0.0034838	0.0033716	0.0032868	0.003267	0.0032847	0.0033366	0.0034439	0.003615	0.0038626	0.0041228	0.0044712	0.004882	0.005323	0.0057955
1660	0.0042049	0.0040761	0.0038839	0.0037875	0.0037527	0.0037582	0.0038269	0.0039622	0.0041785	0.0044515	0.0048312	0.0051657	0.0055834	0.0060402	0.0065671	0.0071421
1665	0.0041296	0.0041077	0.0041986	0.0042394	0.0042842	0.0043793	0.0045826	0.0048725	0.0052251	0.0056136	0.0061023	0.0065085	0.0069771	0.007567	0.0081669	0.0087871
1670	0.0043434	0.0044784	0.004466	0.0046489	0.0049715	0.0053354	0.0057526	0.0061841	0.0066477	0.0070897	0.0075961	0.008088	0.0086597	0.0093482	0.0100059	0.0107825
1675	0.0043655	0.0046353	0.0050827	0.0056696	0.0062618	0.0068061	0.0073297	0.0078385	0.008335	0.0088671	0.0093731	0.0101584	0.0106826	0.0114108	0.0122963	0.0131889
1680	0.005364	0.0060529	0.006888	0.0075268	0.0081667	0.0087279	0.009245	0.0097777	0.0103063	0.0109853	0.0115009	0.0122313	0.0131235	0.01421	0.0150106	0.0160777
1685	0.0086102	0.0090024	0.0096141	0.0101259	0.0104901	0.010981	0.0115306	0.0121594	0.0127364	0.0135714	0.0141063	0.0154906	0.0160826	0.0172289	0.0183071	0.0195022
1690	0.0128472	0.0130157	0.0128679	0.0129195	0.0132861	0.0138599	0.0144692	0.0151073	0.0158298	0.0167265	0.0173836	0.0184106	0.0196695	0.020824	0.0221985	0.0234917
1695	0.0178219	0.0163525	0.0164196	0.0167847	0.0170302	0.0174372	0.0180223	0.0187555	0.0197816	0.0206958	0.0216445	0.0232848	0.0239195	0.0253447	0.0266032	0.0280981
1700	0.019822	0.0213699	0.0212201	0.0211398	0.0213193	0.021794	0.0225557	0.023456	0.0247083	0.0254531	0.0266931	0.0274358	0.0288688	0.0302798	0.0318088	0.0333845

Table 5.15. β for 1550-1700 nm, with b of 2.0 comparison run.

beta:	15	20	25	30	35	40	45	50	55	60	65	70	75	80	85	90
1550	0.8963629	0.8887293	0.8741653	0.8522526	0.8241464	0.7919196	0.7594258	0.7281089	0.6969575	0.66778	0.6396955	0.6136268	0.5891324	0.565289	0.5423487	0.5203156
1555	0.9296734	0.9197279	0.905854	0.8896134	0.8669887	0.8388584	0.8068798	0.7738965	0.7411839	0.7103415	0.6802853	0.6525593	0.6259427	0.5994952	0.5751544	0.5517171
1560	0.9431005	0.938114	0.930508	0.917007	0.8983962	0.8759582	0.849309	0.8191314	0.7881333	0.7554207	0.7236172	0.6938983	0.665743	0.6363833	0.6101863	0.5848292
1565	0.9555445	0.9527718	0.9449208	0.9351588	0.9216577	0.9038835	0.882687	0.8578081	0.8305678	0.7999755	0.7683647	0.7365168	0.7070674	0.6756787	0.6472506	0.6195791
1570	0.9603274	0.955952	0.9514858	0.9442759	0.9341201	0.9219552	0.9067807	0.8878818	0.8650815	0.838974	0.8092687	0.7786279	0.7481067	0.7154439	0.6849381	0.6556416
1575	0.9626349	0.9546201	0.947487	0.9427879	0.9382237	0.931663	0.9222886	0.9090686	0.8911395	0.8698562	0.843658	0.8158618	0.7864287	0.7546805	0.7230085	0.6924561
1580	0.9404308	0.9391987	0.9396746	0.9398593	0.9389468	0.9361817	0.9308386	0.9221959	0.9093036	0.8927312	0.8709807	0.8473079	0.82024	0.7898489	0.7592859	0.7288834
1585	0.9265561	0.9314519	0.9353254	0.9375216	0.9382616	0.9376541	0.9348905	0.9296761	0.9212905	0.9087861	0.8916162	0.8719143	0.8485028	0.8212354	0.7927673	0.7635489
1590	0.9283919	0.9316416	0.9335266	0.9354334	0.9368684	0.9376993	0.9368368	0.9337757	0.9281486	0.9191206	0.9062662	0.8903878	0.8706507	0.8477749	0.8221171	0.7950526
1595	0.9345559	0.9321789	0.9334214	0.9354596	0.9368509	0.9376173	0.9374993	0.9357179	0.9315248	0.9251065	0.9156328	0.9024811	0.8867169	0.867443	0.8456872	0.822076
1600	0.9418544	0.9408598	0.939148	0.9381662	0.9382041	0.9383042	0.9377398	0.9363444	0.9330155	0.928001	0.9206984	0.9102995	0.8971874	0.8814263	0.8636531	0.8432428
1605	0.9501899	0.9475471	0.9456001	0.9437232	0.9419116	0.9403484	0.9386408	0.9365312	0.9332997	0.9285779	0.9224587	0.9134749	0.9027435	0.890159	0.8750236	0.8577561
1610	0.9553081	0.9526293	0.9507109	0.9488181	0.9462575	0.9433988	0.9401447	0.9365087	0.9324092	0.9273441	0.9213778	0.9137924	0.9041868	0.8932931	0.8803915	0.865735
1615	0.9566072	0.9578004	0.9560485	0.9526196	0.9483067	0.9442813	0.9397947	0.9350142	0.9297926	0.9245852	0.9180301	0.9109264	0.9021154	0.8925432	0.8809498	0.8679688
1620	0.9587904	0.9572605	0.9547182	0.95066	0.9454256	0.940296	0.935559	0.9306247	0.9251027	0.9195512	0.9123393	0.9056423	0.8971838	0.8882968	0.8776591	0.8654616
1625	0.9573708	0.9512848	0.9458494	0.940661	0.9368679	0.9331251	0.9285439	0.9231512	0.9172989	0.9114169	0.9048659	0.8979819	0.8899356	0.8805327	0.8706959	0.8586745
1630	0.9449022	0.9342359	0.931013	0.9303547	0.9281343	0.9235421	0.9179291	0.9124336	0.9076769	0.9015115	0.8958293	0.8881893	0.880408	0.8714303	0.8602015	0.8477193
1635	0.9195836	0.9240324	0.9245847	0.9209008	0.9148096	0.9098329	0.905562	0.9016342	0.8976123	0.8911459	0.8854105	0.8770447	0.8682407	0.8578386	0.8458591	0.8322675
1640	0.922457	0.920733	0.9115687	0.903174	0.901756	0.8987007	0.8952811	0.8912553	0.8861686	0.8798949	0.8729694	0.863099	0.8531067	0.83974	0.8272356	0.8123165
1645	0.9072154	0.8983277	0.8984079	0.8974039	0.8943952	0.8900175	0.8857177	0.880877	0.8740402	0.866912	0.8578455	0.8477266	0.834084	0.8202596	0.8044543	0.7886875
1650	0.8965871	0.8967603	0.8923631	0.8886918	0.8857311	0.8815331	0.8762943	0.8698914	0.8611814	0.851317	0.8387629	0.824376	0.8107879	0.7954424	0.7789086	0.7629784
1655	0.885391	0.8854017	0.883623	0.8803308	0.8767748	0.8716091	0.8647641	0.8559161	0.8445174	0.8309978	0.815115	0.8016365	0.7842517	0.7673373	0.7520582	0.7374337
1660	0.8758196	0.8713517	0.8719497	0.8701261	0.865202	0.8579623	0.8485133	0.8358754	0.820851	0.8051701	0.7880091	0.7711323	0.7572129	0.7424567	0.7275729	0.7134921
1665	0.865443	0.8664463	0.8608816	0.8549201	0.8472008	0.8372208	0.8233795	0.8075222	0.7912584	0.7754112	0.7598897	0.74649	0.7318411	0.7173836	0.7040728	0.6916142
1670	0.8468753	0.845567	0.8427427	0.8331505	0.8194368	0.8042362	0.7884504	0.7734993	0.7592923	0.7463017	0.7346475	0.7212228	0.708658	0.6955849	0.6837505	0.6712667
1675	0.8319004	0.8194966	0.8061686	0.7906269	0.7760332	0.7630286	0.7511603	0.7400109	0.7300806	0.719371	0.711366	0.6965249	0.686851	0.6758817	0.663559	0.6521202
1680	0.7886329	0.7687998	0.7507491	0.7401067	0.730255	0.7233225	0.7171301	0.7103348	0.703593	0.6941389	0.6882939	0.677295	0.6655788	0.6532882	0.6444969	0.6340309
1685	0.7109885	0.7112325	0.7032239	0.6976255	0.6946708	0.692245	0.6883592	0.6828781	0.6779467	0.6693068	0.6649717	0.6499134	0.6447308	0.6350942	0.6262902	0.6172763
1690	0.6637718	0.6613	0.6673539	0.6716889	0.6702619	0.6668714	0.6623218	0.6577085	0.6523989	0.6454815	0.6414785	0.6335223	0.6248162	0.6180383	0.6094365	0.6021667
1695	0.6389847	0.6504709	0.6507262	0.647761	0.6463186	0.6440946	0.6399454	0.6350777	0.6282837	0.6234277	0.6184487	0.6102554	0.6071216	0.6013147	0.5955527	0.5885884
1700	0.6442288	0.6338367	0.6323851	0.6310821	0.6285372	0.6236674	0.6186875	0.6142053	0.6081179	0.6056224	0.5998977	0.5984282	0.5922505	0.5877351	0.5824144	0.5764598

Table 5.16. Transmission (TnoH2O) for 1550-1700 nm, with b of 2.5 comparison run.

tnoh2o:	15	20	25	30	35	40	45	50	55	60	65	70	75	80	85	90
1550	0.9963938	0.9941862	0.9917288	0.9887677	0.9854214	0.9820846	0.9791741	0.9769117	0.9753081	0.9742979	0.9736537	0.9733376	0.9731658	0.9730721	0.9730489	0.9729221
1555	0.9979287	0.9943351	0.9888626	0.9827707	0.9774398	0.9736027	0.9711587	0.9698753	0.9693266	0.9692897	0.9693897	0.9696764	0.9698693	0.9701715	0.9701691	0.970196
1560	0.9918311	0.9826513	0.9744662	0.9690409	0.9659765	0.9645656	0.9642333	0.9645476	0.9650649	0.9657115	0.966181	0.966687	0.9668835	0.9670249	0.9672611	0.9674059
1565	0.9605672	0.9549182	0.9537085	0.9544137	0.9561294	0.9579566	0.9597961	0.9612667	0.9623004	0.9629723	0.9633404	0.9636277	0.9637962	0.9640198	0.9642567	0.9645747
1570	0.9222773	0.9306304	0.9381284	0.9448185	0.950245	0.9541706	0.9568406	0.9584865	0.9594225	0.9597782	0.9599686	0.9602691	0.9604189	0.9609496	0.9613542	0.9619085
1575	0.8979353	0.9171845	0.9311541	0.9407047	0.9469488	0.9508517	0.9530186	0.9542207	0.9548425	0.9553062	0.9558061	0.9563199	0.956985	0.957729	0.9587484	0.9596488
1580	0.919809	0.9259064	0.9331206	0.9390841	0.9429203	0.9452277	0.9466415	0.9477766	0.9488229	0.9500253	0.9513863	0.952677	0.9539521	0.9554477	0.9566662	0.9578893
1585	0.9551975	0.9493415	0.9439594	0.9400033	0.9380822	0.9380244	0.9391583	0.9409953	0.9430747	0.945372	0.9477065	0.9496895	0.9516514	0.9535612	0.9550966	0.9565297
1590	0.9787104	0.9624849	0.9489754	0.9402639	0.9357052	0.9343752	0.9351516	0.9372987	0.9398899	0.9427874	0.9455802	0.94806	0.9501577	0.9520773	0.9539453	0.9553891
1595	0.9597154	0.9502211	0.9439712	0.93955	0.9371123	0.9363655	0.9370134	0.9386321	0.9406971	0.9430131	0.9453683	0.9474993	0.9494441	0.9515168	0.9528978	0.954371
1600	0.9245022	0.9303474	0.934641	0.9378876	0.9400827	0.9414545	0.9424931	0.943462	0.9445298	0.9456051	0.9468018	0.9483218	0.9495337	0.9509321	0.952282	0.9535531
1605	0.897891	0.9152427	0.9281062	0.9368615	0.9424697	0.9457971	0.947544	0.9484139	0.9487889	0.9490448	0.9492224	0.9498459	0.9503816	0.9511806	0.952203	0.9531417
1610	0.9138106	0.9213341	0.9301858	0.937966	0.9437655	0.9476599	0.9499578	0.9511685	0.9515431	0.951669	0.9514953	0.9516976	0.951687	0.952263	0.9526308	0.9533045
1615	0.9459109	0.9446155	0.9441711	0.9450216	0.9468619	0.9488887	0.9505936	0.9517881	0.9523857	0.9528009	0.9529488	0.9529728	0.9530113	0.9531465	0.9535499	0.9540146
1620	0.9753976	0.9672204	0.9610065	0.95666	0.9538034	0.9524151	0.9519993	0.9522113	0.9526853	0.9531298	0.9537411	0.9538816	0.9541128	0.9544595	0.9547147	0.9550605
1625	0.9858542	0.9799027	0.9730444	0.9666516	0.9614177	0.957844	0.9555653	0.9544055	0.9542437	0.9541039	0.9548159	0.9548454	0.9551392	0.9556663	0.9558749	0.9562312
1630	0.9824041	0.9788527	0.9746683	0.9704676	0.9663845	0.9629774	0.960307	0.9584077	0.9573433	0.9565621	0.9567875	0.9562248	0.9565021	0.9566487	0.9571933	0.957499
1635	0.9709472	0.9702914	0.9697022	0.9688895	0.9676309	0.9661075	0.9643509	0.9626424	0.9609536	0.9599938	0.9596375	0.9589371	0.9585318	0.9587722	0.9587809	0.9590128
1640	0.9595714	0.9619203	0.9639769	0.9657545	0.9667982	0.9669341	0.966356	0.9653662	0.9640014	0.9632002	0.9626601	0.9615001	0.9611804	0.9610403	0.9607759	0.9609064
1645	0.9525493	0.9572779	0.9610459	0.9636882	0.9652561	0.965884	0.9661929	0.9661307	0.9659579	0.9655258	0.9652362	0.9647563	0.9640056	0.9634969	0.963309	0.9631177
1650	0.9577968	0.9597871	0.9611283	0.9620312	0.9629853	0.9640077	0.9652207	0.9660915	0.9669858	0.9670236	0.9669293	0.9666728	0.9664657	0.9662001	0.9657669	0.9653909
1655	0.9667598	0.9631293	0.9609938	0.961013	0.962147	0.9638447	0.9652582	0.9664209	0.9675903	0.9679983	0.9679391	0.9684165	0.9682697	0.9679913	0.967802	0.9674307
1660	0.9643047	0.9627279	0.9632891	0.9640965	0.9648998	0.9659225	0.966682	0.9674456	0.9680526	0.9688042	0.9687055	0.9694775	0.9694747	0.9694964	0.9693243	0.9690648
1665	0.9638281	0.9675094	0.9686646	0.9688796	0.9689024	0.9688318	0.9689915	0.969145	0.9692569	0.9697891	0.9695626	0.9700494	0.9703471	0.9704902	0.9704241	0.9703061
1670	0.9652098	0.9692047	0.9712466	0.9719943	0.9720742	0.9717008	0.9715102	0.971224	0.9711721	0.9710944	0.9707918	0.9714559	0.9711796	0.9711139	0.9713674	0.9713055
1675	0.9791155	0.9746424	0.9733868	0.9735946	0.973943	0.9738191	0.9735403	0.9731303	0.9729267	0.9725507	0.9722455	0.9719967	0.9721617	0.9723347	0.9721836	0.9722481
1680	0.9829295	0.9813082	0.978929	0.9770681	0.9760032	0.9754484	0.9749539	0.9745244	0.9742961	0.9739199	0.9737271	0.973738	0.9733304	0.9733698	0.9732761	0.9732609
1685	0.982351	0.982153	0.9813485	0.9801287	0.978635	0.9773065	0.9764205	0.9757993	0.9754176	0.9752133	0.9750811	0.9746732	0.9746051	0.9744477	0.9744357	0.9743832
1690	0.98176	0.9816087	0.9809858	0.9803125	0.9795074	0.9786715	0.9779946	0.9773748	0.9768981	0.976631	0.976545	0.9761285	0.9758955	0.9758546	0.9757161	0.9755986
1695	0.9809229	0.97989	0.9793127	0.9792886	0.9793376	0.9793543	0.9791678	0.9788226	0.9785134	0.9780706	0.9779456	0.9775497	0.9771922	0.9770501	0.9770088	0.976885
1700	0.9774696	0.977666	0.9783376	0.9790793	0.9795629	0.9798188	0.9798263	0.9796816	0.9794782	0.9792325	0.9791345	0.9785918	0.9785112	0.978487	0.9783187	0.9782271

Table 5.17. α for 1550-1700 nm with b of 2.5 comparison run.

alpha:	15	20	25	30	35	40	45	50	55	60	65	70	75	80	85	90
1550	0.002907	0.0033116	0.0039509	0.0048591	0.0061047	0.0077011	0.0096802	0.012037	0.0148053	0.0179418	0.0214184	0.0254718	0.0297578	0.0344985	0.0397011	0.0452565
1555	0.0019113	0.0022813	0.0027254	0.0032704	0.004047	0.0050653	0.0064127	0.0081	0.0101418	0.0125322	0.0152255	0.0184062	0.0218921	0.0258594	0.0300829	0.034694
1560	0.0016673	0.0017554	0.0019477	0.0022808	0.0027903	0.0034797	0.0043935	0.005571	0.0070165	0.0088042	0.0108553	0.0133264	0.0160531	0.019202	0.0226433	0.0264634
1565	0.0013787	0.0013752	0.0014983	0.0017175	0.0020564	0.0025318	0.0031703	0.0039911	0.0050227	0.0063091	0.0078354	0.0097156	0.011811	0.0142835	0.0170281	0.0201449
1570	0.0010943	0.0011773	0.0012807	0.0014419	0.0016827	0.0020093	0.0024485	0.0030163	0.0037561	0.0046634	0.0058005	0.0071413	0.008785	0.010688	0.0128795	0.0153685
1575	0.0008368	0.0010154	0.001182	0.0013368	0.0015156	0.0017401	0.0020299	0.0024144	0.0029317	0.0035772	0.0044204	0.0054338	0.0066523	0.0080992	0.0098191	0.0118122
1580	0.0009959	0.0010768	0.0011804	0.0012977	0.0014276	0.0015721	0.0017666	0.0020252	0.0023816	0.0028682	0.0035039	0.0042085	0.005162	0.0062956	0.0076325	0.0091855
1585	0.0012941	0.0013002	0.0013066	0.0013211	0.0013591	0.0014392	0.0015712	0.001753	0.0020124	0.0023831	0.0028575	0.0034011	0.0041189	0.0049871	0.006051	0.0072975
1590	0.0016252	0.0015037	0.0013986	0.0013322	0.0013103	0.0013508	0.001432	0.0015628	0.0017585	0.0020472	0.0024048	0.002815	0.0033975	0.004079	0.0049271	0.0059337
1595	0.0015919	0.0014621	0.0013682	0.0013071	0.0012805	0.0012996	0.0013488	0.00144	0.0015968	0.0018163	0.0021031	0.0024401	0.0029056	0.0034606	0.0041483	0.0049725
1600	0.0012994	0.0012832	0.0012675	0.0012516	0.0012454	0.001252	0.0012915	0.0013604	0.0015002	0.0016659	0.001912	0.0022098	0.0025868	0.0030451	0.0036228	0.0043165
1605	0.0009487	0.001065	0.0011215	0.0011447	0.001164	0.0011833	0.0012313	0.001304	0.0014297	0.0015831	0.0018042	0.0020858	0.0024162	0.0028034	0.0033009	0.0038967
1610	0.0008319	0.0008772	0.0009192	0.000971	0.0010308	0.0010933	0.0011717	0.0012695	0.0013948	0.001563	0.0017738	0.002051	0.0023692	0.0027057	0.0031375	0.0036644
1615	0.0008153	0.0007635	0.000771	0.0008305	0.0009235	0.0010212	0.0011391	0.0012673	0.0014109	0.0015946	0.0018087	0.0020437	0.002372	0.0027271	0.0031234	0.0035866
1620	0.0006705	0.0006912	0.0007448	0.0008226	0.0009204	0.0010335	0.0011674	0.0013167	0.0014832	0.0016796	0.0019099	0.0021588	0.0024487	0.0027962	0.0032124	0.0036704
1625	0.000562	0.0007119	0.0008169	0.0009153	0.0010183	0.0011448	0.0012844	0.001444	0.00163	0.0018278	0.0020597	0.002292	0.0026091	0.0029456	0.0033479	0.0038286
1630	0.0007466	0.0008445	0.0009602	0.0010767	0.0011962	0.0013463	0.0014982	0.0016624	0.001851	0.0020488	0.0022694	0.0025446	0.0028421	0.0031834	0.0035867	0.0040731
1635	0.0011437	0.001158	0.0012452	0.0013612	0.0014986	0.0016457	0.0018003	0.0019571	0.0021282	0.0023347	0.0025392	0.0028275	0.003153	0.0035146	0.00395	0.0044607
1640	0.0015694	0.0016393	0.001735	0.0018316	0.0019379	0.0020434	0.0021693	0.0023082	0.002478	0.0026831	0.0028907	0.0032289	0.003563	0.0039825	0.0044536	0.0050153
1645	0.0021696	0.0022984	0.0023516	0.0023839	0.0024367	0.0025042	0.0025917	0.0027133	0.0028975	0.0031061	0.0033514	0.0037005	0.0041075	0.0045753	0.0051345	0.0057631
1650	0.0029955	0.0029247	0.0029227	0.0029228	0.0029301	0.0029771	0.0030545	0.0031836	0.0033858	0.0036408	0.0039636	0.0043801	0.0048334	0.0053828	0.0060231	0.006744
1655	0.0036868	0.0035904	0.0034809	0.0034166	0.0033951	0.0034549	0.0035737	0.0037525	0.0040056	0.0043443	0.0047836	0.0052143	0.0057959	0.0064658	0.0071967	0.0079951
1660	0.0041589	0.004038	0.0039118	0.003875	0.0039116	0.0040205	0.004213	0.0044842	0.0048387	0.0052819	0.0058499	0.0064035	0.0070381	0.0077763	0.0086224	0.0095507
1665	0.0041761	0.0041707	0.0042511	0.0043616	0.0045262	0.0047479	0.0050711	0.0054822	0.0059759	0.0065278	0.0072169	0.0078451	0.0085905	0.0095041	0.010448	0.0114437
1670	0.0043425	0.0045224	0.004655	0.0049335	0.005333	0.0057696	0.0062829	0.0068402	0.0074798	0.0081081	0.008835	0.0096126	0.0104768	0.0115062	0.0125349	0.0137182
1675	0.0045279	0.0048701	0.0053906	0.0060087	0.0066468	0.0072717	0.0079095	0.0085705	0.0092829	0.0100402	0.0107838	0.0118847	0.0127394	0.013818	0.0151068	0.0164308
1680	0.0056238	0.0063484	0.0071521	0.0078745	0.0085806	0.0092536	0.0099375	0.0106683	0.0114236	0.0123487	0.0131206	0.014197	0.0154458	0.0169114	0.0181248	0.0196457
1685	0.008617	0.0092361	0.0098555	0.0104354	0.0109807	0.0116696	0.012393	0.0132112	0.0140231	0.0151476	0.0159662	0.0177213	0.0186819	0.0202118	0.0217391	0.0234288
1690	0.0128205	0.0130229	0.0131264	0.0134156	0.0139187	0.0146185	0.0154453	0.0163423	0.017336	0.0185351	0.0194714	0.0208744	0.0225445	0.0241253	0.0259967	0.0278433
1695	0.0176746	0.0167159	0.0167652	0.0171708	0.0176582	0.0183258	0.0191988	0.0201874	0.0214771	0.0226688	0.0239152	0.0259489	0.0271063	0.0290426	0.0308369	0.0329569
1700	0.0201724	0.021175	0.0213646	0.0216174	0.0221128	0.0228734	0.0238217	0.0249221	0.0264886	0.0276015	0.0291999	0.0304931	0.0324309	0.0344041	0.0365782	0.0388575

Table 5.18. β for 1550-1700 nm with b of 2.5 comparison run.

beta:	15	20	25	30	35	40	45	50	55	60	65	70	75	80	85	90
1550	0.8900141	0.8719463	0.8454455	0.8119645	0.775458	0.737672	0.7013876	0.6675884	0.6351525	0.605941	0.5778778	0.5532339	0.5295107	0.5070944	0.4858477	0.4657951
1555	0.9214806	0.90449	0.8804962	0.8504074	0.8150427	0.7768035	0.7384847	0.7021409	0.6674749	0.6362931	0.6062835	0.5801368	0.5549394	0.530465	0.5083924	0.4874413
1560	0.939286	0.9268184	0.9070789	0.8799164	0.8471469	0.811141	0.7739854	0.7369896	0.7019313	0.6680358	0.6359174	0.6076666	0.5814315	0.554746	0.5315852	0.5094007
1565	0.9520435	0.9428038	0.925651	0.9024801	0.8737084	0.8410993	0.8065531	0.7707138	0.7359141	0.7007097	0.6671982	0.6366315	0.6086199	0.5802696	0.5552444	0.5315567
1570	0.9579575	0.9491224	0.936158	0.9178593	0.8943173	0.8668076	0.8356528	0.8020406	0.767638	0.7325568	0.6979703	0.6648588	0.63588	0.6057704	0.5788951	0.5538473
1575	0.9587723	0.9486296	0.9374465	0.924534	0.9080567	0.8865728	0.8601112	0.8295587	0.7961903	0.7620398	0.7271281	0.694097	0.6625729	0.6314681	0.6025108	0.576224
1580	0.9405233	0.9374141	0.9335842	0.926911	0.9162231	0.9000168	0.8783838	0.8514636	0.8201949	0.7858205	0.7509034	0.718202	0.6879616	0.6552848	0.6258525	0.5991851
1585	0.9276102	0.931105	0.931634	0.9285219	0.9208917	0.9084657	0.8906652	0.8675759	0.8393872	0.8067335	0.7737508	0.7443317	0.712536	0.6792185	0.6494344	0.6213882
1590	0.9285021	0.9312265	0.9313586	0.9292996	0.9235842	0.9140507	0.8992895	0.8794776	0.8549111	0.8242823	0.7938441	0.765232	0.7349955	0.7031119	0.6725985	0.6440811
1595	0.9345083	0.9328114	0.9322842	0.9307456	0.9263291	0.9183295	0.9058356	0.888546	0.8673368	0.838659	0.8094265	0.7835683	0.7551663	0.7238659	0.6945984	0.6665176
1600	0.9414448	0.9401361	0.9376621	0.9344441	0.9296778	0.9219995	0.91064	0.8951045	0.8763968	0.8510746	0.8221493	0.7979674	0.7727389	0.7430797	0.7156705	0.688097
1605	0.9493076	0.9466763	0.9435081	0.9393759	0.9336466	0.9253593	0.9141034	0.8995798	0.8823581	0.8609222	0.8346779	0.8072574	0.7860326	0.7606547	0.7344638	0.7078279
1610	0.9546041	0.951597	0.9481359	0.9434299	0.9366528	0.9276681	0.9161623	0.9021557	0.885605	0.8670557	0.845417	0.820974	0.7944407	0.7729475	0.7497175	0.7245532
1615	0.9560699	0.9557548	0.9520397	0.9456592	0.9373174	0.9274264	0.9157814	0.9022318	0.8863121	0.869756	0.8512043	0.8280139	0.805024	0.779829	0.758166	0.7367586
1620	0.9578602	0.9549828	0.9502015	0.9431169	0.9341067	0.9236944	0.9122593	0.8993819	0.8845405	0.8692791	0.852185	0.8337595	0.8122665	0.7878096	0.76347	0.7410132
1625	0.9552232	0.9482164	0.9416397	0.9345977	0.926642	0.9172745	0.9064103	0.894213	0.8805966	0.8656595	0.8498158	0.8306366	0.8125724	0.7912668	0.7680596	0.7437417
1630	0.9414443	0.9333022	0.9285492	0.9241756	0.9175631	0.9088737	0.8984088	0.8868862	0.8747242	0.8596118	0.8443673	0.8266562	0.8081596	0.7880406	0.7665015	0.7436526
1635	0.9202769	0.9220016	0.9198196	0.9143064	0.9063877	0.898093	0.8886492	0.8781163	0.8664218	0.8515254	0.8359023	0.8183004	0.7998605	0.7797371	0.7585162	0.7369676
1640	0.920075	0.9164773	0.9087238	0.9018719	0.8952329	0.8877031	0.8790774	0.8686506	0.8558709	0.8413139	0.8245919	0.8063808	0.7879679	0.7662387	0.7464628	0.7252688
1645	0.90698	0.8989866	0.8962555	0.8926767	0.8870227	0.8789878	0.86948	0.8581361	0.8437715	0.8284971	0.8100927	0.7935928	0.7726368	0.7521688	0.7311261	0.7104622
1650	0.8951752	0.8941548	0.8897128	0.8843883	0.8782484	0.8695423	0.8586699	0.845732	0.8298965	0.812919	0.7926753	0.7726789	0.7543972	0.7343773	0.7135913	0.6937506
1655	0.8847751	0.8836121	0.880371	0.8749388	0.8676422	0.857642	0.8451465	0.8300636	0.8128029	0.7936612	0.7725993	0.7555491	0.7340259	0.7134827	0.69455	0.6763273
1660	0.8755132	0.8708308	0.8682192	0.862698	0.8536621	0.8414267	0.8268268	0.8094718	0.7907249	0.77091	0.7504314	0.7298719	0.7129665	0.694607	0.6763147	0.6590562
1665	0.8636443	0.8620886	0.8554237	0.8459659	0.8336321	0.8190731	0.8017765	0.7831269	0.7641113	0.7455225	0.7270939	0.7103894	0.6922349	0.6744717	0.658042	0.6424839
1670	0.8459368	0.8414015	0.8337146	0.8207599	0.8047854	0.78791	0.770173	0.7529301	0.7356356	0.7198372	0.7051825	0.6881167	0.6724252	0.6565077	0.6417152	0.6266505
1675	0.8265519	0.8124154	0.7965727	0.7803602	0.7648886	0.7501702	0.7362401	0.7224945	0.7088738	0.6950911	0.684135	0.6663486	0.6534502	0.6399375	0.6252323	0.6114213
1680	0.7814198	0.7624531	0.7459519	0.733906	0.72286	0.7135862	0.7042615	0.694184	0.6839958	0.6717457	0.663085	0.6490495	0.6350204	0.620936	0.6094642	0.5967716
1685	0.7111472	0.7073435	0.7005173	0.6946189	0.6889642	0.6832644	0.6765423	0.668515	0.6606697	0.6493494	0.6422436	0.6253266	0.6171345	0.605534	0.5942611	0.5827983
1690	0.6648086	0.6635448	0.6660585	0.6667078	0.6634074	0.6588791	0.6522636	0.6452143	0.6375567	0.6282806	0.6219049	0.6113366	0.6001421	0.590816	0.5797307	0.5696548
1695	0.6402059	0.6477868	0.6478466	0.6448983	0.6413617	0.6369126	0.6307214	0.6243265	0.6159816	0.6092058	0.6020858	0.5915965	0.5847703	0.5760341	0.5673708	0.5574529
1700	0.6408838	0.6339532	0.6307572	0.6275292	0.6234852	0.617504	0.6117167	0.606011	0.5980521	0.5931104	0.5853121	0.5802845	0.571378	0.5637763	0.5552667	0.5461628

Table 5.19. Transmission (TnoH2O) for 1550-1700 nm, with b of 3.3 comparison run.

tnoh2o:	15	20	25	30	35	40	45	50	55	60	65	70	75	80	85	90
1550	0.9951041	0.9923881	0.9894577	0.9864145	0.983449	0.9808	0.9786083	0.976913	0.9756537	0.9747745	0.9741188	0.9736982	0.9733875	0.9731592	0.9730126	0.9728211
1555	0.9955215	0.9909957	0.9857209	0.9807709	0.9767742	0.9739605	0.9721026	0.9710222	0.9704182	0.9701736	0.9700359	0.9700988	0.9701216	0.9703197	0.9702725	0.9702983
1560	0.9881211	0.9799949	0.9735705	0.9694195	0.9670819	0.9659683	0.9656143	0.9657041	0.9659318	0.9663028	0.9665972	0.9669865	0.9671863	0.9673797	0.9676745	0.9678809
1565	0.9606932	0.9563109	0.9555311	0.9562982	0.9577326	0.9591069	0.9604763	0.9616027	0.9624596	0.9631181	0.9636097	0.9640733	0.9644286	0.9648132	0.9651754	0.9655417
1570	0.9250929	0.9338717	0.9409891	0.9467521	0.951209	0.9543883	0.9566356	0.9581956	0.9593089	0.9599977	0.9605798	0.9612092	0.9616293	0.9622986	0.9627751	0.9632893
1575	0.9044587	0.9214555	0.9335237	0.9416661	0.9470206	0.9505351	0.9527546	0.9543006	0.9553916	0.9563108	0.957181	0.9579419	0.958726	0.9594775	0.9604291	0.9611874
1580	0.9225688	0.9291937	0.93536	0.9401839	0.9435472	0.945976	0.9477944	0.9493557	0.9507176	0.9521051	0.9535121	0.9547548	0.9559187	0.9572435	0.9582909	0.9593279
1585	0.9534456	0.9479376	0.9439386	0.9416215	0.9408572	0.9413769	0.9426837	0.9444405	0.9462924	0.9482836	0.9502615	0.9519303	0.9535778	0.955218	0.9565404	0.9577888
1590	0.9727684	0.9587604	0.9484505	0.9423051	0.9394451	0.9389769	0.9399065	0.9417233	0.9437813	0.9460768	0.9482945	0.9503272	0.9520478	0.9536819	0.9553197	0.9566145
1595	0.957653	0.9490748	0.9438934	0.9409128	0.9397003	0.9397495	0.9407458	0.9423507	0.9441816	0.9461229	0.9480531	0.9498472	0.9514831	0.9533028	0.9544902	0.9558234
1600	0.9258618	0.9317701	0.9358274	0.9387699	0.9409274	0.9425494	0.9439791	0.9453342	0.9467034	0.9479388	0.9491619	0.9506734	0.951782	0.9530685	0.954266	0.9554164
1605	0.9038969	0.9192011	0.9302011	0.9375795	0.9423561	0.9453847	0.9472848	0.9485837	0.9495013	0.9503029	0.9509259	0.9518639	0.9526162	0.9534868	0.9544933	0.9553717
1610	0.9173052	0.9255062	0.9332905	0.9396075	0.9442232	0.9473776	0.9494058	0.9507299	0.9514766	0.9521468	0.9525316	0.9532214	0.9535984	0.9544119	0.9549205	0.955639
1615	0.946156	0.9453501	0.9456557	0.9467679	0.9482644	0.9497355	0.9509978	0.9519868	0.9526128	0.9532483	0.9537217	0.9540966	0.9545004	0.9549212	0.9555427	0.9561483
1620	0.9726053	0.9653758	0.9601816	0.9567751	0.9546927	0.9537278	0.9534042	0.9535066	0.953828	0.954173	0.9547533	0.954984	0.955372	0.9558954	0.9563429	0.9568516
1625	0.982836	0.9765033	0.9703104	0.9651315	0.9611419	0.9585336	0.9568973	0.9560331	0.9558938	0.9556804	0.9562272	0.9561821	0.9564542	0.9569928	0.9573044	0.9577558
1630	0.9804358	0.9764279	0.9722616	0.9684771	0.9651355	0.9625372	0.9606125	0.9592769	0.9585586	0.9580072	0.9582701	0.9577367	0.9579638	0.9580842	0.9585954	0.9589095
1635	0.9706795	0.9696888	0.9686694	0.9675671	0.9662401	0.9648755	0.9635139	0.9623397	0.9612206	0.9607409	0.9607036	0.9602251	0.9599082	0.9601556	0.9601483	0.9603478
1640	0.9602333	0.9625155	0.9641359	0.9652553	0.9657486	0.9656196	0.9651055	0.9644449	0.9635534	0.9632053	0.963035	0.9622189	0.9620792	0.9620634	0.9618859	0.9620358
1645	0.9542771	0.9584364	0.9614921	0.9635382	0.9647543	0.9652332	0.9654744	0.9654168	0.9653032	0.9650431	0.9649366	0.9647149	0.9641986	0.9639261	0.9639026	0.9638516
1650	0.9583756	0.9602787	0.9616162	0.9626873	0.9636659	0.9644608	0.9652799	0.9657921	0.9664154	0.9663457	0.9662501	0.9661148	0.9660581	0.9660155	0.9657945	0.9656324
1655	0.965872	0.9633436	0.9623177	0.9625862	0.9634416	0.9646791	0.9656326	0.9663982	0.9672431	0.9674279	0.9672599	0.9676911	0.9675892	0.9674361	0.9674183	0.9672465
1660	0.9652315	0.9637639	0.9641166	0.9648319	0.9655753	0.9665036	0.9671015	0.9676498	0.968033	0.9685427	0.968298	0.9689082	0.9688503	0.968879	0.9687757	0.9686421
1665	0.9638285	0.9671388	0.968332	0.9687519	0.9689707	0.9690564	0.9692709	0.9694022	0.9694462	0.9698064	0.9694747	0.9697856	0.9699653	0.9700323	0.9699388	0.9698474
1670	0.9664843	0.9693574	0.9708757	0.9714996	0.9716644	0.9714617	0.9714313	0.9712638	0.9712823	0.9711857	0.9708742	0.9713955	0.9710475	0.9708782	0.9710429	0.9709382
1675	0.9781688	0.9750496	0.973885	0.9736719	0.9736871	0.9734618	0.9732229	0.9729331	0.9728621	0.9725692	0.9723238	0.9720593	0.9721594	0.9722397	0.972012	0.9719964
1680	0.9820175	0.9802111	0.9782745	0.9768792	0.9759531	0.9753498	0.9748206	0.9744038	0.9742287	0.9738908	0.9737338	0.9737326	0.9733169	0.973307	0.9731571	0.9730778
1685	0.9819564	0.9813844	0.9803367	0.9792179	0.9780788	0.9770943	0.9764036	0.975844	0.9754494	0.9751946	0.9750466	0.9746179	0.9745188	0.9743482	0.9743003	0.9742035
1690	0.9814956	0.9810967	0.9803774	0.9797043	0.9789706	0.9782673	0.9777341	0.9772294	0.9767786	0.976536	0.9764511	0.9760008	0.9757525	0.9756929	0.9755267	0.97537
1695	0.9806542	0.9798381	0.9793534	0.9792259	0.9790857	0.9789431	0.9787026	0.9784032	0.9781334	0.9778139	0.9777418	0.9773602	0.9769886	0.9768229	0.9767385	0.976564
1700	0.9778042	0.978075	0.9785632	0.9790606	0.9793391	0.9794676	0.9794211	0.9792861	0.9790958	0.9789023	0.9788299	0.9782981	0.9781882	0.9781259	0.977915	0.9777654

Table 5.20. α for 1550-1700 nm, with b of 3.3 comparison run.

alpha:	15	20	25	30	35	40	45	50	55	60	65	70	75	80	85	90
1550	0.0033528	0.0042732	0.0056029	0.0073768	0.0096361	0.0123908	0.015636	0.0193334	0.0235331	0.0280982	0.0330588	0.0384981	0.0441939	0.0502459	0.0567145	0.0634074
1555	0.0022558	0.0029437	0.0038928	0.0051462	0.0068011	0.0088552	0.0113605	0.0142944	0.0176823	0.0214431	0.0255655	0.0301403	0.0350668	0.0404435	0.0459939	0.0518535
1560	0.0018389	0.0022144	0.0028273	0.0037179	0.0049399	0.0065033	0.008431	0.0107447	0.0134264	0.0165214	0.0199417	0.0238203	0.0279459	0.032523	0.0373377	0.042498
1565	0.0015034	0.0017205	0.0021572	0.0028245	0.003767	0.0049329	0.006437	0.0082638	0.0104023	0.0129165	0.015677	0.0189335	0.02244	0.0263442	0.0304843	0.0349833
1570	0.0011753	0.0014153	0.0017697	0.0022956	0.0029894	0.0039028	0.005085	0.0065321	0.0082669	0.0102866	0.0126274	0.0152791	0.018227	0.0214093	0.0249508	0.0289402
1575	0.0009401	0.0012083	0.0015433	0.001976	0.0025283	0.0032353	0.0041609	0.0053152	0.006723	0.0083638	0.0103148	0.012516	0.0150043	0.0177747	0.0208689	0.0241447
1580	0.0010512	0.0012179	0.0014608	0.0017841	0.0022404	0.0027732	0.003512	0.0044447	0.0055877	0.0069494	0.0085868	0.0104095	0.0125454	0.0149649	0.0176101	0.0205169
1585	0.0013098	0.0013667	0.0014957	0.001698	0.0020254	0.0024393	0.0030386	0.0038064	0.0047541	0.0059027	0.0072826	0.0088504	0.0106722	0.0127389	0.0150404	0.0175875
1590	0.0015786	0.0015097	0.0015284	0.001634	0.001859	0.002203	0.0026912	0.0033378	0.0041409	0.0051255	0.0063053	0.0076539	0.0092476	0.0110263	0.0130548	0.0153018
1595	0.001561	0.0014643	0.0014658	0.0015485	0.0017267	0.0020415	0.0024404	0.0029971	0.003704	0.0045541	0.0055769	0.0067819	0.0081713	0.0097574	0.0115383	0.0135357
1600	0.001294	0.0012928	0.0013431	0.0014449	0.0016152	0.0019081	0.002256	0.0027505	0.0033928	0.004142	0.0050508	0.0061279	0.0073739	0.0087924	0.0103863	0.0121891
1605	0.0009756	0.0010821	0.0011848	0.0013136	0.0014969	0.0017817	0.0021122	0.0025723	0.0031607	0.0038562	0.0046856	0.0056748	0.0068036	0.0080903	0.0095499	0.0111908
1610	0.0008558	0.0009164	0.0010094	0.0011572	0.0013625	0.001663	0.0020016	0.0024524	0.0030105	0.0036794	0.0044592	0.005378	0.0064237	0.0076111	0.0089691	0.0104912
1615	0.0008252	0.0008184	0.0008872	0.0010427	0.0012693	0.001584	0.0019439	0.0023983	0.0029493	0.0035992	0.0043488	0.0052187	0.006212	0.0073332	0.0086175	0.0100511
1620	0.0006997	0.000755	0.0008602	0.0010318	0.0012688	0.0015911	0.00198	0.0024245	0.0029764	0.0036166	0.0043518	0.0051932	0.0061516	0.0072362	0.0084641	0.0098431
1625	0.0006182	0.0007772	0.0009288	0.0011182	0.0013656	0.0016916	0.0021151	0.0025457	0.0030991	0.0037339	0.0044564	0.0052857	0.0062337	0.0073078	0.0084995	0.0098513
1630	0.0008077	0.0009325	0.0010897	0.0012915	0.0015522	0.0018931	0.0023058	0.0028034	0.0033158	0.0039556	0.0046725	0.005521	0.0064567	0.0075201	0.0087226	0.0100717
1635	0.0011891	0.0012539	0.0013898	0.0015864	0.0018611	0.0021955	0.0025982	0.0031038	0.003664	0.0042822	0.0050019	0.005864	0.0068267	0.0079012	0.0091323	0.010509
1640	0.0016104	0.0017175	0.0018542	0.0020325	0.0022947	0.002608	0.0029994	0.0034745	0.0041005	0.0047541	0.005466	0.006386	0.0073569	0.0085117	0.0097579	0.0111775
1645	0.0021962	0.0023303	0.0024356	0.0025736	0.0028013	0.0031004	0.0034806	0.0039584	0.0045947	0.005352	0.0061059	0.0070018	0.0080746	0.0092716	0.0106176	0.0121024
1650	0.002999	0.0029718	0.0030137	0.0031256	0.0033281	0.0036352	0.0040364	0.0045494	0.0052057	0.006019	0.006981	0.0079348	0.0090137	0.0102884	0.0117296	0.0133146
1655	0.0036711	0.0036009	0.0035864	0.0036783	0.0038803	0.0042235	0.0046877	0.0052731	0.0059916	0.006874	0.0079643	0.009023	0.0102327	0.0116444	0.0131794	0.0148468
1660	0.0041297	0.0040709	0.0040798	0.0042278	0.0045087	0.0049326	0.0054929	0.0061901	0.0070176	0.0080281	0.0092173	0.0104247	0.0117894	0.0132618	0.014922	0.016737
1665	0.0042581	0.004326	0.0045122	0.0048257	0.0052663	0.0058283	0.0065332	0.0073788	0.0083817	0.0095024	0.0108263	0.0121071	0.0136027	0.0153289	0.0171569	0.0190223
1670	0.0044366	0.0047383	0.0050869	0.0055996	0.006258	0.0070108	0.0079099	0.0089219	0.0101196	0.0113365	0.0127209	0.0142326	0.0158599	0.0177166	0.0196296	0.0217711
1675	0.0048258	0.0053214	0.0060026	0.0068132	0.0076973	0.0086523	0.009714	0.0108754	0.0121957	0.0135809	0.0149999	0.0168904	0.0185501	0.0204688	0.02268	0.0249649
1680	0.0060256	0.0068739	0.0078014	0.008755	0.0097559	0.0108221	0.0119831	0.0132668	0.0146544	0.016261	0.0177337	0.0196445	0.0217326	0.0240822	0.0262314	0.0287371
1685	0.0088391	0.0096818	0.0105147	0.0113988	0.0123431	0.013496	0.0147446	0.0161486	0.0176056	0.0194703	0.0210198	0.0236528	0.0254864	0.0279246	0.0304273	0.0331361
1690	0.0129743	0.0133464	0.0138518	0.0145814	0.0155257	0.0166892	0.018093	0.0196299	0.0213255	0.0232904	0.02499	0.0273048	0.0299004	0.0324358	0.0353245	0.0382416
1695	0.0176537	0.0172824	0.0176434	0.0184203	0.019404	0.0206365	0.0221618	0.0238314	0.0258766	0.0278507	0.0299036	0.0328623	0.0350662	0.0380349	0.0408802	0.0441398
1700	0.0205816	0.0214452	0.0221017	0.0229678	0.0240707	0.0254596	0.0270464	0.0288574	0.0312415	0.033219	0.0357049	0.0380685	0.0410622	0.0441358	0.0474655	0.0509318

Table 5.21. β for 1550-1700 nm, with b of 3.3 comparison run.

beta:	15	20	25	30	35	40	45	50	55	60	65	70	75	80	85	90
1550	0.863242	0.8217462	0.7752568	0.7279168	0.6839816	0.6430473	0.6066458	0.5744951	0.5445609	0.518521	0.493557	0.4730737	0.4528315	0.4343867	0.4170249	0.4009645
1555	0.893709	0.8530576	0.8061062	0.7569025	0.7099836	0.6658924	0.6266438	0.5921879	0.5607316	0.5334123	0.5074468	0.4861385	0.4653929	0.4457686	0.4283256	0.4120441
1560	0.9189037	0.8795356	0.8318054	0.7809932	0.7320376	0.686471	0.6458569	0.6095496	0.5773306	0.5481284	0.5210704	0.4983852	0.4775849	0.4568701	0.4392233	0.4225257
1565	0.9357921	0.8993655	0.8530681	0.8019232	0.7502189	0.7069035	0.6653482	0.6273689	0.5942574	0.5632232	0.5365991	0.5119702	0.4896059	0.4681844	0.449659	0.4324641
1570	0.9448398	0.91245	0.8707799	0.8212512	0.7752238	0.730179	0.6864232	0.646449	0.6112776	0.5787502	0.5496778	0.5224943	0.5010896	0.4807445	0.461818	0.4426497
1575	0.9469007	0.9184847	0.8826999	0.8397976	0.7967254	0.7536488	0.7085842	0.6663759	0.6285043	0.5945683	0.5640766	0.5370959	0.5124534	0.4896672	0.4691778	0.4527506
1580	0.9363632	0.9188275	0.8915333	0.8573307	0.8135837	0.7742338	0.7292802	0.6853288	0.6451551	0.6099591	0.5779047	0.5473837	0.5236589	0.4992628	0.4785351	0.4601086
1585	0.92708	0.9205095	0.9007205	0.8716357	0.8298112	0.791568	0.7468951	0.7020321	0.660839	0.6243977	0.5911857	0.5614825	0.5348294	0.5094379	0.4886148	0.469401
1590	0.9281721	0.9248862	0.9085308	0.8828349	0.8451217	0.8061764	0.7620044	0.7167796	0.6754661	0.6380704	0.6037705	0.5720897	0.5462195	0.5211537	0.4989967	0.4792683
1595	0.9344193	0.9291071	0.9145858	0.8912823	0.8585106	0.8162701	0.7756492	0.7305501	0.6897745	0.651156	0.6162011	0.5845333	0.558115	0.5319347	0.5099046	0.4899215
1600	0.9407406	0.9360448	0.9219143	0.8992597	0.8689565	0.82459	0.7872981	0.7429268	0.7033662	0.6638194	0.6288072	0.5980379	0.5706654	0.5437698	0.5220013	0.5015349
1605	0.9478613	0.9424496	0.9284986	0.9057854	0.8758097	0.8316608	0.7954149	0.7528863	0.7137035	0.6758182	0.641753	0.609557	0.5838261	0.5575636	0.5348902	0.5139618
1610	0.9530182	0.9470057	0.9329699	0.9088513	0.8784264	0.8354256	0.8001223	0.7602224	0.7213388	0.6866614	0.6545978	0.6256316	0.5971396	0.5711161	0.5479655	0.5265885
1615	0.9542803	0.9497263	0.935812	0.9098635	0.8787177	0.8366713	0.8027965	0.7657042	0.7284064	0.6962586	0.666046	0.633957	0.6096376	0.58384	0.5600826	0.5386682
1620	0.9548711	0.948189	0.9337829	0.9088861	0.877688	0.8387345	0.8027934	0.7704865	0.7355207	0.7045737	0.6759694	0.6478776	0.6204863	0.5948661	0.5715854	0.5493709
1625	0.9501411	0.9401782	0.9266152	0.9048003	0.8753695	0.842118	0.8021868	0.7743485	0.7427174	0.7113953	0.6833022	0.6527523	0.6290289	0.6034107	0.5800105	0.5579526
1630	0.9365032	0.9271866	0.9161159	0.8979065	0.8712741	0.8415838	0.8076541	0.7726647	0.7477896	0.7164585	0.6878976	0.6607429	0.6348158	0.6097609	0.5859153	0.5638903
1635	0.9191044	0.9157203	0.907169	0.8912094	0.8664348	0.8392173	0.8100202	0.7755638	0.7453378	0.7186435	0.6892388	0.6627183	0.6375138	0.6125972	0.5889906	0.5670686
1640	0.915409	0.9089732	0.8984201	0.8834996	0.8610346	0.8355129	0.8079835	0.7781084	0.742896	0.7152114	0.6876984	0.6620772	0.6371836	0.6114448	0.5892834	0.5676851
1645	0.905071	0.8955504	0.8874658	0.8748944	0.8550982	0.8307377	0.8035883	0.7746074	0.7423634	0.7087768	0.6823466	0.6601804	0.6339641	0.6097645	0.5872286	0.5660642
1650	0.8921316	0.8880635	0.8799068	0.8664704	0.8472307	0.8232104	0.7959028	0.7669902	0.7366625	0.7043661	0.6725706	0.6501966	0.6283229	0.6053619	0.5830723	0.5626279
1655	0.8821799	0.8777391	0.8694618	0.8553774	0.8355714	0.8113402	0.7842847	0.7554906	0.7263507	0.696943	0.6665453	0.6424615	0.620152	0.5978248	0.577251	0.5578898
1660	0.8729272	0.8653013	0.8557622	0.8405628	0.8199175	0.7948632	0.7681264	0.7397925	0.7119304	0.6837225	0.6573421	0.6322104	0.6099429	0.5900231	0.5705165	0.5521624
1665	0.858926	0.8522661	0.8396032	0.8212214	0.7988967	0.7737159	0.7470785	0.7201211	0.6933654	0.6680924	0.6445785	0.6232429	0.601468	0.5813749	0.5622903	0.545728
1670	0.8404586	0.829863	0.8144275	0.7937829	0.7709031	0.7466775	0.7217324	0.6974902	0.6731104	0.6512712	0.6312961	0.6098874	0.590703	0.5724244	0.5552692	0.5383372
1675	0.8162148	0.7981218	0.7777337	0.7565706	0.7359877	0.7150967	0.6943489	0.6738185	0.6532117	0.6338952	0.6175919	0.5963622	0.5794932	0.5632825	0.5466799	0.531189
1680	0.770964	0.7510931	0.7327384	0.7161554	0.6998914	0.6841435	0.6678934	0.6510856	0.6343251	0.6168706	0.6029907	0.5848085	0.5680056	0.5520287	0.5376933	0.5232621
1685	0.7085258	0.700841	0.691287	0.6809772	0.6694955	0.657514	0.6443739	0.6303164	0.6166131	0.6004189	0.5883264	0.5689741	0.5564265	0.5423153	0.528529	0.5150676
1690	0.6648542	0.6624411	0.6594445	0.6539443	0.6452551	0.6358762	0.623934	0.6115841	0.5987797	0.584987	0.5738893	0.5593352	0.5451145	0.5326458	0.5192476	0.5067816
1695	0.640539	0.6434608	0.6402922	0.6338547	0.6259705	0.6169008	0.6059002	0.5948575	0.582142	0.570928	0.559612	0.5459491	0.5344533	0.5225866	0.5109757	0.4985883
1700	0.6371241	0.6308699	0.6246758	0.6174303	0.6096372	0.5999665	0.5903372	0.5803624	0.5683251	0.5586662	0.5469527	0.537142	0.524781	0.513719	0.5022407	0.4905792

Table 5.22. Indices 1550-1700 nm. IW/λ – Index Water/Wavelength, II/λ – Index Ice/Wavelength

λ (nm)	IW/λ	II/λ	λ (nm)	IW/λ	II/λ	λ (nm)	IW/λ	II/λ	λ (nm)	IW/λ	II/λ	λ (nm)	IW/λ	II/λ
1550	0.0000863	0.0002738	1582	0.0000671	0.0002063	1614	0.0000537	0.0001643	1646	0.0000467	0.0001454	1678	0.0000446	0.0001232
1551	0.0000857	0.0002717	1583	0.0000664	0.0002042	1615	0.0000534	0.0001637	1647	0.0000464	0.0001449	1679	0.0000446	0.0001225
1552	0.000085	0.0002697	1584	0.0000658	0.000202	1616	0.0000531	0.0001631	1648	0.0000461	0.0001443	1680	0.0000447	0.0001218
1553	0.0000843	0.0002676	1585	0.0000651	0.0001999	1617	0.0000528	0.0001625	1649	0.0000459	0.0001437	1681	0.0000447	0.0001212
1554	0.0000836	0.0002655	1586	0.0000645	0.0001978	1618	0.0000525	0.0001619	1650	0.0000458	0.0001431	1682	0.0000447	0.0001206
1555	0.0000829	0.0002634	1587	0.0000639	0.0001957	1619	0.0000522	0.0001613	1651	0.0000457	0.0001424	1683	0.0000448	0.0001201
1556	0.0000822	0.0002614	1588	0.0000632	0.0001945	1620	0.0000519	0.0001607	1652	0.0000456	0.0001417	1684	0.0000448	0.0001195
1557	0.0000815	0.0002593	1589	0.0000626	0.0001933	1621	0.0000515	0.0001601	1653	0.0000454	0.000141	1685	0.0000448	0.0001189
1558	0.0000809	0.0002572	1590	0.0000622	0.0001921	1622	0.0000512	0.0001596	1654	0.0000453	0.0001403	1686	0.0000449	0.0001183
1559	0.0000802	0.0002551	1591	0.0000618	0.0001909	1623	0.000051	0.000159	1655	0.0000452	0.0001395	1687	0.0000449	0.0001178
1560	0.0000795	0.0002531	1592	0.0000614	0.0001897	1624	0.0000508	0.0001584	1656	0.0000451	0.0001388	1688	0.0000449	0.0001172
1561	0.0000788	0.000251	1593	0.0000611	0.0001885	1625	0.0000506	0.0001578	1657	0.0000449	0.0001381	1689	0.0000449	0.0001166
1562	0.0000781	0.0002489	1594	0.0000607	0.0001874	1626	0.0000504	0.0001572	1658	0.0000448	0.0001374	1690	0.000045	0.000116
1563	0.0000774	0.0002468	1595	0.0000603	0.0001862	1627	0.0000501	0.0001566	1659	0.0000447	0.0001367	1691	0.0000451	0.0001155
1564	0.0000767	0.0002447	1596	0.0000599	0.000185	1628	0.0000499	0.000156	1660	0.0000446	0.000136	1692	0.0000451	0.0001149
1565	0.000076	0.0002426	1597	0.0000595	0.0001838	1629	0.0000497	0.0001554	1661	0.0000445	0.0001353	1693	0.0000452	0.0001143
1566	0.0000754	0.0002404	1598	0.0000592	0.0001826	1630	0.0000496	0.0001549	1662	0.0000445	0.0001346	1694	0.0000453	0.0001137
1567	0.0000747	0.0002383	1599	0.0000588	0.0001814	1631	0.0000494	0.0001543	1663	0.0000445	0.0001339	1695	0.0000454	0.0001132
1568	0.000074	0.0002362	1600	0.0000584	0.0001803	1632	0.0000493	0.0001537	1664	0.0000445	0.0001331	1696	0.0000454	0.0001126
1569	0.0000733	0.000234	1601	0.0000581	0.0001791	1633	0.0000492	0.0001531	1665	0.0000444	0.0001324	1697	0.0000455	0.000112
1570	0.0000726	0.0002319	1602	0.0000577	0.0001779	1634	0.0000491	0.0001525	1666	0.0000444	0.0001317	1698	0.0000456	0.0001114
1571	0.0000722	0.0002298	1603	0.0000574	0.0001767	1635	0.0000489	0.0001519	1667	0.0000444	0.000131	1699	0.0000457	0.0001109
1572	0.0000717	0.0002276	1604	0.000057	0.0001755	1636	0.0000488	0.0001513	1668	0.0000444	0.0001303	1700	0.0000458	0.0001103
1573	0.0000713	0.0002255	1605	0.0000567	0.0001743	1637	0.0000487	0.0001507	1669	0.0000444	0.0001296			
1574	0.0000708	0.0002234	1606	0.0000564	0.0001731	1638	0.0000485	0.0001501	1670	0.0000443	0.0001289			
1575	0.0000704	0.0002212	1607	0.000056	0.000172	1639	0.0000484	0.0001496	1671	0.0000443	0.0001282			
1576	0.00007	0.0002191	1608	0.0000557	0.0001708	1640	0.0000483	0.000149	1672	0.0000444	0.0001275			
1577	0.0000695	0.000217	1609	0.0000553	0.0001696	1641	0.0000482	0.0001484	1673	0.0000444	0.0001268			
1578	0.0000691	0.0002148	1610	0.000055	0.0001684	1642	0.0000479	0.0001478	1674	0.0000444	0.000126			
1579	0.0000686	0.0002127	1611	0.0000546	0.0001672	1643	0.0000476	0.0001472	1675	0.0000445	0.0001253			
1580	0.0000682	0.0002106	1612	0.0000543	0.000166	1644	0.0000473	0.0001466	1676	0.0000445	0.0001246			
1581	0.0000677	0.0002084	1613	0.000054	0.0001648	1645	0.000047	0.000146	1677	0.0000446	0.0001239			

Table 5.23. Transmission (TnoH2O) for 1200-1300 nm, with b of 2.0 comparison run.

tnoh2o:	10	15	20	25	30	35	40	45	50	55	60
1200	0.9919899	0.9908623	0.9912971	0.9921923	0.9928751	0.993243	0.9933805	0.9935538	0.9937505	0.9940254	0.9942192
1202	0.9871702	0.9886152	0.9903502	0.991649	0.9923536	0.9926727	0.9928862	0.9931285	0.9934728	0.9937299	0.9940448
1204	0.9833726	0.987259	0.9898063	0.9911147	0.9916705	0.9919956	0.9923226	0.992769	0.9931495	0.993591	0.9938924
1206	0.9811187	0.9866302	0.9893007	0.9903293	0.9908372	0.9913404	0.9919364	0.9924923	0.9930505	0.9934446	0.9937485
1208	0.9820594	0.9863196	0.9884298	0.9892969	0.9900069	0.9907739	0.9915689	0.9922932	0.9928582	0.9933353	0.9935983
1210	0.9870477	0.9865021	0.9871455	0.9882199	0.989332	0.9904122	0.9913961	0.9921517	0.9927526	0.9931371	0.9934263
1212	0.9910631	0.9872586	0.9863482	0.9874422	0.9888989	0.9901879	0.9912116	0.992045	0.9926674	0.993043	0.993216
1214	0.9920831	0.988039	0.986797	0.9873813	0.9887754	0.9901035	0.9911755	0.9919555	0.9924657	0.9928609	0.9929489
1216	0.9905613	0.9889411	0.9880711	0.9881636	0.9890519	0.990173	0.9911082	0.9918766	0.9924124	0.99261	0.9926034
1218	0.9887968	0.9895637	0.989576	0.9895105	0.9897698	0.9904419	0.9912144	0.9918146	0.9921916	0.9923173	0.9921544
1220	0.9869521	0.9898978	0.9908539	0.9908929	0.9907952	0.9909767	0.9913731	0.991787	0.9920002	0.9919502	0.9915726
1222	0.9863776	0.9900453	0.991669	0.9920247	0.9918842	0.9917089	0.9917566	0.9918122	0.991786	0.9914661	0.9908249
1224	0.9889894	0.9904174	0.9921174	0.992815	0.9928284	0.9925318	0.9921904	0.9918843	0.9914226	0.9907814	0.9898748
1226	0.9924775	0.9919061	0.9925807	0.9933289	0.9935209	0.9932271	0.9926579	0.9919479	0.9911353	0.990078	0.9886827
1228	0.9953437	0.9940754	0.9935611	0.9938232	0.993981	0.9937017	0.9929498	0.9918954	0.9905666	0.9890084	0.9872069
1230	0.997499	0.9960602	0.9950008	0.9945151	0.9943306	0.9939063	0.9929937	0.9915915	0.9897834	0.9876244	0.9854052
1232	0.9986368	0.9976402	0.9964359	0.9954365	0.9947	0.9939018	0.9926832	0.9909022	0.9886258	0.9859739	0.9832448
1234	0.9991655	0.9986176	0.9975951	0.996349	0.9950775	0.9937113	0.9919927	0.9897107	0.9868484	0.9838798	0.9807177
1236	0.999397	0.9991063	0.9983066	0.9969839	0.9952781	0.9932694	0.9908446	0.9879172	0.9845788	0.9810107	0.9778624
1238	0.9995363	0.9992673	0.9985322	0.9971364	0.99506	0.992375	0.9891388	0.9854334	0.9815428	0.9777572	0.9747787
1240	0.9996019	0.9991797	0.9982855	0.996671	0.9941899	0.9907594	0.9866428	0.9821935	0.9778999	0.9745097	0.9716272
1242	0.9994652	0.9987872	0.9975457	0.9955165	0.9924305	0.988135	0.9831872	0.9781921	0.9739324	0.9707034	0.968605
1244	0.9989967	0.9979401	0.9962239	0.9935471	0.9894887	0.9842528	0.978625	0.9735335	0.9695147	0.9669299	0.965901
1246	0.9979795	0.9964667	0.9941379	0.9904007	0.9850162	0.978989	0.9731045	0.9684641	0.9655194	0.9639499	0.9636477
1248	0.9961076	0.9942125	0.9908869	0.9854543	0.9787786	0.9723618	0.9668822	0.9633668	0.9616594	0.9615447	0.9618948
1250	0.9933705	0.9908515	0.9856004	0.9782491	0.9708322	0.9647272	0.9605418	0.9586822	0.9584448	0.9591698	0.9606162
1252	0.9895877	0.9852173	0.977328	0.9687852	0.9615325	0.9566115	0.9546469	0.9547523	0.9561223	0.9574511	0.9597387
1254	0.9837921	0.9754505	0.965909	0.9574488	0.95156	0.9490984	0.9498011	0.9517011	0.9539807	0.956962	0.9591717
1256	0.9719511	0.9612583	0.9517822	0.9447811	0.942095	0.9430055	0.9460611	0.9494608	0.9529714	0.9561263	0.9588279
1258	0.9535286	0.9434079	0.9354621	0.9323559	0.9344367	0.9385824	0.9434193	0.9478813	0.9519274	0.9553602	0.9586341
1260	0.9297683	0.9224301	0.9184622	0.9224352	0.9289677	0.9357108	0.9415235	0.9468083	0.9513168	0.9551215	0.9585344
1262	0.9019124	0.8982509	0.9052338	0.9156637	0.9252361	0.9336191	0.9403064	0.9461091	0.9511079	0.9554359	0.9584899
1264	0.8658577	0.8793386	0.8973973	0.9114383	0.9227743	0.9321894	0.9394927	0.9456772	0.9505705	0.9549481	0.958476
1266	0.8399945	0.8708566	0.8928349	0.9088694	0.9213406	0.9311355	0.9390891	0.9454355	0.9507548	0.9546538	0.9584793
1268	0.8412331	0.8692236	0.8909284	0.9079201	0.9208104	0.9307191	0.9389026	0.945339	0.9505497	0.9549339	0.9584946
1270	0.8528735	0.8740579	0.8925263	0.9085031	0.9211265	0.930869	0.9390129	0.9453739	0.9505482	0.9551281	0.9585227
1272	0.8718602	0.8849353	0.8982549	0.9110323	0.9223999	0.9315971	0.9393331	0.945557	0.950816	0.9548341	0.9585703
1274	0.9078652	0.9014834	0.9078742	0.916144	0.9249582	0.9331806	0.9400458	0.9459385	0.950722	0.9547791	0.9586499
1276	0.9396096	0.9254274	0.9210935	0.9237971	0.9291699	0.935482	0.9412283	0.9466099	0.9514206	0.9555851	0.958782
1278	0.9570419	0.9488725	0.9379261	0.9341787	0.9352602	0.938958	0.9431958	0.947713	0.9519054	0.9558043	0.9589978
1280	0.9704457	0.9644276	0.9549748	0.9466181	0.9432679	0.9437004	0.9461202	0.9494293	0.9529006	0.9561286	0.959343
1282	0.9806905	0.9753141	0.9680787	0.9593976	0.9528646	0.9500434	0.9502297	0.9519407	0.9545726	0.9571013	0.9598807
1284	0.9883733	0.9834026	0.9775192	0.9703026	0.9629372	0.9576532	0.9554665	0.9553671	0.956417	0.9588541	0.9606915
1286	0.9929757	0.9893463	0.9845157	0.978661	0.9720164	0.9657688	0.9616638	0.9597062	0.9596109	0.9603201	0.9618666
1288	0.9954142	0.9932863	0.9896799	0.9849924	0.9793944	0.9734601	0.9682489	0.9647817	0.9630679	0.9626297	0.963492
1290	0.9968194	0.9956261	0.9932913	0.9897058	0.9851308	0.9799145	0.9746096	0.9702276	0.967313	0.9659687	0.965624
1292	0.9976174	0.9970539	0.9956279	0.9930856	0.9894793	0.9850839	0.9802027	0.9755763	0.9719516	0.9695899	0.9682645
1294	0.9982082	0.9979531	0.9970891	0.9953697	0.9926576	0.9890612	0.9848281	0.9804333	0.9763358	0.9732398	0.9713423
1296	0.9987711	0.9985471	0.9980007	0.9968405	0.9948587	0.9920165	0.988494	0.9845893	0.9807637	0.9771731	0.9747129
1298	0.9991901	0.9989894	0.9985775	0.9977505	0.996286	0.9941061	0.9912913	0.9880013	0.9844617	0.9812237	0.9781833
1300	0.9995354	0.9993132	0.9989436	0.9982617	0.9971416	0.9955217	0.9933764	0.9907171	0.987686	0.9845545	0.9815555

Table 5.24. α for 1200-1300 nm, with b of 2.0 comparison run.

alpha:	10	15	20	25	30	35	40	45	50	55	60
1200	0.0939537	0.0861258	0.0842218	0.0847104	0.085445	0.0855525	0.0854313	0.0853135	0.0855206	0.0858516	0.0877886
1202	0.0910024	0.0858078	0.082978	0.0819122	0.0816989	0.0816378	0.0811239	0.0811209	0.0812535	0.0817108	0.0828862
1204	0.0861772	0.0848314	0.082125	0.0796254	0.0779425	0.0774971	0.0770867	0.0768946	0.0770802	0.0777632	0.0782696
1206	0.0803741	0.0822738	0.0801886	0.0769345	0.0744146	0.0733923	0.0727255	0.0726724	0.0726884	0.0731539	0.0738412
1208	0.0756395	0.0778502	0.0762052	0.0733351	0.0710731	0.0694537	0.06885	0.0684781	0.0685764	0.0684385	0.0695754
1210	0.0717113	0.0716164	0.0705676	0.0691607	0.0675412	0.0657227	0.0647697	0.0643873	0.0643405	0.0647133	0.0654505
1212	0.0694573	0.0646271	0.0646394	0.0645233	0.0634945	0.0620234	0.0611104	0.060452	0.0603642	0.0611524	0.0614766
1214	0.0623988	0.0597702	0.0591299	0.0593204	0.0588565	0.0580502	0.0570984	0.0566291	0.0566379	0.0568661	0.0576489
1216	0.0555592	0.0553313	0.0542054	0.0538667	0.053816	0.0536662	0.0532403	0.0528601	0.0528307	0.0529129	0.0539676
1218	0.0487798	0.0498359	0.049358	0.0486645	0.0487062	0.0490229	0.0489297	0.0490673	0.0492767	0.0497717	0.0504619
1220	0.0404025	0.0434298	0.0440614	0.0437779	0.0437919	0.0442753	0.0447753	0.0452074	0.0456528	0.0467235	0.0471068
1222	0.0343859	0.0366499	0.038114	0.0387854	0.0390673	0.0396797	0.0404232	0.0413321	0.0421225	0.0428506	0.0438745
1224	0.0318175	0.0305408	0.0319698	0.033484	0.0344192	0.0352568	0.0364274	0.037503	0.0386629	0.0393843	0.0407315
1226	0.0271213	0.026025	0.0264873	0.0281553	0.0297966	0.0310357	0.032426	0.0337832	0.035084	0.0365232	0.0376532
1228	0.0211452	0.0217665	0.0220857	0.0233653	0.0253069	0.0270045	0.0287317	0.0302316	0.031736	0.0334773	0.0346342
1230	0.0164237	0.0171729	0.0182247	0.0194054	0.0212007	0.0232167	0.0250632	0.0268202	0.0284485	0.0299042	0.0316783
1232	0.0117917	0.013093	0.0145321	0.0159953	0.0176334	0.0196733	0.0216466	0.0235529	0.0253921	0.0269198	0.0288227
1234	0.0075487	0.0095483	0.0112003	0.0128716	0.014555	0.0164691	0.0184231	0.0204601	0.0224307	0.0243633	0.0260792
1236	0.0050076	0.0064475	0.0082971	0.010057	0.0118211	0.0136419	0.0155759	0.0175865	0.0195893	0.0216696	0.0234624
1238	0.0031712	0.0042564	0.005838	0.0076225	0.0093915	0.0111736	0.0130253	0.0149819	0.0169849	0.0189043	0.0209859
1240	0.0018387	0.00275	0.0039992	0.0055746	0.0072765	0.0090021	0.0108047	0.0126642	0.0146016	0.0165661	0.0186668
1242	0.0010878	0.0017368	0.0027064	0.0039698	0.0054957	0.0071216	0.0088297	0.010617	0.0125157	0.0145571	0.0165232
1244	0.0007669	0.0011404	0.0018239	0.0028189	0.0040763	0.0055413	0.0071396	0.0088263	0.0106313	0.0126143	0.0145884
1246	0.0005444	0.0008187	0.0012881	0.00202	0.003014	0.0042543	0.005692	0.007282	0.0090024	0.0108413	0.0128734
1248	0.0004383	0.0006736	0.0009911	0.0015014	0.0022593	0.0032736	0.0045342	0.0059887	0.0076293	0.0093789	0.0113943
1250	0.0005458	0.0006292	0.0008429	0.0011969	0.0017565	0.0025643	0.0036314	0.0049495	0.0064723	0.0082545	0.0101579
1252	0.0006769	0.0006765	0.0007987	0.0010394	0.0014508	0.0020917	0.0030006	0.0041654	0.0056003	0.0072772	0.0091687
1254	0.0007203	0.0007764	0.00083	0.0009811	0.0012958	0.0018171	0.0025814	0.0036254	0.0049433	0.0065127	0.0084372
1256	0.0008506	0.0008684	0.000894	0.0010032	0.00126	0.0017027	0.0023811	0.0033103	0.0045403	0.0060706	0.0079796
1258	0.0010135	0.0009524	0.0009741	0.0010889	0.0013259	0.0017244	0.0023294	0.0032008	0.0043784	0.0059317	0.0078129
1260	0.0010678	0.001047	0.0010875	0.0012331	0.0014761	0.0018632	0.002451	0.0032791	0.0044412	0.0059911	0.0079578
1262	0.0011026	0.001146	0.0012566	0.0014323	0.0016993	0.0021062	0.0026769	0.0035405	0.0047534	0.0063395	0.0084333
1264	0.0012184	0.0012938	0.0014793	0.0016883	0.0019979	0.0024343	0.0030717	0.0039964	0.0053172	0.0070854	0.0092591
1266	0.0012994	0.0015585	0.0017387	0.0020143	0.0023672	0.0028483	0.0035754	0.0046729	0.0061543	0.0080929	0.0104531
1268	0.0016352	0.0018209	0.0020899	0.0024145	0.0028003	0.0033816	0.0043288	0.0056038	0.0073092	0.00944	0.0120385
1270	0.0019671	0.0021847	0.0025465	0.0028624	0.0033301	0.0041065	0.005262	0.0068257	0.0087872	0.0111817	0.0140351
1272	0.0024	0.0027768	0.0030263	0.0033697	0.0040399	0.0050906	0.0065683	0.00838	0.0106469	0.0133845	0.0164635
1274	0.0032512	0.0034196	0.0035173	0.004048	0.0050254	0.0064045	0.0081187	0.0103092	0.0128969	0.0159052	0.0193413
1276	0.004252	0.0039144	0.0041922	0.0050468	0.0063588	0.0080721	0.0101772	0.012667	0.0156132	0.0189279	0.0226766
1278	0.0044691	0.0045476	0.0052336	0.006461	0.0080926	0.0101675	0.0125654	0.0155049	0.0188054	0.0224273	0.0264798
1280	0.0050309	0.0055057	0.0067728	0.0083303	0.0102878	0.0127338	0.0156199	0.0188793	0.022563	0.0265452	0.0307588
1282	0.0058721	0.0072098	0.0087833	0.0106826	0.0130297	0.0158638	0.0191153	0.0228169	0.0267591	0.0310193	0.0355217
1284	0.0076004	0.0094983	0.0113294	0.0136172	0.0164112	0.0196223	0.0234135	0.0273217	0.0315362	0.0358424	0.0407958
1286	0.0099913	0.0122538	0.0145381	0.0172616	0.0205297	0.0241317	0.0281806	0.0323839	0.0367574	0.0414746	0.0466151
1288	0.0140642	0.0157044	0.0185657	0.0217711	0.0255071	0.0294262	0.0337099	0.0379936	0.0425785	0.0478274	0.053025
1290	0.0185431	0.0206908	0.0234917	0.0273042	0.0313699	0.0354821	0.0396704	0.0441774	0.0491058	0.0543758	0.0600873
1292	0.0253004	0.026699	0.0298093	0.0339552	0.0379818	0.0421726	0.0463346	0.050961	0.055947	0.0613456	0.0678702
1294	0.0318016	0.0341656	0.0378052	0.0415297	0.045216	0.0494042	0.0536028	0.0583952	0.0638284	0.0698023	0.0765081
1296	0.0397706	0.0435002	0.0470212	0.0497367	0.0531698	0.0572337	0.0615366	0.066523	0.0721287	0.0790116	0.0860768
1298	0.0505063	0.0546078	0.0564889	0.0587428	0.0619534	0.0657109	0.0702358	0.0754422	0.0815866	0.0886197	0.0967088
1300	0.0657341	0.065516	0.0664197	0.0686585	0.071562	0.0749916	0.0796633	0.0852957	0.0921052	0.09936	0.1085168

Table 5.25. β for 1200-1300 nm, with b of 2.0 comparison run.

beta:	10	15	20	25	30	35	40	45	50	55	60
1200	0.60122	0.6054178	0.6068476	0.6075633	0.6072739	0.6051853	0.6021929	0.5975894	0.5923089	0.5868623	0.5783054
1202	0.5920843	0.5995271	0.6054577	0.6092831	0.6093882	0.6073078	0.6041588	0.5998611	0.5946022	0.5879632	0.5806262
1204	0.5887257	0.5954443	0.6051567	0.6100817	0.6108422	0.6091681	0.6061106	0.6018589	0.5963891	0.5893876	0.5824866
1206	0.5878532	0.5980558	0.605665	0.6097921	0.6113454	0.6104992	0.6075246	0.6034807	0.5982406	0.5918242	0.5840919
1208	0.5983792	0.6042662	0.6071887	0.6095571	0.6111532	0.61125	0.6087995	0.604809	0.5992621	0.5936806	0.5853845
1210	0.6130691	0.6115013	0.6101302	0.6102934	0.6111266	0.6113809	0.6093988	0.6056473	0.6002361	0.5935714	0.5863957
1212	0.6225867	0.6195583	0.6146791	0.6125759	0.6120691	0.6113641	0.6096528	0.6058065	0.6007179	0.5932127	0.5870779
1214	0.6326227	0.6256433	0.6205977	0.6169611	0.6144695	0.6117674	0.6093891	0.6054886	0.6001568	0.5947416	0.587562
1216	0.6437213	0.6317332	0.6275102	0.6230963	0.618184	0.6133524	0.6093043	0.6048582	0.5999994	0.5949812	0.5879887
1218	0.6458504	0.6410664	0.6355457	0.6296489	0.6226431	0.6156643	0.6095746	0.6043306	0.5992052	0.5936487	0.5882312
1220	0.654842	0.6511697	0.6442784	0.6359395	0.6272671	0.6187645	0.6108539	0.604437	0.5989574	0.5924566	0.5884761
1222	0.6661324	0.6618827	0.6530544	0.6424303	0.6320351	0.622022	0.6128067	0.6053112	0.5994598	0.5946311	0.5888736
1224	0.6720054	0.6724198	0.6624363	0.649462	0.6370858	0.6257934	0.6157397	0.6071899	0.6000683	0.5956351	0.5896273
1226	0.6823475	0.6808358	0.6713735	0.6569407	0.6427339	0.6303827	0.6193085	0.6101828	0.6027254	0.5954365	0.5909573
1228	0.7080073	0.689359	0.6782459	0.664645	0.6492748	0.6358137	0.6240118	0.6139696	0.6056622	0.5977786	0.5930448
1230	0.7254642	0.7042966	0.6858197	0.6715931	0.656415	0.6420109	0.6293353	0.6189035	0.6099655	0.6037031	0.5961177
1232	0.7414032	0.7204767	0.6976137	0.6791046	0.6640989	0.6492329	0.6364178	0.6249657	0.6152754	0.607958	0.6000286
1234	0.7705035	0.7366428	0.7119143	0.6898027	0.6727546	0.6576975	0.6440933	0.6321096	0.6212951	0.611375	0.604886
1236	0.7925929	0.759631	0.7274485	0.7037139	0.6837361	0.6674201	0.6534396	0.6404651	0.6292929	0.618959	0.610699
1238	0.8087705	0.7818018	0.747622	0.7198847	0.6974136	0.6790414	0.6635349	0.6500146	0.6378118	0.628105	0.6174713
1240	0.8362185	0.8014718	0.7712727	0.7392975	0.7139212	0.6931367	0.6760064	0.6608093	0.6475021	0.6357319	0.6252088
1242	0.8639706	0.8306984	0.7952743	0.7625018	0.7336276	0.7099376	0.6899163	0.6731561	0.6583077	0.6440548	0.6340092
1244	0.8911685	0.8621842	0.8231901	0.7880856	0.756569	0.7294031	0.7064878	0.6871131	0.6704924	0.6563013	0.6435861
1246	0.9230669	0.8907661	0.8542597	0.8164053	0.7818613	0.7514333	0.7247719	0.7028278	0.6842564	0.6686461	0.6540213
1248	0.9471963	0.9147531	0.8836586	0.8466037	0.8090987	0.7753183	0.7453352	0.719997	0.6988739	0.6805996	0.664957
1250	0.9445317	0.9321347	0.9074988	0.8744498	0.8365631	0.7997512	0.7662472	0.7381724	0.7142784	0.6931358	0.6759825
1252	0.9413996	0.9398261	0.9235871	0.8965763	0.8609636	0.8226965	0.7871159	0.7561552	0.7294965	0.7070656	0.6865487
1254	0.9440088	0.9403808	0.9320002	0.9114352	0.8789074	0.8410702	0.8049752	0.7723258	0.7434521	0.7188903	0.6957386
1256	0.9404095	0.9400818	0.935331	0.9179794	0.8885272	0.8533102	0.8183492	0.7849936	0.7548075	0.7271451	0.7023786
1258	0.9377439	0.9406806	0.9344314	0.9168075	0.8900685	0.8584058	0.8253893	0.7926201	0.761354	0.7317208	0.7054361
1260	0.9431373	0.9397097	0.9287223	0.9097834	0.885933	0.8574656	0.8267605	0.7948287	0.762977	0.733128	0.7041725
1262	0.9453447	0.935692	0.9184489	0.9000651	0.8780876	0.8523397	0.82319	0.7917684	0.7591181	0.7281387	0.6985588
1264	0.9402356	0.9239717	0.90695	0.8891343	0.868041	0.8446087	0.8161731	0.7841164	0.7508667	0.7181129	0.6891731
1266	0.928003	0.9084682	0.8952496	0.8770424	0.8579164	0.8355185	0.8060228	0.7727492	0.73893	0.7061749	0.6770536
1268	0.9037322	0.8967059	0.8805043	0.8651904	0.8484005	0.8241756	0.792797	0.7586344	0.7244496	0.6927013	0.6631379
1270	0.8904026	0.8797162	0.8658835	0.8555681	0.8380333	0.8104376	0.777302	0.742645	0.7087386	0.6771233	0.6483906
1272	0.8733045	0.859473	0.8562531	0.8468863	0.8249168	0.7940803	0.7598667	0.7253783	0.6919604	0.6606588	0.6335083
1274	0.8455604	0.8489678	0.8499991	0.8356141	0.8083954	0.775844	0.7416402	0.7074831	0.6751184	0.6451944	0.6189984
1276	0.8392076	0.8466274	0.8419687	0.8197612	0.7896329	0.7566133	0.7224843	0.6892698	0.6582651	0.630675	0.6052845
1278	0.8424404	0.8459466	0.828552	0.8009779	0.7698467	0.7362069	0.7030649	0.6712413	0.6420585	0.6166155	0.5924984
1280	0.845868	0.8375235	0.8108067	0.7815663	0.7495776	0.7159142	0.6839799	0.6536942	0.6263697	0.6019006	0.5807144
1282	0.8464126	0.8185881	0.7920158	0.7620143	0.7290164	0.6958344	0.6650818	0.637283	0.6126111	0.5897141	0.5699663
1284	0.8299802	0.8002486	0.7724107	0.7413408	0.708343	0.6769331	0.6479324	0.622447	0.599766	0.5803557	0.5600746
1286	0.8093604	0.7818953	0.7520075	0.7199036	0.6879556	0.6589345	0.631882	0.6093723	0.5890344	0.5701552	0.5508864
1288	0.7852007	0.7610267	0.7299512	0.698389	0.6683316	0.6423656	0.6187897	0.5981102	0.5791246	0.5593998	0.5422341
1290	0.7642829	0.736781	0.7073833	0.6773171	0.6503491	0.6276348	0.6068457	0.5883564	0.5699943	0.5517439	0.5339465
1292	0.7373081	0.713208	0.6851593	0.6574733	0.6349851	0.6150916	0.5977309	0.5798988	0.5625632	0.5453642	0.5259358
1294	0.7118996	0.6901144	0.6636665	0.6409469	0.6227143	0.6049956	0.5887513	0.5723315	0.5547024	0.5371304	0.5178424
1296	0.6855276	0.6658595	0.6448709	0.628751	0.6129151	0.5970176	0.5821801	0.56545	0.5480899	0.5283402	0.5097781
1298	0.6579756	0.641575	0.6309664	0.6190425	0.6050478	0.5907158	0.5752629	0.5589636	0.5409005	0.5216616	0.5015972
1300	0.6278282	0.6246484	0.6197178	0.6104152	0.5985953	0.5854309	0.5699546	0.5526406	0.5339167	0.5148239	0.4932988

Table 5.26. Transmission (TnoH2O) for 1200-1300 nm, with b of 2.5 comparison run.

tnoh2o:	10	15	20	25	30	35	40	45	50	55	60
1200	0.9921603	0.991177	0.9916201	0.9923443	0.9928807	0.9932275	0.9934151	0.9936084	0.9937571	0.9939214	0.9939675
1202	0.9874562	0.9890299	0.9905869	0.9916781	0.9923306	0.9927213	0.9929938	0.9932149	0.9934613	0.993574	0.9937102
1204	0.9839193	0.987631	0.9898949	0.9910827	0.9917248	0.9921523	0.9924871	0.9928507	0.9930894	0.9933549	0.9934587
1206	0.9818087	0.9868633	0.9892812	0.9903767	0.9910368	0.9915826	0.99211	0.99253	0.9929118	0.9931078	0.993204
1208	0.982906	0.9865338	0.988497	0.989546	0.9903283	0.9910433	0.9917063	0.9922579	0.9926273	0.9928851	0.992934
1210	0.9869878	0.9868506	0.9876007	0.9886767	0.9897149	0.9906569	0.9914675	0.9920293	0.992417	0.9925813	0.9926347
1212	0.9905165	0.9875754	0.9871233	0.9880756	0.9893162	0.9903958	0.9912155	0.9918333	0.9922258	0.9923624	0.9922906
1214	0.9916528	0.9882339	0.987468	0.9880906	0.9892311	0.9902958	0.9911242	0.9916598	0.9919128	0.9920421	0.9918855
1216	0.9903924	0.9889552	0.9884354	0.9887275	0.9895112	0.9903717	0.9910259	0.9915041	0.9917485	0.9916568	0.9914026
1218	0.988825	0.9895077	0.9896274	0.9897793	0.9901154	0.9906224	0.991098	0.9913678	0.9914144	0.9912469	0.990824
1220	0.987248	0.9898483	0.9906941	0.9908657	0.9909075	0.9910429	0.991188	0.9912516	0.9911032	0.9907407	0.9901314
1222	0.9869608	0.990108	0.9914603	0.9917797	0.9917179	0.9915459	0.9914103	0.9911454	0.9907615	0.9901225	0.989305
1224	0.9893268	0.9907207	0.9920102	0.9924761	0.9924127	0.9920679	0.9915866	0.991016	0.9902382	0.9893445	0.9883232
1226	0.9924325	0.9921717	0.9926499	0.9930145	0.9929351	0.9924617	0.9917302	0.9908051	0.9897637	0.9885567	0.987162
1228	0.9951828	0.9940568	0.9936346	0.993575	0.9933079	0.9926817	0.9916813	0.9904354	0.9889808	0.9874116	0.9857966
1230	0.9972336	0.9958546	0.9948612	0.9942219	0.993594	0.9926928	0.9914251	0.9898241	0.9879978	0.9860166	0.9842035
1232	0.998409	0.9972872	0.9960544	0.9949239	0.9938209	0.9925166	0.9908629	0.9888928	0.9867337	0.9844913	0.9823669
1234	0.9989969	0.9982133	0.9969889	0.9955298	0.993924	0.9921073	0.9899781	0.9875726	0.9849715	0.9826273	0.9802868
1236	0.9992734	0.9986914	0.9975238	0.9958392	0.9937575	0.9913669	0.988668	0.9858019	0.9829589	0.9801948	0.9779887
1238	0.9994144	0.9988277	0.997604	0.9956836	0.9931411	0.9901332	0.9868674	0.9835253	0.9803793	0.9775669	0.9755288
1240	0.999438	0.9986654	0.9972023	0.9949259	0.9918911	0.9882427	0.984417	0.9807035	0.9774087	0.9750305	0.9729937
1242	0.9992388	0.9981446	0.9962596	0.9934654	0.9898224	0.9855348	0.9812579	0.9773362	0.974229	0.9719455	0.9704917
1244	0.9986804	0.9971231	0.9946546	0.9911631	0.9867346	0.9818851	0.9772977	0.9734899	0.9706116	0.9688027	0.9681361
1246	0.9975446	0.9954211	0.9921788	0.9877298	0.9824219	0.9772467	0.9726645	0.9693155	0.9672949	0.9661967	0.9660262
1248	0.9955779	0.9928166	0.9884696	0.9827676	0.9767458	0.9715847	0.967496	0.9650424	0.9638913	0.9639252	0.9642307
1250	0.9926357	0.9889041	0.9829308	0.9759866	0.9697459	0.9651459	0.9621826	0.960943	0.9608634	0.9615203	0.9627791
1252	0.9884071	0.9827816	0.9749089	0.9673616	0.9617058	0.9582619	0.9570372	0.9572727	0.9584906	0.9596251	0.9616645
1254	0.9819078	0.9731178	0.9641908	0.9572524	0.95316	0.9516855	0.9525155	0.9542055	0.9561973	0.9588671	0.9608517
1256	0.9700853	0.9594644	0.9511498	0.9462106	0.9448724	0.9459804	0.9487585	0.9518008	0.954959	0.9578204	0.96029
1258	0.9520003	0.9424368	0.936542	0.9353588	0.9376804	0.941504	0.9459369	0.9500186	0.9537225	0.9568746	0.959924
1260	0.9288189	0.922833	0.9217451	0.9260342	0.9321201	0.9384274	0.9438494	0.9487625	0.952948	0.9564906	0.9597015
1262	0.9014237	0.9017239	0.9093054	0.9190935	0.9282057	0.9361741	0.9424739	0.9479205	0.9526175	0.9566987	0.9595785
1264	0.869677	0.88406	0.9010756	0.9147004	0.9256473	0.9346343	0.941546	0.9473916	0.9520149	0.9561693	0.9595219
1266	0.8458637	0.8751727	0.8965251	0.9121406	0.9241636	0.9335101	0.9410698	0.9470986	0.9521586	0.9558609	0.9595096
1268	0.8452646	0.8737674	0.8949971	0.9112964	0.9236092	0.9330603	0.9408614	0.9469946	0.9519591	0.9561369	0.9595299
1270	0.8561313	0.8783711	0.8967938	0.9120492	0.923991	0.9332464	0.9410057	0.9470664	0.9519932	0.9563548	0.9595814
1272	0.8753683	0.8885801	0.902254	0.9146969	0.9254504	0.9341123	0.9414358	0.9473355	0.9523253	0.9561274	0.9596719
1274	0.9083688	0.9047318	0.9113597	0.9197437	0.9282167	0.9359251	0.9423399	0.9478618	0.9523487	0.9561657	0.9598189
1276	0.9370177	0.9263919	0.9239815	0.9271408	0.9325169	0.9384805	0.9437819	0.948743	0.9532015	0.9570769	0.9600508
1278	0.9553304	0.9468437	0.939078	0.9369125	0.9384636	0.9420998	0.9460102	0.9501036	0.953905	0.9574718	0.9604076
1280	0.9690826	0.9620382	0.9537575	0.9479519	0.9459226	0.9467512	0.9490867	0.9520691	0.9551556	0.9580274	0.9609396
1282	0.9795479	0.9732265	0.9658275	0.9588524	0.954357	0.9526075	0.9531169	0.9547278	0.957054	0.9592499	0.9617042
1284	0.9872782	0.9816046	0.9751757	0.9684953	0.9628845	0.9592414	0.9579258	0.9580919	0.9590594	0.9612087	0.9627588
1286	0.9920945	0.9877491	0.9823278	0.976384	0.9706927	0.9660639	0.9632999	0.9620695	0.9621899	0.9628363	0.9641509
1288	0.9948278	0.9919345	0.9876868	0.9826532	0.9773637	0.9725675	0.9688017	0.9664614	0.9653639	0.9651303	0.9659064
1290	0.9964387	0.994605	0.9915351	0.9874564	0.9828166	0.9782155	0.97409	0.9709982	0.9690397	0.9682003	0.9680187
1292	0.9973877	0.9963086	0.9941782	0.9910198	0.9871234	0.9829495	0.9788572	0.9754068	0.9729113	0.971345	0.9704432
1294	0.9980692	0.9974172	0.9959466	0.9935721	0.99041	0.9867555	0.982971	0.9794729	0.9764728	0.9743499	0.9730996
1296	0.9986592	0.9981661	0.9971176	0.9953383	0.9928286	0.9897439	0.9863889	0.9830679	0.9801394	0.9775234	0.9758821
1298	0.9991055	0.9986991	0.9978926	0.9965298	0.994544	0.9920106	0.9891414	0.9861423	0.9832404	0.9808506	0.9786769
1300	0.9994628	0.9990742	0.9983941	0.9972936	0.9957163	0.9936869	0.9913128	0.9887036	0.9860472	0.9835806	0.9813789

Table 5.27. α for 1200-1300 nm with b of 2.5 comparison run.

alpha:	10	15	20	25	30	35	40	45	50	55	60
1200	0.0927048	0.0865028	0.0849033	0.085044	0.0856824	0.0861319	0.0866564	0.0874472	0.0887266	0.0901891	0.0933
1202	0.0905005	0.0855217	0.0831564	0.0821708	0.0820025	0.0822586	0.0822798	0.0829879	0.0840636	0.0856397	0.0879612
1204	0.0856496	0.0840676	0.0815685	0.0796433	0.078394	0.0782281	0.0781713	0.0786095	0.0796281	0.081314	0.0829169
1206	0.0804732	0.0812377	0.0791572	0.0766962	0.0748355	0.0741509	0.0738507	0.0742981	0.0750413	0.0764026	0.0781344
1208	0.0754199	0.0769243	0.0752609	0.0729065	0.0712228	0.070113	0.0699517	0.0700898	0.0708333	0.0715209	0.0735939
1210	0.0717544	0.0712001	0.0700734	0.0686015	0.067379	0.0661773	0.0658287	0.0660073	0.0665719	0.0676773	0.0692432
1212	0.0688412	0.0650378	0.064474	0.0640232	0.0631874	0.0622685	0.0620256	0.0620117	0.0625428	0.0640022	0.0650988
1214	0.0623376	0.0598709	0.059198	0.0590989	0.0586362	0.0582045	0.0578976	0.0580855	0.0587515	0.0596221	0.0611377
1216	0.0553928	0.0550471	0.0542812	0.0539691	0.053869	0.0539233	0.0539467	0.0541921	0.0548186	0.0556049	0.0573378
1218	0.048546	0.0495721	0.0492811	0.0488894	0.0490573	0.0494775	0.0496769	0.0503112	0.0511466	0.0523326	0.0537124
1220	0.0408103	0.0432973	0.0439389	0.0439975	0.0443188	0.0449607	0.0456475	0.0464488	0.0474316	0.0491109	0.0502314
1222	0.0350209	0.0368735	0.0381991	0.0390439	0.0396532	0.0405016	0.0414517	0.0426324	0.0438626	0.0451565	0.0468778
1224	0.0317168	0.031189	0.0324512	0.0339062	0.0350446	0.0361493	0.0375668	0.0388985	0.0404136	0.0416726	0.0436377
1226	0.026979	0.0264651	0.0272855	0.0288718	0.0305462	0.0319989	0.0336451	0.035277	0.0368985	0.038787	0.0404948
1228	0.0213266	0.0219906	0.0228459	0.0243433	0.0262713	0.0280735	0.0300084	0.0317863	0.0336224	0.0357333	0.0374685
1230	0.0166178	0.0175505	0.0188492	0.0204213	0.0223631	0.0244303	0.0264224	0.0284415	0.0304059	0.03227	0.0345551
1232	0.0119832	0.0135469	0.0151678	0.0169314	0.0188654	0.0210456	0.0231474	0.0252703	0.0274108	0.0293852	0.0317564
1234	0.0079732	0.0099871	0.0118669	0.0137783	0.0157553	0.0179169	0.0200431	0.0222867	0.0245527	0.0268911	0.0290995
1236	0.0053289	0.0070053	0.0089782	0.0109588	0.0129824	0.0150928	0.0172871	0.019533	0.0218274	0.0242739	0.0265828
1238	0.0034131	0.0047888	0.0065658	0.0085204	0.0105337	0.0125969	0.0147587	0.0170182	0.0193474	0.0216532	0.0242341
1240	0.0020705	0.0031946	0.0047033	0.0064867	0.0084117	0.0104113	0.0125504	0.0147599	0.0170696	0.0194668	0.0220573
1242	0.0012634	0.0021144	0.0033348	0.0048632	0.0066273	0.0085265	0.0105736	0.0127494	0.0150682	0.0175932	0.0200798
1244	0.0008689	0.0014396	0.0023718	0.0036423	0.0051862	0.0069503	0.0088932	0.0109894	0.0132634	0.015743	0.018307
1246	0.000622	0.0010452	0.0017408	0.0027574	0.0040684	0.0056504	0.0074541	0.0094781	0.0116962	0.0140844	0.0167538
1248	0.0005136	0.0008363	0.0013548	0.0021462	0.003239	0.0046326	0.006303	0.0082196	0.0103917	0.012759	0.0154398
1250	0.00058	0.0007608	0.0011365	0.0017518	0.0026568	0.0038712	0.005388	0.0072121	0.0093073	0.0117533	0.0143659
1252	0.0006882	0.0007761	0.0010408	0.0015213	0.002276	0.0033398	0.0047392	0.0064541	0.0085086	0.0108685	0.0135528
1254	0.0007439	0.0008416	0.001032	0.0014146	0.0020603	0.0030095	0.0042921	0.0059361	0.0079343	0.0102465	0.0130067
1256	0.000864	0.0009229	0.0010733	0.0014038	0.0019818	0.0028532	0.0040771	0.0056481	0.0076108	0.0099597	0.0127416
1258	0.0010086	0.0010126	0.00115	0.0014705	0.0020214	0.0028548	0.0040229	0.0055816	0.0075486	0.0099734	0.0127761
1260	0.0010747	0.0011097	0.0012705	0.0016103	0.0021656	0.0029981	0.0041751	0.0057288	0.0077277	0.0101852	0.0131253
1262	0.0011302	0.0012243	0.0014452	0.0018208	0.0024068	0.0032738	0.0044625	0.0060911	0.0081755	0.0107049	0.0138042
1264	0.0012421	0.0013927	0.0016798	0.0021047	0.0027441	0.0036727	0.0049642	0.0066774	0.0088921	0.0116333	0.0148331
1266	0.0013621	0.0016489	0.0019768	0.0024671	0.0031825	0.004202	0.0056075	0.0075084	0.0098949	0.0128372	0.0162314
1268	0.0016641	0.0019523	0.0023539	0.0029208	0.003732	0.0048886	0.006528	0.0086125	0.0112319	0.0143637	0.0180176
1270	0.0020413	0.0023434	0.0028306	0.0034715	0.0044195	0.0057836	0.0076418	0.010025	0.0129116	0.016282	0.0202153
1272	0.0024918	0.0029132	0.003388	0.004134	0.0053039	0.0069463	0.0091425	0.0117838	0.0149681	0.0187079	0.0228437
1274	0.0033034	0.0035714	0.0040278	0.0049809	0.0064593	0.0084476	0.0109065	0.0139301	0.0174393	0.0214485	0.0259235
1276	0.0041904	0.0042024	0.0048512	0.0061303	0.0079655	0.0103259	0.0131814	0.0165057	0.0203515	0.0246437	0.029475
1278	0.0046112	0.0049435	0.0060137	0.0076821	0.0098857	0.0126454	0.015797	0.0195569	0.0237518	0.028339	0.0335119
1280	0.0052252	0.0060454	0.007636	0.0097046	0.0122824	0.015435	0.0190583	0.0231257	0.0277069	0.0327106	0.0380568
1282	0.0062048	0.007785	0.0097736	0.0122358	0.0152254	0.0187606	0.0227431	0.0272425	0.032106	0.0374568	0.0431307
1284	0.0078872	0.0101296	0.012478	0.0153475	0.0187916	0.0226825	0.0271806	0.0319346	0.0371416	0.0425777	0.0487595
1286	0.0105154	0.0130177	0.0158335	0.01916	0.0230653	0.0273049	0.032098	0.0372099	0.0426467	0.0485406	0.0549683
1288	0.0144503	0.0167152	0.019999	0.0238215	0.028122	0.0326783	0.0377881	0.0430832	0.0488051	0.0552864	0.0618051
1290	0.0191936	0.0216909	0.0251599	0.0294299	0.0340006	0.0388566	0.0439926	0.0495653	0.0556823	0.0622808	0.0693221
1292	0.0255673	0.0278791	0.0315496	0.0360434	0.0406721	0.0457345	0.0509175	0.056694	0.0629626	0.0697201	0.0775838
1294	0.0324648	0.035341	0.039328	0.0435722	0.0480916	0.0532068	0.0584795	0.0645163	0.0712916	0.0786254	0.0866654
1296	0.0404732	0.0444578	0.0482668	0.0518906	0.0562422	0.0612953	0.0667636	0.0730946	0.0801001	0.0883373	0.0966531
1298	0.0513593	0.0551	0.0578317	0.0610094	0.0651594	0.0700327	0.075889	0.0825131	0.0900631	0.0984091	0.1076389
1300	0.0653588	0.0661965	0.0678936	0.0709507	0.074877	0.0796569	0.0857942	0.0928816	0.1010511	0.1095256	0.1197161

Table 5.28. β for 1200-1300 nm, with b of 2.5 comparison run.

beta:	10	15	20	25	30	35	40	45	50	55	60
1200	0.6016211	0.605115	0.6061473	0.605822	0.6037838	0.5999852	0.5952672	0.5886148	0.5808535	0.5727309	0.5616055
1202	0.5932948	0.6003219	0.6050215	0.6070416	0.605707	0.6021421	0.5972176	0.5910213	0.5834863	0.5742577	0.5644593
1204	0.590169	0.5973371	0.604668	0.6076559	0.6070981	0.6040007	0.5993425	0.593004	0.5853756	0.5761808	0.5669873
1206	0.5899855	0.5991384	0.605327	0.6078278	0.6078284	0.6054316	0.6006692	0.5947108	0.5874516	0.5790551	0.5691396
1208	0.5992511	0.6044484	0.6070799	0.6083344	0.6081406	0.6062657	0.6019074	0.5960399	0.5886577	0.5810363	0.5708577
1210	0.6123745	0.6111987	0.609987	0.6096141	0.6086444	0.6066188	0.6025108	0.5968832	0.58975	0.5812663	0.5723366
1212	0.6217271	0.6183259	0.6142324	0.6118919	0.6098174	0.6069797	0.603136	0.597414	0.5906259	0.5814506	0.5734442
1214	0.6319509	0.624549	0.6195395	0.6156039	0.6120408	0.6077682	0.6033368	0.5976393	0.5904868	0.5833697	0.5743103
1216	0.6416184	0.6312003	0.6256604	0.6205333	0.6151779	0.609428	0.6040062	0.5977411	0.5909984	0.5838732	0.5750894
1218	0.6455672	0.639366	0.6330178	0.6262791	0.6189399	0.6117049	0.6047206	0.5979471	0.5909	0.5831458	0.5756835
1220	0.6534832	0.6485747	0.640927	0.6320826	0.6229513	0.6143699	0.6060728	0.5984807	0.5911923	0.5828347	0.5762878
1222	0.6639642	0.6586449	0.648924	0.6378406	0.6271988	0.6172326	0.60779	0.5995192	0.5920948	0.5852197	0.577018
1224	0.6710195	0.6680664	0.6571801	0.6441547	0.6317581	0.6205007	0.6102783	0.6011681	0.5928248	0.5862656	0.5779994
1226	0.6823409	0.6766186	0.6650559	0.650766	0.6366521	0.6242718	0.6130891	0.6034873	0.595099	0.5861384	0.5794343
1228	0.7041426	0.6864424	0.6721617	0.6571928	0.6420804	0.6287325	0.6169257	0.6065211	0.5973113	0.5883467	0.581217
1230	0.7211713	0.6994548	0.6802333	0.6635763	0.6479234	0.6338277	0.6211601	0.6103016	0.6005337	0.5928628	0.5834916
1232	0.7375215	0.7134138	0.6905745	0.6710156	0.6545133	0.6393901	0.6264989	0.6147381	0.6045606	0.5956334	0.5863763
1234	0.7624969	0.7287985	0.7025945	0.6803876	0.6621164	0.6462604	0.632349	0.6200615	0.60873	0.597804	0.5896645
1236	0.78267	0.7476847	0.7160532	0.691707	0.6712826	0.6541297	0.639399	0.6260387	0.6143008	0.6033509	0.593522
1238	0.8004432	0.7660312	0.7320883	0.7045896	0.6820577	0.6632999	0.6470252	0.6328765	0.6200637	0.6093912	0.5976987
1240	0.8236867	0.7843292	0.7500327	0.7192436	0.6944861	0.6737052	0.6560765	0.6403329	0.6263756	0.6137519	0.6023155
1242	0.8490366	0.8077947	0.7693193	0.7360107	0.708615	0.6856209	0.6656476	0.648577	0.6333285	0.6184542	0.607075
1244	0.8767891	0.8346829	0.7913396	0.7548404	0.7242224	0.6984947	0.6766182	0.6573932	0.6404753	0.625908	0.6120296
1246	0.907508	0.8615583	0.8161303	0.775636	0.7412756	0.7124626	0.6876687	0.6666756	0.648299	0.6323248	0.6169879
1248	0.9315971	0.8872454	0.8418302	0.7979677	0.7594507	0.7271474	0.6996517	0.6760239	0.6556993	0.6373243	0.621523
1250	0.9376086	0.9081348	0.8656422	0.8198223	0.7776768	0.7416329	0.7107929	0.6851099	0.6627485	0.6425503	0.6256039
1252	0.9379789	0.9213421	0.8849988	0.8394694	0.7947201	0.7551893	0.721732	0.6933161	0.6690061	0.6483248	0.6286357
1254	0.9405982	0.9273703	0.8981391	0.8548812	0.8087077	0.7664154	0.7305336	0.7001568	0.673735	0.6513734	0.6304429
1256	0.9387169	0.9296498	0.9052048	0.8646695	0.8183758	0.7749158	0.7376259	0.7050979	0.6772289	0.6523154	0.6307226
1258	0.9371885	0.9304497	0.9067613	0.8681082	0.8232299	0.7799673	0.7413204	0.7076474	0.678168	0.6519834	0.6291534
1260	0.9407797	0.9293429	0.9034083	0.8659986	0.8236348	0.7816254	0.7428111	0.7077434	0.6769122	0.6503375	0.6257269
1262	0.9414148	0.9243997	0.8957977	0.8601996	0.8204114	0.7801196	0.7407559	0.7053478	0.6735582	0.6456272	0.6206291
1264	0.9357284	0.9135193	0.8857817	0.8522474	0.8146451	0.7756158	0.7369506	0.7007142	0.6681914	0.6391129	0.6140404
1266	0.923138	0.8993427	0.8744803	0.8429654	0.8071204	0.7689716	0.7301867	0.6940377	0.6612145	0.6315193	0.60627
1268	0.9012953	0.8861899	0.8618184	0.8327215	0.7983766	0.7601591	0.7220814	0.6856401	0.6526695	0.6236102	0.5976806
1270	0.8861955	0.8706286	0.8488502	0.8223718	0.7884244	0.7500123	0.711639	0.675811	0.6431376	0.6144072	0.5885038
1272	0.8689026	0.8537565	0.8379261	0.8118579	0.7766592	0.7381721	0.7003352	0.6648862	0.6328331	0.6040223	0.5790407
1274	0.8464279	0.8425012	0.82857	0.7999108	0.7631509	0.7248917	0.6874348	0.6531492	0.6219404	0.5937812	0.5695063
1276	0.839072	0.8372529	0.8183458	0.7856485	0.7480639	0.710409	0.6743301	0.6409329	0.6109142	0.5844159	0.5600659
1278	0.8396643	0.8326586	0.8051865	0.7695521	0.7321215	0.6948273	0.6601863	0.6284729	0.59982	0.5748293	0.5509182
1280	0.8406165	0.8224014	0.7891135	0.7526892	0.7156397	0.6792026	0.646506	0.6160848	0.5887226	0.563958	0.5420931
1282	0.8383186	0.8055575	0.7715646	0.7354326	0.6988147	0.6638556	0.6324012	0.604148	0.5786189	0.5545074	0.5336363
1284	0.8230824	0.7877572	0.7533645	0.7175292	0.6819197	0.6492354	0.6196418	0.5928706	0.5685751	0.5471343	0.5255527
1286	0.8015727	0.7692291	0.7344206	0.6989871	0.6652097	0.6351549	0.6069827	0.5825154	0.5598779	0.5388842	0.5178694
1288	0.7789343	0.7487755	0.714312	0.6803151	0.6491372	0.6219165	0.5963795	0.5730991	0.5514889	0.5296249	0.510471
1290	0.7571025	0.7264755	0.6936929	0.6621725	0.6342272	0.6094742	0.5859599	0.5646546	0.5436236	0.5228444	0.5032867
1292	0.7323647	0.7039185	0.6737045	0.6453824	0.621068	0.5984159	0.5779111	0.5570056	0.5367751	0.517123	0.4962356
1294	0.7068817	0.6819314	0.6549214	0.6310487	0.6099198	0.5891989	0.5696604	0.5499998	0.529627	0.5098997	0.4892468
1296	0.6810591	0.6596432	0.6382314	0.6194761	0.6007768	0.5816885	0.5634299	0.5434709	0.5234243	0.5019124	0.482259
1298	0.6544445	0.6383089	0.6246478	0.609968	0.593232	0.575585	0.5566541	0.5372471	0.5167671	0.4959434	0.4752341
1300	0.6274906	0.6218835	0.6138154	0.601648	0.5867751	0.5701212	0.5513683	0.5311682	0.5103806	0.4899736	0.4681595

Table 5.29. Transmission (TnoH2O) for 1200-1300 nm, with b of 3.3 comparison run.

tnoh2o:	10	15	20	25	30	35	40	45	50	55	60
1200	0.9923509	0.9915984	0.9919723	0.99251	0.9928936	0.9931583	0.9932916	0.9934026	0.9934204	0.9934241	0.993305
1202	0.9879729	0.9895387	0.9908679	0.9917548	0.9923164	0.9926729	0.9928923	0.9930064	0.9930888	0.9930222	0.9929677
1204	0.9846946	0.9881028	0.9900584	0.9911197	0.991753	0.9921627	0.9924092	0.9926198	0.9926587	0.9927213	0.9926226
1206	0.9828069	0.9872229	0.9893829	0.9904785	0.991164	0.9916499	0.9920262	0.9922457	0.992396	0.9923669	0.9922638
1208	0.9839039	0.9869486	0.9887357	0.9898248	0.9905654	0.9911348	0.9915818	0.9918887	0.9920084	0.9920249	0.9918844
1210	0.9871143	0.9873643	0.988197	0.9891846	0.990035	0.9907291	0.9912698	0.9915573	0.9916798	0.9916219	0.9914761
1212	0.9900589	0.9880612	0.9879857	0.9887605	0.9896824	0.9904303	0.9909372	0.991253	0.9913738	0.991283	0.9910298
1214	0.9912075	0.9886228	0.9882428	0.988786	0.9895953	0.9902861	0.9907646	0.9909766	0.990946	0.9908437	0.9905357
1216	0.9902529	0.9891034	0.988897	0.9892315	0.9897907	0.9902998	0.9905936	0.9907252	0.9906814	0.9903647	0.9899837
1218	0.9888724	0.9895005	0.9897271	0.9899634	0.9902033	0.9904408	0.9905674	0.9904912	0.9902509	0.9898977	0.989363
1220	0.9876105	0.9897838	0.9905077	0.9907088	0.9907159	0.9906688	0.9905178	0.9902579	0.989843	0.9893167	0.9886617
1222	0.9876449	0.9901332	0.9911435	0.991343	0.9912121	0.9909009	0.9905296	0.9899989	0.9894059	0.988644	0.9878671
1224	0.9897367	0.9909226	0.9917227	0.9918713	0.9916175	0.9911052	0.9904417	0.9896781	0.9887692	0.9878678	0.9869649
1226	0.9924255	0.9922811	0.9924232	0.9923354	0.9919106	0.9911907	0.9902959	0.9892527	0.9881956	0.987099	0.9859399
1228	0.9949282	0.9938866	0.993314	0.992824	0.9921055	0.9911425	0.9899688	0.9886772	0.9873283	0.9860035	0.984777
1230	0.9968035	0.9954023	0.9942852	0.9933001	0.9922118	0.9909311	0.9894845	0.9879072	0.9863187	0.9847397	0.9834631
1232	0.9979494	0.9965943	0.9951563	0.9937088	0.9922	0.9905528	0.9887465	0.9869006	0.9851319	0.9834667	0.9819905
1234	0.998562	0.9973621	0.995766	0.9939488	0.9919922	0.9899295	0.9877591	0.9856167	0.9835521	0.9819265	0.9803597
1236	0.9988561	0.9977274	0.9960091	0.9938738	0.991477	0.9889725	0.9864178	0.9840161	0.9818982	0.9799669	0.9785833
1238	0.9989645	0.9977427	0.9958262	0.9933593	0.9905299	0.987565	0.9847004	0.9820629	0.9798068	0.9779258	0.9766874
1240	0.9988952	0.9974131	0.9951649	0.992284	0.9890263	0.9856287	0.9824896	0.9797322	0.9774692	0.9760102	0.9747125
1242	0.9985601	0.9966679	0.9939432	0.9905543	0.9868436	0.9830846	0.9797891	0.977022	0.974999	0.9735675	0.9727116
1244	0.9978216	0.9953706	0.992031	0.9880642	0.9838598	0.9798785	0.9765245	0.973966	0.9721155	0.971026	0.9707463
1246	0.9964691	0.9933354	0.9892375	0.9846037	0.9799619	0.9760087	0.9727997	0.9706432	0.9694613	0.968849	0.9688805
1248	0.9942579	0.9903173	0.9852877	0.979937	0.975077	0.9713939	0.9686542	0.9671783	0.9665865	0.9668347	0.9671732
1250	0.9909497	0.9859394	0.9798025	0.973894	0.9692283	0.9661751	0.9643402	0.9637318	0.9638941	0.9645573	0.9656714
1252	0.9861711	0.9795594	0.9723775	0.9664542	0.9625886	0.9605179	0.960009	0.9604762	0.9616302	0.9626213	0.9644045
1254	0.9790297	0.9703028	0.9628301	0.9578911	0.9555019	0.9549531	0.9559956	0.9575668	0.9593111	0.9616508	0.9633824
1256	0.9673895	0.9577141	0.9514236	0.9485921	0.9484587	0.9498655	0.9524256	0.9551135	0.9578872	0.9604108	0.9625963
1258	0.9501321	0.9422329	0.9388577	0.9393416	0.942019	0.9455814	0.9495429	0.9531645	0.9564558	0.9592672	0.9620228
1260	0.9281626	0.9247894	0.9262179	0.9309729	0.9366664	0.9424032	0.947284	0.9517073	0.9554806	0.9586897	0.9616293
1262	0.9025809	0.9066783	0.915038	0.9242245	0.9326491	0.9399738	0.9457207	0.9506868	0.9549826	0.9587328	0.9613796
1264	0.875481	0.8909696	0.906872	0.9196908	0.9299452	0.9382848	0.9446496	0.9500293	0.9542826	0.9581287	0.9612402
1266	0.8545489	0.8820527	0.9023042	0.9171014	0.9283941	0.937087	0.9440895	0.9496663	0.9543569	0.9577838	0.9611845
1268	0.8520932	0.8806641	0.9010834	0.9163972	0.9278674	0.9366345	0.9438678	0.9495519	0.9541563	0.9580376	0.9611963
1270	0.8618741	0.8849937	0.9030117	0.9173184	0.9283597	0.9368961	0.9440712	0.9496749	0.9542351	0.9582802	0.9612716
1272	0.8809339	0.894512	0.9081869	0.9200291	0.9299868	0.9379232	0.944647	0.9500628	0.9546553	0.9581465	0.9614204
1274	0.9099028	0.9096583	0.9167308	0.9249701	0.932908	0.9399507	0.945772	0.9507774	0.9548444	0.9583205	0.961665
1276	0.9348999	0.928304	0.9282206	0.9319716	0.9372172	0.9427035	0.9474673	0.9518986	0.9558914	0.9593731	0.9620378
1278	0.9529908	0.9456895	0.9411266	0.940742	0.9428424	0.9463534	0.9498913	0.953503	0.9568375	0.9599845	0.9625759
1280	0.9668486	0.9596711	0.95345	0.9501087	0.9494706	0.9507329	0.9529896	0.9556393	0.9583158	0.9607826	0.9633176
1282	0.9774692	0.9705659	0.9640461	0.9591548	0.9565749	0.9558903	0.9567595	0.958306	0.9603454	0.9622073	0.9642959
1284	0.9852872	0.9789559	0.9727138	0.9673499	0.963587	0.9614455	0.9609731	0.961439	0.9623771	0.9642581	0.9655321
1286	0.9903854	0.9852107	0.9796084	0.9743409	0.9700678	0.9670159	0.9654572	0.9649153	0.9652783	0.965914	0.9670299
1288	0.9935141	0.989643	0.9849351	0.9801345	0.9757707	0.9723446	0.9699201	0.9685732	0.968047	0.9680424	0.9687727
1290	0.9954606	0.9926735	0.9889195	0.9847351	0.9806051	0.9770547	0.9741877	0.9722422	0.9711053	0.9707242	0.9707242
1292	0.9966813	0.9947329	0.991823	0.9882973	0.9845783	0.9811217	0.9780819	0.9757715	0.974241	0.973349	0.972831
1294	0.9975512	0.9961526	0.9939055	0.9910059	0.9877556	0.9845067	0.981534	0.9790476	0.9770476	0.9757393	0.9750298
1296	0.9982448	0.997155	0.995388	0.9930168	0.9902358	0.9873009	0.9845012	0.9819997	0.9799873	0.9782268	0.9772547
1298	0.9987715	0.9978726	0.9964384	0.9944944	0.9921318	0.9895521	0.9869996	0.9845963	0.9824705	0.9808859	0.9794438
1300	0.9991778	0.9983809	0.99717	0.995548	0.9935555	0.9913386	0.9890668	0.9868371	0.9847773	0.9830329	0.9815447

Table 5.30. α for 1200-1300 nm, with b of 3.3 comparison run.

alpha:	10	15	20	25	30	35	40	45	50	55	60
1200	0.0915279	0.0870234	0.0860088	0.0863077	0.0874072	0.088769	0.0904438	0.092557	0.0952393	0.0979717	0.1022482
1202	0.0896784	0.0854079	0.0837123	0.0832115	0.0836395	0.084775	0.0858777	0.0878258	0.0902298	0.0931856	0.0966796
1204	0.0849049	0.0832495	0.0814115	0.0803318	0.0799817	0.0806761	0.0816199	0.0832314	0.0855238	0.0885588	0.0914102
1206	0.0800765	0.0800927	0.0784862	0.0770783	0.0762703	0.0765388	0.0772582	0.0787953	0.0807677	0.0833989	0.0864387
1208	0.0750719	0.0758452	0.074559	0.073091	0.0724211	0.0723308	0.0732082	0.0744784	0.0764155	0.0783791	0.0817054
1210	0.0715841	0.0706901	0.069726	0.0687121	0.0683373	0.0681953	0.0689741	0.0702777	0.07205	0.0744262	0.0772208
1212	0.0681567	0.0652392	0.0645118	0.0641932	0.0640334	0.0641181	0.0650036	0.0661706	0.0679099	0.0705901	0.072937
1214	0.0621286	0.0599802	0.0594425	0.0594936	0.0595666	0.0599977	0.060791	0.0621479	0.0639936	0.0660765	0.0688673
1216	0.0551968	0.0548576	0.0545461	0.0546278	0.0550052	0.0558027	0.056791	0.0581585	0.0599738	0.0620314	0.064969
1218	0.0482991	0.0493802	0.0495292	0.0497022	0.050434	0.0515281	0.052595	0.0542399	0.0562277	0.0586412	0.0612549
1220	0.0412667	0.0433311	0.0442439	0.0448915	0.0458699	0.0471785	0.0486383	0.050391	0.0524597	0.0552903	0.0576881
1222	0.0357777	0.0373399	0.0387783	0.0400754	0.0413343	0.0428602	0.0445805	0.0466307	0.0488864	0.0513103	0.0542839
1224	0.0318329	0.0320445	0.0334674	0.0352114	0.0368751	0.0386403	0.0407983	0.0429783	0.0454684	0.0478913	0.0510145
1226	0.0270474	0.0272725	0.0286014	0.030502	0.032584	0.0346335	0.036999	0.0394542	0.042025	0.0449922	0.0478899
1228	0.0217075	0.0226984	0.0242067	0.0262011	0.0285441	0.0308864	0.033482	0.0360764	0.0388403	0.0419611	0.0449214
1230	0.017025	0.0183749	0.020196	0.022376	0.024821	0.0274242	0.0300621	0.0328648	0.0357437	0.0386442	0.042094
1232	0.0124879	0.0144334	0.0165455	0.0189125	0.0214334	0.0241905	0.026949	0.0298407	0.0328838	0.0359313	0.0394243
1234	0.0086811	0.0109324	0.0132734	0.0157752	0.0183744	0.0211783	0.0239985	0.0270231	0.0301927	0.0335687	0.0369213
1236	0.0059649	0.0080362	0.0104216	0.0129736	0.0156307	0.018429	0.0213653	0.0244283	0.0276362	0.0310901	0.0345955
1238	0.0039653	0.0057983	0.0080425	0.0105506	0.0132074	0.0159793	0.0189388	0.0220664	0.025352	0.0287036	0.0324526
1240	0.0025686	0.0041256	0.0061501	0.0085273	0.0111095	0.0138439	0.0168207	0.0199397	0.0232526	0.0267518	0.0305172
1242	0.0016733	0.0029424	0.0047043	0.0068836	0.0093391	0.0120081	0.0149255	0.0180599	0.0214255	0.0250922	0.0287891
1244	0.001167	0.0021542	0.0036404	0.0055987	0.0078887	0.010472	0.0133281	0.0164288	0.0198103	0.0234275	0.0272855
1246	0.0008589	0.0016465	0.00289	0.0046228	0.0067369	0.0092	0.0119608	0.0150475	0.018414	0.0220244	0.0260131
1248	0.0007142	0.0013407	0.0023845	0.003909	0.0058563	0.008189	0.0108833	0.0139195	0.0172997	0.0209677	0.0249881
1250	0.0007193	0.0011905	0.0020661	0.0034172	0.0052132	0.0074212	0.010028	0.013041	0.0164095	0.0201991	0.0242207
1252	0.0007832	0.001145	0.0018897	0.0031028	0.0047763	0.0068811	0.0094409	0.0124093	0.0158002	0.0195456	0.0237187
1254	0.0008362	0.0011609	0.0018193	0.0029335	0.004518	0.0065502	0.0090518	0.0120232	0.0154361	0.0192074	0.0234959
1256	0.0009401	0.0012207	0.001827	0.0028839	0.0044174	0.0064082	0.0089095	0.0118759	0.0153145	0.0192063	0.0235609
1258	0.0010633	0.0013099	0.0018989	0.0029401	0.0044602	0.00645	0.0089453	0.0119653	0.0154789	0.0194956	0.0239283
1260	0.001144	0.0014176	0.002034	0.0030953	0.0046372	0.006663	0.0092168	0.0122911	0.0158957	0.0199943	0.0246118
1262	0.0012254	0.0015584	0.0022379	0.0033488	0.0049462	0.0070447	0.0096585	0.0128594	0.0165933	0.0208139	0.0256238
1264	0.0013475	0.0017611	0.0025212	0.0037045	0.0053885	0.007596	0.0103527	0.0136802	0.0175851	0.0220471	0.0269818
1266	0.0015082	0.002045	0.0028911	0.0041701	0.0059739	0.0083216	0.0112299	0.014771	0.0188621	0.023566	0.0287065
1268	0.0018069	0.0024096	0.0033578	0.004761	0.0067175	0.0092477	0.0124116	0.016156	0.0204966	0.0253943	0.0308153
1270	0.0022326	0.0028728	0.0039413	0.0054967	0.0076472	0.0104085	0.013818	0.0178644	0.0224867	0.0276002	0.0333309
1272	0.0027258	0.0034867	0.0046562	0.0063961	0.0088046	0.0118617	0.0156175	0.0199338	0.0248419	0.0303519	0.0362763
1274	0.0035024	0.0042372	0.0055179	0.0075092	0.0102478	0.0136659	0.0177081	0.0223979	0.0276408	0.0334274	0.03967
1276	0.0043515	0.005055	0.0065855	0.0089249	0.0120465	0.0158665	0.0202993	0.0252983	0.0308567	0.0369178	0.0435421
1278	0.0050007	0.0060015	0.0079721	0.0107364	0.0142646	0.0185184	0.0232573	0.0286728	0.0345887	0.0409156	0.0479142
1280	0.0057596	0.0073127	0.0098004	0.0130247	0.0169684	0.021635	0.0268256	0.0325596	0.0388662	0.0456514	0.0528076
1282	0.006903	0.0091895	0.0121655	0.0158363	0.0202156	0.025277	0.0308418	0.0369948	0.0435933	0.0507674	0.0582517
1284	0.0086613	0.0116737	0.0151172	0.0192313	0.0240741	0.0294805	0.0355577	0.0420082	0.0489927	0.0562614	0.064268
1286	0.0115067	0.0147998	0.018726	0.0233085	0.0286059	0.0343635	0.0407923	0.0476291	0.0548757	0.0626222	0.0709006
1288	0.015451	0.0187833	0.0231453	0.0282023	0.0338807	0.0399831	0.0467732	0.0538713	0.0614744	0.0698055	0.0781722
1290	0.0204074	0.0238941	0.0285479	0.0340021	0.0399486	0.0464211	0.0533452	0.0607779	0.0687882	0.0772804	0.0861232
1292	0.0265512	0.0302155	0.0350638	0.0407234	0.0468271	0.0536142	0.060666	0.0683682	0.0765788	0.0852135	0.0948214
1294	0.0337212	0.0377111	0.0427519	0.0483274	0.0545072	0.0614639	0.0686813	0.0766827	0.0853958	0.0945646	0.1043064
1296	0.041907	0.0466039	0.0515362	0.0568044	0.0629646	0.0699643	0.0774636	0.0857961	0.0947338	0.1047349	0.1146534
1298	0.0526575	0.0569159	0.0611679	0.0661549	0.072206	0.0791313	0.0871033	0.095759	0.1052003	0.115239	0.12595
1300	0.0656235	0.0680409	0.071444	0.0762995	0.0822498	0.0892227	0.097565	0.1066676	0.116639	0.1267012	0.1382319

Table 5.30. β for 1200-1300 nm, with b of 2.0 comparison run.

beta:	10	15	20	25	30	35	40	45	50	55	60
1200	0.6019014	0.6037529	0.6028445	0.600081	0.5950654	0.5880896	0.580285	0.5706615	0.5599622	0.5494917	0.5366556
1202	0.5947611	0.6001182	0.6020851	0.6011208	0.5968556	0.5902508	0.5823163	0.5730726	0.5627245	0.5509068	0.5394205
1204	0.592128	0.5981464	0.6018917	0.6017948	0.5981942	0.5922257	0.5845417	0.575168	0.5647474	0.5530321	0.5418758
1206	0.5925632	0.5994872	0.6027934	0.6023526	0.5992805	0.5936819	0.5857512	0.5768005	0.5667201	0.5559682	0.5438835
1208	0.6002169	0.6039397	0.6047774	0.6034994	0.6000807	0.5947931	0.5871809	0.5781317	0.5679693	0.5576931	0.5456078
1210	0.611334	0.6100755	0.6077346	0.6052459	0.6010572	0.5954315	0.5878479	0.5791226	0.5690598	0.5579157	0.5469133
1212	0.6205069	0.6163052	0.611647	0.607544	0.6024451	0.5961001	0.588793	0.5798287	0.5700429	0.558412	0.5479831
1214	0.6304754	0.6224282	0.6162913	0.6106256	0.60442	0.5970962	0.5892477	0.5802476	0.5702168	0.5603425	0.548696
1216	0.6387935	0.6289812	0.6216275	0.6144916	0.6070529	0.5987248	0.5902475	0.5807272	0.5707625	0.5604405	0.5492592
1218	0.6440076	0.6359418	0.6278186	0.6192371	0.6100225	0.6006362	0.590878	0.5811151	0.5707892	0.5598938	0.5495687
1220	0.6509033	0.6439472	0.6344784	0.6241325	0.6132397	0.6027794	0.5921517	0.5815772	0.5710503	0.5597804	0.5498474
1222	0.6600837	0.6529402	0.64137	0.6288942	0.6165939	0.6048127	0.5931186	0.5821771	0.5715716	0.5614077	0.5499884
1224	0.6682747	0.661207	0.6481753	0.6338264	0.6200375	0.6069812	0.5946824	0.5829622	0.5716001	0.5613041	0.5502082
1226	0.6800923	0.6693489	0.6547464	0.638864	0.6234689	0.6093519	0.5960364	0.5839479	0.5725635	0.560554	0.5504608
1228	0.6980243	0.6791955	0.6613638	0.6437768	0.6270339	0.6118934	0.5981473	0.5851502	0.5731443	0.5614627	0.5506743
1230	0.7136941	0.690297	0.6685408	0.6485612	0.6307854	0.6146762	0.5998322	0.5865628	0.5740665	0.5632829	0.5510166
1232	0.7291855	0.7017022	0.6765048	0.6539304	0.634817	0.6175699	0.6023128	0.5881557	0.5753019	0.5632014	0.5513825
1234	0.7491451	0.7142049	0.685268	0.660198	0.6392082	0.6209453	0.6044896	0.5898843	0.5761285	0.5627642	0.551726
1236	0.7654464	0.727886	0.69462	0.6670142	0.6440719	0.6244745	0.6074047	0.5916711	0.5776324	0.5646294	0.5519924
1238	0.7812611	0.7405629	0.7044277	0.6740364	0.6491987	0.6283085	0.6097373	0.5934284	0.5785429	0.5656007	0.5521832
1240	0.7986995	0.7530258	0.7144634	0.68099	0.6544213	0.6319193	0.6126044	0.5951365	0.5793636	0.5650144	0.5520649
1242	0.8172441	0.7678335	0.7249152	0.6880927	0.6595627	0.6355401	0.6145952	0.5965387	0.580171	0.5646269	0.5517094
1244	0.8401511	0.7849748	0.7363843	0.6957883	0.6645018	0.6388532	0.6169246	0.5975296	0.580188	0.5656311	0.5509666
1246	0.866469	0.8035368	0.7491708	0.7038745	0.6692814	0.6416682	0.6181087	0.598049	0.5803259	0.5646667	0.5498399
1248	0.8908838	0.8234469	0.763353	0.7124597	0.6739159	0.6442152	0.6194232	0.5979702	0.5794883	0.5625474	0.5482036
1250	0.9082057	0.8442832	0.7782317	0.7210124	0.6784931	0.6462118	0.619439	0.5973769	0.578098	0.5611708	0.5460452
1252	0.9174826	0.8619739	0.7927949	0.7298741	0.6829785	0.6478697	0.6198616	0.596362	0.5765432	0.5596634	0.5434303
1254	0.9237275	0.8742937	0.8053904	0.7384861	0.6872399	0.6490492	0.6191733	0.5949516	0.5741582	0.5565133	0.5403528
1256	0.9258664	0.8815089	0.8144134	0.7458165	0.6910405	0.6503875	0.6193396	0.593376	0.5720368	0.5531634	0.5369301
1258	0.9267328	0.8851322	0.8192717	0.750553	0.6941069	0.6516916	0.6183472	0.5917075	0.5693755	0.5502696	0.5332022
1260	0.9287765	0.8853706	0.8202159	0.7528682	0.6962329	0.6528765	0.6185195	0.5900032	0.5666193	0.5470299	0.5292385
1262	0.9277695	0.8814453	0.8177504	0.7529216	0.6972191	0.6535915	0.617165	0.5881916	0.563982	0.5431469	0.5251427
1264	0.9211897	0.8730778	0.8125801	0.7513313	0.6970499	0.6530233	0.6167768	0.5861911	0.5609884	0.5395589	0.5209402
1266	0.9085296	0.8617788	0.805775	0.748292	0.6956156	0.6515388	0.6144332	0.5838587	0.5580742	0.535593	0.5166113
1268	0.8892139	0.8498405	0.7977188	0.7437545	0.6929955	0.6488987	0.612758	0.5810865	0.5546653	0.531939	0.5121955
1270	0.8732265	0.8369521	0.7889003	0.7381638	0.689124	0.6458385	0.6089243	0.5777867	0.550912	0.5280437	0.5076682
1272	0.8570574	0.8237992	0.780208	0.7317814	0.6840391	0.6417259	0.6055746	0.5738391	0.5469365	0.5235367	0.5030137
1274	0.8396885	0.8130948	0.7718769	0.7244296	0.6778008	0.6366449	0.6001059	0.5693118	0.5423529	0.5185434	0.4982875
1276	0.8310351	0.8058386	0.763134	0.7158585	0.6704335	0.6303039	0.5951353	0.5641918	0.5376068	0.5143167	0.493427
1278	0.8279482	0.7985818	0.7531186	0.7061706	0.6621792	0.622689	0.5882692	0.5585901	0.5323642	0.5098081	0.4884836
1280	0.8252332	0.7881519	0.741451	0.695607	0.653044	0.6146063	0.5820693	0.5526282	0.5268172	0.5038115	0.4835121
1282	0.8201483	0.7745056	0.7283682	0.6843253	0.6432263	0.6061619	0.5742915	0.5464243	0.5214734	0.4982958	0.4785061
1284	0.8056907	0.7592227	0.7144403	0.672114	0.6327843	0.5979128	0.567546	0.5401641	0.5156907	0.4941241	0.4735291
1286	0.7853781	0.7426557	0.6996185	0.6590835	0.6220397	0.5894632	0.5596756	0.5339536	0.510448	0.4891125	0.4685099
1288	0.7648044	0.724757	0.68373	0.6456324	0.6112334	0.5810152	0.5532282	0.5279962	0.504925	0.4828117	0.4635364
1290	0.7436822	0.7056943	0.6674106	0.632203	0.600771	0.572518	0.5459491	0.5222202	0.4996414	0.4781293	0.4586011
1292	0.7214096	0.6861131	0.6513916	0.6195995	0.5911003	0.5644441	0.5403118	0.5167438	0.4946771	0.4741444	0.4535995
1294	0.6972252	0.6666807	0.6362618	0.6083952	0.5824848	0.5573461	0.5339664	0.5115517	0.4894851	0.4690068	0.4485949
1296	0.6726544	0.6474048	0.6223769	0.5986527	0.574998	0.551316	0.5291052	0.5064853	0.4847971	0.4629503	0.4435214
1298	0.6482427	0.629252	0.6102831	0.5901336	0.5684299	0.5461886	0.5235419	0.5015689	0.4796935	0.4585288	0.4383093
1300	0.6247928	0.6142162	0.6002361	0.5825871	0.562584	0.5413545	0.5190969	0.4966586	0.4747802	0.4541019	0.4330823

Table 5.31. Indices 1200-1300 nm. IW/λ – Index Water/Wavelength, II/λ – Index Ice/Wavelength

λ (nm)	IW/λ	II/λ	λ (nm)	IW/λ	II/λ	λ (nm)	IW/λ	II/λ
1200	0.00001	0.0000056	1234	0.0000093	0.0000094	1267	0.0000086	0.0000106
1201	0.00001	0.0000057	1235	0.0000093	0.0000095	1268	0.0000086	0.0000106
1202	0.00001	0.0000059	1236	0.0000093	0.0000096	1269	0.0000086	0.0000106
1203	0.0000099	0.0000061	1237	0.0000092	0.0000096	1270	0.0000086	0.0000106
1204	0.0000099	0.0000062	1238	0.0000092	0.0000097	1271	0.0000086	0.0000106
1205	0.0000099	0.0000064	1239	0.0000092	0.0000098	1272	0.0000086	0.0000106
1206	0.0000099	0.0000065	1240	0.0000092	0.0000098	1273	0.0000087	0.0000106
1207	0.0000099	0.0000067	1241	0.0000091	0.0000099	1274	0.0000087	0.0000105
1208	0.0000099	0.0000068	1242	0.0000091	0.0000099	1275	0.0000087	0.0000105
1209	0.0000099	0.000007	1243	0.0000091	0.00001	1276	0.0000088	0.0000105
1210	0.0000098	0.0000072	1244	0.000009	0.00001	1277	0.0000088	0.0000105
1211	0.0000098	0.0000073	1245	0.000009	0.0000101	1278	0.0000089	0.0000104
1212	0.0000098	0.0000074	1246	0.0000089	0.0000101	1279	0.0000089	0.0000104
1213	0.0000098	0.0000075	1247	0.0000089	0.0000102	1280	0.000009	0.0000104
1214	0.0000098	0.0000076	1248	0.0000089	0.0000102	1281	0.000009	0.0000104
1215	0.0000098	0.0000078	1249	0.0000088	0.0000103	1282	0.000009	0.0000104
1216	0.0000097	0.0000079	1250	0.0000088	0.0000103	1283	0.0000091	0.0000103
1217	0.0000097	0.000008	1251	0.0000088	0.0000103	1284	0.0000091	0.0000103
1218	0.0000097	0.0000081	1252	0.0000087	0.0000104	1285	0.0000092	0.0000103
1219	0.0000097	0.0000082	1253	0.0000087	0.0000104	1286	0.0000092	0.0000103
1220	0.0000096	0.0000084	1254	0.0000087	0.0000104	1287	0.0000093	0.0000103
1221	0.0000096	0.0000084	1255	0.0000087	0.0000104	1288	0.0000093	0.0000103
1222	0.0000096	0.0000085	1256	0.0000086	0.0000104	1289	0.0000094	0.0000102
1223	0.0000096	0.0000086	1257	0.0000086	0.0000104	1290	0.0000094	0.0000102
1224	0.0000096	0.0000087	1258	0.0000086	0.0000104	1291	0.0000095	0.0000102
1225	0.0000095	0.0000088	1259	0.0000086	0.0000105	1292	0.0000096	0.0000102
1226	0.0000095	0.0000089	1260	0.0000086	0.0000105	1293	0.0000097	0.0000102
1227	0.0000095	0.0000089	1261	0.0000086	0.0000105	1294	0.0000099	0.0000102
1228	0.0000095	0.000009	1262	0.0000086	0.0000105	1295	0.00001	0.0000102
1229	0.0000095	0.0000091	1263	0.0000086	0.0000105	1296	0.0000102	0.0000102
1230	0.0000094	0.0000092	1264	0.0000086	0.0000105	1297	0.0000103	0.0000102
1231	0.0000094	0.0000093	1265	0.0000086	0.0000106	1298	0.0000105	0.0000102
1232	0.0000094	0.0000093	1266	0.0000086	0.0000106	1299	0.0000106	0.0000102
1233	0.0000094	0.0000094				1300	0.0000108	0.0000102

Table 5.32. Transmission (TnoH2O) for 900-1000 nm, with b of 2.0 comparison run.

tnoh2o:	10	15	20	25	30	35	40	45	50	55	60
900	0.5973711	0.6408673	0.6627287	0.676886	0.6870217	0.6956848	0.7036055	0.7085875	0.7104299	0.7084491	0.7038357
902	0.5961879	0.6023747	0.6226239	0.6418396	0.6575438	0.671742	0.6819167	0.6881162	0.6893306	0.6856716	0.6817617
904	0.5862001	0.5772207	0.5891993	0.6093631	0.6306718	0.6490377	0.6606548	0.6660766	0.6661536	0.6636312	0.6578755
906	0.5851586	0.5636751	0.5654902	0.5840707	0.6080273	0.6274225	0.6378029	0.6418887	0.6409069	0.6381861	0.6327448
908	0.5760838	0.5551425	0.5538024	0.5695071	0.5900431	0.6057039	0.6133664	0.6149699	0.6127868	0.6088715	0.6067165
910	0.5330448	0.546476	0.5531827	0.5645981	0.5758331	0.5831343	0.5861902	0.5856749	0.5838538	0.5808181	0.5801649
912	0.5002276	0.5349255	0.55787	0.5637345	0.563063	0.5599446	0.5574587	0.5548689	0.5534283	0.553878	0.553825
914	0.4983042	0.5344523	0.5577174	0.5589061	0.5480558	0.5356576	0.5278812	0.5240926	0.5234145	0.5255699	0.5278101
916	0.5237325	0.5455017	0.5516002	0.5447562	0.5276985	0.5103328	0.4991796	0.4947475	0.4951679	0.4968036	0.5027405
918	0.5553766	0.5545146	0.5414358	0.5215573	0.5008445	0.4833291	0.4719104	0.4676524	0.4681851	0.472653	0.4788114
920	0.5851995	0.5559239	0.522633	0.4917812	0.4695603	0.4556603	0.4466814	0.4431712	0.4447747	0.4504102	0.4563676
922	0.6044437	0.5435618	0.4929884	0.4586611	0.4380449	0.4280192	0.4222879	0.4207573	0.4225534	0.4278045	0.435725
924	0.5886542	0.5115737	0.4564705	0.4247243	0.4088118	0.401828	0.3995377	0.3996223	0.402518	0.4075282	0.4172502
926	0.513562	0.459501	0.416811	0.3931055	0.3825394	0.3776785	0.3773143	0.3796048	0.384341	0.3918572	0.4007579
928	0.4058115	0.3892314	0.3752026	0.3646262	0.3584398	0.3553936	0.3571507	0.3609687	0.3669284	0.3766093	0.3865153
930	0.2946299	0.3148067	0.330995	0.3357557	0.3349272	0.3348764	0.3380766	0.3439799	0.3521921	0.3613472	0.374186
932	0.1926412	0.2489565	0.2850923	0.3029338	0.3104109	0.3151417	0.3210487	0.3286573	0.3385757	0.3497455	0.3640156
934	0.1269829	0.1950106	0.2391847	0.2666418	0.2839744	0.2955527	0.3047837	0.315104	0.3268259	0.3412761	0.3558917
936	0.1094083	0.153765	0.1960128	0.2305845	0.2565877	0.2755462	0.2895405	0.3030344	0.3175387	0.3331597	0.349726
938	0.1151	0.1295593	0.1622358	0.1984759	0.229657	0.2547655	0.2746589	0.2923426	0.3092962	0.3265576	0.3457792
940	0.1273109	0.1236041	0.1427809	0.1734347	0.2057316	0.235143	0.260441	0.2827987	0.3036342	0.3235845	0.3436575
942	0.1394806	0.1304614	0.1374086	0.158341	0.187584	0.218228	0.2481221	0.2747892	0.2992104	0.3226281	0.3432435
944	0.1458488	0.1421652	0.1416457	0.1539653	0.1775784	0.2070914	0.2386172	0.268801	0.2965059	0.3214717	0.3442245
946	0.1423868	0.1507233	0.151062	0.1587924	0.1764985	0.2030034	0.2342291	0.2659479	0.2957857	0.3217175	0.346352
948	0.1454899	0.1542299	0.1623402	0.169531	0.1836285	0.2069037	0.2358308	0.2670203	0.2969713	0.3249095	0.3495715
950	0.1533637	0.1617264	0.1730179	0.1833547	0.1975897	0.2185943	0.2440775	0.2726296	0.3011511	0.3286	0.353948
952	0.1686584	0.1754432	0.1853565	0.1999324	0.2168667	0.2362639	0.2583055	0.2826222	0.3082949	0.3341144	0.3598894
954	0.1889592	0.1922433	0.2033734	0.2207428	0.2402377	0.2583763	0.2767621	0.2967115	0.3192841	0.3430758	0.3681683
956	0.2026205	0.2139887	0.2283564	0.2478157	0.266997	0.2825352	0.2980886	0.3144923	0.3337323	0.3564799	0.3789264
958	0.2278511	0.240875	0.2608599	0.2806821	0.2959398	0.3084299	0.32116	0.3353384	0.3521999	0.3716356	0.3925238
960	0.2625091	0.2779836	0.300751	0.3160571	0.3257482	0.3353068	0.3459058	0.3588612	0.3737649	0.3900421	0.409066
962	0.301782	0.3294989	0.3443533	0.3507024	0.3558809	0.3636619	0.3730565	0.3848039	0.3980351	0.4128321	0.4281135
964	0.3637516	0.3848013	0.386144	0.3845885	0.3872843	0.394047	0.4024309	0.4131095	0.4246042	0.4372414	0.4493676
966	0.4426329	0.434014	0.4240927	0.419622	0.4210984	0.4265835	0.4345269	0.4433492	0.4524372	0.4617748	0.4721747
968	0.5087286	0.4770588	0.4610059	0.4565914	0.4577467	0.4619333	0.4684537	0.4751082	0.4821178	0.4882444	0.4960854
970	0.5531191	0.5163146	0.5009594	0.4964159	0.497234	0.4994247	0.5040156	0.5080678	0.5119515	0.5170457	0.5209037
972	0.5837337	0.5564047	0.5435821	0.5390372	0.538635	0.5390999	0.5403234	0.5416311	0.5428918	0.5447106	0.5463655
974	0.5960565	0.5950746	0.5881015	0.5838931	0.5812964	0.5795487	0.5772839	0.5754194	0.5738167	0.5720808	0.5721148
976	0.6004418	0.62674	0.6321245	0.6289794	0.6241586	0.619478	0.6137622	0.6090855	0.6045006	0.600669	0.597997
978	0.6222276	0.6548206	0.6712197	0.6717567	0.6655969	0.6583157	0.6498505	0.6421513	0.6354166	0.6299101	0.6238827
980	0.669813	0.6883466	0.7051864	0.7096331	0.7043448	0.6950445	0.6847273	0.6745816	0.6651237	0.6569623	0.6497933
982	0.7305867	0.7319049	0.7382752	0.7423741	0.7388477	0.7290864	0.7176477	0.7057515	0.6944451	0.683538	0.6753228
984	0.7890181	0.7800458	0.7743379	0.772987	0.7690874	0.7597366	0.7483751	0.7354001	0.7227604	0.7112528	0.7004809
986	0.8431675	0.8257599	0.8129082	0.8037861	0.7964454	0.7873513	0.7760969	0.7630022	0.7495286	0.7375387	0.7251062
988	0.8856438	0.867766	0.8500776	0.8345954	0.8226574	0.8124769	0.8010728	0.7883755	0.7750805	0.7612402	0.7490039
990	0.9183899	0.9027576	0.8830592	0.8639522	0.848372	0.8358735	0.8237634	0.8115173	0.7982946	0.7843877	0.7718546
992	0.9419513	0.9286978	0.9099048	0.8905367	0.8730588	0.8582787	0.8450656	0.8327	0.8200478	0.8073388	0.7936568
994	0.9565189	0.9455631	0.9302964	0.9132848	0.8956229	0.8795561	0.8654203	0.8525559	0.8399526	0.8274657	0.8140619
996	0.9649639	0.9555432	0.9451039	0.9312021	0.9151935	0.8992232	0.8847163	0.8712699	0.858446	0.8452146	0.8330377
998	0.9686355	0.9625883	0.9551106	0.9443367	0.9313389	0.9168546	0.9026722	0.8888708	0.8758864	0.8631708	0.8507235
1000	0.9700758	0.9675235	0.9614337	0.9538454	0.9440807	0.9319343	0.9186737	0.9051741	0.8920105	0.8800708	0.8672922

Table 5.33. α for 900-1000 nm, with b of 2.0 comparison run.

alpha:	10	15	20	25	30	35	40	45	50	55	60
900	0.1255156	0.1060335	0.0976418	0.0921746	0.0882798	0.0853036	0.0828522	0.0820956	0.0833057	0.0866398	0.0915635
902	0.1258453	0.1203586	0.1109695	0.1032647	0.0973252	0.0924519	0.0895914	0.0891905	0.0914762	0.0964056	0.1017728
904	0.1280479	0.1294181	0.1225559	0.1137509	0.1056649	0.0993887	0.0968021	0.0975338	0.101319	0.1068735	0.1133939
906	0.1226376	0.1325508	0.1305315	0.1220867	0.1128345	0.1065201	0.1052687	0.1077907	0.1131214	0.1192649	0.1262673
908	0.1218413	0.1321095	0.1330725	0.1264312	0.1186845	0.1146025	0.1156955	0.1205036	0.1273795	0.1343938	0.1400695
910	0.1376757	0.1316556	0.1302571	0.1266958	0.1236785	0.1243541	0.128824	0.135886	0.1431843	0.1500524	0.1544174
912	0.1487456	0.1336959	0.1255235	0.1251812	0.1290482	0.1362736	0.1448439	0.1535689	0.1606319	0.1654051	0.1689914
914	0.1452373	0.1319234	0.1233282	0.125995	0.1369672	0.1511139	0.163354	0.1726061	0.1785784	0.1815322	0.1835167
916	0.1330569	0.1247402	0.1242689	0.1329067	0.1501812	0.1689027	0.1831105	0.1917645	0.1959412	0.1982036	0.197828
918	0.1179441	0.1185046	0.1285696	0.1477192	0.1701933	0.1895403	0.2030746	0.2100434	0.2130893	0.213433	0.2117403
920	0.1022352	0.1167494	0.141176	0.1708441	0.195552	0.2116382	0.2219497	0.2271005	0.2285348	0.2272182	0.2250516
922	0.0919861	0.125283	0.1664133	0.2007961	0.2226673	0.2337697	0.240305	0.2431772	0.2435463	0.2415061	0.2375399
924	0.09954	0.1536056	0.2028656	0.2334925	0.2483299	0.2549929	0.2575905	0.2586779	0.2577003	0.2545864	0.249018
926	0.1456419	0.2044211	0.2448443	0.2642089	0.2713736	0.2747013	0.2751182	0.2737653	0.2704882	0.2658322	0.2593157
928	0.2353833	0.27192	0.2869309	0.2911834	0.2928383	0.2939265	0.2916435	0.2882662	0.2833189	0.2760493	0.2683887
930	0.3531445	0.3442169	0.3273963	0.3176792	0.3148194	0.3123811	0.3080614	0.3018812	0.2942261	0.2858888	0.27618
932	0.482053	0.4113307	0.3677873	0.3482387	0.3385172	0.3308488	0.3230567	0.3143736	0.3045047	0.2943711	0.2827016
934	0.5914739	0.469588	0.413437	0.3837146	0.3639691	0.349408	0.337677	0.325661	0.3135752	0.3005809	0.2879113
936	0.620742	0.5256072	0.4641911	0.4211584	0.3907574	0.3682984	0.3512221	0.3357414	0.3205931	0.3059408	0.2917751
938	0.5964078	0.5686978	0.5102012	0.4573227	0.4177737	0.3879129	0.3645345	0.3447199	0.3270516	0.3102013	0.2943537
940	0.562355	0.5764946	0.5391834	0.4884004	0.4430502	0.4065999	0.3768956	0.3526213	0.3315391	0.3132497	0.2957247
942	0.5283992	0.5541865	0.5441115	0.5075601	0.463081	0.4229007	0.3879191	0.3592801	0.3350723	0.3140801	0.2960902
944	0.5065699	0.5231867	0.5288731	0.5096975	0.4734471	0.4334033	0.396096	0.3641534	0.3375271	0.3146143	0.2956668
946	0.5183787	0.4998667	0.5040376	0.4958779	0.4712122	0.4360897	0.3997837	0.3664831	0.3379458	0.3146534	0.2946196
948	0.5155477	0.4916998	0.47906	0.4726414	0.4568298	0.4292125	0.3971782	0.3653888	0.3372944	0.3135782	0.2929795
950	0.4900968	0.4793066	0.4593432	0.4471348	0.4338736	0.4131739	0.3877484	0.3602054	0.3341298	0.3108767	0.2905829
952	0.460373	0.4527295	0.4394995	0.4221644	0.4068601	0.3911451	0.372058	0.3506815	0.3283328	0.3066214	0.2871233
954	0.4258017	0.422423	0.4122118	0.3954341	0.3788713	0.3658718	0.3525199	0.3371972	0.3195689	0.3009002	0.2822455
956	0.3981983	0.389648	0.3788281	0.3646061	0.3508298	0.3407159	0.3311807	0.3206505	0.3071338	0.2915588	0.2755645
958	0.3634292	0.3542292	0.3421021	0.3310661	0.3228487	0.3160972	0.3095458	0.3021288	0.2923768	0.2803034	0.2668989
960	0.3232804	0.3148559	0.3037097	0.2981719	0.2955058	0.2921649	0.2881542	0.2825854	0.2756232	0.2666696	0.2563073
962	0.2820464	0.2707696	0.2669878	0.2679854	0.269243	0.2683774	0.2663214	0.2625813	0.2576409	0.251672	0.2440609
964	0.2356628	0.2294386	0.234392	0.2403691	0.2438712	0.244766	0.2445207	0.2423689	0.239484	0.2354366	0.230625
966	0.1862029	0.1961988	0.2064873	0.2142968	0.2190257	0.2215557	0.2222119	0.222104	0.2209695	0.2192408	0.2164661
968	0.1497572	0.168928	0.1816858	0.1893106	0.1946236	0.1984588	0.2005896	0.2020412	0.2027495	0.2029211	0.2019854
970	0.1263606	0.1462634	0.1579374	0.1654321	0.170974	0.1759316	0.1792164	0.1824847	0.185039	0.1865786	0.1874734
972	0.1128269	0.1259113	0.1354031	0.1425804	0.14848	0.1540475	0.1591661	0.1636653	0.1675397	0.1707666	0.1731042
974	0.107332	0.108768	0.1145661	0.1210553	0.1274708	0.1336118	0.13994	0.1457614	0.1509549	0.1553553	0.1589871
976	0.1053918	0.0959982	0.0964727	0.1016518	0.108289	0.1149742	0.1223213	0.1289068	0.1350505	0.1407115	0.1452242
978	0.0966869	0.0859959	0.0822371	0.0851478	0.0912919	0.098289	0.1058894	0.1131975	0.1199959	0.1261751	0.1319073
980	0.0797803	0.0751198	0.071202	0.0719311	0.0767972	0.083668	0.0911709	0.0987284	0.106131	0.1127837	0.119129
982	0.0597608	0.0617032	0.0612219	0.0615422	0.0649113	0.0709897	0.0779308	0.0855506	0.0930539	0.1003885	0.1069462
984	0.0425598	0.0473702	0.0507492	0.0525636	0.0552958	0.0602954	0.0665392	0.0737387	0.0812045	0.0885499	0.0954378
986	0.027993	0.0346429	0.0399448	0.0438734	0.0471414	0.0513192	0.0567438	0.0633384	0.0704665	0.077473	0.0846669
988	0.0182781	0.0239195	0.0299972	0.035345	0.0396589	0.0436562	0.0485702	0.0543413	0.0608415	0.067781	0.074691
990	0.011844	0.0159873	0.0216488	0.0274608	0.0325283	0.0368724	0.0414636	0.0466183	0.0525269	0.0590875	0.0655531
992	0.0077502	0.0107213	0.0153133	0.0206541	0.0259048	0.0306287	0.0352414	0.0399272	0.0451834	0.0509915	0.0572925
994	0.0054904	0.0075493	0.0108903	0.0151916	0.0200903	0.0249227	0.0294647	0.0340067	0.038831	0.0440231	0.049898
996	0.0043235	0.0058118	0.0079455	0.0111814	0.0153029	0.0198198	0.0242588	0.0286612	0.0332129	0.0381665	0.0433281
998	0.0038431	0.0047319	0.0061076	0.0084207	0.0115891	0.0154681	0.0195602	0.0238235	0.0281309	0.0327102	0.0375053
1000	0.0036645	0.0040325	0.0050276	0.0065621	0.0088451	0.0119418	0.0155796	0.0195192	0.0236385	0.0277432	0.0323307

Table 5.34. β for 900-1000 nm, with b of 2.0 comparison run.

beta:	10	15	20	25	30	35	40	45	50	55	60
900	0.6427006	0.6527181	0.654569	0.6567873	0.6587641	0.6589206	0.6577653	0.6527128	0.6426095	0.6284513	0.6118413
902	0.6432548	0.6543664	0.6606318	0.663207	0.6646544	0.6642309	0.6610057	0.652159	0.6384906	0.6210681	0.6032556
904	0.6499871	0.6581104	0.6655686	0.6695881	0.6704183	0.6690255	0.6619541	0.6494636	0.6320054	0.6119453	0.5945599
906	0.6711478	0.6664787	0.670906	0.6747745	0.6752813	0.6718211	0.6608893	0.6436057	0.6232058	0.6034681	0.5860971
908	0.6871971	0.6799476	0.6785073	0.6797453	0.6789444	0.6716941	0.6558169	0.6348478	0.6129097	0.5944318	0.5788468
910	0.6915399	0.6935218	0.6891009	0.6857389	0.6807448	0.6677555	0.6472513	0.6237108	0.6025422	0.5856068	0.5734979
912	0.7001324	0.7023351	0.6994156	0.6924296	0.6795286	0.6591138	0.6348338	0.6118248	0.5933641	0.579412	0.5697233
914	0.7135196	0.7090526	0.707659	0.69626	0.6733415	0.6456023	0.6206936	0.6007223	0.5861523	0.5757876	0.56782
916	0.7196444	0.7194204	0.7127169	0.6915852	0.6592053	0.6289594	0.6069106	0.5916988	0.5813428	0.5739775	0.567046
918	0.7312413	0.730284	0.7112427	0.6749871	0.6380185	0.6118646	0.5951996	0.5853037	0.578069	0.5716037	0.5672969
920	0.7539008	0.7351119	0.6941639	0.6481454	0.6153947	0.5971571	0.5868863	0.5808787	0.5759889	0.5714901	0.5682904
922	0.7736307	0.7201118	0.6585296	0.6172744	0.5963116	0.5867568	0.5813812	0.5778867	0.5749516	0.5722079	0.5698034
924	0.7610326	0.6705199	0.6153946	0.5914226	0.5832391	0.5798722	0.5781038	0.5760815	0.5742082	0.573512	0.5714639
926	0.6921077	0.6080618	0.5797046	0.5745388	0.5754526	0.5759226	0.5756831	0.5750918	0.5747091	0.5732988	0.5735506
928	0.61134	0.5662483	0.5591627	0.5655522	0.5706277	0.5727099	0.5740838	0.5746601	0.5751653	0.5750179	0.5755625
930	0.5649835	0.5512741	0.5538893	0.5616851	0.5668299	0.5704316	0.5727951	0.574695	0.5762099	0.5779609	0.577801
932	0.5591653	0.5543378	0.5585866	0.5608794	0.564377	0.5688826	0.572351	0.5752704	0.5774606	0.5790157	0.5797617
934	0.5687354	0.5676979	0.5649343	0.5629319	0.5647587	0.5686585	0.5725702	0.5761227	0.5787076	0.5800127	0.5815039
936	0.5784747	0.578177	0.5715294	0.5680165	0.5676991	0.5701413	0.5739115	0.577386	0.5802175	0.5820459	0.5830712
938	0.5861226	0.5821559	0.578491	0.5748128	0.5729375	0.5734026	0.5759538	0.5788658	0.5814565	0.5839651	0.583957
940	0.5911426	0.5863191	0.5842387	0.5813478	0.5790238	0.5779136	0.5791227	0.5806718	0.5823641	0.5832186	0.5844723
942	0.5988693	0.5923719	0.5889782	0.5868936	0.5847321	0.5829101	0.5821057	0.5823946	0.5831094	0.5832062	0.5844235
944	0.607637	0.598955	0.5948885	0.5918493	0.5893245	0.5871429	0.5851907	0.5839601	0.5831993	0.5838751	0.5838584
946	0.6027933	0.6058607	0.6015387	0.5967878	0.5930814	0.5900571	0.5868306	0.5847394	0.5835446	0.5835118	0.5828361
948	0.6002237	0.6077925	0.606993	0.6021508	0.5966769	0.591827	0.5876645	0.5847155	0.5829256	0.5810903	0.5813878
950	0.610648	0.6077062	0.6098885	0.6068401	0.6000262	0.5929984	0.5876411	0.5839954	0.5819463	0.5804326	0.5797064
952	0.6154419	0.6128634	0.6117562	0.6091573	0.6023757	0.5940523	0.5877789	0.5834072	0.5809329	0.5798482	0.5778037
954	0.6209387	0.6198334	0.6151652	0.6100342	0.6032705	0.5953177	0.5885121	0.5833848	0.5794938	0.5772974	0.5753589
956	0.631965	0.6260093	0.6192278	0.6107169	0.6032511	0.5966389	0.5898408	0.5839446	0.5795631	0.5750463	0.5729502
958	0.6387966	0.6330321	0.6226612	0.6120783	0.6041497	0.5980481	0.5916557	0.5850453	0.5790698	0.5742118	0.5706497
960	0.6462765	0.6383741	0.6258946	0.6150665	0.6070614	0.600347	0.5934879	0.5863265	0.5792405	0.5741173	0.5685322
962	0.6582755	0.6421789	0.6301346	0.6205702	0.6120277	0.6038644	0.5957417	0.5876382	0.5798801	0.5721482	0.5670315
964	0.6629155	0.6490485	0.6376644	0.6281307	0.6182085	0.6081594	0.598209	0.5889449	0.5800417	0.5719439	0.5660374
966	0.6719245	0.658976	0.6481522	0.6368451	0.6250666	0.6129781	0.6016678	0.5907791	0.5816122	0.5733104	0.5657959
968	0.6858389	0.6723636	0.6598042	0.6467146	0.6326481	0.6184332	0.6052371	0.5934101	0.5827714	0.5744401	0.5663157
970	0.7030115	0.6865041	0.6718814	0.6567407	0.6406729	0.6247912	0.610334	0.5967584	0.585285	0.574733	0.5673972
972	0.7111611	0.700058	0.6847297	0.6674488	0.6495457	0.6321574	0.6156078	0.6011306	0.5887533	0.5775721	0.569106
974	0.7158703	0.7112694	0.6978524	0.678893	0.6591454	0.6402506	0.622445	0.6065675	0.5929248	0.5823233	0.5717578
976	0.7176788	0.7202169	0.7095627	0.6906855	0.6693895	0.6493366	0.6298705	0.6130808	0.5987746	0.5857993	0.575396
978	0.7239482	0.7254622	0.718406	0.7016622	0.68037	0.6588941	0.638871	0.6209109	0.6050731	0.5908726	0.580023
980	0.7345985	0.7298908	0.7238179	0.7109162	0.6909426	0.6688853	0.6481359	0.6294857	0.6126179	0.5985229	0.5853455
982	0.7549288	0.7377502	0.7284983	0.7177424	0.700702	0.6795347	0.6593047	0.6392189	0.6215739	0.6063866	0.5918261
984	0.7814434	0.7541594	0.7360615	0.7231708	0.7089613	0.6902924	0.6697429	0.6496509	0.6307328	0.6132812	0.5991299
986	0.8225406	0.7780454	0.7490733	0.7305221	0.716551	0.7003091	0.6811913	0.6607242	0.6412188	0.6228465	0.6071647
988	0.8618692	0.8100935	0.7687554	0.7428825	0.7253645	0.7098019	0.6912273	0.6717859	0.6518046	0.633745	0.6158249
990	0.8976762	0.8447596	0.7956651	0.7611762	0.7374809	0.7197601	0.7019681	0.6825069	0.6626577	0.6432808	0.6252476
992	0.9299532	0.8790419	0.8278543	0.785118	0.7538621	0.7315435	0.7117025	0.6930906	0.6733577	0.6528111	0.6347548
994	0.9518695	0.9118066	0.8612171	0.8132523	0.7747888	0.7458901	0.7238057	0.7034284	0.6836755	0.6640565	0.6446905
996	0.9603446	0.9363078	0.8924597	0.8430405	0.7993325	0.764086	0.7369461	0.7146671	0.6940976	0.6749358	0.6548782
998	0.9627098	0.9496798	0.918224	0.8725224	0.825802	0.785036	0.7533816	0.727438	0.7053701	0.6843706	0.6649585
1000	0.9626368	0.9569306	0.9361982	0.8985058	0.8522936	0.8080502	0.7712547	0.741865	0.7171558	0.6950164	0.6747047

Table 5.35. Transmission (TnoH2O) for 900-1000 nm fw1p25_parms comparison run.

tnoh2o:	10	15	20	25	30	35	40	45	50	55	60
900	0.6028045	0.6435348	0.6651076	0.6789101	0.6886289	0.6957145	0.7010314	0.7032449	0.7030677	0.7004132	0.696311
902	0.5974659	0.6088354	0.6281645	0.645969	0.6602912	0.6715004	0.6783728	0.6819035	0.681961	0.6784656	0.67572
904	0.5887114	0.5836132	0.5972338	0.6162692	0.6339431	0.6479583	0.6560331	0.6594922	0.6594376	0.6578931	0.6539597
906	0.5843716	0.5686786	0.574988	0.5923468	0.6110407	0.6253628	0.6327789	0.6358792	0.6357411	0.6347343	0.6312278
908	0.5713532	0.5588956	0.5621177	0.5763743	0.5920874	0.6034176	0.6090914	0.6107421	0.6100756	0.6080004	0.6075837
910	0.5348833	0.54814	0.5572738	0.5674108	0.5760761	0.581398	0.5838642	0.5843621	0.5840649	0.5827632	0.5836466
912	0.507251	0.5374446	0.5555755	0.5612541	0.5611994	0.5592876	0.5580496	0.5569987	0.5569332	0.5585747	0.5595514
914	0.505016	0.5361774	0.5523406	0.5522511	0.5444123	0.5361411	0.5314363	0.5295685	0.5300384	0.5329105	0.5359901
916	0.5244613	0.5436352	0.5455841	0.5368109	0.5238013	0.512018	0.5051867	0.5028834	0.5043883	0.5066627	0.5132108
918	0.5539122	0.5490283	0.5342342	0.5154441	0.4985974	0.4860953	0.4790134	0.4774144	0.4793595	0.4846638	0.4914012
920	0.5800447	0.5476023	0.5154837	0.4888289	0.4702229	0.4595811	0.4539318	0.4534432	0.4570638	0.464258	0.4711161
922	0.5942367	0.5340351	0.4881255	0.4583239	0.4409396	0.4331142	0.4296488	0.4311154	0.4357992	0.4429184	0.4524023
924	0.5750727	0.502939	0.4539708	0.4264052	0.4128414	0.4075492	0.407284	0.4103356	0.4161871	0.4238984	0.4353794
926	0.5043805	0.4524334	0.4154865	0.3953262	0.3866832	0.3840527	0.3860394	0.3910411	0.3987039	0.4089091	0.4201099
928	0.4041215	0.3865319	0.3739871	0.3658375	0.3622561	0.3620313	0.3666512	0.3732369	0.3820406	0.3943751	0.4066221
930	0.2974921	0.3173548	0.3304401	0.335805	0.3383619	0.3418103	0.3482793	0.3570768	0.3681738	0.3798121	0.3949315
932	0.2013441	0.2541747	0.2864615	0.3039111	0.3139134	0.3221795	0.3316249	0.3424094	0.3551414	0.3688031	0.3851947
934	0.138288	0.2021111	0.2437961	0.2703919	0.2885489	0.3028817	0.3155958	0.3292852	0.3439284	0.3607285	0.3771363
936	0.1171574	0.1636309	0.2047887	0.237622	0.2630264	0.2835842	0.3006963	0.3174756	0.3347193	0.352691	0.3708881
938	0.1198469	0.1405112	0.1743474	0.2089752	0.2391243	0.2647178	0.2865644	0.3069567	0.3265031	0.3457678	0.3665471
940	0.1293498	0.1328815	0.1559703	0.1871357	0.2186922	0.2477153	0.2739474	0.2978875	0.3207058	0.342308	0.3637557
942	0.1400483	0.1365198	0.1495489	0.1740416	0.2038923	0.2340262	0.2637658	0.2908016	0.3161115	0.3406999	0.3625582
944	0.1453782	0.1451914	0.1517329	0.1697712	0.1959643	0.2257999	0.2567575	0.286198	0.3135033	0.3390565	0.3628704
946	0.14476	0.1524019	0.1588279	0.1730112	0.1955094	0.2237709	0.2543274	0.284653	0.313371	0.3391976	0.3646585
948	0.1477787	0.1573428	0.168215	0.1817332	0.2017596	0.2280599	0.2569213	0.286864	0.3156332	0.3430181	0.3678285
950	0.1558097	0.1657806	0.1791441	0.1942564	0.2137983	0.2381927	0.2648717	0.292964	0.3209819	0.3478377	0.3726575
952	0.17059	0.1797211	0.19296	0.2102746	0.2305403	0.253072	0.2774924	0.3030991	0.3291144	0.3543621	0.3794895
954	0.1894518	0.1972535	0.2116214	0.2308821	0.2515417	0.2722627	0.294053	0.3167525	0.3405078	0.3640322	0.3882401
956	0.2059091	0.219068	0.2363365	0.2564673	0.2761802	0.2942641	0.313601	0.3334438	0.3546535	0.3775449	0.3992036
958	0.2312904	0.246924	0.2673527	0.2867401	0.3035177	0.3190131	0.3354041	0.3529149	0.3719014	0.391958	0.4124234
960	0.2658515	0.2839881	0.3045401	0.3201375	0.3326212	0.3455477	0.3590846	0.3746224	0.3914776	0.4087972	0.4279732
962	0.3064518	0.3315371	0.3457891	0.3544441	0.3628106	0.3734776	0.3851245	0.3986966	0.4135162	0.4293773	0.4453526
964	0.3661415	0.383339	0.3867974	0.3888518	0.3941998	0.4031252	0.4129099	0.4248379	0.4376065	0.4515602	0.4646066
966	0.4400393	0.432536	0.4254369	0.423978	0.427463	0.4342874	0.4431849	0.4528201	0.4631989	0.4737322	0.4854403
968	0.5037554	0.4760833	0.4633652	0.4605144	0.46292	0.467874	0.4750153	0.482484	0.4904209	0.4979042	0.5072437
970	0.5497052	0.5160399	0.5027536	0.4994764	0.500751	0.50337	0.5084381	0.5131389	0.5183077	0.5246045	0.5300636
972	0.5799126	0.5556279	0.5445323	0.5406862	0.5402542	0.5409782	0.5427346	0.5447004	0.547102	0.5503789	0.5536597
974	0.5940819	0.5929467	0.5873799	0.5834933	0.5809592	0.5794179	0.5776015	0.5766231	0.5762093	0.5759512	0.5775143
976	0.6035279	0.6248964	0.6290909	0.6261794	0.6216936	0.6174974	0.6123885	0.6085318	0.6052218	0.6027464	0.6017545
978	0.6274628	0.6553336	0.6671123	0.666698	0.6609506	0.6542459	0.6466162	0.639917	0.6343784	0.6304086	0.6260631
980	0.6734529	0.6905508	0.7021635	0.7034859	0.6976376	0.6888796	0.6796068	0.6706877	0.6625599	0.6559319	0.650287
982	0.730532	0.7331567	0.7368525	0.736805	0.7311161	0.7212877	0.7108905	0.7001998	0.6903034	0.6808714	0.674274
984	0.7876864	0.7789287	0.7730644	0.7685949	0.7616307	0.7511235	0.7401413	0.7282582	0.7170307	0.7070013	0.6977427
986	0.840173	0.8230301	0.810031	0.7997031	0.7899193	0.7789294	0.7670355	0.7546218	0.7422932	0.7316973	0.7207878
988	0.8822547	0.8632509	0.845449	0.8299141	0.8168031	0.8047103	0.791967	0.7791138	0.7665133	0.7539355	0.7431184
990	0.9148849	0.8971188	0.8770576	0.8583432	0.8424382	0.82872	0.8150867	0.8020083	0.7888803	0.7757779	0.7644866
992	0.9386421	0.922924	0.9032739	0.8839227	0.8664602	0.8512002	0.8367646	0.823315	0.810185	0.7977698	0.784987
994	0.9538477	0.9405613	0.9237018	0.9058783	0.8882197	0.872036	0.8571819	0.8432991	0.8299148	0.8172569	0.8043548
996	0.9630346	0.9518422	0.9389227	0.9236282	0.9072181	0.89107	0.8761926	0.8620239	0.8483794	0.8347934	0.8226609
998	0.9674103	0.9596405	0.949841	0.9372811	0.9231292	0.9080962	0.8936023	0.8794253	0.8658379	0.8525205	0.839841
1000	0.968985	0.9649395	0.9573844	0.9476556	0.9360688	0.9228588	0.9091154	0.8953552	0.881767	0.8692739	0.8560498

Table 5.36. α for 900-1000 nm fw1p25_parms comparison run.

alpha:	10	15	20	25	30	35	40	45	50	55	60
900	0.1233905	0.1052518	0.0968635	0.0917869	0.0884756	0.0866659	0.0859049	0.0868271	0.0891564	0.0927491	0.0970688
902	0.1249925	0.1177674	0.1092197	0.1022697	0.0974704	0.09443	0.0936102	0.0947857	0.0976947	0.1021807	0.1063776
904	0.126225	0.12662	0.119747	0.1120601	0.106057	0.1023244	0.1018739	0.1037316	0.1073955	0.1118027	0.1166841
906	0.1231104	0.1301133	0.1269797	0.12008	0.1138704	0.1105259	0.111146	0.1140224	0.1183648	0.1228373	0.1279468
908	0.124167	0.1306909	0.1300283	0.1251828	0.1207711	0.1194892	0.1217307	0.1259311	0.1310998	0.1361241	0.140018
910	0.1370762	0.1316662	0.1295862	0.1275738	0.1271589	0.1296525	0.1340705	0.1395746	0.1448097	0.1497872	0.1527043
912	0.1457519	0.1335138	0.1281272	0.1291828	0.1341686	0.1412774	0.148214	0.1547841	0.1599275	0.1632648	0.1657289
914	0.1430335	0.1320179	0.1281031	0.1331176	0.1434503	0.1549929	0.1642107	0.1711423	0.1756711	0.1776932	0.1788428
916	0.1330568	0.1270778	0.1305421	0.1416756	0.1566954	0.1709477	0.1814691	0.1880455	0.1912176	0.1927721	0.1917828
918	0.1189157	0.1235352	0.1369129	0.1558532	0.1746841	0.1894454	0.1996691	0.2048809	0.2069615	0.206619	0.2043139
920	0.1056725	0.1246772	0.1503819	0.1763604	0.1967302	0.2096503	0.2177206	0.2212198	0.2213952	0.2191553	0.2162732
922	0.0989604	0.1355839	0.1735362	0.2025934	0.2209482	0.2305549	0.2357199	0.2368816	0.2355571	0.2322128	0.2274959
924	0.1102678	0.1631141	0.2060786	0.2321161	0.2452461	0.2512223	0.2526326	0.2518342	0.2489218	0.2443444	0.2378618
926	0.1558562	0.2101083	0.2447062	0.2616307	0.2682825	0.2705939	0.2693184	0.2660737	0.2609584	0.2547814	0.2472803
928	0.2395287	0.2722656	0.2854311	0.2894177	0.2900832	0.2891015	0.2847857	0.279545	0.2729151	0.2642784	0.2556843
930	0.3501056	0.3398328	0.3259386	0.316968	0.3117419	0.3066142	0.3001136	0.2921663	0.2830668	0.2735024	0.2630228
932	0.4706038	0.4045261	0.3662304	0.3465019	0.3344062	0.3242169	0.3142926	0.3038336	0.2926278	0.2815055	0.2692729
934	0.5706362	0.4621633	0.4087952	0.3789401	0.3583681	0.3419918	0.3282402	0.3145137	0.3011801	0.2874309	0.2743826
936	0.6050206	0.5125737	0.453513	0.4126805	0.3829873	0.3597576	0.3411507	0.3241717	0.3079502	0.2927347	0.2783708
938	0.5870944	0.5490462	0.4931951	0.444403	0.4069292	0.3775334	0.3535207	0.3327634	0.3143378	0.2971526	0.2812876
940	0.5581231	0.5584364	0.5180104	0.4702333	0.4280317	0.3934666	0.3644102	0.3401355	0.3189087	0.3005358	0.2831626
942	0.5284036	0.5431281	0.5233026	0.4851083	0.4434383	0.4062941	0.3734067	0.3459712	0.3224563	0.3018503	0.2840842
944	0.5106891	0.5187148	0.512444	0.486444	0.450275	0.4132002	0.3791186	0.3497229	0.3246974	0.3027217	0.2841101
946	0.5157602	0.4996	0.4933746	0.47586	0.4472463	0.4134197	0.3806045	0.3507309	0.3245997	0.3026552	0.2832541
948	0.5100862	0.4884892	0.4730553	0.4576666	0.4352532	0.4064356	0.3768385	0.348438	0.323065	0.3010047	0.2814475
950	0.4867716	0.4728987	0.4534738	0.4363542	0.4168305	0.3929973	0.3679485	0.3425274	0.3188324	0.2974793	0.2785853
952	0.4581206	0.4473491	0.4315229	0.4132057	0.3945824	0.3753352	0.3544567	0.3331524	0.3121892	0.2923403	0.2745177
954	0.4251978	0.4177748	0.404404	0.387208	0.3702154	0.3545183	0.3379021	0.3208015	0.3032691	0.2859294	0.2690492
956	0.3957284	0.3856401	0.3728216	0.3581781	0.3444918	0.3324489	0.3195148	0.3061891	0.2916678	0.276654	0.2620921
958	0.3610979	0.3505819	0.3383863	0.3273791	0.3180958	0.3094192	0.3001528	0.2900265	0.2786064	0.2662385	0.2536467
960	0.3212591	0.3121123	0.3025865	0.2966095	0.2919065	0.2864606	0.2804493	0.2728075	0.2640565	0.2541798	0.2438457
962	0.2806506	0.2708801	0.2676276	0.2673409	0.266491	0.2637392	0.2601734	0.2549161	0.2483953	0.2411345	0.2328727
964	0.2351763	0.2317895	0.2357601	0.2399664	0.2419091	0.2414241	0.2399217	0.2365929	0.2323608	0.2269184	0.221024
966	0.1886854	0.1984967	0.2078367	0.2142927	0.2179963	0.2196049	0.2193018	0.2180841	0.2157371	0.2126042	0.2085704
968	0.1529042	0.1709929	0.1828085	0.1899676	0.1946858	0.1978956	0.1992234	0.1996635	0.1991775	0.1980363	0.1957292
970	0.1289532	0.1480482	0.159352	0.166736	0.1721447	0.1766689	0.1792822	0.181562	0.1829501	0.1832187	0.1827344
972	0.1149861	0.1278716	0.1373211	0.1446476	0.1506204	0.1559314	0.1604285	0.1640336	0.1667985	0.168735	0.1697537
974	0.1085897	0.1109782	0.1171475	0.1239444	0.1304634	0.1364388	0.1422502	0.1472541	0.1514102	0.1545943	0.1569033
976	0.1045225	0.0978929	0.0996799	0.1052836	0.1120356	0.1185874	0.1254978	0.1313746	0.136552	0.1410655	0.1443247
978	0.0951825	0.0867915	0.085391	0.089287	0.0956646	0.1025693	0.1098207	0.1165072	0.1224481	0.1275617	0.1321076
980	0.078852	0.0751006	0.0735226	0.0760112	0.0815561	0.0885015	0.0957434	0.1027672	0.1093972	0.1151222	0.1203408
982	0.0602037	0.0618045	0.0626384	0.0649543	0.069635	0.0761567	0.0830092	0.0902138	0.0970639	0.1035363	0.1091021
984	0.0433199	0.048222	0.0518754	0.0551699	0.0595133	0.065439	0.0719203	0.0788975	0.0858555	0.0924557	0.0984518
986	0.0292873	0.0359401	0.0413979	0.046025	0.0506504	0.0560578	0.0621269	0.068812	0.0756193	0.0820628	0.0884615
988	0.0194756	0.0256385	0.0318556	0.0374814	0.0426312	0.0478126	0.0536813	0.0598834	0.0663421	0.0728976	0.0791655
990	0.0128485	0.0178046	0.0237992	0.0297687	0.0352997	0.0405285	0.0461278	0.0519938	0.0581654	0.0645592	0.0705843
992	0.0085568	0.0123577	0.0175188	0.0231461	0.0287094	0.0340089	0.0394695	0.044981	0.0507499	0.0566788	0.0627327
994	0.0060752	0.0088735	0.0129341	0.0177613	0.0229855	0.0282257	0.0334035	0.0387103	0.0441853	0.0497264	0.055583
996	0.0047059	0.0067803	0.0097297	0.0136387	0.0182202	0.0231341	0.0280552	0.0330898	0.0382873	0.0437203	0.0491035
998	0.0040788	0.0054504	0.0075638	0.0106136	0.0144066	0.0187732	0.0233001	0.0280775	0.0329695	0.0380938	0.0432426
1000	0.0038525	0.0045985	0.0061397	0.0084285	0.0114521	0.0151442	0.0192616	0.023663	0.0282922	0.0329312	0.0379566

Table 5.37. β for 900-1000 nm, with b of 2.5 comparison run.

beta:	10	15	20	25	30	35	40	45	50	55	60
900	0.6424028	0.6518171	0.6542299	0.6552101	0.654914	0.6516562	0.6460183	0.6371014	0.6253784	0.6122592	0.5989878
902	0.6444612	0.6545905	0.659275	0.6609831	0.6594269	0.6550071	0.6471875	0.6353785	0.6215206	0.6071569	0.5935701
904	0.6528554	0.658844	0.6643165	0.6659297	0.6635957	0.6575261	0.6463556	0.6324176	0.6167103	0.6009625	0.587985
906	0.6705381	0.6678553	0.6699656	0.6702502	0.6665772	0.658219	0.6440969	0.6275817	0.6107891	0.5954988	0.582464
908	0.6853458	0.6796206	0.6774146	0.6744673	0.6680188	0.65611	0.6391404	0.6212099	0.6039099	0.5899209	0.5777115
910	0.6910285	0.6911895	0.6857516	0.6786221	0.6677663	0.6512752	0.6324589	0.6134263	0.597099	0.5836026	0.5735459
912	0.7001314	0.6995247	0.6932743	0.6815968	0.6644388	0.6436224	0.6235399	0.6052678	0.5904817	0.578788	0.570603
914	0.7116513	0.7063797	0.6978595	0.6805083	0.6573137	0.6334089	0.6135063	0.597217	0.5846947	0.575595	0.5684741
916	0.7186652	0.7135372	0.6986161	0.6733841	0.6451277	0.6212462	0.6031047	0.5899388	0.5803428	0.5736562	0.56732
918	0.7295461	0.7189732	0.6924534	0.6587618	0.6291153	0.608506	0.5937513	0.5840869	0.5769787	0.5708697	0.5672172
920	0.7463046	0.716755	0.6749734	0.6375276	0.611811	0.596464	0.586457	0.5798206	0.5748601	0.570318	0.567561
922	0.7555109	0.6971632	0.6457895	0.613648	0.5961928	0.5866678	0.5809331	0.5768561	0.5735251	0.571066	0.5684091
924	0.7340688	0.654599	0.6114185	0.5920093	0.583908	0.5795398	0.577322	0.5749646	0.5729661	0.5717805	0.5696216
926	0.6734152	0.6045557	0.5816136	0.5762475	0.5755346	0.5748883	0.5745782	0.5738972	0.573227	0.5714452	0.5710804
928	0.6054956	0.5690147	0.5630519	0.5668219	0.5702075	0.5720285	0.5731581	0.5734636	0.5734922	0.5728446	0.5726806
930	0.5653021	0.5539224	0.5566103	0.5626439	0.5670357	0.5703053	0.5720392	0.5733601	0.5740297	0.5752725	0.5743219
932	0.5577278	0.555089	0.5587763	0.5619258	0.5655517	0.5693089	0.5716963	0.5737084	0.5750374	0.5757684	0.5757013
934	0.5658504	0.5648838	0.5639566	0.5637962	0.5660025	0.5691832	0.5719174	0.5742863	0.575817	0.576278	0.5771219
936	0.5758522	0.5742317	0.5697213	0.5678486	0.5684716	0.5705525	0.5730549	0.5752442	0.5771285	0.5779049	0.5782854
938	0.5846976	0.5797203	0.575536	0.5731112	0.5722356	0.5728096	0.5747207	0.576512	0.5780041	0.579664	0.5789118
940	0.5910586	0.584769	0.5813283	0.5784066	0.5767857	0.5761787	0.5770217	0.5779519	0.5786604	0.578801	0.5793417
942	0.597926	0.5912871	0.5868853	0.5835175	0.5812029	0.5797504	0.5790438	0.5791684	0.5793637	0.5788094	0.5793444
944	0.6047145	0.597921	0.5929424	0.5886871	0.5854513	0.5831572	0.5812396	0.580102	0.579474	0.5795367	0.5789166
946	0.6012221	0.6034319	0.5990359	0.5938209	0.5891715	0.5856678	0.5826314	0.580757	0.5797766	0.5794615	0.5780776
948	0.6013704	0.6058827	0.6037465	0.5986215	0.5926818	0.5876136	0.5837714	0.5809309	0.5791034	0.5772109	0.5770679
950	0.6098892	0.6076042	0.606624	0.6021818	0.5955805	0.5893303	0.5843145	0.5809832	0.5784248	0.5765988	0.5757456
952	0.6147529	0.6119608	0.6091051	0.6044321	0.5977411	0.5906183	0.5850838	0.5808278	0.577875	0.5764495	0.5739855
954	0.6208729	0.6177123	0.6123641	0.6058676	0.5988737	0.5917098	0.5857933	0.5809042	0.5769136	0.5745741	0.5723071
956	0.6301836	0.6237369	0.6157914	0.6074772	0.5997417	0.5929312	0.5866747	0.5813236	0.5771369	0.5728642	0.5706337
958	0.637092	0.6297427	0.6192277	0.6094611	0.6013494	0.5945215	0.58795	0.5818577	0.5766467	0.5724787	0.5691004
960	0.6448053	0.6346958	0.6228133	0.6123605	0.6040868	0.5966145	0.5895035	0.5828528	0.5768197	0.5726603	0.5676088
962	0.6546624	0.6394581	0.6272656	0.6170329	0.608128	0.599655	0.5914339	0.5838979	0.5772601	0.5709375	0.5667011
964	0.6608993	0.6462198	0.6342064	0.6236127	0.6133133	0.6031467	0.5938124	0.585277	0.5774695	0.5706336	0.5660083
966	0.6691667	0.6555328	0.6435055	0.6314089	0.6192475	0.6073397	0.596765	0.5871086	0.5788251	0.5719872	0.5655845
968	0.6829419	0.6680911	0.6539903	0.6401439	0.6259099	0.6121335	0.5999218	0.5892781	0.5800824	0.5729199	0.5659599
970	0.6985016	0.6813503	0.6654631	0.6491558	0.6329527	0.6177005	0.6043264	0.5923408	0.581986	0.5728778	0.5667197
972	0.7080525	0.6941101	0.6770223	0.6586425	0.6408185	0.6240561	0.6087085	0.5958939	0.5849787	0.5751966	0.5679048
974	0.7134777	0.7052441	0.6887628	0.6687378	0.6490707	0.6309098	0.6145371	0.6002063	0.5881319	0.5790299	0.5700414
976	0.7168511	0.7141823	0.699427	0.6790674	0.6577144	0.6382874	0.6202868	0.6052844	0.592663	0.5815626	0.5726453
978	0.7229764	0.7204285	0.7082319	0.6886247	0.666842	0.6461952	0.6275183	0.6113622	0.5975043	0.5851187	0.5759544
980	0.7337286	0.7260944	0.7147847	0.6972064	0.6758377	0.6543365	0.634796	0.6178825	0.6031129	0.59088	0.5799367
982	0.7516768	0.7345048	0.7209721	0.7045449	0.6842816	0.6627915	0.6433686	0.6252625	0.6097777	0.5969868	0.5845411
984	0.7766198	0.7486666	0.7289919	0.7111078	0.6920915	0.6715384	0.6513975	0.6331017	0.6164071	0.6015753	0.5899592
986	0.8113639	0.769119	0.7405357	0.7192221	0.7000381	0.6801385	0.6605555	0.641214	0.6241595	0.6083867	0.5955911
988	0.8471347	0.7949469	0.7564456	0.7301154	0.7088251	0.6889896	0.6685635	0.6496619	0.631846	0.6164324	0.6016019
990	0.8806226	0.8228153	0.7768613	0.7442814	0.7192922	0.6980445	0.6776551	0.6578259	0.6396083	0.623202	0.6081455
992	0.910918	0.8512321	0.8005744	0.7616377	0.7318271	0.7079167	0.6860693	0.6661868	0.6474264	0.6293613	0.6146022
994	0.9335706	0.8794541	0.8256791	0.7812515	0.7465574	0.7187236	0.6958663	0.6745965	0.6552245	0.6375089	0.6213787
996	0.9466214	0.9034298	0.8503014	0.8019945	0.7627861	0.7311542	0.7053946	0.6832135	0.6632687	0.6455014	0.6281341
998	0.9533449	0.9205549	0.8726664	0.8231922	0.7801504	0.7446336	0.7165616	0.6921715	0.6711331	0.6518932	0.6350481
1000	0.9564151	0.9326022	0.8916429	0.8433313	0.7975906	0.7590901	0.7276182	0.7015294	0.6791866	0.6589743	0.6415964

Table 5.38. Transmission (TnoH2O) for 900-1000 nm, with b of 3.3 comparison run.

tnoh2o:	10	15	20	25	30	35	40	45	50	55	60
900	0.610784	0.647924	0.6681015	0.6805464	0.6887429	0.6936345	0.6965526	0.6970021	0.6958621	0.6933269	0.6903853
902	0.6016411	0.6171589	0.6349548	0.650476	0.661739	0.6697126	0.6740017	0.6758261	0.6756148	0.6730619	0.6718759
904	0.5933805	0.5930385	0.6068863	0.6231556	0.6365194	0.6463918	0.6518374	0.6542867	0.6545708	0.6544924	0.6525385
906	0.5850682	0.5769047	0.5858158	0.6003664	0.6139674	0.6240999	0.6293741	0.6320792	0.6330991	0.6338658	0.632705
908	0.5685488	0.5647569	0.5713317	0.5830991	0.5944626	0.6026501	0.6071972	0.609451	0.6104812	0.6104727	0.6122587
910	0.5379175	0.5516156	0.5615756	0.5704214	0.5772254	0.5815319	0.5845398	0.5863298	0.5879701	0.5888031	0.5916835
912	0.515482	0.5402846	0.5541743	0.5596126	0.5608256	0.5608247	0.5617889	0.5628734	0.5648008	0.5682661	0.5709759
914	0.5120534	0.5366747	0.5470474	0.5472045	0.5432209	0.5393894	0.5384811	0.539334	0.5417813	0.5462105	0.550715
916	0.5252004	0.5394415	0.5386303	0.5310244	0.5231138	0.5172548	0.515068	0.5158909	0.5194125	0.5232239	0.5309149
918	0.549912	0.5411252	0.5263866	0.5113433	0.5000899	0.4935491	0.4912541	0.4930228	0.4972315	0.504085	0.5121334
920	0.5709638	0.5368732	0.5083629	0.487581	0.4747648	0.4692099	0.4680391	0.4709202	0.4770967	0.4861022	0.4943001
922	0.5788888	0.5223175	0.4835133	0.4605742	0.4483756	0.4447261	0.4452705	0.4501317	0.4576041	0.466907	0.4778735
924	0.5564936	0.492387	0.452174	0.4311406	0.4222008	0.4206533	0.4240162	0.4305711	0.4395934	0.4495174	0.4626705
926	0.4916779	0.4447894	0.4155991	0.4012238	0.3969109	0.3981992	0.4038923	0.4124678	0.4232753	0.4359764	0.4490568
928	0.4009638	0.3844823	0.3752591	0.3714839	0.372559	0.3769521	0.3855989	0.39582	0.4078878	0.4227161	0.4367723
930	0.3020614	0.3210448	0.3333851	0.3414555	0.3488761	0.3572797	0.36815	0.3806977	0.3949028	0.409274	0.42613
932	0.2136638	0.2622881	0.2921523	0.3109929	0.3250567	0.3382966	0.3520833	0.3668701	0.3828681	0.3989256	0.4169816
934	0.154404	0.2138795	0.2534273	0.2805636	0.3014849	0.3198622	0.3368036	0.3542722	0.3721337	0.3913228	0.4093208
936	0.1304527	0.1790171	0.2194773	0.2520184	0.2788163	0.3021936	0.3227389	0.3430629	0.3632639	0.3834474	0.403139
938	0.1297181	0.1577534	0.1933169	0.2277117	0.2583109	0.2855477	0.3100419	0.3331234	0.3551889	0.3763746	0.3984334
940	0.1358916	0.1489825	0.176998	0.2095835	0.2417672	0.2715148	0.2993321	0.3250317	0.3494924	0.3727456	0.3952136
942	0.143763	0.1495792	0.1702619	0.198979	0.2302601	0.2610642	0.2912514	0.3190733	0.3452594	0.370746	0.3935069
944	0.1471094	0.1548245	0.1706713	0.1952222	0.2246242	0.2554764	0.2864871	0.3157196	0.3431703	0.36897	0.3933604
946	0.1481524	0.1603452	0.1755539	0.1975624	0.2249093	0.2550099	0.2856377	0.3153891	0.3436202	0.3693574	0.3946887
948	0.1525418	0.1661272	0.1832592	0.2045142	0.2303499	0.2594562	0.2888989	0.3183564	0.3464382	0.3734458	0.397867
950	0.161094	0.1753109	0.1939047	0.2154692	0.2406593	0.2683893	0.2964366	0.3246978	0.3521712	0.3785278	0.4028184
952	0.1752662	0.1894135	0.2081421	0.2303593	0.2550088	0.2810064	0.307752	0.3342845	0.360469	0.3851319	0.4096001
954	0.1931929	0.2073972	0.2268232	0.2495531	0.2734076	0.2974228	0.3222857	0.3469808	0.3713881	0.394893	0.4182412
956	0.2121427	0.2293275	0.250411	0.2730793	0.2953751	0.3170515	0.3398621	0.3623081	0.3848155	0.4078174	0.4287336
958	0.2379398	0.257363	0.2794408	0.300622	0.3204654	0.3398578	0.3597262	0.3799529	0.4004268	0.4209435	0.441026
960	0.2722596	0.2929506	0.3136778	0.3314754	0.3479315	0.3647616	0.3816707	0.3996769	0.4180662	0.436029	0.4550259
962	0.313121	0.3362646	0.3518612	0.3643034	0.3769809	0.3911695	0.4056373	0.4213094	0.4377295	0.4544377	0.4706037
964	0.3693446	0.3844624	0.3913945	0.3981732	0.407348	0.4190482	0.4312067	0.4448662	0.459009	0.4740418	0.4877604
966	0.4371076	0.4323533	0.4299576	0.4326077	0.4391664	0.4479929	0.4587136	0.4698827	0.4816623	0.4936326	0.5060004
968	0.4982226	0.4763017	0.4679921	0.4681681	0.4725571	0.4789089	0.4875807	0.4964711	0.5060139	0.5149508	0.5254494
970	0.5450408	0.5163696	0.5065421	0.505267	0.5078014	0.5115999	0.5178849	0.5242125	0.5308299	0.5387146	0.5457526
972	0.5750281	0.554904	0.5463602	0.5440356	0.5444913	0.5460868	0.5491305	0.5526318	0.5567493	0.5618513	0.5667124
974	0.591536	0.5905295	0.5866189	0.5835857	0.5819409	0.5813556	0.5809671	0.5816731	0.5831093	0.5846515	0.5882856
976	0.6064494	0.622584	0.6252909	0.6229971	0.6192746	0.6162702	0.6128085	0.6106452	0.6094888	0.6090766	0.6099811
978	0.6331089	0.6544575	0.6618621	0.6604769	0.6554183	0.650057	0.6441295	0.6394484	0.6358893	0.6340964	0.6319146
980	0.6776289	0.6909069	0.6971011	0.6956022	0.6896002	0.681982	0.6743314	0.6674368	0.6615767	0.6570565	0.6536294
982	0.7306832	0.7324271	0.7324746	0.7288243	0.7215839	0.7121222	0.7031428	0.6944475	0.6868388	0.6795999	0.6751141
984	0.7851177	0.7758131	0.7683039	0.7607141	0.7514859	0.7405971	0.7303878	0.7202575	0.7110925	0.7033265	0.6963473
986	0.8352106	0.8176479	0.8036908	0.7915556	0.7797553	0.7676024	0.7560058	0.7447503	0.7342356	0.7256317	0.7169475
988	0.8762506	0.8556389	0.837168	0.8209705	0.8065238	0.7931618	0.7800734	0.7679009	0.7566743	0.7459142	0.7370438
990	0.9083673	0.8878944	0.8671079	0.8482284	0.8317119	0.8169392	0.8027137	0.7897434	0.777536	0.7658874	0.7563233
992	0.9322249	0.9132671	0.8924231	0.8726884	0.8548549	0.8389928	0.823946	0.8102421	0.7975199	0.7861385	0.7748355
994	0.9483938	0.931628	0.9126581	0.8938056	0.8757228	0.8590773	0.8437649	0.8295668	0.8163263	0.8042727	0.7925304
996	0.9587634	0.9443105	0.9283075	0.911244	0.8939942	0.8773235	0.862051	0.847594	0.8339631	0.8207056	0.8093685
998	0.9641869	0.9532151	0.9401625	0.9252349	0.9095934	0.893697	0.878731	0.8642512	0.850554	0.837413	0.8253145
1000	0.9663398	0.959354	0.9489539	0.9363933	0.9226336	0.908109	0.8936253	0.8794579	0.8657111	0.853253	0.8403336

Table 5.39. α for 900-1000 nm, with b of 3.3 comparison run.

alpha:	10	15	20	25	30	35	40	45	50	55	60
900	0.1203054	0.1040908	0.096466	0.0923892	0.0903557	0.090025	0.0906586	0.0925364	0.0951419	0.0982914	0.1015897
902	0.1229534	0.114844	0.1075656	0.1022934	0.0993453	0.0982103	0.0988572	0.1007353	0.1034777	0.1070147	0.1098288
904	0.1237021	0.123002	0.1171181	0.1115786	0.1081343	0.1066556	0.1075305	0.1096414	0.1125715	0.1155679	0.1187145
906	0.1230131	0.1270754	0.1239837	0.1195432	0.1164055	0.1153565	0.1168841	0.1193701	0.1223868	0.125093	0.1282517
908	0.126051	0.12915	0.1280691	0.1256009	0.1240891	0.1245604	0.1269532	0.1300516	0.1334	0.1363797	0.1383673
910	0.1362971	0.1318941	0.1303612	0.1301811	0.1315496	0.1345575	0.1380734	0.1417507	0.1448732	0.1477855	0.1489723
912	0.1429027	0.1344772	0.1322498	0.1346447	0.1396393	0.1454611	0.1502336	0.1544476	0.1574165	0.1589323	0.159895
914	0.1413211	0.1343821	0.1348109	0.1409317	0.1494505	0.1577949	0.1637634	0.1680256	0.1705289	0.1710491	0.1709698
916	0.1341072	0.132374	0.139166	0.1503689	0.16197	0.1716836	0.1783509	0.1822518	0.1836344	0.1838785	0.1819753
918	0.1225387	0.1318535	0.1469976	0.1635892	0.1776948	0.1876165	0.1940923	0.1968301	0.197258	0.1957907	0.1927392
920	0.1128988	0.1358514	0.1603712	0.1813659	0.1964502	0.2051969	0.2101592	0.211408	0.2100106	0.2066853	0.2030641
922	0.1106305	0.1483058	0.1809768	0.2037351	0.2174077	0.2238827	0.2265713	0.2256891	0.2227056	0.2181966	0.2128315
924	0.1254729	0.1742085	0.2092953	0.2295809	0.2393602	0.2429514	0.24225	0.2393986	0.2347898	0.2290067	0.2219045
926	0.169147	0.2164069	0.2439676	0.2569473	0.261206	0.2612132	0.2576702	0.2523916	0.2456309	0.2383159	0.2302284
928	0.2447653	0.2721322	0.2822356	0.2841947	0.2824551	0.2787017	0.2719262	0.2645963	0.2563795	0.2467801	0.2377184
930	0.345396	0.3339449	0.3214127	0.3115449	0.3033671	0.2950439	0.2859187	0.2760099	0.2655289	0.2551216	0.2443666
932	0.4542676	0.3946439	0.3601975	0.3394816	0.3244677	0.3112616	0.298883	0.2866212	0.2742454	0.2624581	0.2501381
934	0.5434756	0.4487695	0.3987537	0.3683254	0.346027	0.3274195	0.3116463	0.2964147	0.2821333	0.2680124	0.2550235
936	0.5801219	0.4922605	0.4361942	0.3970595	0.3674575	0.3432444	0.3233379	0.3053301	0.2885283	0.2731618	0.2590191
938	0.5688494	0.5211298	0.4678818	0.4228753	0.3873135	0.3584318	0.334226	0.3131557	0.2945845	0.2775774	0.2621194
940	0.5462115	0.5304551	0.4874894	0.4426797	0.403626	0.3711083	0.3432089	0.3196273	0.2988989	0.2810264	0.2643103
942	0.5233507	0.5216264	0.4923039	0.4532004	0.4143141	0.3803139	0.3499638	0.3243245	0.3020945	0.2824833	0.2655644
944	0.511136	0.5049765	0.4852275	0.4535751	0.4180414	0.3840818	0.3533966	0.3267974	0.3038189	0.2833757	0.2658377
946	0.5110778	0.4905792	0.4718714	0.4457138	0.4146502	0.3826284	0.3532144	0.3266473	0.3031445	0.2830943	0.2650557
948	0.501523	0.478169	0.4560817	0.4321423	0.405046	0.3761134	0.3489497	0.3236316	0.3010089	0.2810522	0.2631844
950	0.4795458	0.4608524	0.4380766	0.4150846	0.3907526	0.3652269	0.3410192	0.3177398	0.2964119	0.2772076	0.2601463
952	0.4526412	0.4365608	0.41648	0.3949797	0.3729917	0.3513399	0.3298079	0.3092059	0.2898415	0.2719258	0.2559007
954	0.4216017	0.4083348	0.3909507	0.3716809	0.3526773	0.3345506	0.3161184	0.2984608	0.2815586	0.2656376	0.2504412
956	0.390839	0.3776804	0.3621295	0.3458767	0.3304516	0.316011	0.3007353	0.2859632	0.2712642	0.2570547	0.243805
958	0.356708	0.3442072	0.3309576	0.3185576	0.307069	0.2958119	0.284079	0.2721569	0.2599731	0.2477883	0.2360746
960	0.317983	0.3079004	0.2984664	0.2907604	0.2833251	0.2751812	0.2668332	0.2573995	0.2475592	0.2373943	0.2273705
962	0.2786568	0.2701732	0.2662065	0.2635294	0.2598451	0.2545891	0.2489364	0.2419688	0.2342281	0.2262743	0.2178406
964	0.2353999	0.233764	0.235959	0.2374928	0.2369689	0.2343696	0.2310226	0.2261076	0.2205384	0.2140965	0.2076604
966	0.1921335	0.2012288	0.2086545	0.2129711	0.2147821	0.2146753	0.2127858	0.2099935	0.2062269	0.2018809	0.1969665
968	0.1573306	0.1738175	0.184028	0.1898974	0.193269	0.1950829	0.1949455	0.1938607	0.1919017	0.1894073	0.1859466
970	0.1329741	0.1508272	0.1613267	0.1679747	0.1724933	0.1758769	0.1771496	0.1778993	0.1777076	0.1765364	0.1747375
972	0.1184848	0.1310978	0.1402676	0.1472506	0.1526201	0.1569721	0.1601728	0.1622978	0.1634973	0.1638615	0.1634788
974	0.1108293	0.1146409	0.1211808	0.1278857	0.133945	0.139093	0.1437084	0.1472648	0.149871	0.1514792	0.1523079
976	0.104477	0.1012417	0.1045323	0.1104009	0.1168099	0.1226348	0.1284233	0.1329419	0.1366145	0.1395753	0.1413155
978	0.0941552	0.0891434	0.09031	0.0951341	0.1014666	0.1077919	0.1140562	0.119482	0.1239953	0.1275857	0.1306213
980	0.078361	0.0766304	0.0778013	0.0819541	0.087981	0.094638	0.1010693	0.1069651	0.1122557	0.1165541	0.1202901
982	0.0610392	0.0633772	0.0661949	0.0704694	0.0761971	0.0828557	0.0891853	0.0954559	0.1011178	0.1062418	0.1104017
984	0.0448973	0.0503668	0.0551447	0.0601076	0.0658153	0.0723333	0.0786528	0.0849653	0.0909284	0.096325	0.1010182
986	0.0314942	0.0386191	0.0448202	0.050605	0.0565418	0.0628182	0.0691153	0.0754592	0.0815082	0.0869507	0.0921637
988	0.0217118	0.0287686	0.0355856	0.0419806	0.0481812	0.0543042	0.0606793	0.06687	0.0728698	0.0786287	0.0838763
990	0.0149038	0.0210754	0.0277658	0.0343312	0.0406781	0.0467577	0.0530037	0.0591135	0.0651011	0.070932	0.0761525
992	0.0103374	0.0154571	0.0215139	0.0277909	0.0340445	0.0400756	0.0461905	0.052105	0.0579209	0.0635515	0.0689952
994	0.0074868	0.0116018	0.0167453	0.0223958	0.0283147	0.0342177	0.0400092	0.0457876	0.0514818	0.056935	0.0623908
996	0.0057607	0.0090507	0.0132181	0.0181105	0.0234877	0.0290753	0.0345808	0.0401127	0.0456218	0.0511165	0.0563197
998	0.004858	0.0073305	0.0106443	0.0147856	0.0195123	0.0246298	0.0297612	0.0350506	0.040323	0.0456469	0.05076
1000	0.0044595	0.0061699	0.008787	0.0122209	0.0162961	0.0208324	0.0256262	0.0305774	0.0356367	0.0405656	0.0456895

Table 5.40. β for 900-1000 nm, with b of 3.3 comparison run.

beta:	10	15	20	25	30	35	40	45	50	55	60
900	0.6419461	0.6497921	0.6510612	0.6493954	0.645142	0.63809	0.6296447	0.6195015	0.6089233	0.5986596	0.5888911
902	0.6457516	0.653403	0.6555725	0.6535784	0.6483475	0.6401792	0.6298857	0.6181913	0.6063299	0.5954061	0.5856156
904	0.655207	0.6582926	0.6600383	0.6573199	0.6506999	0.6411901	0.6286364	0.6157827	0.6033136	0.5914863	0.5824592
906	0.6698875	0.6668776	0.6652251	0.660449	0.6521196	0.6407059	0.6265212	0.6127075	0.5997465	0.5885859	0.5790627
908	0.6824753	0.6767833	0.6712939	0.663266	0.6521938	0.6383383	0.6228724	0.6085057	0.5953814	0.5853402	0.5760531
910	0.6894894	0.6855924	0.6770126	0.6651443	0.6506689	0.6341816	0.6180903	0.6035286	0.5912241	0.580951	0.5730981
912	0.6981933	0.692373	0.6808124	0.665052	0.6467743	0.6281858	0.6121395	0.5980246	0.5866438	0.577383	0.5707875
914	0.707819	0.697624	0.6819551	0.6615301	0.6403013	0.6208229	0.6051668	0.5923079	0.5822279	0.574755	0.5687429
916	0.7140922	0.7007003	0.6790361	0.6541414	0.6309833	0.6123195	0.5978953	0.5869517	0.5788099	0.5730971	0.5674623
918	0.7214369	0.7001896	0.6707256	0.6421667	0.6193793	0.6032171	0.5907673	0.5820854	0.5755936	0.5699862	0.5664875
920	0.7291979	0.6924043	0.6551582	0.6264126	0.6066239	0.5939327	0.5845577	0.5781675	0.5732418	0.5688578	0.5662263
922	0.7271007	0.672164	0.6326674	0.6082243	0.5941536	0.5854105	0.5792898	0.5749161	0.5714871	0.568926	0.5661676
924	0.7015213	0.6384798	0.6066492	0.5910719	0.583283	0.5784395	0.575551	0.5727285	0.570235	0.5690526	0.5666713
926	0.6528237	0.6007872	0.582849	0.5771477	0.5750208	0.5734093	0.5725535	0.5713027	0.5701699	0.5680029	0.5672142
928	0.5995764	0.5717763	0.566602	0.5681247	0.569589	0.5702415	0.570738	0.5705051	0.5698703	0.5687448	0.5681444
930	0.5657076	0.5572695	0.5593128	0.5634848	0.5663924	0.5686484	0.5694968	0.5700227	0.5700416	0.5703837	0.5689462
932	0.5566227	0.5557831	0.5591177	0.5623529	0.5653703	0.5678185	0.5691975	0.5699633	0.5702546	0.5703438	0.5697564
934	0.5619529	0.5618671	0.5626076	0.5636915	0.5656026	0.5677266	0.5691099	0.5702615	0.570634	0.5702439	0.5705004
936	0.5715709	0.5694597	0.5671141	0.56639	0.5669969	0.5683852	0.5698468	0.5706619	0.5714067	0.5713391	0.5711133
938	0.5817617	0.575803	0.5717766	0.5700375	0.569483	0.5697341	0.5706457	0.5714827	0.5719455	0.5727959	0.5715425
940	0.5897635	0.5816147	0.5768833	0.5740337	0.5724351	0.5718566	0.5720363	0.5722421	0.5723822	0.5716661	0.5717496
942	0.5961975	0.5882969	0.5824959	0.5782208	0.57591	0.5742044	0.5733764	0.5730341	0.5727874	0.5717866	0.5717121
944	0.6015139	0.5947288	0.5884676	0.5831861	0.5794497	0.5769913	0.5749787	0.5737675	0.5727869	0.5725483	0.5714256
946	0.599885	0.599264	0.5938511	0.5878114	0.5827699	0.579326	0.5762931	0.5743899	0.5732403	0.5725212	0.571119
948	0.6014615	0.6020308	0.5979631	0.5920742	0.5860856	0.581348	0.5776795	0.5749028	0.5729648	0.5707579	0.5704001
950	0.6084567	0.6049672	0.6008919	0.5951883	0.5886573	0.5831511	0.5786023	0.5753537	0.5728671	0.5707379	0.5695354
952	0.613216	0.6089253	0.6038052	0.5975266	0.5909367	0.5846139	0.579574	0.5758167	0.5727981	0.5713171	0.56859
954	0.6193571	0.6138328	0.6069634	0.5996855	0.592609	0.5860732	0.5806891	0.5761614	0.5724845	0.5698675	0.5676332
956	0.6271705	0.6192991	0.6104073	0.6018921	0.5942695	0.587378	0.5815332	0.5766535	0.5728176	0.5687608	0.5667318
958	0.6337616	0.6244174	0.6138123	0.6043337	0.5961787	0.5890511	0.5828569	0.5773427	0.5728095	0.569105	0.5659461
960	0.6412135	0.6295047	0.6175932	0.6073017	0.5986695	0.5911097	0.5842072	0.5782686	0.5731194	0.5697002	0.5653299
962	0.6495461	0.6347728	0.6221663	0.6113673	0.6020899	0.593819	0.586078	0.5794641	0.5736719	0.5682764	0.564932
964	0.656504	0.6409682	0.628126	0.6167688	0.6063734	0.5968114	0.58814	0.5807329	0.5741495	0.5684056	0.5645619
966	0.6646159	0.6495406	0.6360543	0.6234096	0.6113087	0.600394	0.5908124	0.5825539	0.575621	0.5697579	0.5647344
968	0.6772259	0.6603531	0.6450475	0.6305331	0.6168929	0.6044617	0.5935518	0.584496	0.5765727	0.5706773	0.5650149
970	0.690963	0.6724469	0.6548619	0.6381667	0.6227377	0.6088637	0.5972142	0.5868141	0.578378	0.5706664	0.5656762
972	0.7014219	0.6837785	0.6648439	0.6459314	0.6290044	0.6140123	0.6006249	0.5897751	0.5806913	0.5725337	0.5667458
974	0.7079247	0.6940093	0.6744647	0.6543571	0.6356673	0.6193483	0.6050522	0.5929074	0.5828474	0.5757555	0.5679877
976	0.7126759	0.7024482	0.6837052	0.6623939	0.6424394	0.6248876	0.6091625	0.5966992	0.5860424	0.5769055	0.5699021
978	0.7190825	0.709698	0.6915397	0.6701602	0.6491901	0.6304308	0.6143	0.6006336	0.5894045	0.5792428	0.5719717
980	0.7293987	0.7162826	0.6982602	0.6773004	0.6557425	0.6359514	0.6192493	0.6051638	0.5930124	0.5834015	0.5746741
982	0.745104	0.7245262	0.704634	0.6834003	0.6619779	0.6418964	0.625093	0.6099708	0.597293	0.5874547	0.5777116
984	0.766529	0.7361043	0.71197	0.6895775	0.6681611	0.6478594	0.630305	0.6149655	0.6015187	0.5897057	0.5807717
986	0.7935238	0.751478	0.7210521	0.6964348	0.6742912	0.6542497	0.6362407	0.6200491	0.6063995	0.5940241	0.5842976
988	0.8218219	0.7691405	0.7319813	0.7042322	0.6807547	0.6603616	0.6414027	0.6251327	0.6107252	0.5989053	0.5877063
990	0.8482702	0.7874465	0.7446584	0.7133981	0.6875526	0.6664007	0.6472536	0.6301461	0.6153217	0.6027961	0.5914277
992	0.8716961	0.8054642	0.7581722	0.7232964	0.6951738	0.6722909	0.6523137	0.6352811	0.6201258	0.6059362	0.5951309
994	0.8906124	0.8233138	0.7723662	0.7336559	0.7030472	0.6783356	0.6580989	0.6400356	0.6242819	0.6106542	0.5987451
996	0.9053464	0.8399063	0.7863394	0.7443535	0.7111344	0.6846765	0.6630581	0.6446282	0.6286268	0.6153631	0.6022074
998	0.9174601	0.8544313	0.7997819	0.7551799	0.7192152	0.6908734	0.6684558	0.6490336	0.6325505	0.617909	0.6054631
1000	0.927693	0.8674095	0.8126342	0.7656258	0.7271076	0.6971985	0.6731493	0.6532221	0.6361905	0.6208242	0.6084657

Table 5.41. Transmission (TnoH2O) for 1300-1400 nm with b of 2.0 comparison run.

tnoh2o:	10	15	20	25	30	35	40	45	50	55	60
1300	0.870119103	0.8705078	0.8690867	0.8658882	0.8620751	0.8578241	0.8521806	0.8457629	0.838237	0.8306708	0.821281
1302	0.848571402	0.8506326	0.8499262	0.8472209	0.8443105	0.8406749	0.8351115	0.8286672	0.8212846	0.8125649	0.8037158
1304	0.827783771	0.8300074	0.8293535	0.8281817	0.8259557	0.8220988	0.8167412	0.8100736	0.8021648	0.793452	0.7850544
1306	0.805439815	0.8080677	0.8082987	0.8087506	0.8065109	0.8023481	0.7969525	0.7900335	0.7823034	0.7741468	0.7654408
1308	0.787035259	0.7848751	0.7885417	0.7882325	0.7856389	0.781155	0.7756504	0.7683927	0.7607898	0.7533804	0.7448419
1310	0.765153628	0.7671291	0.7681223	0.7665556	0.7639188	0.7588722	0.7525068	0.7454458	0.7382516	0.7309025	0.7235126
1312	0.74972755	0.7508875	0.7466087	0.7443902	0.7408705	0.7347621	0.7278226	0.7212666	0.7154205	0.7082218	0.701001
1314	0.734332523	0.7293957	0.7257939	0.7220419	0.7156996	0.7084754	0.7020099	0.6967683	0.6913253	0.6855014	0.6774955
1316	0.709578814	0.7068167	0.7047592	0.6972287	0.6881202	0.6810059	0.6760896	0.6719246	0.6671553	0.6607341	0.6525485
1318	0.684649988	0.6860566	0.6804862	0.668867	0.6590019	0.6534437	0.6501141	0.6465147	0.6414628	0.6342733	0.6264618
1320	0.672252273	0.663701	0.6498705	0.6372418	0.6303257	0.6269424	0.6243703	0.6203862	0.6145092	0.6071383	0.5989192
1322	0.648768587	0.6340782	0.61417	0.6057315	0.6027701	0.6009461	0.5979622	0.592828	0.5863248	0.5793318	0.5704554
1324	0.610682479	0.5909709	0.5789723	0.5766375	0.5763614	0.5743741	0.5700815	0.5638015	0.5564797	0.5486557	0.541429
1326	0.563123568	0.5435866	0.5471721	0.5493723	0.54923	0.5462036	0.540338	0.5330336	0.5255687	0.5181973	0.5122071
1328	0.504528106	0.5088999	0.518007	0.521757	0.5202689	0.5152695	0.5081928	0.5006943	0.4936649	0.4875825	0.4827536
1330	0.456654341	0.4817989	0.4897756	0.4916139	0.4884494	0.4815691	0.4744077	0.4677287	0.4617191	0.4579064	0.4536558
1332	0.423300546	0.4520853	0.4600698	0.4584308	0.4527643	0.4458408	0.4393626	0.4341356	0.4300914	0.4264517	0.4246829
1334	0.400008936	0.4194563	0.4249936	0.420782	0.414116	0.4081688	0.4041401	0.4004174	0.3982788	0.396767	0.3962942
1336	0.394368092	0.3869866	0.3836427	0.3789609	0.3739503	0.3704983	0.3679686	0.3672647	0.3670787	0.3679027	0.3685294
1338	0.390875975	0.3542705	0.3400877	0.335152	0.3332898	0.3326985	0.3336068	0.3348506	0.3367477	0.3392375	0.3409713
1340	0.355763281	0.3210279	0.2986993	0.2922253	0.2929288	0.2961454	0.2990722	0.3032626	0.3070357	0.3104792	0.3144428
1342	0.297366632	0.2764704	0.2591644	0.2528009	0.2548234	0.2605861	0.2664614	0.2721824	0.2777878	0.2829869	0.2885045
1344	0.227711431	0.2223379	0.2189827	0.2172731	0.2200733	0.2269419	0.2346746	0.2424667	0.2499016	0.2567581	0.2631379
1346	0.155877623	0.1676778	0.1769829	0.1830921	0.1888596	0.1961332	0.2053314	0.2138869	0.2227678	0.2309134	0.2383483
1348	0.091127425	0.1166274	0.1353278	0.1489549	0.1590849	0.1676625	0.1772319	0.1870591	0.1966654	0.2060367	0.214973
1350	0.04856241	0.0723977	0.0967675	0.1160033	0.1301849	0.1415851	0.1519427	0.161856	0.1726274	0.1822935	0.1926439
1352	0.020238605	0.0402256	0.0633778	0.0850688	0.1023869	0.1162917	0.1277184	0.1386621	0.1498355	0.1610522	0.1714481
1354	0.007102996	0.0194789	0.0376744	0.0577632	0.0764896	0.0923105	0.1054791	0.1172554	0.1287604	0.1400606	0.1511554
1356	0.001810609	0.0080477	0.020036	0.03615	0.0535594	0.0702173	0.0843545	0.0976194	0.1095941	0.1212484	0.1325892
1358	0.000380663	0.0027832	0.009395	0.0207298	0.035138	0.0506528	0.0657094	0.079095	0.0917322	0.103419	0.1151424
1360	8.98341E-05	0.0008528	0.0039553	0.0108935	0.0216057	0.0348648	0.0487948	0.0625642	0.0753023	0.0873103	0.098872
1362	3.82995E-05	0.0002808	0.0016139	0.0054795	0.0126105	0.0227727	0.0351049	0.0476912	0.0602648	0.0724157	0.0837917
1364	2.65047E-05	0.0001371	0.0007757	0.0028176	0.007194	0.0143168	0.023873	0.0350968	0.0468043	0.0586864	0.0701466
1366	3.20327E-05	0.000151	0.0005935	0.0016985	0.0041732	0.0087504	0.0159063	0.0249915	0.0354407	0.0466064	0.0577147
1368	7.90647E-05	0.0003139	0.0006723	0.0012343	0.0025458	0.005353	0.0102983	0.0174055	0.0262412	0.036084	0.0466015
1370	0.00027755	0.0006383	0.0007921	0.0010116	0.0017138	0.003455	0.0067313	0.0119242	0.0189551	0.027542	0.0369242
1372	0.000799894	0.0009522	0.0008404	0.0008897	0.0013025	0.0024018	0.0045046	0.008187	0.0136382	0.0206337	0.0290121
1374	0.001295557	0.0010624	0.0008472	0.0008456	0.0011368	0.0018576	0.0032825	0.0058321	0.0098513	0.0154723	0.0225317
1376	0.001334446	0.0010984	0.0008775	0.0008914	0.0011031	0.0015878	0.0025487	0.0043683	0.0073264	0.0116753	0.0175823
1378	0.001228135	0.0011301	0.0009672	0.001007	0.001147	0.0014829	0.0022227	0.003534	0.0057918	0.0091757	0.0139302
1380	0.001065343	0.0012019	0.0011416	0.0011495	0.0012343	0.0014909	0.0020618	0.0031089	0.0047986	0.007498	0.0113351
1382	0.000725763	0.001141	0.0012385	0.0012819	0.0013669	0.0016072	0.0021144	0.0029287	0.0043482	0.0064313	0.0096808
1384	0.000441057	0.0010766	0.0012733	0.0014234	0.0015583	0.0018033	0.0022281	0.0029681	0.0041471	0.0060291	0.0087515
1386	0.000499865	0.0008872	0.0012316	0.0015613	0.0017995	0.002066	0.0024869	0.0031474	0.0042551	0.0060127	0.0083542
1388	0.000787745	0.0008343	0.0012471	0.0017376	0.0020715	0.0023787	0.0027776	0.0035107	0.0046283	0.0061765	0.0084455
1390	0.000928123	0.0009992	0.0014397	0.0019727	0.0023468	0.0027081	0.0032317	0.004023	0.0051536	0.0066791	0.0089332
1392	0.001196787	0.0013308	0.001807	0.0022657	0.0026268	0.0031172	0.0037691	0.0047352	0.0060415	0.0077462	0.0097075
1394	0.001567279	0.0017943	0.0023481	0.0026195	0.0029913	0.0036493	0.0045664	0.0056813	0.0070245	0.0088693	0.0108642
1396	0.00147355	0.0024285	0.0028337	0.0030613	0.003555	0.0044117	0.0055232	0.0068334	0.0083661	0.0100128	0.0122607
1398	0.002209839	0.0028019	0.0032858	0.0036749	0.004425	0.0054935	0.0068229	0.0082563	0.0099629	0.011688	0.0140141
1400	0.002857203	0.0031566	0.0038609	0.0046101	0.0056439	0.0068701	0.0082892	0.0099241	0.0117309	0.0140549	0.0160156

Table 5.42. α for 1300-1400 nm with b of 2.0 comparison run.

alpha:	10	15	20	25	30	35	40	45	50	55	60
1300	0.0496262	0.0498199	0.0509317	0.0527284	0.0548838	0.057423	0.060918	0.0652305	0.0705978	0.0765633	0.0840194
1302	0.059128	0.0587489	0.0594581	0.0610283	0.0628323	0.0652375	0.0689794	0.0736611	0.0794098	0.0865023	0.0942764
1304	0.0688999	0.0682604	0.0688226	0.0696932	0.0712782	0.0739611	0.077931	0.0831427	0.0897031	0.0974384	0.1056814
1306	0.0796913	0.0785814	0.078623	0.0787833	0.0804939	0.0835847	0.0879194	0.0937945	0.1009182	0.1090687	0.1182979
1308	0.0887804	0.0897309	0.0880918	0.0886495	0.0906786	0.0942519	0.0991438	0.1058192	0.1136717	0.1222821	0.1322847
1310	0.0997885	0.0985053	0.0981865	0.0994002	0.1016873	0.1059907	0.1118672	0.1192521	0.12776	0.1373565	0.1477054
1312	0.107565	0.1068581	0.1091614	0.1107824	0.1138539	0.1192346	0.1262093	0.134194	0.1430266	0.1536403	0.1649714
1314	0.1153159	0.118111	0.1200997	0.1227639	0.1277663	0.13442	0.1420363	0.1504246	0.1602055	0.1711463	0.184237
1316	0.1283968	0.1300275	0.1314926	0.1366582	0.1438213	0.151248	0.159147	0.1681546	0.1789327	0.1916369	0.2059864
1318	0.141778	0.1412728	0.1451609	0.1533551	0.1617655	0.1693262	0.1775736	0.1878046	0.2003381	0.2149795	0.2303237
1320	0.1487661	0.1539543	0.1632881	0.1729762	0.1806778	0.1882336	0.1976528	0.2098715	0.2246437	0.2409049	0.2576658
1322	0.1622456	0.1719077	0.1858014	0.1938407	0.2002499	0.2085223	0.2201926	0.2352246	0.2521545	0.2694255	0.2879016
1324	0.1856673	0.199808	0.209675	0.2146193	0.2208144	0.2314392	0.246417	0.2644429	0.2837628	0.3031091	0.3209205
1326	0.2174807	0.2329058	0.232895	0.2358343	0.2440601	0.2582981	0.2771542	0.2982183	0.3192144	0.3393102	0.3565082
1328	0.261339	0.2595381	0.255904	0.2594883	0.2717659	0.2908788	0.3136746	0.3369337	0.3589036	0.3782919	0.394679
1330	0.3007132	0.28241	0.2801648	0.2882167	0.3060538	0.3303488	0.3559842	0.3802879	0.4021589	0.4194581	0.4349187
1332	0.3323043	0.3088349	0.3087972	0.3243291	0.3492202	0.3770962	0.4045417	0.4284708	0.448413	0.4654286	0.4773523
1334	0.355515	0.3408204	0.3472755	0.3713755	0.402175	0.4323348	0.4586905	0.4811817	0.4985728	0.512168	0.5215027
1336	0.3637635	0.3778678	0.4003625	0.4317994	0.4650894	0.4948093	0.519411	0.5377909	0.5514931	0.5601657	0.5672639
1338	0.3710721	0.4243002	0.4681317	0.5057435	0.5381944	0.565123	0.5841163	0.5980902	0.6071885	0.6121561	0.6151361
1340	0.4176493	0.484769	0.547577	0.5916548	0.6214295	0.6413974	0.6547807	0.6620026	0.6656845	0.6666934	0.6642652
1342	0.509517	0.57519	0.6397614	0.6866989	0.7122762	0.7240928	0.7294836	0.7300925	0.7271631	0.72207	0.7153686
1344	0.6542065	0.7027488	0.7515271	0.7887142	0.8083938	0.8125387	0.8092702	0.801356	0.7909406	0.7791709	0.7688496
1346	0.8544424	0.8715574	0.8888992	0.9019483	0.9090286	0.904701	0.8922329	0.8764351	0.8582383	0.8417271	0.8252465
1348	1.143092	1.0892398	1.053874	1.033649	1.0189215	1.0023371	0.9798874	0.9546466	0.9295066	0.9061465	0.8836643
1350	1.5054859	1.3608129	1.2537572	1.1879345	1.1419262	1.1047186	1.0701098	1.036785	1.0030127	0.9731459	0.9452202
1352	1.975785	1.6886055	1.4996508	1.3703018	1.282267	1.2187908	1.1675936	1.1227307	1.0810103	1.0427172	1.0102541
1354	2.5232096	2.0902941	1.7924701	1.5862283	1.4450439	1.3465806	1.2726731	1.2143188	1.1639103	1.1204023	1.0798408
1356	3.2329581	2.5684865	2.1327734	1.8381156	1.6357431	1.491817	1.3916131	1.3135217	1.252085	1.199533	1.1521207
1358	4.0415311	3.1156332	2.5240793	2.1275368	1.8535829	1.6602669	1.5235966	1.4259708	1.3488541	1.2848339	1.2290207
1360	4.7405539	3.6971381	2.9560709	2.4494433	2.0972421	1.8494092	1.6781199	1.5509081	1.455056	1.3769813	1.3109862
1362	5.1536469	4.2227635	3.3860493	2.780134	2.3611732	2.0642908	1.8491503	1.6933781	1.5726438	1.4769245	1.3988364
1364	5.2796516	4.5500016	3.7172551	3.0892494	2.6336761	2.297909	2.0455325	1.8517852	1.7035545	1.5864131	1.4923221
1366	5.2361631	4.4877067	3.8253329	3.3225434	2.898133	2.5444577	2.2506933	2.0240221	1.8459507	1.7045325	1.5935743
1368	4.74575	4.1175313	3.7554333	3.4735887	3.137696	2.78613	2.4650538	2.2045577	1.9980394	1.83548	1.7030921
1370	4.0914783	3.7415428	3.6688588	3.5714686	3.3274865	2.9958441	2.6706812	2.3898144	2.1593099	1.9711843	1.8205653
1372	3.5477574	3.519805	3.6329453	3.6293685	3.4531386	3.1631589	2.8601091	2.5708897	2.3206067	2.1133714	1.9412158
1374	3.2648196	3.4640443	3.6217239	3.6389718	3.5068018	3.2744813	3.0074863	2.732439	2.4767785	2.253948	2.0654683
1376	3.2410948	3.4601135	3.5918729	3.5954411	3.5050235	3.3384697	3.121814	2.8672636	2.6180296	2.3903224	2.18575
1378	3.3187726	3.4445546	3.5257034	3.5189638	3.4700301	3.3610642	3.1798503	2.9634199	2.727699	2.5029345	2.2967131
1380	3.4507339	3.4154329	3.4291971	3.438693	3.4218397	3.3489873	3.2069468	3.017796	2.8122005	2.5956972	2.3925691
1382	3.72964	3.4283061	3.3813348	3.3753567	3.3640375	3.3053701	3.1843359	3.0368416	2.8520408	2.6635156	2.463798
1384	3.8993204	3.415736	3.3457546	3.3266401	3.2962391	3.2410512	3.1498511	3.0205309	2.864336	2.6879864	2.5064881
1386	3.7647786	3.5114884	3.3682675	3.293344	3.2264004	3.1677139	3.085768	2.9813354	2.8432333	2.6792934	2.5215135
1388	3.4890034	3.5353823	3.3813288	3.2560251	3.1620245	3.0930979	3.0251806	2.9191289	2.7922382	2.6578019	2.5084522
1390	3.3951049	3.4314458	3.3303699	3.2029169	3.1060588	3.0278883	2.9441023	2.8442309	2.7313433	2.6101828	2.4730496
1392	3.3160379	3.2792952	3.2320933	3.1322696	3.0528195	2.9606876	2.8670864	2.7581463	2.6451979	2.5294034	2.4236286
1394	3.205807	3.1427703	3.090452	3.0485842	2.9856069	2.8844442	2.7703419	2.6647663	2.5635369	2.4554465	2.3606391
1396	3.2710228	3.0083525	2.9883075	2.9568758	2.8917718	2.7888227	2.6766534	2.5705643	2.4731503	2.3882291	2.2932382
1398	3.0825667	2.9681413	2.9127021	2.856874	2.7728477	2.6734903	2.5678735	2.4742246	2.382431	2.3058431	2.2207105
1400	2.9407451	2.9322891	2.8344343	2.7402673	2.6431956	2.5529928	2.4661992	2.3784676	2.2979591	2.2096355	2.1485176

Table 5.43. β for 1300-1400 nm with b of 2.0 comparison run.

beta:	10	15	20	25	30	35	40	45	50	55	60
1300	0.9383248	0.9318523	0.9224233	0.9144767	0.9054879	0.8941448	0.878722	0.8584946	0.833837	0.8056108	0.7751571
1302	0.9297065	0.9220124	0.9157524	0.9096997	0.9018821	0.8906081	0.8740156	0.8525574	0.8264979	0.7966842	0.7651462
1304	0.9185313	0.9140072	0.910383	0.9057932	0.8982274	0.8866076	0.868901	0.8461085	0.8184195	0.7871422	0.7541497
1306	0.9091603	0.9081189	0.9064156	0.9021682	0.8944311	0.8817792	0.863229	0.8386657	0.8092375	0.7765933	0.7420071
1308	0.9032425	0.903936	0.9030327	0.8987896	0.8907107	0.8768726	0.8565104	0.8302731	0.7988396	0.7643912	0.7287424
1310	0.8981642	0.9011347	0.8996316	0.8954666	0.8864825	0.8708863	0.8491408	0.8206419	0.7874762	0.7510751	0.713995
1312	0.8966064	0.8977095	0.8962754	0.8920807	0.8816859	0.8644392	0.840296	0.81002	0.7743916	0.7363147	0.6981885
1314	0.8965828	0.8944532	0.8934239	0.8880549	0.876031	0.8570184	0.8307491	0.7976001	0.7598053	0.720299	0.6810971
1316	0.8946277	0.8934294	0.8908457	0.8832982	0.8693942	0.8485264	0.8191947	0.7833389	0.7429522	0.7020113	0.6632632
1318	0.8946481	0.8929526	0.8877244	0.8775787	0.8620034	0.8387266	0.8063003	0.7669728	0.7243931	0.6830067	0.6446968
1320	0.8937341	0.8914109	0.8834332	0.8714992	0.8536289	0.8268909	0.7904251	0.7481136	0.704168	0.6628373	0.6261428
1322	0.8928403	0.8871374	0.8779969	0.8649136	0.8441597	0.8127464	0.7720318	0.7270588	0.6827993	0.6427265	0.6077421
1324	0.8892255	0.881041	0.8719879	0.8574785	0.8323677	0.7952791	0.7504321	0.7039362	0.6602817	0.6219758	0.5898873
1326	0.8838109	0.8757534	0.8659253	0.8484311	0.8176172	0.7743614	0.7263336	0.6795637	0.6378122	0.602011	0.5729647
1328	0.8759524	0.8706942	0.8593093	0.8366115	0.7985191	0.7500067	0.7001188	0.6547827	0.6157016	0.5836594	0.5575853
1330	0.8720395	0.8647251	0.8512884	0.8207072	0.7742898	0.722604	0.6730502	0.6300809	0.5945421	0.5659207	0.5437778
1332	0.8651831	0.859385	0.8391984	0.7987038	0.745798	0.6934257	0.6458228	0.6066638	0.5754082	0.5506296	0.5320325
1334	0.8617616	0.8517587	0.8208349	0.7702954	0.7144117	0.6634036	0.6195604	0.5852383	0.5582309	0.5374952	0.5222279
1336	0.8548844	0.8385571	0.7942045	0.7369907	0.6817898	0.6339489	0.5960404	0.5661292	0.5436882	0.5274466	0.5144343
1338	0.8454372	0.814041	0.7597082	0.7016201	0.6496397	0.6066684	0.5743212	0.5497109	0.5312558	0.5176579	0.5089349
1340	0.8247262	0.7753382	0.7204375	0.6663254	0.6198527	0.5829322	0.5567489	0.5362108	0.5216801	0.5116633	0.5050586
1342	0.7893732	0.732124	0.6799317	0.6320923	0.5935151	0.5635268	0.5415575	0.5260587	0.5153463	0.5084705	0.5029262
1344	0.7428967	0.6923182	0.6403933	0.601117	0.5710161	0.5476909	0.5305595	0.5187589	0.5110543	0.5067581	0.5023146
1346	0.7074151	0.6529058	0.6070169	0.5757365	0.5518373	0.5353057	0.5219603	0.5144422	0.5092074	0.5048558	0.5029585
1348	0.6734438	0.618431	0.5831921	0.5560836	0.5371376	0.5256936	0.5175713	0.5124842	0.5091687	0.5059018	0.5039707
1350	0.6351323	0.5982274	0.5662211	0.5417506	0.5276154	0.5194963	0.5149857	0.5127265	0.5100827	0.5089201	0.5054005
1352	0.6190106	0.5856302	0.5547965	0.5341964	0.5234835	0.5173594	0.5158823	0.5144368	0.5124821	0.5100185	0.50708
1354	0.6128621	0.5766144	0.5496706	0.5338119	0.5242978	0.5194032	0.5183574	0.5172073	0.5151572	0.5116914	0.509252
1356	0.6093018	0.5734029	0.5517612	0.538177	0.5296394	0.5251048	0.5232584	0.520411	0.5175821	0.5140256	0.5113183
1358	0.6070307	0.5787585	0.5595828	0.5460396	0.5383007	0.5332829	0.5283773	0.5244536	0.5202653	0.5176485	0.5139433
1360	0.6150899	0.5897174	0.5705495	0.5575771	0.549324	0.5424722	0.5348803	0.5284579	0.5235355	0.5201127	0.5171682
1362	0.6187304	0.6016099	0.583618	0.5711343	0.5610188	0.5511653	0.5407361	0.5335104	0.5280053	0.5236109	0.5210069
1364	0.6291077	0.6101909	0.5969083	0.584594	0.571515	0.5589353	0.5480472	0.539503	0.5336547	0.5286299	0.5251422
1366	0.6201252	0.6127828	0.6042181	0.5935929	0.5797014	0.5660198	0.5549806	0.5464427	0.5397212	0.534391	0.5298741
1368	0.6264829	0.61208	0.6056006	0.5975778	0.5860257	0.5732468	0.5630392	0.5538157	0.5460837	0.5399839	0.535192
1370	0.6316584	0.6154307	0.6061734	0.5989318	0.590954	0.580366	0.5709954	0.5616178	0.5533251	0.5462227	0.541081
1372	0.6354746	0.6201463	0.6075481	0.601087	0.5956148	0.587495	0.5789388	0.5693076	0.560339	0.5532107	0.5468935
1374	0.6473932	0.6202374	0.6093296	0.6052417	0.6000298	0.593987	0.5850241	0.5759177	0.5675062	0.5597255	0.5532037
1376	0.6499738	0.6168399	0.612331	0.6093881	0.6045329	0.5988097	0.5904663	0.5818299	0.5735685	0.5657482	0.5593412
1378	0.6397612	0.6171301	0.6165764	0.6130205	0.6084251	0.6022653	0.5943286	0.5866331	0.5787249	0.5718349	0.5652587
1380	0.6233795	0.6165523	0.6198335	0.6163892	0.6112407	0.6047879	0.5977306	0.5905173	0.5836006	0.5770698	0.5709224
1382	0.6022965	0.6201432	0.6216149	0.6185372	0.6127722	0.6061602	0.6004561	0.594156	0.5874472	0.5817019	0.5757223
1384	0.6224513	0.6312625	0.6274724	0.6173455	0.6130374	0.6076119	0.6025928	0.5969705	0.5914212	0.5849509	0.5796812
1386	0.6395464	0.6315116	0.6259013	0.6135625	0.6120353	0.6086352	0.6047747	0.5996374	0.5938764	0.5883842	0.583121
1388	0.6526266	0.6332682	0.6206793	0.6087427	0.6098797	0.6093414	0.6058869	0.601409	0.5962256	0.5909172	0.58578
1390	0.6563283	0.6369681	0.6147371	0.6053572	0.60757	0.6089805	0.6068924	0.6028595	0.5979092	0.5932669	0.5879502
1392	0.6440164	0.6396822	0.6098368	0.6051927	0.6062003	0.6074855	0.6062696	0.6035326	0.5991899	0.59454	0.5901447
1394	0.6375497	0.6363613	0.6120681	0.6078892	0.606337	0.6060291	0.6056682	0.6033689	0.6004722	0.5958365	0.5917326
1396	0.6278685	0.6315002	0.6139535	0.6115107	0.6079584	0.6054173	0.6042728	0.6030286	0.6004794	0.5974355	0.5934291
1398	0.6234732	0.6218674	0.6140116	0.6136388	0.6101422	0.6062902	0.6042638	0.6025941	0.6006359	0.5982779	0.5946093
1400	0.6272734	0.6142784	0.6127657	0.6139919	0.6119268	0.6082941	0.6047971	0.6029212	0.6006456	0.5985407	0.5957643

Table 5.44. Transmission (TnoH2O) for 1300-1400 nm with b of 2.5 comparison run.

tnoh2o:	10	15	20	25	30	35	40	45	50	55	60
1300	0.870778217	0.8696757	0.8674788	0.8638393	0.8593643	0.8542356	0.8475796	0.8401236	0.8314304	0.8227402	0.8121771
1302	0.848508301	0.8498786	0.8485383	0.8454646	0.8418166	0.8371003	0.8305727	0.8230769	0.814709	0.805021	0.7949365
1304	0.827495638	0.8293814	0.8284867	0.8265988	0.8233138	0.8186013	0.8123448	0.8047976	0.7961217	0.7862957	0.7767155
1306	0.805782762	0.8077811	0.8077353	0.8069041	0.8038956	0.7989474	0.7929012	0.7852598	0.7768469	0.7675449	0.7573655
1308	0.786980846	0.7857364	0.7873026	0.7864074	0.7832802	0.7781665	0.7720203	0.76445	0.7558215	0.7471618	0.7368926
1310	0.766288447	0.766799	0.7669374	0.7648999	0.7615027	0.7560274	0.7497656	0.7422189	0.7340306	0.7248941	0.7155353
1312	0.748762023	0.7494086	0.7458662	0.7428476	0.7386285	0.7329888	0.7261596	0.7190527	0.7113577	0.7022702	0.6933474
1314	0.733127181	0.7283985	0.7244529	0.7199411	0.7140394	0.7080001	0.7014361	0.6947677	0.6873508	0.6794511	0.6699234
1316	0.709146655	0.7058888	0.701961	0.6952231	0.6881504	0.6821211	0.6760665	0.6699056	0.662972	0.654887	0.6457588
1318	0.685768805	0.6835955	0.6771236	0.6679996	0.6605614	0.6550766	0.6500648	0.6443263	0.6371883	0.6287333	0.6204129
1320	0.669512806	0.6601215	0.648021	0.6384784	0.6326602	0.6282902	0.6238108	0.6180395	0.6105991	0.6024732	0.5939527
1322	0.644428129	0.6302875	0.615276	0.6083663	0.6049352	0.6016313	0.5967527	0.5904525	0.5829638	0.5755676	0.5668094
1324	0.60812911	0.590185	0.5810993	0.578965	0.5773574	0.5741543	0.5685943	0.5617418	0.5539162	0.5464461	0.5392161
1326	0.561939519	0.547054	0.5486614	0.5504414	0.5495228	0.5456301	0.5392102	0.5316693	0.5243015	0.5169617	0.5110755
1328	0.506969382	0.511665	0.5190238	0.5218131	0.5201996	0.514821	0.5076823	0.5004211	0.4938001	0.4878732	0.4826093
1330	0.45935462	0.4823043	0.4903329	0.4917984	0.488128	0.48166	0.4749949	0.4683251	0.4627975	0.4588345	0.45442
1332	0.426169538	0.4519189	0.4597874	0.4585785	0.4532629	0.446657	0.4406128	0.435789	0.4318571	0.4283293	0.4263246
1334	0.403182417	0.4200593	0.4245625	0.4213467	0.41594	0.4101008	0.4062018	0.4028778	0.4006393	0.3990812	0.3988821
1336	0.394892575	0.3880867	0.3851337	0.3807669	0.3764895	0.3731846	0.3710433	0.3703177	0.3702423	0.3706472	0.3713715
1338	0.385831839	0.356332	0.3436738	0.3389487	0.3367766	0.3362229	0.3370855	0.3384348	0.3400413	0.3426753	0.3447014
1340	0.351425372	0.3207229	0.3030641	0.297638	0.2976	0.300354	0.3032603	0.3070788	0.3109812	0.3148089	0.3189341
1342	0.295147275	0.2758206	0.2626711	0.2583655	0.2603723	0.2655626	0.2711098	0.2768379	0.2827051	0.2876476	0.2936772
1344	0.22800922	0.2235795	0.2213151	0.2219044	0.2262209	0.2327027	0.2401076	0.2478911	0.2553118	0.2625313	0.2689672
1346	0.157933373	0.1702879	0.1796354	0.186512	0.1939359	0.2023173	0.2113259	0.2200206	0.2290609	0.2374496	0.2452703
1348	0.09596849	0.1204376	0.1386584	0.1526389	0.1635449	0.1734364	0.1836975	0.1941219	0.2037991	0.2133651	0.2226255
1350	0.052498651	0.0776861	0.1011464	0.120014	0.1346045	0.1471133	0.1586277	0.1694969	0.180472	0.1903908	0.200683
1352	0.023949767	0.0457464	0.0690213	0.0899094	0.1072663	0.1216337	0.1345163	0.1464818	0.1579036	0.1694499	0.1799115
1354	0.009431857	0.0242358	0.0436853	0.0638586	0.0821857	0.098335	0.1123405	0.1249946	0.1374286	0.1490811	0.1603609
1356	0.003128893	0.011675	0.0256946	0.0426839	0.0602313	0.0766396	0.0914492	0.1052823	0.1181145	0.1303947	0.142068
1358	0.000973313	0.0051553	0.0140598	0.0270901	0.0422742	0.0579153	0.0730361	0.0868217	0.1000611	0.1127996	0.124731
1360	0.000339858	0.0022158	0.0074157	0.016491	0.0285994	0.0424322	0.0564499	0.0705608	0.0837772	0.0965373	0.1087276
1362	0.000154288	0.0010321	0.0039136	0.0098477	0.0188837	0.0301654	0.0431145	0.0559547	0.0689386	0.081758	0.094069
1364	9.49969E-05	0.0005745	0.0022452	0.0060168	0.0123921	0.0211773	0.031925	0.0437885	0.0559887	0.0681253	0.0802554
1366	8.61382E-05	0.0004479	0.0015454	0.0039277	0.0082568	0.0147144	0.0235263	0.0336862	0.0447504	0.0565091	0.0681433
1368	0.000140286	0.0005266	0.0012962	0.0028049	0.0056731	0.010395	0.0170912	0.0255867	0.0354226	0.0460774	0.0572563
1370	0.000344382	0.0007576	0.0012249	0.002166	0.0040748	0.0074976	0.0126708	0.0194893	0.0279328	0.0375643	0.0478398
1372	0.000812325	0.0010045	0.0011764	0.0017689	0.0030993	0.0055973	0.0094442	0.0149363	0.022041	0.0304321	0.0398515
1374	0.00138157	0.0011205	0.0011269	0.001526	0.0025206	0.0043731	0.0073825	0.0117328	0.0175036	0.0247866	0.0332124
1376	0.001627024	0.0011572	0.0011191	0.0014349	0.002211	0.0036079	0.0059172	0.0094174	0.0142265	0.0203704	0.027934
1378	0.001598619	0.0011958	0.0011699	0.0014545	0.0020611	0.0031659	0.0050752	0.0079047	0.0119429	0.0172014	0.0237224
1380	0.001404255	0.0012602	0.0012954	0.0015299	0.0020298	0.0029502	0.0045041	0.0068895	0.010257	0.0147605	0.0205347
1382	0.000920879	0.0013088	0.0014359	0.0016365	0.002076	0.0028913	0.0042675	0.006283	0.0092099	0.0131005	0.0182017
1384	0.00061794	0.0012524	0.0015191	0.0017501	0.0022065	0.0029706	0.0041801	0.0059926	0.0085888	0.0121756	0.0166618
1386	0.000726759	0.0011266	0.0015288	0.001897	0.0024069	0.003159	0.0043181	0.0059636	0.0083597	0.0117149	0.0157049
1388	0.00089475	0.0011251	0.0015988	0.0021012	0.002648	0.0034543	0.0045317	0.0061716	0.0084905	0.0114472	0.0153224
1390	0.001059905	0.0013316	0.0018222	0.0023469	0.0029592	0.0038002	0.0049764	0.0066165	0.0088199	0.0116039	0.0153737
1392	0.001292281	0.0017345	0.0021787	0.0026578	0.0033367	0.0042744	0.0055249	0.0072788	0.0095689	0.0124405	0.0158219
1394	0.001639922	0.002226	0.0026756	0.0030778	0.003825	0.0048674	0.0063543	0.0081425	0.0103918	0.0133907	0.0166471
1396	0.001903055	0.0028181	0.0032132	0.0036331	0.0044789	0.0057173	0.007342	0.0093288	0.0116972	0.0143662	0.0178448
1398	0.002591935	0.0034157	0.0037357	0.0043643	0.0054344	0.0068576	0.0086407	0.0107402	0.0131887	0.0159243	0.0194227
1400	0.003439075	0.00396	0.0043668	0.0053625	0.0066651	0.0082812	0.0102109	0.012458	0.0149848	0.0182144	0.0212164

Table 5.45. α for 1300-1400 nm with b of 2.5 comparison run.

alpha:	10	15	20	25	30	35	40	45	50	55	60
1300	0.0494413	0.0504982	0.0523266	0.0550634	0.058578	0.0628606	0.0682822	0.0745224	0.0817517	0.0893095	0.0982211
1302	0.0592831	0.0593707	0.0608507	0.0634417	0.0668308	0.0712318	0.0770349	0.0837541	0.0913268	0.0999934	0.1091362
1304	0.0690726	0.0688499	0.0700925	0.0722989	0.0757861	0.0805525	0.0867283	0.0940082	0.1023157	0.1116407	0.1211362
1306	0.079578	0.079042	0.079899	0.0818233	0.0855111	0.0908624	0.0974734	0.1054062	0.1142231	0.1238723	0.1343943
1308	0.0888412	0.0897081	0.0898662	0.0920565	0.0962036	0.1022161	0.1094732	0.1180773	0.12773	0.1377797	0.1490314
1310	0.0992635	0.0991474	0.1001541	0.103166	0.1079594	0.1148268	0.1228494	0.1322271	0.1424814	0.1536356	0.1650712
1312	0.1081124	0.1081504	0.1111657	0.1150732	0.1208888	0.1286114	0.1377653	0.1477982	0.1586154	0.1706188	0.1826309
1314	0.1160693	0.119237	0.1227911	0.1279943	0.1354316	0.1442358	0.1542624	0.1650348	0.1766717	0.1887104	0.2020897
1316	0.1287791	0.1313686	0.1354293	0.1426304	0.1516499	0.161451	0.1723249	0.183874	0.196256	0.2095057	0.2233673
1318	0.1414165	0.14378	0.1500084	0.159564	0.1699104	0.1805551	0.1921026	0.2046059	0.2182469	0.2327422	0.246899
1320	0.1506489	0.1574979	0.1679629	0.1789906	0.1897494	0.2011342	0.2136909	0.2275043	0.2425291	0.2577436	0.2728564
1322	0.1653391	0.1760214	0.1894628	0.200247	0.2110694	0.2234178	0.2376892	0.2532397	0.2694294	0.2849527	0.3011579
1324	0.187924	0.2024734	0.2135282	0.2227791	0.2341767	0.2483851	0.2647273	0.2821198	0.2997471	0.3164932	0.3317913
1326	0.2191858	0.2331773	0.2383902	0.2467875	0.2598151	0.2765953	0.295386	0.3147171	0.3330477	0.3504086	0.3649447
1328	0.2603166	0.2610005	0.2634547	0.2734179	0.2894771	0.3095623	0.3308599	0.3513413	0.3699812	0.3862733	0.4005609
1330	0.2997925	0.2865787	0.2904073	0.3044021	0.3249981	0.3483025	0.3710939	0.3921461	0.4103855	0.4249278	0.4382058
1332	0.33118	0.3153659	0.3224396	0.3423366	0.3676753	0.393258	0.4170738	0.437127	0.4537558	0.4680029	0.4780504
1334	0.3550338	0.3491643	0.3637085	0.3898403	0.4185809	0.4454992	0.4679707	0.4864904	0.5009307	0.5122212	0.5195786
1336	0.366892	0.3887509	0.4167105	0.4486414	0.478794	0.5044301	0.5247315	0.5397603	0.5506559	0.5578586	0.5635476
1338	0.3823722	0.43665	0.4821822	0.5186465	0.5478119	0.5704794	0.5858441	0.596692	0.6038988	0.6072136	0.6090646
1340	0.4312444	0.5004293	0.559064	0.5991647	0.6255538	0.6422501	0.6523997	0.6575813	0.6594482	0.6590245	0.6560628
1342	0.5232958	0.591138	0.6497069	0.6891348	0.7106019	0.7199332	0.7230608	0.7218386	0.717576	0.7125978	0.7051486
1344	0.6638635	0.7152231	0.7590876	0.7878128	0.8010729	0.8028308	0.798145	0.7892969	0.7787151	0.7666911	0.756537
1346	0.8610135	0.8771013	0.8908179	0.8992094	0.8990045	0.8897488	0.8765737	0.8605301	0.8426282	0.8263044	0.8098101
1348	1.1333642	1.0826324	1.0491092	1.0254048	1.0055003	0.9839891	0.9598404	0.934184	0.9101658	0.8874515	0.8651525
1350	1.4767175	1.3355002	1.2370343	1.1717011	1.1235497	1.0830137	1.0461326	1.0120333	0.9796354	0.9506014	0.9235835
1352	1.9062378	1.6349242	1.4596938	1.3408715	1.2561257	1.1931859	1.1395537	1.0941424	1.0539149	1.0163542	0.9846117
1354	2.4028678	1.989887	1.7188854	1.5338153	1.4058545	1.3123569	1.2398047	1.181797	1.1308863	1.0880928	1.0484241
1356	2.9921391	2.3920333	2.0098512	1.7530881	1.5744992	1.4463462	1.3509886	1.2755342	1.2139053	1.1614804	1.1151855
1358	3.6145046	2.8257444	2.3282752	1.9938133	1.7608705	1.593894	1.4712799	1.3791039	1.3039472	1.2394149	1.1861066
1360	4.1474996	3.2545867	2.6559241	2.2482719	1.9613994	1.7543743	1.6063153	1.4900625	1.3997276	1.3241993	1.2603898
1362	4.5372205	3.628166	2.9704399	2.5030789	2.1702082	1.9293921	1.7478509	1.6123397	1.5031151	1.4135407	1.3381205
1364	4.7679477	3.9018686	3.230397	2.7391899	2.3794203	2.1103356	1.9028802	1.7408433	1.6124582	1.5091094	1.4218591
1366	4.7883005	3.9979811	3.3944569	2.9405079	2.5798099	2.2953749	2.0596807	1.8762656	1.7288837	1.6065156	1.5077168
1368	4.4944038	3.8845115	3.4615245	3.0995803	2.7638156	2.4703197	2.2202902	2.0157733	1.8488952	1.7123485	1.5977851
1370	4.0048051	3.671643	3.4730301	3.2208204	2.9234788	2.6299241	2.3691015	2.1520824	1.9691149	1.8164535	1.6897596
1372	3.5508778	3.5078092	3.479759	3.3104222	3.050647	2.7677367	2.5108674	2.282835	2.0868793	1.9215004	1.7821453
1374	3.256165	3.4462483	3.4903314	3.3671317	3.1397781	2.877748	2.6274343	2.3998022	2.1989822	2.0231783	1.8729771
1376	3.1847825	3.4348476	3.4818192	3.3807452	3.1887007	2.9603407	2.7285249	2.5033286	2.2994478	2.1197066	1.9581521
1378	3.2688851	3.4216721	3.443825	3.3579159	3.2067208	3.0131183	2.7953053	2.5837507	2.3819854	2.1993973	2.0368054
1380	3.395308	3.3993349	3.3812389	3.3174789	3.2002602	3.03759	2.844389	2.643465	2.4511418	2.2700045	2.1045847
1382	3.6174676	3.3888223	3.3273005	3.2743092	3.1787062	3.0382724	2.8598402	2.6796336	2.4962251	2.3237185	2.1592126
1384	3.7994404	3.4165764	3.3072119	3.240644	3.1433494	3.0155742	2.8609376	2.6930559	2.5213706	2.3534415	2.197104
1386	3.6004322	3.4445751	3.3164988	3.20907	3.0995939	2.9776402	2.8345439	2.6855755	2.5264707	2.3633721	2.219394
1388	3.4420309	3.4305279	3.3046715	3.1696138	3.0535753	2.9275904	2.8038006	2.6595507	2.5095265	2.3667035	2.2243195
1390	3.3496244	3.3391972	3.240593	3.1188889	3.0007179	2.8770664	2.7501597	2.6174023	2.4826396	2.350987	2.2148771
1392	3.2815018	3.1981564	3.1434128	3.0523472	2.9406137	2.8176296	2.6950994	2.563473	2.433944	2.3079865	2.1927123
1394	3.1920371	3.0878134	3.0326343	2.9699638	2.8683345	2.7505608	2.6204946	2.5015712	2.3844588	2.2644432	2.1597879
1396	3.1503043	3.0019343	2.9349914	2.8778851	2.7819736	2.6666889	2.5456386	2.429163	2.3204937	2.2222495	2.1180892
1398	3.0382948	2.9141784	2.8567364	2.7805388	2.6781204	2.5690167	2.4571702	2.3533733	2.2541203	2.1643021	2.0694485
1400	2.869642	2.8393965	2.7770772	2.6737556	2.5686018	2.4665735	2.3689687	2.2733181	2.1856866	2.0908513	2.0186706

Table 5.46. β for 1300-1400 nm with b of 2.5 comparison run.

beta:	10	15	20	25	30	35	40	45	50	55	60
1300	0.9367549	0.9257984	0.9097642	0.8898882	0.8653081	0.8363391	0.8051428	0.7729205	0.7414321	0.7113342	0.6831295
1302	0.9277341	0.9174049	0.903782	0.8857197	0.8614984	0.8326722	0.8006008	0.7678815	0.7356521	0.7047725	0.676559
1304	0.9179277	0.9098585	0.8988135	0.8815724	0.8575316	0.8284982	0.7954963	0.7621186	0.7293714	0.6982552	0.6692196
1306	0.9086627	0.9043133	0.894739	0.8774551	0.8530391	0.8231767	0.7895434	0.7555386	0.7220973	0.6906989	0.6613041
1308	0.9028821	0.9000367	0.8908858	0.8732867	0.848148	0.8170541	0.7829524	0.7481064	0.7142579	0.682036	0.6528063
1310	0.8979121	0.896697	0.8868824	0.8689926	0.8426471	0.8103065	0.7755079	0.7399747	0.7052459	0.6727833	0.6434759
1312	0.8960491	0.8930099	0.8828082	0.8638658	0.8362642	0.8026403	0.7670806	0.7306502	0.6955751	0.6629031	0.6333247
1314	0.8954848	0.8897544	0.8784879	0.8581851	0.8292947	0.7946353	0.7576897	0.7204413	0.6848587	0.6524966	0.6228145
1316	0.8935364	0.8875287	0.8742855	0.8516057	0.8210419	0.7852203	0.7468618	0.7088568	0.6728745	0.6401829	0.6115612
1318	0.8930404	0.8855807	0.8694631	0.8443846	0.8121156	0.7749262	0.7348754	0.6960288	0.6600625	0.6281168	0.6001322
1320	0.891598	0.8826266	0.8637394	0.8364631	0.8017166	0.7623563	0.7211405	0.6818784	0.6462932	0.6153015	0.588669
1322	0.8896618	0.8775143	0.8568683	0.8274024	0.789792	0.7479028	0.7060107	0.6668504	0.6322318	0.6025298	0.5771053
1324	0.8859292	0.8712789	0.8492842	0.8168285	0.7760312	0.7315867	0.6894116	0.6508329	0.6175427	0.5887441	0.5656207
1326	0.8800325	0.8651484	0.8405851	0.8041487	0.7598667	0.7136435	0.6714277	0.634249	0.6026068	0.5760142	0.5546797
1328	0.8730752	0.8582485	0.8301226	0.7888648	0.7412366	0.6945366	0.6529182	0.6173869	0.5876788	0.5638989	0.5444937
1330	0.8679582	0.8500793	0.8171538	0.7704936	0.7204581	0.6741969	0.6337014	0.6006035	0.5733581	0.5517653	0.5349838
1332	0.8610876	0.8407587	0.8005673	0.7491423	0.6976577	0.6531635	0.6149025	0.5843017	0.5601963	0.5409048	0.5265923
1334	0.8551102	0.8282365	0.7798296	0.7247161	0.6734689	0.6312912	0.5962015	0.5691381	0.5480747	0.531656	0.5191688
1336	0.8457884	0.8099857	0.7540828	0.6976916	0.6490717	0.6097735	0.5791564	0.555248	0.5372433	0.5244126	0.5133849
1338	0.8306315	0.7828219	0.7238944	0.6692603	0.6248543	0.5893239	0.5629905	0.5429399	0.5280246	0.5165073	0.5087124
1340	0.8063101	0.7471593	0.6905456	0.6411629	0.6020268	0.5711061	0.5495171	0.5327199	0.5203513	0.5113525	0.5051415
1342	0.7706899	0.7088944	0.6567848	0.614342	0.581201	0.5558756	0.5376257	0.5244666	0.5148715	0.5086343	0.5029175
1344	0.7287542	0.672925	0.6249098	0.5894942	0.5625779	0.5431148	0.5286732	0.518235	0.5110648	0.5064458	0.5019467
1346	0.6940026	0.6392262	0.5972012	0.5685284	0.547329	0.5329611	0.5213798	0.5142708	0.5088705	0.504187	0.5017908
1348	0.6613394	0.6102488	0.5761836	0.5516179	0.5354123	0.5250868	0.5173392	0.5118568	0.5081436	0.5045127	0.5022909
1350	0.6289344	0.5905423	0.5610285	0.539798	0.5273542	0.5195465	0.5145718	0.5113673	0.5082247	0.5067124	0.5035976
1352	0.6114607	0.5778553	0.5507876	0.5332839	0.5234452	0.5174849	0.5147775	0.5122817	0.5100845	0.5076312	0.5052649
1354	0.6036143	0.5694688	0.5457742	0.5317953	0.5235285	0.518357	0.5163064	0.5143617	0.511956	0.5089552	0.5071918
1356	0.5972777	0.5651026	0.545966	0.5345573	0.5271118	0.5227838	0.5200025	0.517069	0.5144122	0.5114412	0.5093259
1358	0.5931101	0.5669207	0.5508605	0.540015	0.5333048	0.5285837	0.5241339	0.520803	0.5173538	0.5148929	0.511972
1360	0.5964864	0.5736448	0.5582406	0.5479901	0.5411554	0.5355952	0.5296695	0.5245025	0.5204904	0.5173922	0.5148266
1362	0.6005622	0.5819442	0.5678799	0.557963	0.5496078	0.5423761	0.5343792	0.529048	0.524514	0.5204642	0.517902
1364	0.6043697	0.5901642	0.5784718	0.5681386	0.5576415	0.5484	0.5401096	0.5335342	0.5287896	0.524921	0.5218414
1366	0.6100628	0.5978926	0.5874831	0.5765069	0.5645452	0.5540496	0.5453317	0.5386277	0.5334642	0.5292242	0.5256718
1368	0.6190058	0.6047918	0.5940697	0.5822579	0.5704038	0.5592372	0.5514282	0.5443336	0.5384102	0.5336094	0.5300137
1370	0.6268463	0.6111349	0.5987657	0.5865147	0.5757339	0.5651554	0.5569744	0.5499746	0.5436013	0.5383843	0.5345268
1372	0.6327037	0.6162285	0.602474	0.5911055	0.5811507	0.5714774	0.5633405	0.5558	0.5490854	0.5438148	0.5391977
1374	0.6409664	0.6178244	0.6054892	0.5966126	0.5869365	0.5783218	0.5688906	0.5611402	0.5548577	0.5488507	0.5440195
1376	0.6382509	0.6165083	0.6086413	0.6015432	0.5925816	0.584239	0.5746557	0.5666321	0.5596812	0.5534938	0.5486717
1378	0.6170189	0.6155874	0.6126681	0.605815	0.5978485	0.5890604	0.579484	0.5713883	0.5642829	0.5585962	0.5534804
1380	0.6006238	0.614417	0.6155207	0.6097776	0.6019267	0.5927885	0.5839776	0.5760801	0.5689917	0.5634905	0.5581309
1382	0.5996041	0.6120654	0.6159519	0.6121968	0.6047707	0.595731	0.5880893	0.580406	0.5735549	0.5676048	0.562628
1384	0.60545	0.6106624	0.6135979	0.6120301	0.6059266	0.5983327	0.5911875	0.5843159	0.5778909	0.5712803	0.5666582
1386	0.6342169	0.6175407	0.6101498	0.6093096	0.605657	0.6001843	0.5942095	0.5877092	0.5812086	0.5753772	0.5705246
1388	0.6485948	0.6214331	0.6070938	0.6056012	0.604741	0.6013756	0.5960279	0.5904614	0.5843765	0.5788136	0.5738941
1390	0.6511292	0.6231229	0.6062338	0.6038103	0.6034315	0.6017653	0.5976828	0.5924615	0.5868861	0.5821064	0.5770383
1392	0.6431005	0.6253263	0.6077908	0.6045434	0.602881	0.6013563	0.597966	0.5939427	0.5890976	0.5845777	0.5799063
1394	0.6350598	0.6208432	0.6094136	0.606644	0.603471	0.6013463	0.5986917	0.5952185	0.5914989	0.586512	0.582447
1396	0.6256684	0.6106675	0.6106256	0.6088225	0.6051185	0.6015981	0.5986962	0.5958495	0.5923527	0.588672	0.5846193
1398	0.6125852	0.6073585	0.6110118	0.6099396	0.6066058	0.6029305	0.6002125	0.5968466	0.5938736	0.5903598	0.5864055
1400	0.6202843	0.607011	0.6109755	0.6104124	0.6082658	0.6048407	0.6009244	0.5980619	0.5946824	0.5917539	0.5883858

Table 5.47. Transmission (TnoH2O) for 1300-1400 nm with b of 3.3 comparison run.

tnoh2o:	10	15	20	25	30	35	40	45	50	55	60
1300	0.8704234	0.8682992	0.8652019	0.8601533	0.8537367	0.8461367	0.836855	0.8269298	0.8161374	0.8053252	0.7932728
1302	0.8478323	0.8486531	0.8465531	0.8422583	0.83645	0.8291469	0.8200452	0.8101139	0.79955	0.788077	0.7765637
1304	0.8269099	0.8284376	0.826993	0.8236785	0.8181797	0.8108757	0.8021311	0.7922301	0.7814558	0.7700012	0.7588317
1306	0.8057668	0.807391	0.80683	0.8040923	0.7989038	0.7915225	0.7829694	0.7732605	0.7627804	0.751701	0.7402675
1308	0.7868254	0.7863472	0.7863938	0.7836785	0.7786251	0.7711435	0.7628218	0.7530598	0.7425862	0.7320797	0.7207051
1310	0.7669303	0.7667479	0.7660127	0.7626187	0.7572563	0.7497429	0.7413597	0.7317919	0.7215344	0.7106792	0.7001656
1312	0.7475634	0.7480721	0.7451818	0.7407415	0.7347798	0.7273293	0.7186295	0.709326	0.6996788	0.688827	0.6789308
1314	0.7311784	0.7274596	0.723294	0.7179212	0.7111243	0.7036335	0.6949814	0.6859293	0.6763116	0.6670351	0.656554
1316	0.7083915	0.704675	0.7001744	0.6934698	0.6861962	0.6787213	0.6702751	0.661723	0.652621	0.6434305	0.6336021
1318	0.6860001	0.6815404	0.675146	0.6672941	0.6600003	0.6524551	0.644709	0.6365759	0.6276192	0.618375	0.6098869
1320	0.665807	0.6573571	0.6476948	0.6395729	0.6327655	0.625783	0.6185772	0.6105322	0.6022365	0.5933749	0.5851617
1322	0.6395929	0.6279916	0.6171446	0.6104036	0.6048332	0.5987509	0.5917245	0.5838773	0.5759829	0.5683486	0.560153
1324	0.6054466	0.5912754	0.5844725	0.5808987	0.5764525	0.5708653	0.5638254	0.5560632	0.5485141	0.5409788	0.5343254
1326	0.5618323	0.5520145	0.5520545	0.5512161	0.5477597	0.5422455	0.5348104	0.5276959	0.5207756	0.5137948	0.5081527
1328	0.5108112	0.5161312	0.5214952	0.5216228	0.51789	0.5120278	0.504842	0.4979095	0.4917473	0.4864352	0.4818043
1330	0.4638738	0.4846456	0.4914376	0.4910571	0.4864029	0.4800037	0.473548	0.4678335	0.462646	0.4591907	0.4554627
1332	0.4305071	0.4535454	0.4597435	0.4580409	0.4524879	0.446377	0.4411115	0.4366705	0.4335855	0.4306294	0.4293115
1334	0.4080842	0.4220906	0.4249703	0.4218363	0.4165555	0.4114906	0.4083357	0.4058189	0.4039449	0.4028732	0.4030966
1336	0.3966721	0.3911241	0.3872003	0.3831285	0.3792132	0.3766029	0.3747363	0.3745068	0.3750427	0.3759526	0.3773825
1338	0.3822826	0.3591458	0.3481374	0.3433222	0.3414676	0.3412338	0.342258	0.3438551	0.346072	0.3493748	0.3518672
1340	0.3468888	0.321708	0.3084507	0.3040044	0.3041265	0.3068423	0.3098879	0.3138067	0.318351	0.3226829	0.3270969
1342	0.2932772	0.2767072	0.267632	0.2657894	0.2684934	0.273381	0.2792368	0.2850466	0.2912652	0.2969144	0.3031631
1344	0.2287448	0.2260079	0.2260418	0.2290927	0.2346849	0.241572	0.2494065	0.2573781	0.2649188	0.2726387	0.2797004
1346	0.1619291	0.1746468	0.1845944	0.1936292	0.2027429	0.2118632	0.2217541	0.2309414	0.2400026	0.248852	0.2572089
1348	0.1028388	0.1267105	0.1451853	0.1597259	0.172218	0.1837506	0.1947678	0.2058063	0.2159163	0.2259727	0.2357313
1350	0.0593755	0.086017	0.1089876	0.1280281	0.1435093	0.157483	0.1703157	0.1819929	0.1935302	0.2040242	0.214883
1352	0.0304127	0.0545518	0.0781473	0.0990169	0.116905	0.1326432	0.1465323	0.1595079	0.1721026	0.1839328	0.1951214
1354	0.0142381	0.0324154	0.0535344	0.0740427	0.0928706	0.1097436	0.1246212	0.1387139	0.1518107	0.164377	0.1764694
1356	0.0062629	0.018503	0.0353137	0.0535516	0.0718873	0.0889347	0.1042951	0.1189882	0.1329696	0.1459802	0.1585712
1358	0.0028456	0.010378	0.0226535	0.0379484	0.0542709	0.0706462	0.0866761	0.1013879	0.1155902	0.1288814	0.1418566
1360	0.0014293	0.0058971	0.0144797	0.0263963	0.0405439	0.0556019	0.0706377	0.0853745	0.0995941	0.1133061	0.1263559
1362	0.0008102	0.0035592	0.0094086	0.0184599	0.0300767	0.0431974	0.0573684	0.0713103	0.0852224	0.0988323	0.1120982
1364	0.0005239	0.0023433	0.0063768	0.0130641	0.0223156	0.0336026	0.0459942	0.0591966	0.072535	0.0858913	0.0991105
1366	0.0004005	0.0017191	0.0046437	0.0096053	0.0168455	0.0261445	0.0371891	0.0489713	0.0615082	0.074499	0.0874073
1368	0.0004012	0.0014799	0.0036575	0.0073956	0.0130288	0.0206126	0.0299185	0.0406739	0.0522715	0.0642654	0.0767244
1370	0.0005636	0.0014701	0.0030774	0.0058932	0.0103201	0.0165621	0.0245355	0.0337632	0.0443607	0.0557289	0.0675749
1372	0.0009404	0.0015539	0.0026994	0.0048399	0.0083537	0.0135114	0.0201836	0.028351	0.0378167	0.0483198	0.0594067
1374	0.0014192	0.0016014	0.0024192	0.004125	0.0070179	0.0113105	0.016996	0.0241726	0.0326015	0.0421468	0.0526094
1376	0.0016676	0.001594	0.002231	0.003644	0.0060972	0.0096853	0.0145783	0.0208865	0.0285095	0.0371135	0.0470446
1378	0.0016852	0.0015866	0.0021443	0.0033953	0.0054787	0.0085376	0.012875	0.0184189	0.0252521	0.0333551	0.0422214
1380	0.0014602	0.0015897	0.0021504	0.0032719	0.005076	0.0077918	0.0115958	0.0166046	0.0227671	0.0301339	0.0384081
1382	0.0010137	0.0015697	0.0021974	0.0032229	0.0048906	0.0073645	0.0108414	0.0153163	0.0209985	0.0275617	0.0354761
1384	0.000811	0.0015219	0.002232	0.0032371	0.0048193	0.0071201	0.0103153	0.0144592	0.019641	0.025969	0.0333138
1386	0.0009954	0.0015185	0.0022566	0.0033229	0.0048795	0.0071292	0.0101317	0.0139677	0.0188721	0.0248549	0.0316877
1388	0.0011708	0.0016014	0.0023637	0.0034882	0.0050782	0.0072545	0.010096	0.013873	0.0185449	0.0241043	0.0306751
1390	0.0013157	0.0018242	0.0025927	0.0037751	0.0053743	0.0075509	0.0103782	0.0140049	0.018434	0.0236891	0.0300814
1392	0.0015885	0.0022424	0.0029937	0.0041538	0.0057953	0.007999	0.0108633	0.0145113	0.0188976	0.0242618	0.0301361
1394	0.0020168	0.0027572	0.0035102	0.0046717	0.0063697	0.0086618	0.0116529	0.0152529	0.0195276	0.0247375	0.030541
1396	0.0024778	0.0032968	0.0040858	0.0053334	0.0071668	0.0095607	0.0125728	0.0162452	0.0205968	0.0254218	0.0312789
1398	0.0033048	0.0039044	0.004763	0.0061754	0.0081878	0.0107319	0.0139345	0.0175907	0.0219286	0.0267003	0.0324762
1400	0.0043145	0.0045843	0.0055801	0.0072736	0.0095221	0.0122437	0.0154714	0.0193215	0.0235904	0.0288533	0.0341364

Table 5.48. α for 1300-1400 nm with b of 3,3 comparison run.

alpha:	10	15	20	25	30	35	40	45	50	55	60
1300	0.0498015	0.0528713	0.0569385	0.0620774	0.0680172	0.0747579	0.0824878	0.0907755	0.0997451	0.1088395	0.1189329
1302	0.0598319	0.0618198	0.0657064	0.0708266	0.076907	0.083915	0.092059	0.1008095	0.1100989	0.1201438	0.1302928
1304	0.0695951	0.0713434	0.075148	0.0801912	0.086585	0.0940445	0.1025672	0.1118224	0.1217381	0.1322737	0.142719
1306	0.0798973	0.0815553	0.0852154	0.0903927	0.0971362	0.1052074	0.1141803	0.1239129	0.1342272	0.1449947	0.1562036
1308	0.0893199	0.0921018	0.0957608	0.1014073	0.1086453	0.1174264	0.1268718	0.137252	0.1481933	0.159239	0.1709238
1310	0.0994703	0.1022517	0.1067026	0.113218	0.1212534	0.1308077	0.1409236	0.1518843	0.1633875	0.1753355	0.1869755
1312	0.1094572	0.1123016	0.118319	0.1259978	0.1350963	0.145398	0.1564385	0.1680063	0.1798198	0.1924179	0.2043208
1314	0.1181236	0.1236968	0.1310118	0.1399446	0.1503564	0.1615016	0.173421	0.1856346	0.1981699	0.2102993	0.2233335
1316	0.130508	0.1366335	0.1450043	0.1556208	0.1672661	0.1793113	0.192081	0.2048642	0.2178486	0.2307822	0.2438255
1318	0.1430527	0.1503856	0.1608191	0.1732736	0.1860341	0.1990865	0.2125269	0.2259481	0.239679	0.2533568	0.2660432
1320	0.1549682	0.1655015	0.1791089	0.1930493	0.2067666	0.220682	0.2347817	0.2490809	0.2632464	0.2771926	0.290302
1322	0.1710258	0.1848336	0.2006304	0.2151553	0.2295088	0.2441803	0.2592121	0.2743383	0.2889394	0.3025378	0.3162777
1324	0.1930003	0.2102731	0.2252454	0.2393028	0.2543974	0.2702155	0.2862858	0.3023461	0.3174741	0.3319097	0.3444825
1326	0.2232743	0.2396719	0.2518022	0.2657309	0.2817251	0.298938	0.316494	0.3330267	0.348315	0.362784	0.3747283
1328	0.2620893	0.2693044	0.2794591	0.2946541	0.3125549	0.3314337	0.3501107	0.3673368	0.3825966	0.3955951	0.407004
1330	0.3019403	0.2984223	0.3095198	0.3273477	0.3479194	0.368635	0.3879541	0.4048029	0.4195525	0.4308774	0.4412565
1332	0.3344353	0.330259	0.3444811	0.3658622	0.3893434	0.4110495	0.4303623	0.446411	0.4590712	0.4701174	0.4773975
1334	0.359824	0.3664329	0.3869499	0.4123306	0.4376434	0.4596383	0.4772404	0.4912733	0.5022619	0.5106397	0.515745
1336	0.3771948	0.4075462	0.438769	0.4679992	0.4934488	0.5136415	0.5294052	0.540372	0.5478456	0.5524699	0.5558165
1338	0.4012668	0.4568435	0.500463	0.5330857	0.5568414	0.5742705	0.5854099	0.5928177	0.5969591	0.5978147	0.5980005
1340	0.4542851	0.5221532	0.5732992	0.6070233	0.6277888	0.6399607	0.6463826	0.6488101	0.6480537	0.6457825	0.6417514
1342	0.5450959	0.6112987	0.660298	0.6900885	0.7052359	0.7110177	0.7108005	0.7075806	0.7016807	0.6950919	0.6869807
1344	0.6807038	0.7300365	0.764489	0.7829795	0.7892893	0.7870548	0.7796283	0.7694294	0.7582361	0.7454656	0.7342748
1346	0.8691155	0.881762	0.8888568	0.8879456	0.8803401	0.8672155	0.8512908	0.8342723	0.8167196	0.7999701	0.7830548
1348	1.1198683	1.0706223	1.0347587	1.0065922	0.9802185	0.953789	0.9281973	0.9021853	0.8783917	0.8556466	0.833336
1350	1.4317294	1.2965422	1.2053369	1.1401089	1.0896335	1.0460743	1.0075184	0.9734485	0.9416822	0.9129603	0.8859705
1352	1.8060987	1.5579444	1.3999444	1.2906069	1.2096438	1.1463717	1.0935066	1.0485318	1.0080472	0.972098	0.9403455
1354	2.22334	1.8534228	1.6171185	1.4563361	1.340732	1.2537884	1.1847169	1.1270386	1.078045	1.0357306	0.9965464
1356	2.6777494	2.1699154	1.8506778	1.636459	1.4825943	1.3691639	1.2826061	1.2114881	1.1514308	1.1009071	1.0556184
1358	3.1167436	2.4889464	2.0926304	1.8241428	1.634056	1.4928278	1.3837955	1.2990698	1.2284076	1.1683068	1.1167221
1360	3.4877613	2.788101	2.3292859	2.0157104	1.7883528	1.6195167	1.493132	1.3918953	1.3093351	1.239396	1.1797734
1362	3.7799997	3.0449493	2.5489178	2.1987748	1.9432445	1.7521883	1.6040343	1.4882923	1.3929281	1.3134555	1.2445588
1364	3.9885681	3.2472625	2.7381878	2.3697805	2.0951748	1.8836186	1.7198508	1.5871406	1.4787092	1.3881307	1.3106956
1366	4.0885067	3.3791089	2.884042	2.5193939	2.2368946	2.0138314	1.8313217	1.6868074	1.5660498	1.4633958	1.3776286
1368	4.0277548	3.4169614	2.9854627	2.6452003	2.3652015	2.1356626	1.9430683	1.7836262	1.6516609	1.5416528	1.4460034
1370	3.7980649	3.3805234	3.0524299	2.7512934	2.4794693	2.2450178	2.0442586	1.8787192	1.7363822	1.6155944	1.512255
1372	3.5010831	3.3234403	3.1011715	2.8389032	2.579396	2.3432899	2.1408689	1.9665999	1.81701	1.6878456	1.5781856
1374	3.2665987	3.293488	3.1422462	2.9060831	2.6580508	2.4249599	2.2235773	2.0452821	1.8905855	1.7567157	1.6397648
1376	3.1938798	3.2932358	3.1697121	2.9539664	2.7168779	2.4939594	2.2953413	2.1152096	1.9567019	1.8203601	1.6957247
1378	3.2479959	3.2989924	3.1758566	2.9757071	2.7571268	2.5476687	2.3502793	2.1734378	2.0142181	1.8712493	1.7482095
1380	3.3726196	3.3020363	3.1634417	2.9801884	2.7820919	2.5845487	2.3950863	2.2193615	2.0619872	1.9186124	1.7930405
1382	3.5661035	3.3128006	3.1479571	2.976361	2.790786	2.6049473	2.420023	2.2528126	2.0966516	1.9589812	1.8293881
1384	3.6657276	3.3313248	3.1420739	2.9699588	2.790895	2.6126781	2.4375103	2.274008	2.1226368	1.9838459	1.8567041
1386	3.5309126	3.3315885	3.1414404	2.9589648	2.7806802	2.6049261	2.4375782	2.2833815	2.1363988	1.9985746	1.8764713
1388	3.3511925	3.2978106	3.1217251	2.9379182	2.7587767	2.5883598	2.4328279	2.2794647	2.1376953	2.0082686	1.8869579
1390	3.266417	3.223774	3.0725515	2.8977838	2.72755	2.56302	2.4108543	2.2669752	2.1335223	2.0095239	1.8901687
1392	3.1939905	3.117486	2.9947083	2.8435013	2.6850107	2.5290728	2.3830121	2.2423375	2.11342	1.9903915	1.883067
1394	3.1060863	3.0159335	2.9086115	2.7764103	2.6308806	2.4839642	2.3399806	2.2101479	2.0890782	1.9734893	1.8697388
1396	3.080132	2.9323907	2.8270731	2.7020879	2.5643551	2.427984	2.2956879	2.1709397	2.0557971	1.9531077	1.8508211
1398	2.9538693	2.8511229	2.7472401	2.6230009	2.4895864	2.3613155	2.2354774	2.1236184	2.0166442	1.9212562	1.8253305
1400	2.8046751	2.7668712	2.6639841	2.535476	2.4064491	2.2868171	2.1762915	2.0693488	1.973702	1.8748125	1.7940258

Table 5.49. β for 1300-1400 nm with b of 3.3 comparison run.

beta:	10	15	20	25	30	35	40	45	50	55	60
1300	0.9328249	0.8942651	0.8495526	0.8069648	0.7679437	0.7319999	0.700629	0.6725039	0.6475784	0.6260245	0.6065843
1302	0.9237518	0.8886498	0.8467898	0.8058631	0.7668654	0.7311192	0.6989131	0.670514	0.6453182	0.6228324	0.6035957
1304	0.9144655	0.8829991	0.8441092	0.8040286	0.7651032	0.7296715	0.6966093	0.6678532	0.6425217	0.6199074	0.6002424
1306	0.9051011	0.8778785	0.8408707	0.8014846	0.762623	0.7268435	0.693691	0.6645101	0.6387981	0.6164621	0.5962961
1308	0.8987409	0.8731292	0.8374427	0.7983021	0.7593892	0.7231042	0.6899141	0.6606367	0.6346986	0.6118329	0.5919716
1310	0.8931504	0.868863	0.8333612	0.7944505	0.7554357	0.718469	0.685525	0.6560224	0.6298155	0.6068987	0.5872717
1312	0.8898227	0.8643404	0.8288889	0.7899633	0.7506839	0.7134072	0.6805581	0.6508311	0.6245658	0.601922	0.5819553
1314	0.8872865	0.8600276	0.8240116	0.7846861	0.7451257	0.7078822	0.6745555	0.6448259	0.6188188	0.5963337	0.5765213
1316	0.8842148	0.8562474	0.8186353	0.778565	0.738728	0.7015286	0.6678562	0.6379668	0.6120615	0.5893227	0.570513
1318	0.8817551	0.8518707	0.8129232	0.7717373	0.7314579	0.6945809	0.660225	0.6304369	0.604856	0.5828825	0.5642133
1320	0.8783738	0.8466587	0.8063115	0.7641565	0.7232087	0.6857291	0.651571	0.622232	0.596778	0.5760163	0.5579442
1322	0.8743511	0.8402169	0.7990364	0.7558955	0.7138608	0.675573	0.641907	0.6131521	0.588694	0.5685858	0.551262
1324	0.8697224	0.8336812	0.7908999	0.7461314	0.7032394	0.6642849	0.6316274	0.6037041	0.58022	0.5604734	0.5447825
1326	0.8635114	0.826418	0.7813659	0.734684	0.691045	0.6522369	0.6205969	0.5935213	0.5712714	0.5528601	0.5383432
1328	0.856725	0.817857	0.7698243	0.7212886	0.6775942	0.6398242	0.6089423	0.5834538	0.5625172	0.5459293	0.5320523
1330	0.8499326	0.8071525	0.7562584	0.706276	0.6629063	0.6268359	0.5969804	0.5729484	0.5536359	0.5382019	0.5260199
1332	0.8413124	0.7946303	0.7404911	0.6900142	0.6475025	0.6135955	0.5850964	0.5629548	0.5452551	0.5310336	0.5203515
1334	0.8307206	0.77922	0.7224265	0.6724383	0.6313964	0.5993899	0.5730383	0.5529208	0.537445	0.5250511	0.5154407
1336	0.8161646	0.75948	0.7020117	0.6533932	0.6148875	0.5848421	0.5619464	0.5438511	0.5300222	0.5201194	0.5110831
1338	0.7955191	0.7347061	0.6789586	0.6334146	0.59833	0.5708562	0.5508283	0.5354214	0.5235885	0.5141002	0.5076435
1340	0.7701718	0.706021	0.6541258	0.613265	0.5823405	0.5580375	0.5413072	0.5280788	0.5177783	0.5101617	0.5048618
1342	0.7382675	0.6760976	0.6292371	0.5938278	0.5670841	0.5470775	0.5323576	0.5216773	0.513511	0.5078118	0.502749
1344	0.7039667	0.6476772	0.6056113	0.575614	0.553288	0.5375219	0.5254678	0.5165939	0.510357	0.505919	0.5015981
1346	0.6730704	0.6213127	0.5846535	0.5594734	0.5414398	0.5296614	0.5193662	0.5128782	0.5080116	0.5034805	0.5010571
1348	0.6449862	0.5983021	0.5672787	0.5462257	0.5322368	0.5229409	0.5158624	0.5105341	0.506822	0.5032602	0.5010604
1350	0.6182586	0.5804563	0.5544993	0.5364933	0.525704	0.518196	0.5129623	0.5095192	0.5062736	0.5047212	0.5018463
1352	0.6003586	0.568268	0.545535	0.5308527	0.5219886	0.5156881	0.5126474	0.5097469	0.5071018	0.5051007	0.5030168
1354	0.5901439	0.5600427	0.5402079	0.5286529	0.5210513	0.5157831	0.5134242	0.5107787	0.5086807	0.5058945	0.5044917
1356	0.5816233	0.5543889	0.5383711	0.5292864	0.5226588	0.518387	0.5158376	0.5130806	0.5105719	0.5082954	0.5065314
1358	0.5749988	0.5527251	0.5400162	0.5317134	0.5264657	0.5223993	0.5183368	0.5155411	0.5127614	0.511308	0.5087668
1360	0.573714	0.5555982	0.5441626	0.5365937	0.5311542	0.5269999	0.5222549	0.5186387	0.5154483	0.5130363	0.5111678
1362	0.5761183	0.5607834	0.5503873	0.5428941	0.5366291	0.5315669	0.5258379	0.5219496	0.5186229	0.5156134	0.5137212
1364	0.5813503	0.5673266	0.5580659	0.5503218	0.542515	0.5357348	0.5301645	0.5254295	0.5219408	0.5188686	0.5164216
1366	0.5906088	0.5765041	0.5662175	0.5569468	0.5478802	0.5398402	0.5337446	0.5290918	0.5251876	0.5221003	0.5192702
1368	0.6040533	0.5875382	0.5743355	0.5624264	0.5526502	0.5439	0.538081	0.5326533	0.5283628	0.5250522	0.5226073
1370	0.6170484	0.5982196	0.5817358	0.5678129	0.5573109	0.5483551	0.5419192	0.5368252	0.5320842	0.5284883	0.5257701
1372	0.6266351	0.605955	0.5877081	0.573538	0.5624737	0.5534616	0.5466021	0.540976	0.5362468	0.5325642	0.5294387
1374	0.6343352	0.609944	0.5924444	0.5791388	0.5676896	0.5591224	0.5513312	0.5451142	0.5404513	0.5363234	0.5329529
1376	0.6321595	0.6106764	0.5966772	0.5845872	0.5732165	0.564555	0.5560656	0.5495591	0.5441435	0.5397716	0.5363243
1378	0.615366	0.609736	0.6008077	0.5892994	0.5787239	0.5695874	0.5608968	0.5539509	0.5482987	0.5437129	0.5402333
1380	0.6012967	0.6086249	0.6039517	0.5938413	0.5837668	0.5738088	0.5653322	0.5582479	0.5522413	0.5477471	0.5440112
1382	0.6000273	0.6074458	0.605204	0.5974052	0.5873162	0.5771667	0.5695403	0.5623944	0.5563212	0.5516935	0.5476531
1384	0.6039372	0.6067187	0.6045847	0.5986694	0.5897907	0.5807034	0.5729407	0.5663286	0.5607209	0.5551762	0.5511473
1386	0.6114613	0.6069619	0.6031272	0.5978797	0.5910079	0.5831733	0.576481	0.5699844	0.5640411	0.5593102	0.5548007
1388	0.6373857	0.6087557	0.6019062	0.5966033	0.5913534	0.5857655	0.5789562	0.5729959	0.5674893	0.5624297	0.5582519
1390	0.6448304	0.6108108	0.6023347	0.5963193	0.5918978	0.5872909	0.5817391	0.5759816	0.5706372	0.5660963	0.5617959
1392	0.6390101	0.6110415	0.6034395	0.5977983	0.592975	0.5886255	0.5831633	0.5783221	0.5735748	0.5689756	0.56475
1394	0.6300572	0.6098099	0.6047179	0.5998192	0.5946572	0.5898748	0.5855159	0.5807009	0.5765668	0.5719729	0.5677397
1396	0.6069949	0.6073516	0.6058111	0.6017646	0.5964912	0.5914978	0.587244	0.5831741	0.5787723	0.5746837	0.5707465
1398	0.6003218	0.6055842	0.6061425	0.6029465	0.598539	0.5939339	0.589791	0.5854824	0.5814662	0.5774063	0.5734479
1400	0.6039894	0.6061487	0.6067924	0.6040694	0.6003988	0.5962682	0.5916533	0.5876547	0.5834838	0.5799857	0.575855

Table 5.50. Transmission (TnoH2O) for 970-1070 nm with b of 2.0 comparison run.

tnoh2o:	10	15	20	25	30	35	40	45	50	55	60
970	0.9998599	0.9998535	0.9998436	0.9998279	0.9998056	0.9997767	0.9997438	0.9997106	0.9996799	0.9996522	0.9996259
972	0.9998778	0.9998693	0.9998575	0.9998397	0.9998149	0.9997845	0.9997517	0.9997194	0.9996886	0.9996589	0.9996287
974	0.9998911	0.9998813	0.9998661	0.9998443	0.9998162	0.9997852	0.9997547	0.9997252	0.9996957	0.9996644	0.99963
976	0.9998992	0.9998875	0.9998677	0.9998404	0.9998097	0.9997807	0.9997543	0.9997284	0.9997001	0.9996674	0.9996284
978	0.9999012	0.9998856	0.9998595	0.9998273	0.9997975	0.9997734	0.9997522	0.9997294	0.9997016	0.9996663	0.9996223
980	0.9998949	0.999872	0.9998387	0.9998062	0.9997827	0.9997656	0.9997489	0.9997277	0.9996987	0.99966	0.99961
982	0.9998761	0.9998423	0.9998057	0.9997819	0.9997687	0.9997582	0.9997442	0.9997225	0.9996907	0.999647	0.99959
984	0.999837	0.9997935	0.999768	0.9997596	0.9997566	0.9997505	0.9997367	0.9997127	0.9996765	0.9996264	0.999561
986	0.9997647	0.999736	0.9997346	0.9997417	0.9997456	0.999741	0.9997253	0.9996971	0.9996544	0.9995964	0.9995212
988	0.9996726	0.9996864	0.9997092	0.999727	0.9997337	0.9997278	0.9997084	0.9996741	0.9996237	0.9995557	0.9994692
990	0.9995982	0.9996511	0.9996909	0.9997131	0.999719	0.9997096	0.9996844	0.9996423	0.9995819	0.9995028	0.9994034
992	0.999555	0.9996307	0.9996758	0.999697	0.9996997	0.9996846	0.9996516	0.9995997	0.9995281	0.999436	0.9993218
994	0.9995524	0.9996216	0.9996608	0.9996774	0.9996741	0.999651	0.9996079	0.9995447	0.9994602	0.9993534	0.9992225
996	0.9995971	0.9996219	0.9996457	0.9996533	0.9996405	0.9996066	0.9995517	0.9994754	0.9993761	0.9992526	0.9991031
998	0.9996607	0.9996359	0.9996324	0.9996234	0.9995967	0.9995495	0.9994808	0.9993898	0.999274	0.9991315	0.9989609
1000	0.9997069	0.9996588	0.9996215	0.9995867	0.999541	0.9994779	0.9993937	0.9992856	0.9991506	0.9989871	0.9987928
1002	0.9997261	0.9996709	0.9996063	0.9995415	0.9994726	0.9993905	0.9992881	0.9991604	0.9990037	0.9988161	0.9985957
1004	0.9997121	0.9996552	0.9995739	0.9994841	0.9993905	0.9992861	0.9991618	0.9990112	0.9988297	0.998615	0.998366
1006	0.9996614	0.9996021	0.9995131	0.9994076	0.9992913	0.9991617	0.9990118	0.9988346	0.9986249	0.9983804	0.9980998
1008	0.9995791	0.9995095	0.9994184	0.9993042	0.9991689	0.9990134	0.9988346	0.998627	0.9983855	0.998108	0.9977931
1010	0.9994588	0.9993821	0.9992883	0.9991669	0.9990152	0.9988346	0.9986249	0.9983838	0.9981069	0.9977931	0.9974419
1012	0.9992954	0.9992217	0.9991223	0.9989908	0.9988227	0.9986179	0.9983768	0.9980995	0.9977843	0.9974315	0.9970416
1014	0.999091	0.9990239	0.9989172	0.9987717	0.9985853	0.9983556	0.9980822	0.9977677	0.9974126	0.9970186	0.9965877
1016	0.9988512	0.9987826	0.9986669	0.9985054	0.9982973	0.9980401	0.9977339	0.9973813	0.996985	0.9965485	0.996075
1018	0.9985735	0.9984937	0.9983653	0.9981858	0.9979525	0.9976647	0.9973239	0.9969333	0.9964951	0.9960145	0.9954984
1020	0.998254	0.9981534	0.9980075	0.9978056	0.9975433	0.9972224	0.9968463	0.9964164	0.9959347	0.9954095	0.9948528
1022	0.9978801	0.9977584	0.9975877	0.9973567	0.9970621	0.9967073	0.9962939	0.9958227	0.9952963	0.9947269	0.9941342
1024	0.9974405	0.9972993	0.9970972	0.9968306	0.9965024	0.9961133	0.9956599	0.9951435	0.9945714	0.9939635	0.9933405
1026	0.9969234	0.9967611	0.9965231	0.9962208	0.9958594	0.9954327	0.9949337	0.9943693	0.9937534	0.9931126	0.9924724
1028	0.9963168	0.9961254	0.9958531	0.9955224	0.9951265	0.9946552	0.9941053	0.9934914	0.9928374	0.9921731	0.991534
1030	0.9956042	0.9953736	0.9950836	0.9947287	0.9942921	0.9937665	0.9931614	0.992503	0.9918203	0.991152	0.9905343
1032	0.9947523	0.9945093	0.9942122	0.9938272	0.993339	0.9927518	0.9920957	0.9914016	0.9907091	0.9900604	0.9894865
1034	0.9937625	0.9935403	0.9932283	0.9927984	0.9922466	0.9915996	0.9908996	0.9901886	0.9895085	0.9889067	0.9884089
1036	0.9926652	0.9924568	0.9921112	0.9916167	0.9909968	0.9903017	0.9895767	0.9888717	0.9882371	0.9877108	0.9873236
1038	0.9914556	0.9912369	0.9908276	0.9902553	0.9895794	0.9888549	0.9881284	0.9874659	0.9869141	0.9865055	0.9862552
1040	0.9901243	0.9898422	0.9893389	0.9887016	0.9879906	0.9872605	0.9865732	0.9859954	0.985569	0.9853165	0.9852285
1042	0.9886596	0.9882154	0.9876297	0.9869531	0.9862307	0.9855325	0.9849334	0.9844933	0.9842398	0.9841725	0.9842662
1044	0.986936	0.9863397	0.9857065	0.9850092	0.9843106	0.9836996	0.9832503	0.9830008	0.9829581	0.9830976	0.9833857
1046	0.9848247	0.9842362	0.983564	0.9828749	0.9822602	0.9818057	0.981571	0.9815636	0.9817653	0.9821251	0.9825984
1048	0.9824287	0.981864	0.9811951	0.9805813	0.9801314	0.9799121	0.9799528	0.9802262	0.9806823	0.9812612	0.9819093
1050	0.9797012	0.9791886	0.9786206	0.9781873	0.9779944	0.9780886	0.9784546	0.9790258	0.9797324	0.9805127	0.9813184
1052	0.9766075	0.9762353	0.9759053	0.9757702	0.975936	0.9764117	0.9771236	0.9779866	0.9789236	0.9798763	0.9808217
1054	0.9732609	0.973117	0.9731444	0.9734348	0.9740529	0.9749442	0.975996	0.977119	0.9782522	0.9793586	0.9804141
1056	0.9698699	0.9700075	0.9704768	0.9713094	0.9724346	0.9737293	0.97508	0.9764234	0.9777202	0.9789459	0.9800895
1058	0.9665225	0.967092	0.968112	0.9695342	0.9711426	0.9727822	0.9743801	0.9758937	0.9773121	0.9786274	0.9798427
1060	0.9634012	0.9645932	0.9662707	0.9682178	0.9702049	0.9721041	0.9738819	0.9755211	0.9770271	0.9784052	0.9796689
1062	0.9609498	0.9628158	0.9650931	0.9674084	0.9696298	0.971692	0.9735827	0.9752975	0.9768579	0.978275	0.979565
1064	0.9596311	0.9620416	0.9646202	0.9671035	0.9694166	0.9715396	0.9734703	0.9752169	0.9767963	0.9782314	0.9795287
1066	0.9598243	0.9623257	0.9648525	0.9672874	0.969558	0.9716458	0.9735496	0.9752774	0.9768472	0.9782641	0.9795586
1068	0.9614451	0.963572	0.96577	0.9679528	0.9700457	0.9720055	0.9738154	0.9754803	0.9770019	0.9783894	0.9796549
1070	0.9642969	0.9656569	0.9673138	0.9690824	0.9708747	0.9726202	0.9742785	0.9758295	0.9772705	0.9785998	0.9798189

Table 5.51. α for 970-1070 nm with b of 2.0 comparison run.

alpha:	10	15	20	25	30	35	40	45	50	55	60
970	0.1603764	0.1855026	0.2014947	0.2124535	0.2213816	0.2301097	0.2366839	0.2433852	0.2490211	0.2531349	0.2563364
972	0.1395676	0.1585341	0.1723536	0.1837269	0.1934593	0.2027718	0.2115558	0.2195319	0.2267625	0.2327852	0.2375107
974	0.1315341	0.1357625	0.1457719	0.1564142	0.1668419	0.1767743	0.186929	0.1964183	0.2049762	0.2125293	0.2187374
976	0.129082	0.1196511	0.1226781	0.1315263	0.1420405	0.1526072	0.1639826	0.1742773	0.1839492	0.1928908	0.2001195
978	0.1199618	0.1079315	0.1046262	0.1100812	0.1197735	0.1305646	0.1422116	0.1532816	0.1636301	0.1728861	0.181893
980	0.1007827	0.0952896	0.090954	0.0929114	0.1006224	0.1110636	0.1223401	0.1336489	0.1446322	0.1546555	0.1642243
982	0.0764381	0.0790232	0.0786276	0.079605	0.0849416	0.0940096	0.1043609	0.11555	0.1266493	0.1375905	0.1472333
984	0.0551327	0.0609479	0.0654771	0.0682232	0.0723254	0.0796541	0.0886933	0.0992159	0.1100875	0.1208216	0.1311197
986	0.0366907	0.044693	0.0516708	0.0570749	0.0616547	0.0675887	0.0753301	0.0847962	0.0951467	0.1052889	0.1159512
988	0.0237263	0.0310021	0.0388294	0.0459517	0.0517997	0.0573206	0.0641433	0.0723398	0.0816751	0.0918067	0.1018517
990	0.0151363	0.0206297	0.0279818	0.03559	0.0423433	0.0482266	0.0545225	0.0617086	0.0700628	0.0796057	0.0889429
992	0.0097486	0.0136568	0.0196719	0.0266209	0.0335279	0.0398335	0.0461008	0.0525613	0.0599411	0.0680987	0.07729
994	0.0067826	0.0095085	0.0138468	0.0194195	0.0258041	0.0321857	0.0383139	0.0445121	0.0511781	0.0584902	0.0668944
996	0.0053174	0.0072733	0.0100009	0.0141382	0.0194646	0.0253793	0.0313077	0.0372638	0.0435157	0.0504678	0.0577058
998	0.0047604	0.0059066	0.0076299	0.0105401	0.0145776	0.0196167	0.0250134	0.0307315	0.0365951	0.0428974	0.049625
1000	0.004596	0.0050221	0.0062614	0.0081551	0.0110064	0.0149704	0.0197063	0.0249358	0.0304798	0.0360685	0.0424791
1002	0.0047029	0.0047897	0.0054257	0.0065594	0.0085105	0.0114541	0.0153622	0.0199602	0.0250061	0.0303798	0.0361403
1004	0.0051241	0.004912	0.0048932	0.005498	0.0068162	0.0089295	0.0120055	0.0158357	0.0202868	0.0253686	0.030495
1006	0.005367	0.0048894	0.0045935	0.0048296	0.0056896	0.0071891	0.0094758	0.0125378	0.0163178	0.0206218	0.0254993
1008	0.0047098	0.0046191	0.0044004	0.0044533	0.0049621	0.0059844	0.0076268	0.009981	0.0130761	0.0167384	0.0211313
1010	0.0043046	0.0041469	0.0041889	0.0042385	0.0044981	0.005144	0.00628	0.0080388	0.0104995	0.0136895	0.0173855
1012	0.0040631	0.0038179	0.0039315	0.004049	0.0041731	0.0045457	0.0053018	0.0065825	0.0084835	0.011089	0.0142363
1014	0.0034237	0.0036656	0.0037191	0.0038032	0.0038833	0.0040867	0.0045801	0.0054964	0.0069406	0.0089429	0.0116482
1016	0.0028577	0.0034202	0.0035375	0.0035348	0.0035801	0.0037087	0.0040318	0.0046833	0.0057665	0.0073461	0.0095611
1018	0.0027766	0.0030841	0.0032619	0.0032578	0.0032653	0.0033558	0.0035902	0.0040629	0.0048819	0.006177	0.0079028
1020	0.0029089	0.0028375	0.0028985	0.0029408	0.0029499	0.0030275	0.0032125	0.0035734	0.0042005	0.0051857	0.0066017
1022	0.0029002	0.0026631	0.0025574	0.0025819	0.0026295	0.002706	0.0028738	0.0031692	0.0036615	0.0044232	0.0055879
1024	0.0028457	0.0024632	0.0022711	0.0022405	0.0023077	0.0024056	0.0025701	0.002822	0.0032326	0.00385	0.0048001
1026	0.0024863	0.002213	0.0020211	0.0019596	0.0020105	0.0021212	0.0022821	0.0025167	0.0028643	0.0034188	0.0041875
1028	0.0019527	0.0018798	0.0017792	0.0017242	0.0017556	0.0018608	0.0020238	0.0022437	0.0025642	0.00303	0.0037102
1030	0.0013443	0.001483	0.0015127	0.0015104	0.0015388	0.0016344	0.0017783	0.0019985	0.0023025	0.0027165	0.0033393
1032	0.0008946	0.0010655	0.0012157	0.0012889	0.0013435	0.0014336	0.0015755	0.0017825	0.0020736	0.0024824	0.0030566
1034	0.0004848	0.000722	0.0009092	0.0010532	0.0011533	0.0012555	0.0013897	0.001598	0.001893	0.0023021	0.0028508
1036	0.0002596	0.0004357	0.0006375	0.0008159	0.0009599	0.0010865	0.001242	0.0014469	0.0017376	0.0021597	0.0027185
1038	0.0001354	0.0002453	0.0004137	0.0005969	0.0007684	0.0009284	0.0011011	0.0013279	0.0016411	0.0020576	0.0026607
1040	0.0000714	0.0001339	0.0002523	0.0004143	0.0005937	0.0007789	0.0009885	0.0012406	0.0015832	0.0020544	0.0026835
1042	0.0000396	0.0000737	0.0001509	0.0002782	0.0004493	0.0006505	0.0008887	0.0011875	0.0015778	0.0021141	0.002795
1044	0.0000223	0.0000432	0.0000938	0.0001919	0.0003456	0.0005553	0.000829	0.0011775	0.0016348	0.0022256	0.0030061
1046	0.000012	0.0000286	0.0000671	0.000147	0.0002883	0.000507	0.0008141	0.001225	0.0017555	0.0024273	0.0033283
1048	0.0000082	0.000025	0.0000607	0.0001366	0.0002795	0.0005182	0.0008676	0.0013483	0.0019775	0.0027848	0.0037773
1050	0.0000133	0.0000308	0.0000715	0.0001587	0.0003217	0.0005996	0.0010079	0.0015676	0.0022985	0.0032467	0.0043716
1052	0.0000252	0.0000476	0.0001025	0.0002157	0.0004235	0.0007622	0.0012445	0.0019011	0.00275	0.0037803	0.0051334
1054	0.0000454	0.0000801	0.0001616	0.0003197	0.0006012	0.0010171	0.0016056	0.0023668	0.0033444	0.0045619	0.0060907
1056	0.0000766	0.0001408	0.0002611	0.0004977	0.0008746	0.0013847	0.0020836	0.0029808	0.0041083	0.0055811	0.0072723
1058	0.0001518	0.0002325	0.0004362	0.0007813	0.001263	0.0018888	0.0027277	0.0037632	0.0050776	0.0066958	0.0087179
1060	0.0002407	0.0004024	0.0007303	0.001194	0.0017865	0.0025589	0.003512	0.0047374	0.0062634	0.0080933	0.0104662
1062	0.0004014	0.0007242	0.0011686	0.0017496	0.0024665	0.0033911	0.0045181	0.0059339	0.0077183	0.0099426	0.01257
1064	0.0007792	0.001225	0.0017786	0.0024626	0.0033263	0.0044147	0.0057166	0.0073881	0.0094459	0.0120284	0.0150861
1066	0.0014237	0.0019327	0.0025917	0.0033804	0.0043939	0.0056491	0.0072122	0.0091456	0.0115488	0.0143947	0.0180832
1068	0.0022857	0.0029028	0.0036345	0.0045494	0.0057052	0.0071481	0.0089807	0.0112545	0.0140583	0.0174961	0.021644
1070	0.0035966	0.0041288	0.0049386	0.0059862	0.007316	0.0089916	0.0111525	0.013782	0.0170802	0.021217	0.0258586

Table 5.52. β for 970-1070 nm with b of 2.0 comparison run.

beta:	10	15	20	25	30	35	40	45	50	55	60
970	0.5828863	0.5668604	0.5492131	0.5304258	0.5099713	0.488529	0.4688298	0.4501363	0.4337733	0.4191141	0.4074899
972	0.6040115	0.5840775	0.5631864	0.5393998	0.515682	0.4927012	0.4709648	0.4517389	0.4345254	0.4196209	0.40762
974	0.6136098	0.5996522	0.5763596	0.5494625	0.5229088	0.4983021	0.4754559	0.4549361	0.437094	0.4225945	0.4090308
976	0.6156488	0.6091985	0.5882057	0.5603917	0.5320767	0.5057247	0.4810233	0.4598852	0.4414512	0.4251552	0.4119411
978	0.6150151	0.6107184	0.5966139	0.5717335	0.542788	0.5148967	0.4892141	0.4668104	0.4474328	0.4305836	0.4162644
980	0.6164589	0.6094359	0.5999102	0.5813432	0.554082	0.5253565	0.4989991	0.4757213	0.4553361	0.437847	0.4219822
982	0.6304108	0.612386	0.6016893	0.5872082	0.5643225	0.537124	0.5110071	0.4866092	0.4648577	0.4460604	0.429146
984	0.650288	0.6262686	0.6066585	0.5907676	0.572683	0.5488731	0.5239564	0.4990656	0.4761351	0.4552702	0.4375392
986	0.6850929	0.6487383	0.6182671	0.5968897	0.5802296	0.5604249	0.5373605	0.5125892	0.4887123	0.4670408	0.4472608
988	0.7290902	0.6782731	0.6375232	0.6094349	0.5896816	0.5714868	0.5500498	0.5264741	0.5022855	0.4795704	0.4581989
990	0.7720765	0.7148066	0.6651346	0.6293086	0.6033856	0.583239	0.5627231	0.5400666	0.5162582	0.4917676	0.4701063
992	0.8118232	0.755263	0.7001764	0.6558943	0.6225675	0.5978031	0.5752134	0.553284	0.5297032	0.5058152	0.4827425
994	0.842425	0.7931021	0.7383092	0.6879672	0.6472214	0.6157716	0.5902302	0.5666316	0.5433043	0.5197529	0.4958861
996	0.8529653	0.8202866	0.7740819	0.7229645	0.6765659	0.6380207	0.6071054	0.5812244	0.5567873	0.5329032	0.5092627
998	0.851501	0.8346312	0.8031842	0.7570899	0.7084262	0.6637532	0.6281519	0.5978311	0.571579	0.546569	0.5225821
1000	0.844796	0.8428398	0.8224055	0.7863568	0.7399744	0.6924559	0.6514483	0.6171195	0.5877611	0.5615803	0.5360373
1002	0.8387501	0.8430327	0.8337526	0.808615	0.7684264	0.7222626	0.6779075	0.6388777	0.6055469	0.5765345	0.5497184
1004	0.8328195	0.840066	0.8396979	0.8237416	0.7919284	0.7505566	0.7045856	0.6626198	0.6254551	0.5923082	0.564069
1006	0.8345014	0.8391497	0.8420062	0.8332093	0.8098642	0.7748239	0.7311396	0.6872551	0.646526	0.6110836	0.5792751
1008	0.844743	0.8420709	0.8429905	0.8385427	0.8225385	0.7938902	0.7547408	0.7114167	0.6686316	0.6301689	0.5955205
1010	0.8512084	0.8490096	0.8449991	0.8416282	0.8309917	0.808388	0.7753221	0.7339988	0.6906921	0.6489413	0.6126741
1012	0.8534195	0.8535847	0.8491006	0.844359	0.8365868	0.8190281	0.7915977	0.7540698	0.7115961	0.6692117	0.6306128
1014	0.8617246	0.8555789	0.8529569	0.8480504	0.8411178	0.8273539	0.8046161	0.7711257	0.7311108	0.6897261	0.6488304
1016	0.8690603	0.8595009	0.8555704	0.852091	0.8454046	0.8338377	0.8141349	0.7851161	0.7481814	0.7078223	0.6668607
1018	0.8706731	0.8638522	0.859413	0.8558023	0.8493903	0.8392995	0.8217459	0.796424	0.7630107	0.7236111	0.6842762
1020	0.864053	0.8670771	0.8644419	0.8592978	0.8529101	0.843403	0.8275899	0.805436	0.7755401	0.7395131	0.7005406
1022	0.8627547	0.8686922	0.8683846	0.8631555	0.8561227	0.8468816	0.832769	0.812718	0.7857941	0.7531997	0.7153048
1024	0.8656845	0.8693236	0.8701655	0.8665762	0.859326	0.8497778	0.8368012	0.8187679	0.7942386	0.7634786	0.7283006
1026	0.8701311	0.8704691	0.8703808	0.8684031	0.8621591	0.8525612	0.8407841	0.8237398	0.8012261	0.7720633	0.7393338
1028	0.8760579	0.8724285	0.8706492	0.8688374	0.8641282	0.8554642	0.8436823	0.8277672	0.8063702	0.7799475	0.7482652
1030	0.8903351	0.8763444	0.8719571	0.8688623	0.8651137	0.8576728	0.8467101	0.8309703	0.8105921	0.785417	0.7550193
1032	0.900557	0.8860241	0.8751661	0.8698878	0.8657506	0.8593087	0.8481492	0.8330974	0.8131914	0.7880079	0.7593187
1034	0.9187916	0.8965128	0.8818164	0.8726664	0.8666028	0.8599929	0.8493884	0.8341132	0.8140138	0.7893903	0.7610558
1036	0.9308414	0.9094137	0.8903843	0.8774541	0.8683095	0.8603384	0.848866	0.8335952	0.813395	0.7883735	0.7598593
1038	0.9460889	0.9213439	0.8998557	0.883694	0.8712391	0.8604268	0.8481793	0.8313465	0.8098089	0.784745	0.7555519
1040	0.9629796	0.9328329	0.9093481	0.8900726	0.8748174	0.8605015	0.8454714	0.8268442	0.8036963	0.7768962	0.7478828
1042	0.9736848	0.945825	0.9178454	0.8961727	0.877775	0.8599042	0.8413561	0.8195994	0.7944648	0.7661704	0.7369875
1044	0.9812785	0.9564297	0.9258749	0.9003235	0.8779443	0.8563983	0.8334459	0.8087534	0.781617	0.753303	0.7231457
1046	0.9853494	0.9631072	0.9314119	0.900829	0.8732418	0.8475198	0.8211239	0.793922	0.7657589	0.7369332	0.7070841
1048	0.9889441	0.9655556	0.9319142	0.895765	0.8628749	0.8329514	0.804292	0.7756282	0.7468918	0.717295	0.6895313
1050	0.9902019	0.9649333	0.926527	0.8860796	0.8489377	0.8150164	0.7843649	0.7551599	0.7264617	0.6979394	0.6713189
1052	0.9881408	0.9601429	0.9181994	0.8743861	0.8336538	0.7973862	0.7648338	0.7344935	0.7062176	0.6802011	0.6532257
1054	0.9830813	0.950834	0.9082193	0.8612141	0.8182506	0.7802551	0.7453285	0.7149284	0.68715	0.6608677	0.63572
1056	0.9737099	0.9400098	0.8943719	0.8461517	0.8022515	0.7629161	0.7280896	0.6973719	0.6699756	0.6431789	0.6192822
1058	0.9592161	0.9268941	0.8760447	0.8289252	0.7848388	0.7455436	0.7111822	0.6817249	0.6544121	0.629533	0.6038073
1060	0.950143	0.9057158	0.8557685	0.8091348	0.7660078	0.7283121	0.6969454	0.6676723	0.6406234	0.61518	0.5894181
1062	0.9306571	0.8805169	0.8342519	0.7872403	0.7473031	0.7134321	0.683027	0.6546443	0.6271563	0.6004118	0.5758278
1064	0.8992719	0.8566343	0.8091693	0.7657576	0.7304347	0.6995366	0.6704879	0.6423152	0.6150016	0.5883043	0.5629511
1066	0.8726047	0.8292609	0.7824988	0.7465685	0.715533	0.686524	0.6580747	0.630243	0.602966	0.5772306	0.5506208
1068	0.8458301	0.7967671	0.7596415	0.7301938	0.701918	0.6740975	0.6460956	0.6184355	0.5911105	0.5646459	0.5385898
1070	0.8043371	0.7690552	0.7420179	0.7156452	0.6887257	0.6615148	0.6340292	0.6068168	0.5798922	0.551955	0.5266889

Chapter 6

Strategy and Requirements for the PACE OCI Solar Calibration

Gerhard Meister, NASA Goddard Space Flight Center, Greenbelt, Maryland [6]

Robert E. Eplee, Science Applications International Corporation, Reston, Virginia

Executive Summary

The Phytoplankton, Aerosol, Cloud, ocean Ecosystem (PACE) Ocean Color Instrument (OCI) has a threshold requirement to perform daily solar calibrations. Solar calibration has been a major component of the calibration strategy for every NASA ocean color mission. This paper presents an overview of the planned PACE OCI solar calibration strategy and the specific requirements to enable accurate calibration results. The document describes how on-orbit solar diffuser measurements, using daily and monthly solar diffusers, will be used, in conjunction with lunar observations, to trend the radiometric gain changes of the OCI instrument.

6.1. Introduction

The primary radiometric stability monitors for NASA and ESA ocean color missions for the past 20 years have been solar calibrations, through observations of sunlight reflected by solar diffusers, and lunar calibrations. Solar diffuser observations provide daily measurements of instrument performance, while lunar observations provide twice-monthly to monthly measurements. The primary uncertainty in solar calibration measurements is degradation of the solar diffuser reflectance under solar UV exposure, while the primary uncertainty in lunar calibration measurements is observational scatter in the individual calibrations.

SeaWiFS used a relatively simple solar calibration concept, with no specific approach for monitoring the on-orbit degradation of diffuser reflectance [*Eplee Jr et al.*, 2007]. MODIS and VIIRS used special devices (SDSM: solar diffuser stability monitor) to track the degradation of diffuser reflectance [*Xiong et al.*, 2014]. MERIS and OLCI used two solar diffusers with different solar UV exposure times to track the degradation of diffuser reflectance [*Delwart and Bourg*, 2013]. For OCI, a two-diffuser approach (one measured daily, one measured monthly) was chosen because an SDSM is a rather costly device that measures the reflectance at a different view angle than the ocean color instrument, which is a problem if the reflectance changes as a function of view angle. Because of the large range of radiances to be measured, i.e., bright clouds and dark ocean, the OCI will have a third "dark" diffuser to examine system linearity over the course of the mission, but that topic is not discussed in this chapter.

The SeaWiFS diffuser was an aluminum plate coated with YB71 paint. MODIS, VIIRS, MERIS and OLCI used a Spectralon diffuser, which degrades strongly in the UV and is therefore not a good candidate

[6] Cite as: Meister, G., and R. E. Eplee (2018), Strategy and Requirements for the PACE OCI Solar Calibration, in *PACE Technical Report Series, Volume 7: Ocean Color Instrument (OCI) Concept Design Studies (NASA/TM-2018 – 2018-219027/ Vol. 7)*, edited by I. Cetinić, C. R. McClain and P. J. Werdell, NASA Goddard Space Flight Space Center Greenbelt, MD.

for OCI. Quasi-Volume Diffusers (QVDs) where chosen for OCI, based on their excellent performance for the OMI sensor [*Jaross*, 2017].

In the following sections, the solar calibration strategy, requirements, and measurement analysis approach (in appendices) will be presented.

6.2. Overview of the Solar Calibration Strategy

The OCI solar calibration strategy is based on MODIS and VIIRS heritage, modified to use two diffusers instead of a single diffuser and an SDSM:

- The spacecraft is maneuvered once per day to point the boresight of the solar calibration aperture at the Sun. This avoids uncertainty due to the position of the Sun on the solar diffuser, i.e, maintain constant azimuth and zenith angles of incidence to minimize errors due to uncertainties in the diffuser bidirectional reflectance distribution function (BRDF).
- The daily solar diffuser will be used to detect short-term variations in the OCI gain. The monthly solar diffuser will be used to detect medium-term (up to two years) variations in the OCI gain.
- Lunar measurements will be sued to detect long-term (more than two years) variations in the OCI gain.

The OCI solar calibration strategy will use observations of the daily and monthly solar diffusers to determine the degradation of the solar diffuser reflectance from the diffuser measurements and the differences in the diffuser solar exposure times (daily and monthly, two minutes per measurement. The strategy will be implemented as follows. For this discussion, a simplified OCI calibration equation will be used:

$$L_r(t) = K1 * K2(t) * dn(t), \quad \text{(Eq 6.1)}$$

where K1 is the absolute gain factor, K2 is the relative gain factor as a function of time, and dn are the dark-subtracted instrument counts.

During the first 18 months of the mission, the two solar diffusers will be used to derive the trend in K2. The daily solar diffuser measurements will be used to track the short-term variations in K2. The daily exposure of the solar diffuser to UV radiation will lead to a degradation of the reflectance of the diffuser. The monthly solar diffuser receives only $1/30^{th}$ of the solar exposure of the daily diffuser. Combining the measurements of the two diffusers allows the degradation of the diffuser reflectance to be estimated, as is described in Appendices 1-3. The reflectance of the daily solar diffuser as a function of time can be computed as:

$$f_r^d(t) = f_r^d(t_0) * d^d(t) \quad \text{(Eq 6.2)}$$

where d^d is the degradation estimate. The radiance reflected by the solar diffuser becomes:

$$L^{SD}(t) = f_r^d(t) * E^{sun}, \quad \text{(Eq 6.3)}$$

Where E^{sun} is the solar irradiance. $K2^{SD}$ can then be derived as:

$$K2^{SD}(t) = L^{SD}(t) / (K1 * dn(t)) = (f_r^d(t) * E^{sun}) / (K1 * dn(t)). \quad \text{(Eq 6.4)}$$

After approximately 18 months of operation, lunar measurements will be used to improve the trending accuracy of the OCI gains. As discussed in the lunar calibration TM chapter, the solar-derived K2 trends will be used to calibrate the lunar observations. Any residual trends over time in the calibrated

lunar time series will be assumed to arise from inaccuracies in the diffuser degradation correction. Fits to the lunar residuals ($K2^{L}$) will represent adjustments that are required for the solar-derived K2. The lunar-corrected gain trend K2(t) is defined as:

$$K2(t) = K2^{SD}(t) / K2^{L}(t). \quad \text{(Eq 6.5)}$$

This K2 will be the final temporal radiometric gain for the OCI on-orbit calibration.

6.3. Solar Calibration Requirements and Rationale

The threshold requirement for the solar calibration is stated in the Program Level Requirements as follows.

PACE shall provide:

- *Monthly characterizations of OCI instrument detector and optical component temporal stability. This will include lunar observations through the earth viewing port that illuminate all detector elements*

The baseline requirement is:

- *Twice-monthly characterizations of OCI instrument detector and optical component temporal stability. This will include lunar observations through the earth viewing port that illuminate all detector elements.*
- *Daily characterizations of OCI instrument detector and optical component changes using an independent, on-board capability that illuminates all detector elements.*

The solar calibration strategy is being developed to meet the baseline requirement.

The driving requirement for the solar calibration accuracy is stated in the Mission Requirements [*Werdell*, 2018]:

MRD-110 Long Term Radiometric Stability: OCI radiometric response shall vary by less than 0.5% per month with a characterization accuracy of 0.1%

The solar calibration will be performed to meet this requirement in conjunction with the lunar calibration. In addition, the following requirements are stated for the Space Segment:

MRD-373 The PACE Space Segment shall perform daily solar calibrations of the OCI to characterize the detector and optical component changes.

MRD-374 The PACE Space Segment shall perform the OCI solar calibration maneuver without violating OCI or Polarimeter(s) coverage requirements.

MRD-375 The PACE Space Segment shall perform the OCI solar calibration maneuver by pointing the boresight of the solar calibration aperture at the sun for between 30 and 120 seconds.

The requirements for performing the solar calibration, including the calibration maneuver and the use of two solar diffusers, have been developed to minimize the uncertainty in the radiometric trends computed from the solar measurements, in order to meet MRD-110.

6.4. Summary

The PACE mission has a requirement to perform solar calibrations, in conjunction with lunar calibrations, as part of the overall calibration strategy for OCI, in particular to determine the temporal response, as has

been performed for other NASA ocean color missions. The overall strategy is based on that used for MODIS and VIIRS, using two solar diffusers in place of a single diffuser and a Solar Diffuser Stability Monitor. The requirements have been specified at the program and mission level to accomplish the solar calibrations.

The key challenge when using solar diffuser measurements for trending on-orbit OCI gain changes is to track the reflectance of the solar diffuser. The approach chosen for OCI is to use two identical solar diffusers, exposing these two solar diffusers to different solar exposure amounts (daily versus monthly). The reflectance of the monthly solar diffuser is assumed to degrade at the same rate (per solar exposure) as the daily solar diffuser. Equations derived in Appendices 1 and 2 show that the degradation rate can be calculated from the measured dn (the solar diffuser measurements by OCI, both daily and monthly) and the solar exposure times for the two solar diffusers.

Appendix 6.3 provides an estimate of the maximum allowable degradation of the solar diffuser to achieve the desired gain trending accuracies (the monthly solar diffuser must not degrade by more than 0.6% for 2 years of on-orbit measurements). The appendix also provides an estimate for the expected degradation when using a Quasi Volume Diffuser as the monthly solar diffuser (0.13%), demonstrating that this type of solar diffuser is appropriate for OCI. These estimates should be updated once the final OCI on-orbit solar diffuser maneuvers are finalized and more exact solar exposure times are available.

Note that this document does not estimate the actual uncertainty for an individual solar diffuser measurement or the derived trending accuracy. These estimates are updated as the mission evolves. Currently, the best estimate for an individual measurement uncertainty of a solar diffuser measurement is 0.26%, the best estimate for trending accuracy after 2 years is 0.19% (without lunar adjustments).

Table 6.1. Glossary of terms

BRDF, f_r	Bidirectional reflectance distribution function (unitless)
c1	factor describing the difference of degradation rates of daily and monthly solar diffuser [unitless]
D	relative solar diffuser reflectance degradation [unitless]
superscript d	Daily
Dn	digital number (after background subtraction)
E_s	solar irradiance [Wm^{-2}]
g1	degradation rate of the daily solar diffuser in the first month [1/time]
g2	degradation rate of the daily solar diffuser in the second month [1/time]
K1	absolute gain factor [radiance/dn]
K2	temporal change of the instrument gain (unitless)
L_r	reflected radiance [$W/(m^2\ sr^{-1}\ m^{-2})$]
superscript m	Monthly
S	relative error in K2 (unitless)
t	Instrument/mission time [s]
T_{se}	solar exposure time (cumulative) [s]
2y	2 years

6.5. Appendix - Solar diffuser reflectance degradation

We will assume that both solar diffusers degrade mostly proportionally to the solar exposure. [Any deviation from this proportionality shall be captured by the constant *c1* (introduced in Appendix 4 below). Therefore, the temporal dimension for the solar diffuser degradation is the solar exposure time (called T_{se} in this chapter). It needs to be converted to instrument time (called *t* in this memo) before applying the calibration equations. Therefore, the solar exposure times T_{se} for all calibration events need to be recorded. Note that it will be necessary to not only count the time of the actual measurement, but all the time needed to bring the solar diffuser into full illumination, adding times of partial illumination with an appropriately smaller weighting.

The daily solar diffuser reflectance at a given wavelength, f_r^d, will degrade as

$$f_r^d (T_{se}=T_{se}^d) = f_r^d (T_{se}=0) * d^d(T_{se}= T_{se}^d) \quad \text{(Eq 6.6)}$$

where T_{se}^d is the total solar exposure time of the daily solar diffuser. d^d is a dimensionless function of T_{se} that describes the degradation of the reflectance (d^d is equal to one initially, equal to zero for a reflectance that does not reflect anymore) This is based on the assumption that the solar diffuser will only degrade during periods of solar exposure, which has been a good assumption for heritage instruments (OMI, MERIS, MODIS; see also Jaross 2017). $d^d(T_{se})$ is expected to be close to an exponential function, but deviations are likely and have been observed, so we will not assume a specific functional form for $d^d(T_{se})$. However, we do assume that for times t1 and t2 separated by a month or less, $d^d(T_{se})$ can be approximated reasonably well as linear:

$$d^d(t2) = d^d(t1) * (1+g1 * (T_{se}^d(t2) - T_{se}^d(t1))) \quad \text{(Eq 6.7)}$$

If the data suggest a nonlinear behavior, this will slightly modify our approach (see Jaross 2017 below). Note that the linear coefficient *g1* is expected to be negative. Also, *g1* is only valid for the time period t1 to t2.

The monthly solar diffuser reflectance, f_r^m, will degrade with

$$f_r^m (T_{se}^m) = f_r^m (T_{se}=0) * d^m(T_{se}^m) \quad \text{(Eq 6.8)}$$

where T_{se}^m is the total solar exposure time of the monthly solar diffuser.

The key assumption in our approach is that both the daily and monthly solar diffusers will degrade identically for a given amount of solar exposure. This is captured by this equation:

$$d^m(T_{se}^m) = d^d(T_{se}^m) \quad \text{(Eq 6.9)}$$

6.6. Appendix 2. Measuring the solar diffuser degradation

The OCI instrument will be used to detect the degradation of the solar diffuser via its measurements of $L_r(t)$. The fact that the OCI gain will change with time as well will be considered in the approach outlined in this document.

6.6.1. Definitions

The basic equation [*Barnes et al.*, 1998] used to calculate the radiance reflected off a solar diffuser is the definition of BRDF:

$$f_r(\theta_i,\theta_r,\varphi_i,\varphi_r) = L_r(\theta_i,\theta_r,\varphi_i,\varphi_r) / E_i(\theta_i) \quad \text{(Eq 6.10)}$$

$$(\text{or } f_r(\theta_i,\varphi_i;\theta_r,\varphi_r) = dL_r(\theta_i,\varphi_i,\theta_r\,\varphi_r; E_\iota) / dE_i(\theta_i,\varphi_i)) \quad \text{(Eq 6.11)}$$

Where f_r = BRDF of the solar diffuser. BRDF is wavelength dependent; L_r = radiance reflected off the solar diffuser at a given geometry; and E_i= solar irradiance = E_s. $(\theta_i,\theta_r,\varphi_i,\varphi_r)$ = (incidence zenith angle relative to the normal of the solar diffuser, reflected zenith angle relative to the normal of the solar diffuser, azimuth angle of the incident irradiance, azimuth angle of the reflected radiance).

Above the earth's atmosphere, the solar irradiance can be calculated from

$$E_s = F_0 * \cos(\theta_i) * d_{ES}^2 \quad \text{(Eq 6.12)}$$

d_{ES} is the Earth-Sun distance in Astronomical units. For F_0, the OBPG uses the *Thuillier et al.* [2003] solar spectrum and values are provided at https://oceancolor.gsfc.nasa.gov/docs/rsr/f0.txt.

For the PACE mission, all angles on the solar diffuser will be identical for each solar diffuser calibration measurement, so we do not need to carry the angles in the equations. In this memo, we will use a simplified version of the OCI calibration equation:

$$L_r(t) = K1 * K2(t) * dn(t) \quad \text{(Eq 6.13)}$$

K1 represents the OCI counts-to-radiance conversion (with units of radiance/dn). K2(t) represents the change of the counts-to-radiance conversion with time, with K2(t=0)=1 [dimensionless]. Determining K2(t) from the solar diffuser measurements is the purpose of the solar diffuser measurements. Using a simplified version of the OCI calibration equation simplifies the equations provided here; in practice, the full calibration equation (adding terms for temperature sensitivity (e.g. K3), linearity (K4), etc.) will be used for all equations containing dn(t) in this memo, so there will be no loss of accuracy.

6.6.2. Calculations for the First Month

Let t1 and t2 be the instrument times of the first two monthly solar diffuser measurements (e.g. t1 = January 2023 and t2 = February 2023). Associated with these times are the accumulative solar exposure durations for the daily solar diffuser $T1_{se}^d$ and $T2_{se}^d$ (e.g. $T1_{se}^d$ = 0 seconds and $T2_{se}^d$=120 seconds *30) and for the monthly solar diffuser $T1_{se}^m$ and $T2_{se}^m$ (e.g. $T1_{se}^m$ = 0 seconds and $T2_{se}^m$=120 seconds). The total time label for subsequent months will follow the same convention, e.g., T3 for the second month as discussed in the following section. Here we define the solar exposure duration as the total time the solar diffuser was exposed before the start of the solar diffuser measurement. We are assuming that the daily solar diffuser is measured at the same time as the monthly solar diffuser (both are measured either at t1 or t2). In reality, they will be measured on two consecutive orbits, but that difference is not relevant.

The solar diffuser reflectances at times t1 and t2 are given by

$f_r^d(t1) = f_r^d(T1_{se}^d) = f_r^d(0) * d^d(T1_{se}^d)$ (Eq 6.14)

$f_r^d(t2) = f_r^d(T2_{se}^d) = f_r^d(0) * d^d(T2_{se}^d)$ (Eq 6.15)

$f_r^m(t1) = f_r^m(T1_{se}^m) = f_r^m(0) * d^m(T1_{se}^m)$ (Eq 6.16)

$f_r^m(t2) = f_r^m(T2_{se}^m) = f_r^m(0) * d^m(T2_{se}^m)$ (Eq 6.17)

The measured reflected radiance of the daily solar diffuser in the first month is given by

$L_r(t1) = K1 * K2(t1) * dn^d(t1) = f_r^d(0) * d^d(T1_{se}^d) * E_s$ (Eq 6.18)

The measured reflected radiance of the daily solar diffuser in the second month is given by

$L_r(t2) = K1 * K2(t2) * dn^d(t2) = f_r^d(0) * d^d(T2_{se}^d) * E_s$ (Eq 6.19)

The ratio of these two equations is

$K2(t1)/K2(t2) * dn^d(t1)/ dn^d(t2) = d^d(T1_{se}^d)/ d^d(T2_{se}^d)$ (Eq 6.20)

Similarly, for the monthly solar diffuser:

$K2(t1)/K2(t2) * dn^m(t1)/ dn^m(t2) = d^m(T1_{se}^m)/ d^m(T2_{se}^m)$ (Eq 6.21)

where $dn^m(t1)$ and $dn^m(t2)$ are the measured dn for the monthly solar diffuser at times t1 and t2, resp.

Taking the ratio of the above two equations yields

$A = d^d(T1_{se}^d)/ d^d(T2_{se}^d) / (d^m(T1_{se}^m)/ d^m(T2_{se}^m))$ (Eq 6.22)

where A is a function of the measured dn (the terms K2(t1)/K2(t2) are eliminated in the ratio):

$A = dn^d(t1)/ dn^d(t2) / (dn^m(t1)/ dn^m(t2))$ (Eq 6.23)

Assuming the degradation of the daily solar diffuser within the month is linear (this is a reasonable assumption for slowly degrading materials like QVD, but may need to be reevaluated for materials like Spectralon in the UV), we can rewrite the degradation at time t2 as a function of the solar exposure time:

$d^d(T2_{se}^d) = d^d(T1_{se}^d) * (1+g1 * (T2_{se}^d - T1_{se}^d))$ (Eq 6.24)

$d^m(T2_{se}^m) = d^m(T1_{se}^m) * (1+g1 * (T2_{se}^m - T1_{se}^m))$ (Eq 6.25)

By definition, for the very first month of the mission, $d^d(T_{se}=T1_{se}^d=0)=1$ and $d^m(T_{se}= T1_{se}^m=0)=1$. This leads to

$A = d^m(T2_{se}^m) / d^d(T2_{se}^d) = (1+g1 * (T2_{se}^m - T1_{se}^m)) / (1+g1 * (T2_{se}^d - T1_{se}^d))$ (Eq 6.26)

The variable A and the solar exposure times are known, so this equation allows g1 to be retrieved:

$g1 = (A-1)/((T2_{se}^m - T1_{se}^m) - A*(T2_{se}^d - T1_{se}^d))$ (Eq 6.27)

With g1 determined, the daily and monthly solar diffuser degradation for time t2 can be calculated.

6.6.3. Calculations for the Second Month and Beyond

The next monthly solar diffuser calibration will occur one month later, at time t3. We will again assume that a daily solar diffuser measurement is performed at the same time. The degradation for the two solar diffusers at time t3 as a function of the solar exposure time can be calculated as:

$$d^d(T3_{se}^d) = d^d(T2_{se}^d) * (1 + g2 * (T3_{se}^d - T2_{se}^d)) \quad \text{(Eq 6.28)}$$

$$d^m(T3_{se}^m) = d^m(T2_{se}^m) * (1 + g1 * (T3_{se}^m - T2_{se}^m)) \quad \text{(Eq 6.29)}$$

Note that in the above equation for the monthly solar diffuser, g1 is used (not g2) because $T3_{se}^m - T1_{se}^m < T2_{se}^d - T1_{se}^d$. The degradation rate of the daily solar diffuser may change from one month to the next, so we cannot use g1 in equation 6.29 for the daily solar diffuser, and need to introduce a new variable (g2). g2 will be determined in the following steps.

We can use the monthly solar diffuser to calculate K2(t3):

$$K1 * K2(t3) * dn^d(t3) = f_r^m (T_{se}=0) * d^m(T_{se}= T3_{se}^m) * E_s \quad \text{(Eq 6.30)}$$

With K2(t3), we can calculate $d^d(T3_{se}^d)$:

$$K1 * K2(t3) * dn^d(t3) = f_r^d (0) * d^d(t3_{se}^d) * E_s \quad \text{(Eq 6.31)}$$

This allows us to calculate g2 from eq.(6.28). With g2, we can calculate $d^d(T_{se})$ for any time of the second month ($T2_{se}^d < T_{se} < T3_{se}^d$). With $d^d(T_{se})$ known, we can calculate K2(t) for the second month for each solar diffuser measurement:

$$K1 * K2(t) * dn^d(t) = f_r^d (0) * d^d(T_{se}) * E_s \quad \text{(Eq 6.32)}$$

This process can be repeated until the solar exposure time of the monthly solar diffuser reaches the total solar exposure time of the daily solar in the first month. After that, g1 in eq. 6.29 must be replaced by g2.

6.7. Appendix 3. Maximum allowable degradation of the solar diffuser reflectance

If the assumptions made above hold true, there is almost no limit to the maximum allowable degradation of the reflectance of the solar diffuser. Random noise errors like uncertainties of angles or SNR of the instrument are not important over longer periods of time because of the large number of measurements. The assumption that is most likely not 100% true is that the degradation of the monthly and the daily solar diffuser is only dependent on the amount of exposure to solar radiation, and that the rate is identical. A more realistic assumption is that the degradation of both solar diffusers is proportional to the solar exposure, but that the rate might be different. We will modify equation 6.29 above to

$$d^m(T2_{se}^m) = d^m(T1_{se}^m) * (1+c1*g1 * (T2_{se}^m - T1_{se}^m)) \quad \text{(Eq 6.33)}$$

where c1 is a factor that describes by how much the rate of degradation for the monthly solar diffuser is different from that of the daily solar diffuser. Note that with this approach, we can even realistically describe degradation processes that are not dependent on the amount of solar exposure, as long as they are proportional to time on-orbit and the time on-orbit is proportional to solar exposure time. If the calibration maneuvers are scheduled consistently (e.g. daily for the daily solar diffuser, monthly for the monthly solar diffuser), the time on-orbit will be proportional to solar exposure time for long periods of time (such as 1 year of on-orbit time).

The factor c1 is unknown. In the following, we will evaluate how different values for c1 impact the calculation of K2(t). It will be shown that the impact is a function of c1 and g1, which will allow us to provide an upper limit for the allowable degradation of the solar diffuser (i.e. g1). The limit will be a function of the allowable error in the calculation of K2(t), we will assume a value of 0.1% for that. The evaluation will be for 2 years of on-orbit measurements, because for longer time periods the lunar measurements will be used for long term trending. For simplicity, we will assume that after 2 years of measurements, we are still using g1 (not g2). This is a good assumption because g2 is only needed after 30 monthly measurements (assuming that both the monthly and the daily measurement have the same exposure time per measurement), which is larger than the 24 monthly measurements we expect during 2 years.

In the ideal case of c1=1.0 after 2 years of on-orbit measurements, we correctly calculate the degradation of the sensor after 2 years K2(2y) with the equation that describes the radiance reflected off the solar diffuser:

$$K1 * K2(2y) * dn^d(2y) = f_r^m(0) * d^m(T2y_{se}^m) * E_s \quad \text{(Eq 6.34)}$$

where $T2y_{se}^m$ is the total solar exposure time for the monthly solar diffuser. To describe the degradation of the monthly solar diffuser after 2 years, eq. 6.25 becomes

$$d^m(T2y_{se}^m) = d^m(0) * (1 + g1 * (T2y_{se}^m - 0)) = 1 + g1 * T2y_{se}^m \quad \text{(Eq 6.35)}$$

Note that since we do not know c1, we will have to assume c1=1.0 in the actual calculations we will perform on-orbit.

In the case of c1 not equal to 1.0 (which is most likely the true case), eq. 6.35 becomes

$$d^m(T2y_{se}^m) = d^m(0) * (1 + c1 * g1 * (T2y_{se}^m - 0)) = 1 + c1*g1 * T2y_{se}^m \quad \text{(Eq 6.36)}$$

Let us call $K2^{c1}(2y)$ the K2(2y) we would calculate for c1 not equal to 1.0. $K2^{c1}(2y)$ is the true K2 after two years. Equation 6.35 becomes

$K1 * K2^{c1}(2y) * dn^{d}(2y) = f_r^{m}(0) * (1 + c1*g1* T2y_{se}^{m}) * E_s$ (Eq 6.37)

Not knowing that c1 is not equal to 1, we would have used eq. 6.34 to calculate K2(2y). The relative error S in the K2 term is the ratio $S = K2(2y)/ K2^{c1}(2y)$, or the ratio of equation 6.34 and 6.37:

$S = (1 + g1* T2y_{se}^{m}) / (1 + c1*g1* T2y_{se}^{m})$ (Eq 6.38)

$c1*g1* T2y_{se}^{m}$ is the relative degradation of the monthly solar diffuser after 2 years on-orbit. E.g., if the solar diffuser has degraded by 2%, $c1*g1* T2y_{se}^{m}= -0.02$, see eq. 6.36. Solving eq.6.38 for $g1* T2y_{se}^{m}$ leads to

$g1* T2y_{se}^{m} = (S-1)/(1-S*c1)$ (Eq 6.39)

As an example, we will set c1=1.2, i.e. the monthly solar diffuser degraded 20% more than we expected based on our initial assumptions. For S=1.001 (a 0.1% error in the K2 term, see following subsection, 'Calculation of S'), we get

$c1*g1* T2y_{se}^{m} = -0.006$ (Eq 6.40)

This means that to achieve an error of 0.1% in the calculation of K2, the monthly solar diffuser must not degrade by more than 0.6% for 2 years of on-orbit measurements. Lower values of c1 (e.g. 1.1, i.e. higher confidence in our assumptions) will lead to higher allowable degradation (1.1% for c1=1.1).

6.7.1. Calculation of the Relative Error S

It is not intuitively obvious whether for c1>1, a 0.1% error in K2 means S=1.001 or S=0.999. If S=1.001, K2(2y) is larger than $K2^{c1}(2y)$. In the case considered here, the unexpectedly large degradation of the solar diffuser (described by c1>1) leads to an unexpected decrease in the reflected radiance. However, this is not known to the user of equation 7: he thinks the dn he measures corresponds to a radiance that is higher than the actual radiance, and therefore the gain he calculates (K2(t=2y)) is too high relative to the true gain ($K2^{c1}(2y)$). This means that $S = K2(2y)/ K2^{c1}(2y) > 1$.

6.7.2. Example Calculations for a QVD Diffuser

As an example, we will calculate the expected degradation of a Quart-Volume-Diffuser (QVD). Based on a plot of reflectance data measured with OMI (provided by *Jaross* [2017] private communication), the degradation rate of QVD at 350nm for OMI is -0.00013/hour. For longer wavelengths, the magnitude of the degradation is smaller, so 350nm is the worst case. The OMI design is different from the OCI design in two important ways that require an adjustment of the rate to infer OCI specific degradation rates:

- OMI uses a screen with a transmission of 10%. This means the rate needs to be multiplied by 10.
- The incidence angle for the OMI solar diffuser is ~30^{O}. For OCI, it will be 58^{O}. This means the rate needs to be multiplied by $\cos(58^{O})/\cos(30^{O})=0.61$.

Therefore, the expected degradation rate for an OCI QVD is -0.00079/hour. We will assume that the total solar exposure time for an OCI solar diffuser measurement is 4 minutes (two minutes of measurement, one minute each (this estimate should be updated based on feedback from the spacecraft team) to move the solar diffuser in and out of illumination (after adjusting for the actual illumination profile).

After 2 years of monthly measurements, the monthly solar diffuser will have degraded by

$d^{m}(T2y_{se}^{m}) = 1 + g1* T2y_{se}^{m} = 1 - 0.00096*(4/60*12*2) = 0.9987$ (Eq 6.41)

a degradation of 0.13%, less than the maximum allowable degradation calculated above (0.6%).

This memo does not deal with the maximum allowable degradation of the daily solar diffuser, but we will evaluate the expected degradation anyway. After 3 years of daily measurements, a rough estimate for the daily solar diffuser degradation is

$$d^{d}(T3y_{se}^{d}) = 1 + g1 * T3y_{se}^{d} = 1 - 0.00079*(4/60*30*12*3) = 0.94, \quad \text{(Eq 6.42)}$$

a degradation of 6%. The above calculation assumed that the degradation does not change from one month to the next. Most likely the degradation will level off [*Jaross*, 2017], so 6% is likely too high. In any case, it is important to know that the predicted radiance change is on the order of 5% for the daily solar diffuser, i.e. for a QVD daily solar diffuser, there are no concerns regarding a lack of SNR after 3 years or linearity concerns.

6.8. Appendix 4. Absolute calibration coefficient

As was shown above (Section 'Calculations for first month', above), the measured reflected radiance of the daily solar diffuser in the first month is given by

$$L_r(t1) = K1 * K2(t1) * dn^d(t1) = f_r^d(0) * d^d(T1_{se}^d) * E_s \quad \text{(Eq 6.43)}$$

This equation can be solved for K1. This is the first exposure of the daily diffuser to solar radiation, so there has been no degradation, i.e. $d^d(T1_{se}^d) = 1$. There has also been no degradation of the sensor, i.e. K2(t1)=1.0 (per definition, the trending of the OCI gain starts with the first measurement). This allows the calculation of K1 with the prelaunch solar diffuser reflectance ($f_r^d(0)$) of the daily diffuser:

$$K1 = f_r^d(0) * E_s / dn^d(t1) \quad \text{(Eq 6.44)}$$

See section 'Definitions' how to calculate E_s.

The same approach can be used to calculate K1 with the prelaunch solar diffuser reflectance ($f_r^d(T_{se}=0)$) of the monthly diffuser:

$$K1 = f_r^m(0) * E_s / dn^m(t1) \quad \text{(Eq 6.45)}$$

Note that a vicarious calibration coefficient (Franz et al., 2007) will be applied for certain (most) bands for ocean color processing. Top-of-atmosphere radiances calculated with K1 from the above equation(s) will be used to calculate the vicarious calibration coefficients.

Chapter 7

Strategy and Requirements for the PACE OCI Lunar Calibration

Frederick S. Patt, Science Applications International Corporation, Reston, Virginia[7]

Robert E. Eplee, Science Applications International Corporation, Reston, Virginia

Executive Summary

The Phytoplankton, Aerosol, Cloud, ocean Ecosystem (PACE) Ocean Color Instrument (OCI) has a threshold requirement to perform monthly lunar calibrations. Lunar calibration has been a major component of the calibration strategy for every NASA ocean color mission. This paper presents an overview of the planned PACE OCI lunar calibration strategy and the specific requirements to enable accurate calibration results.

7.1. Introduction

The lunar calibration has been an integral element of the radiometric calibration methodology for every NASA ocean color sensor since it was first used for the Sea-viewing Wide Field-of-view Sensor (SeaWiFS) in 1997 [*Eplee et al.*, 2012; *Woodward et al.*, 1993]. The Moderate-resolution Imaging Spectroradiometer (MODIS) on the Terra and Aqua spacecraft and the Visible and Infrared Imaging Radiometer Suite (VIIRS) on the Suomi National Polar-orbiting Partnership (SNPP) and the Joint Polar Satellite System (JPSS) all depend on the lunar calibration to achieve the radiometric stability required for climate-quality ocean color remote sensing [*Eplee et al.*, 2015; *Sun et al.*, 2007; *Xiong et al.*, 2016]. For SeaWiFS, the lunar calibration was the sole source for trending temporal response changes over the 13-year mission life, and enabled the achievement of radiometric stability that is still considered a standard for ocean remote sensing instruments. Both MODIS and VIIRS have a solar diffuser (SD) that includes a stability monitor for tracking changes in the diffuser reflectance; however, even with these capabilities the instrument temporal response still required adjustment using the lunar calibration to produce climate-quality ocean color data. Lunar calibration has also been performed or proposed for non-NASA ocean remote sensing missions, and for other Earth remote sensing instruments whose primary purpose is not ocean color [*Wagner et al.*, 2015]. The approaches to and benefits of lunar calibration for ocean color missions has been well documented in the scientific literature [National Research *Council*, 2011; *Eplee et al.*, 2012; *Eplee et al.*, 2015; *IOCCG*, 2013].

The lunar calibration strategy for all missions is based on these common elements:

- The lunar calibration is used to determine the relative temporal response of the instrument. It is not used as an absolute calibration reference, although work has been done in that direction.
- The radiance measurements of the Moon for a given calibration are combined to generate a disk-integrated irradiance (DII). There is no model of the lunar surface [*Woodward et al.*, 1993] that

[7] Cite as: Patt, F. S., and R. E. Eplee (2018), Strategy and Requirements for the PACE OCI Lunar Calibration, in PACE Technical Report Series, Volume 7: Ocean Color Instrument (OCI) Concept Design Studies (NASA/TM-2018 – 2018-219027/ Vol. 7), edited by I. Cetinić, C. R. McClain and P. J. Werdell, NASA Goddard Space Flight Space Center Greenbelt, MD.

allows specific locations on the Moon to be used as individual calibration sources. The calculation of the DII is described in Appendix A.

The model of the lunar irradiance is provided by the Robotic Lunar Observatory (ROLO) model developed by the U. S. Geological Survey [*Kieffer and Stone*, 2005]. The ROLO model provides the DII for each instrument spectral band, given the band spectral responses and observation parameters (i.e., spacecraft position and time of observation), and incorporates all known effects that result in DII variations, including Sun and Moon distances, lunar phase and libration. The calculation and use of the ROLO model irradiances is summarized in Appendix 7.A.

In the following sections, the lunar calibration strategy, requirements and error budget are presented.

7.2. Overview of the Lunar Calibration Strategy

The OCI lunar calibration strategy is based on the SeaWiFS approach, which incorporated two key elements:

- The spacecraft is maneuvered to allow the Moon to be viewed within the Earth-viewing scan angle range. This avoids any uncertainty due to RVS differences between the lunar and Earth view angle of incidence (AOI) on the half-angle mirror.
- The Moon is viewed as close as possible to 7 degrees phase each month. This minimizes uncertainties in the modeled lunar radiance due to such effects as lunar libration and polarization that increase at larger phase angles.

The OCI lunar calibration will incorporate a number of refinements to the SeaWiFS calibration approach to further improve the quality of the calibration measurements.

- The PACE spacecraft rotation rate will be controlled in order to perform all lunar calibrations with nearly the same oversampling ratio (OSR), and will also be determined from spacecraft telemetry for each calibration. The OSR determines the overlap between successive scans on the lunar surface; an OSR of 1 results in no overlaps or gaps and only ~37 pixels. A larger OSR results in more samples collected on the lunar disk, reducing the effects of random noise. For SeaWiFS, the lunar calibration was performed with an open-loop (uncontrolled) pitch maneuver, and there were no rate measurements (e.g., from gyros), so the OSR could not be determined from spacecraft telemetry and had to be estimated by analysis of the lunar image. This was the largest source of uncertainty for SeaWiFS [*Eplee et al.*, 2012]. For the OCI lunar measurements the rotation rate should be known with acceptable accuracy and should be controlled to a repeatable value. The required OSR is 8, which will result in ~300 data samples (radiance measurements) of the lunar disk. To reduce the effects of rate knowledge uncertainty, this OSR will be achieved by performing two lunar view maneuvers in opposite directions, with an OSR of 4 for each maneuver. The spacecraft pointing requirements are discussed in Section III.
- PACE will also be able to control the spacecraft maneuver to allow the Moon to be viewed close to the center of the OCI Earth view. This will minimize the effects of RVS uncertainty on the lunar measurements. For SeaWiFS, again the pitch maneuver was uncontrolled, and therefore the Moon was observed over a range of scan angles.
- Although the threshold requirement is for one lunar calibration per month, the baseline requirement is for two per month, at 7 degrees phase before and after the full Moon. This will

involve performing the two calibrations about one day apart. Performing two calibrations per month will significantly reduce the uncertainty in the temporal response change over the mission compared to one per month.

A list of parameters relevant to the lunar calibration is provided in Table 7.1.

Table 7.1. Lunar Calibration Parameters

Parameter	Value
Mean Lunar Radius	1738 km
Mean Earth-Moon Distance	384,401 km
Lunar Month	29.53 days
OCI FOV	0.089 degree
OCI scan rate	5.8 Hz

The maneuvers must be designed to maintain the instrument thermal stability by observing the instrument keep-out zone (KOZ) constraints. Specifically, the maneuvers must prevent any Sun illumination of the OCI radiator while the spacecraft is in sunlight, and must also minimize Earth shine on the radiator. This is accomplished by orienting the spacecraft to maximize the Y axis (radiator normal) angle to the nadir vector throughout the maneuver sequence, and also by having OCI view the Moon at other than the scan center.

The lunar calibration operations will be performed following the science data collection period, in the orbit corresponding to the 7-degree lunar phase. The OCI tilt will be +20 degrees (forward) at the end of science data collection for that orbit.

The spacecraft will perform four attitude maneuvers in sequence. First, the spacecraft will perform a rapid setup maneuver from the nadir orientation to position the OCI scan approximately 0.75 degree from the center of the lunar disk, or about 0.5 degree from the Moon's limb. This maneuver will position the Moon at the specified OCI scan angle, and also point the OCI radiator away from the Earth. Algorithms for determining the first maneuver are presented in Appendix 7.B.

Second, the spacecraft will rotate about an axis perpendicular to the Moon in the OCI scan plane, to cause OCI to view the moon at the specified OSR. An OSR of 4 corresponds to a pitch rate of 0.125 degree/sec. The total pitch rotation will be ~1.5 degrees. Third, the spacecraft will repeat this maneuver in the opposite direction. Finally, the spacecraft will maneuver back to the nadir orientation. The total time required for the three maneuvers is TBD minutes. The lunar calibration sequence of operations is illustrated in Figure 7.1.

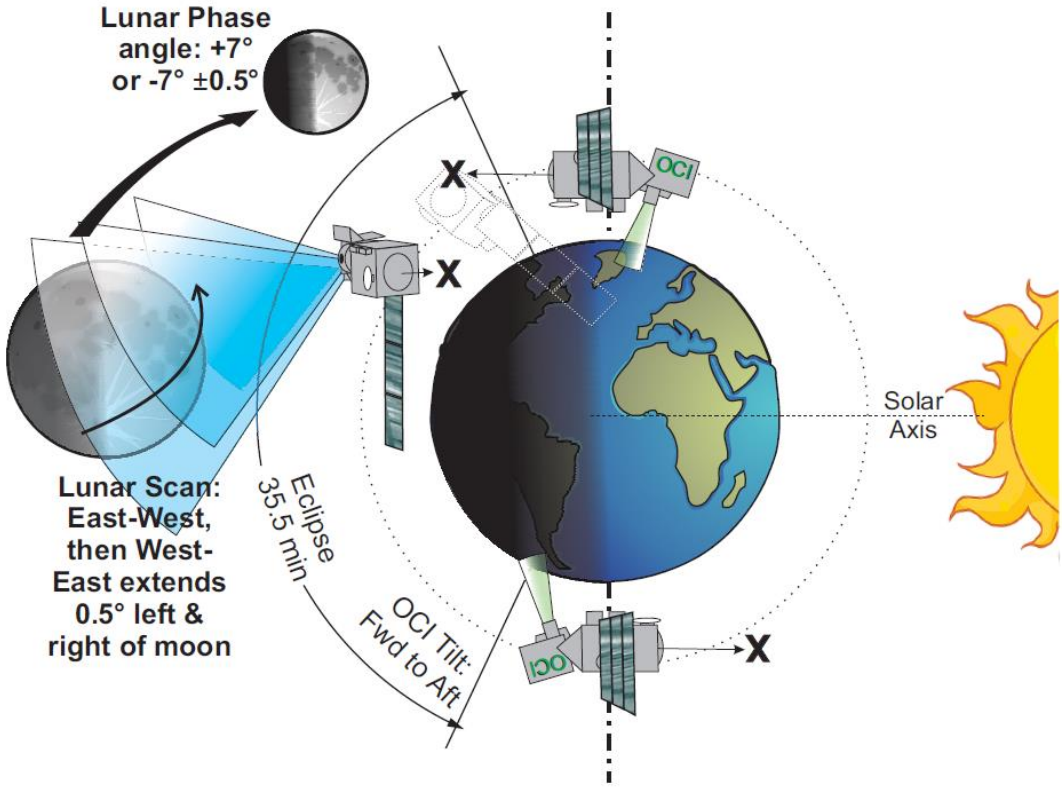

Figure 7.1. OCI Lunar Calibration Operations Sequence

7.3. Lunar Calibration Requirements and Rationale

The threshold requirement for the lunar calibration is stated in the Program Level Requirements as follows.

PACE shall provide:

g) Monthly characterizations of OCI instrument detector and optical component temporal stability. This will include lunar observations through the earth viewing port that illuminate all detector elements

The baseline requirement is:

g) Twice-monthly characterizations of OCI instrument detector and optical component temporal stability. This will include lunar observations through the earth viewing port that illuminate all detector elements

The lunar calibration strategy is being developed to meet the baseline requirement.

The driving requirement for the lunar calibration accuracy is stated in the Mission Requirements [*Werdell*, 2018]:

MRD-110 Long Term Radiometric Stability: OCI radiometric response shall vary by less than 0.5% per month with a characterization accuracy of 0.1%

The lunar calibration will be performed to meet this requirement in conjunction with the solar calibration. In addition, the following requirements are stated for the Space Segment:

MRD-367 The PACE Space Segment shall perform 2 monthly lunar calibrations of the OCI to characterize the detector and optical component changes.

MRD-368 The PACE Space Segment shall perform the OCI lunar calibration maneuver without impacting science collection

MRD-369 The PACE Space Segment shall perform the OCI lunar calibration maneuver at the same lunar phase angle each month, with those angles being +7 deg +/- 0.5 deg, and -7 deg +/- 0.5 deg.

MRD-370 The PACE Space Segment shall perform the OCI lunar calibration maneuver with the instrument boresight moving perpendicular to the scan direction and bisecting the lunar disk to obtain full lunar disk coverage.

The requirements for performing the lunar sweep maneuver have been developed to minimize the uncertainty in the radiometric trends computed from the lunar measurements, in order to meet MRD-110. The complete error budget is presented in Section IV. As for SeaWiFS, the primary contributions to the lunar calibration uncertainty are geometric. With this in mind, the following requirements have been developed.

Repeatability of the pitch rate (i.e., between lunar calibrations) within 10% of the specified rate.

This will minimize variation in the OSR between calibrations.

Knowledge of the pitch rate to 0.2%

The uncertainty in the OSR is equivalent to the pitch rate knowledge uncertainty. This requirement will limit this contribution to the calibration uncertainty to 0.2%.

Stability of the pitch rate to 1%

The lunar disk reflectance is not uniform. At the OCI resolution, the variation in the disk reflectance is approximately +/-10%. Variations in the pitch rate will result in uncertainty in the DII when viewing the non-uniform lunar surface. This requirement will limit this contribution to 0.1%.

OCI views the Moon at the same scan angle for every calibration, within 1 degree.

Spacecraft rotation axis perpendicular to the Moon direction, within 1 degree

The effective OCI sweep rate across the Moon is affected by the angle of the rotation axis to the Moon's direction. These requirements minimize the contributions from both effects, and are not difficult for the spacecraft to meet. The OCI scan angle requirement also minimizes RVS effects.

7.4. Lunar Calibration Error Budget

A complete error budget has been developed for the OCI lunar calibration. The budget is divided into geometric, radiometric (i.e., instrumental) and model (ROLO) terms. Each of these is described below.

1. Geometric terms

These terms were discussed in the previous section:

- Pitch rate knowledge error
- Pitch rate stability
- OCI scan center offset from the Moon's center
- Rotation axis offset from pitch axis

2. Radiometric terms

The instrument characteristics that potentially affect the lunar measurements are:

- Random errors (SNR): Effect of instrument random errors on the DII.
- Temperature: This represents the effect of CCD and electronics temperature variations between lunar measurements.
- Linearity: Depends on the range of DN for the lunar measurements.
- Polarization: Depends on the degree of polarization of the lunar disk radiance and the polarization sensitivity of the instrument.
- Crosstalk: Lunar signals should be largely coherent across bands, so probably small.
- Spectral response: Results from bandpass variations with time.
- Threshold: Lower limit on measurements included in the IDR. This has been a significant source of uncertainty for heritage sensors.
- Dark count: Determined from the image background around the Moon.

3. Model terms

The ROLO model is subject to potential uncertainties from the following:

- Phase angle: May vary by up to +/-1 degree due to scheduling conflicts
- Libration: lunar libration angles will be different for each lunar measurement. SeaWiFS results suggest that wavelength variations at 7 degrees phase will be small.
- Sun-Moon distance: Negligible, included for completeness
- S/C-Moon distance: The model for the lunar distance is the limiting factor.
- Temporal: This term reflects possible changes in the lunar disk reflectance, which are not included in ROLO. It is negligible and included for completeness.

The allocations, current best estimates (CBE) and bases-of-estimate are summarized in Table 7.2 for the visible and near-infrared (NIR) bands and in Table 7.3 for the short-wave infrared (SWIR) bands. The CBEs will be updated as information becomes available. The pitch rate knowledge and stability are the dominant terms in the budget. The tables also show the RMS of all uncertainties and the corresponding temporal trend uncertainties after 18 months (threshold mission), 24 months and 36 months (baseline mission). The method for computing the temporal trend uncertainty is described in Appendix 7.C. As shown in the tables, the 36-month trend uncertainty using the CBEs meets the MRD-110 long-term stability requirement of 0.1%.

7.5. Conclusion

The PACE mission has a requirement to perform lunar calibrations as part of the overall calibration strategy for the OCI, in particular to determine the temporal response, as has been performed for other NASA ocean color missions. The overall strategy is based on that used for SeaWiFS, with refinements to improve the quality of the lunar measurements. The requirements have been specified at the program and mission level to accomplish the lunar calibrations. An error budget has been developed that verifies that the lunar calibration is capable of meeting the OCI radiometric stability requirements.

Table 7.2. Lunar Calibration Error Budget for Visible/NIR Bands

Term	**Allocation**	**CBE**	**Basis/Confidence**
Pitch rate knowledge error	0.240%	0.200%	The pitch rate knowledge requirement is 0.2%.
Pitch rate stability	0.120%	0.100%	Analysis of MODIS images shows that at OCI resolution, the variability is ~10%. The pitch rate stability requirement is 1%.
OCI scan center offset from the Moon	0.015%	0.015%	The requirement is 1 degree, and the equivalent oversampling error is (1 - cos(1°)).
Rotation axis offset from pitch (Y) axis	0.015%	0.015%	Same as above for oversampling error.
Random errors (SNR)	0.010%	0.010%	The minimum RSB SNR is 600, and the number of pixels collected per measurement will be ~300 (with 8x oversampling)
Temperature	0.020%	0.010%	OCI temperature controller should maintain temperatures within range during lunar maneuvers.
Linearity	0.010%	0.010%	The range of DN values should not change significantly between measurements.
Polarization	0.010%	0.010%	Estimated lunar radiance polarization at 7 degrees phase is 1%, and the OCI visible and NIR polarization sensitivity requirement is 1%
Crosstalk	0.020%	0.010%	Placeholder estimate
Spectral response	0.020%	0.010%	Placeholder estimate
Threshold	0.006%	0.006%	From analysis of uncertainties in disk-integrated irradiances for VIIRS lunar images using 1% of peak brightness as the reference point for the threshold.
Dark count	0.020%	0.020%	From analysis of the dark sky around VIIRS lunar images.
Phase angle	0.070%	0.070%	From analysis of SeaWiFS low phase angle lunar observations
Libration	0.080%	0.080%	From analysis of SeaWiFS low phase angle lunar observations
Sun-Moon distance	0.000%	0.000%	
S/C-Moon distance	0.003%	0.003%	Assumes lunar distance accuracy of 0.001 Earth radius.
Temporal	0.000%	0.000%	
RSS Error	**0.293%**	**0.251%**	
18-month Trend	**0.169%**	**0.145%**	
24-month Trend	**0.146%**	**0.125%**	
36-month Trend	**0.120%**	**0.102%**	

Table 7.3. Lunar Calibration Error Budget for SWIR Bands

Term	Allocation	CBE	Basis/Confidence
Pitch rate knowledge error	0.240%	0.200%	The pitch rate knowledge requirement is 0.2%.
Pitch rate stability	0.120%	0.100%	Analysis of MODIS images shows that at OCI resolution, the variability is ~10%. The pitch rate stability requirement is 1%.
OCI scan center offset from the Moon	0.015%	0.015%	The requirement is 1 degree, and the equivalent oversampling error is (1 - cos(1°)).
Rotation axis offset from pitch (Y) axis	0.015%	0.015%	Same as above for oversampling error.
Random errors (SNR)	0.010%	0.010%	The minimum RSB SNR is 600, and the number of pixels collected per measurement will be ~300 (with 8x oversampling)
Temperature	0.020%	0.010%	OCI temperature controller should maintain temperatures within range during lunar maneuvers.
Linearity	0.010%	0.010%	The range of DN values should not change significantly between measurements.
Polarization	0.020%	0.020%	Estimated lunar radiance polarization at 7 degrees phase is 1%, and the OCI SWIR sensitivity requirement is 2%
Crosstalk	0.020%	0.010%	Placeholder estimate
Spectral response	0.020%	0.010%	Placeholder estimate
Threshold	0.006%	0.006%	From analysis of uncertainties in disk-integrated irradiances for VIIRS lunar images using 1% of peak brightness as the reference point for the threshold.
Dark count	0.020%	0.020%	From analysis of the dark sky around VIIRS lunar images.
Phase angle	0.070%	0.070%	From analysis of SeaWiFS low phase angle lunar observations
Libration	0.080%	0.080%	From analysis of SeaWiFS low phase angle lunar observations
Sun-Moon distance	0.000%	0.000%	
S/C-Moon distance	0.003%	0.003%	Assumes lunar distance accuracy of 0.001 Earth radius.
Temporal	0.000%	0.000%	
RSS Error	**0.293%**	**0.251%**	
18-month Trend	**0.169%**	**0.145%**	
24-month Trend	**0.146%**	**0.125%**	
36-month Trend	**0.120%**	**0.102%**	

7.6. Appendix 7.A – Lunar Calibrations Equations

These are the equations that describe how the PACE OCI lunar observations will be used to generate the lunar calibration time series.

1. DISK-INTEGRATED IRRADIANCES

The disk-integrated lunar radiances are computed for all pixels on the lunar disk where the pixel brightness is at least 1% of the peak brightness in the lunar image:

$$L_{moon}(\lambda, t) = \sum c_i(\lambda)\, dn_{moon}(\lambda, t) \quad \text{(Eq. 7.1)}$$

where dn_{moon} is he dark-subtracted counts of the lunar pixels, and c_i is the counts-to-radiance conversion coefficient.

The ROLO model requires disk-integrated lunar irradiances as input, which are computed from the disk-integrated lunar radiances and the instantaneous field of view (IFOV) of OCI:

$$E_{inst}(\lambda, t) = IFOV\ L_{moon}(\lambda, t) \quad \text{(Eq 7.2)}$$

where: IFOV is the instantaneous field-of-view in radians, assumed to be the same for all bands.

2. ROLO MODEL IRRADIANCES

The radiometric output of ROLO is the modeled lunar irradiance at the location of the instrument for the time of observation:

$$E_{ROLO}(r, \lambda, t) = (A_{Moon}(r, \lambda, t)\, E_{Sun}(\lambda))/K_d(r, t) \quad \text{(Eq 7.3)}$$

where A_{Moon} is the lunar reflectance from the ROLO model, K_d represents the distance corrections, and E_{Sun} is the solar irradiance. The Sun/Moon and Instrument/Moon distance corrections are given by:

$$K_d(r, t) = (R_{Sun\text{-}Moon}(r, t)/AU)^2\, (R_{Inst\text{-}Moon}(r, t)/MLD)^2 \quad \text{(Eq 7.4)}$$

where $R_{Sun\text{-}Moon}$ is the Sun – Moon distance, AU is the Astronomical Unit, $R_{Inst\text{-}Moon}$ is the Instrument – Moon distance, and MLD is the mean Earth – Moon distance (384401 km).

3. OCI/ROLO COMPARISONS

The lunar calibration time series are comprised of the ratios of the observed disk-integrated lunar irradiances from OCI to the modeled irradiances from ROLO. The OCI temporal gains K2 are relative gains, so the lunar calibration time series will be normalized to the first observation:

$$F_{Moon}(\lambda, t) = (E_{inst}(\lambda, t) / E_{ROLO}(\lambda, t)) / (E_{inst}(\lambda, t_0) / E_{ROLO}(\lambda, t_0)) \quad \text{(Eq 7.5)}$$

where t_0 is the time of the first lunar measurement.

The OCI lunar observations will occur twice per month. The temporal gains will need to be applied continually throughout the mission. The determination of the temporal gains will use the results from both the lunar and solar calibrations, possibly following the same approach used for VIIRS (Eplee et al., 2015). If the temporal response is sufficiently well-behaved, the gains could be derived from functional fits to the lunar data alone, as for SeaWiFS [*Eplee et al.*, 2012].

The lunar calibration time series F_{Moon} is the radiometric response over time. The temporal gain over time as derived from the lunar observations is the inverse of the radiometric response:

$$K2(\lambda, t) = 1/F_{Moon}(\lambda, t) \quad \text{(Eq 7.6)}$$

7.7. Appendix 7.B – Calculation of the Lunar Calibration Setup Maneuver

The lunar calibration setup maneuver calculation will be based on a predicted PACE orbit ephemeris, consisting of a set of Cartesian position and velocity vectors with associated time tags. The first step is to determine whether the 7-degree lunar phase angle occurs within the time range of the ephemeris. This is performed as follows.

The lunar and solar vectors are computed from models or ephemerides, for each sample in the predicted PACE ephemeris, in the same reference frame as the PACE orbit vectors. The PACE-to-Moon and Sun-to-Moon unit vectors are then computed as follows:

$$\mathbf{R_{P2M}} = \mathbf{R_M} - \mathbf{P} \quad \text{(Eq 7.7)}$$

$$\hat{\mathbf{R}}_{\mathbf{P2M}} = \mathbf{R_{P2M}} / |\, \mathbf{R_{P2M}} \,| \quad \text{(Eq 7.8)}$$

$$\mathbf{R_{S2M}} = \mathbf{R_M} - \mathbf{R_S} \quad \text{(Eq 7.9)}$$

$$\hat{\mathbf{R}}_{\mathbf{S2M}} = \mathbf{R_{S2M}} / |\, \mathbf{R_{S2M}} \,| \quad \text{(Eq 7.10)}$$

Where $\mathbf{R_M}$ is the Earth-to-Moon vector,

$\mathbf{P}$ is the PACE orbit position vector,

$\mathbf{R_S}$ is the Earth-to-Sun vector,

$\hat{\mathbf{R}}_{\mathbf{P2M}}$ is the PACE-to-Moon unit vector, and

$\hat{\mathbf{R}}_{\mathbf{S2M}}$ is the Sun-to-Moon unit vector.

The lunar phase is computed as:

$$\Phi = \cos^{-1}(\hat{\mathbf{R}}_{\mathbf{P2M}} \bullet \hat{\mathbf{R}}_{\mathbf{S2M}}) \quad \text{(Eq 7.11)}$$

If the target phase of 7 degrees falls within the range of computed phase angles, the maneuver calculation can proceed.

The next step is to determine the maneuver start times. This will be specified according to the solar zenith angle at the subsolar point. OCI is required to collect data to at least 75 degrees solar zenith angle, which therefore represents the earliest possible maneuver start time. This time is defined by the condition

$$\mathbf{P} \bullet \mathbf{R_S} / (|\, \mathbf{P} \,|\, |\, \mathbf{R_S} \,|) \leq \cos(\text{solz}) \quad \text{(Eq 7.12)}$$

For each orbit, the first time at which this condition is satisfied represents the maneuver start time. Based on the previous calculation of the lunar phase angles, the maneuver start time is selected for which the phase is closest to 7 degrees. If the ephemeris time range spans both of the 7-degree phase angles for a month, then the maneuver start times closest to 7 degrees before and after full phase are selected. Alternatively, if a range of possible maneuver orbits is needed (e.g., to allow for conflict resolution), all of the maneuver start times within a specified tolerance of 7 degrees phase may be selected.

For each selected maneuver time, the maneuver quaternion is calculated as follows. First, the orbital frame transformation matrix **[S]** is computed from the orbit position and velocity vectors according to the following conditions: Z axis parallel to the local (geodetic) nadir; X axis in the nadir-velocity plane and perpendicular to Z; Y axis normal to the X-Z plane to form a right-handed orthogonal triad.

The matrix **[S]** is used to transform the PACE-to-Moon vector to the observatory reference frame:

$$\hat{\mathbf{R}}_{\mathbf{P2M\_O}} = \mathbf{[S]}\ \hat{\mathbf{R}}_{\mathbf{P2M}} \qquad \text{(Eq 7.13)}$$

This vector represents the Moon vector in the observatory frame at the start of the maneuver. The desired maneuver is to position the OCI scan plane 0.5 degrees from the Moon's limb, at a specified scan angle. Since the size of the lunar disk as viewed from Earth is approximately 0.5 degree, the scan plane will be positioned 0.75 degree from the center of the Moon, which is represented by $\hat{\mathbf{R}}_{\mathbf{P2M\_O}}$.

As stated in the assumptions, OCI will be tilted forward by 20 degrees. Thus, the desired direction of the Moon at the end of the maneuver will be 0.75 degrees from the scan plane at the specified scan angle, in the direction of the scan rotation axis. Specifically:

$$\hat{\mathbf{R}}_{\mathbf{P2M\_D}} = \begin{vmatrix} \sin(0.75)\cos(20) + \cos(0.75)\cos(-\Phi)\sin(20) \\ \cos(0.75)\sin(-\Phi) \\ \cos(0.75)\cos(-\Phi)\cos(20) - \sin(0.75)\sin(20) \end{vmatrix} \qquad \text{(Eq 7.14)}$$

where Φ is the scan angle, assuming a positive rotation about the OCI +X axis.

The calculation of the maneuver depends on the type of maneuver to be performed. The calculations are described here for three types of maneuvers: the minimum-angle maneuver; a pitch-roll maneuver sequence; and a single-axis maneuver to maximize the angle between the spacecraft +Y axis and the nadir vector at the end of the maneuver. This last type is based on the need to minimize Earth shine on the OCI radiator, which is normal to the +Y axis.

Minimum Angle Maneuver

The minimum angle maneuver is equivalent to a simple rotation of the Moon vector at the initial orientation, $\hat{\mathbf{R}}_{\mathbf{P2M\_O}}$, to the desired viewing direction, $\hat{\mathbf{R}}_{\mathbf{P2M\_D}}$. The rotation angle is simply the angle between the two vectors, and the axis is the normal to the plane represented by the vectors. The angle and vector for the desired maneuver are computed as follows:

$$\Theta = \text{acos}(\hat{\mathbf{R}}_{\mathbf{P2M\_O}} \bullet \hat{\mathbf{R}}_{\mathbf{P2M\_D}}) \qquad \text{(Eq 7.15)}$$

$$\hat{\mathbf{e}} = \hat{\mathbf{R}}_{\mathbf{P2M\_O}} \times \hat{\mathbf{R}}_{\mathbf{P2M\_D}} \,/\, |\, \hat{\mathbf{R}}_{\mathbf{P2M\_O}} \times \hat{\mathbf{R}}_{\mathbf{P2M\_D}}\, | \qquad \text{(Eq 7.16)}$$

where Θ is the angle and $\hat{\mathbf{e}}$ is the vector. The maneuver quaternion is then computed as:

$$Q = (\hat{\mathbf{e}}\ \sin(\Theta/2), \cos(\Theta/2)) \qquad \text{(Eq 7.17)}$$

Pitch/Roll Maneuver Sequence

The pitch/roll sequence involves sequential rotations about the +Y and +X axes to position the Moon vector in the desired direction. The calculations for the pitch and roll angles are based on the fact that each maneuver affects two of the three components of the Moon vector in the spacecraft frame; the pitch maneuver affects the X and Z components, and the roll maneuver, the Y and Z components. Thus, after the pitch maneuver, the X component must have the value for the desired vector.

In addition, the Z component after the pitch maneuver can be predicted from this knowledge and the following: the Y component will not be changed by the maneuver, and the sign of the Z component will be positive, based on the OCI scan geometry. Thus, the vector at the end of the pitch maneuver will be:

$$\hat{\mathbf{R}}_{\mathbf{P2M\_P}} = \begin{vmatrix} R_{P2M\_DX} \\ R_{P2M\_OY} \end{vmatrix} \qquad \text{(Eq 7.18)}$$

$$| \sqrt{(1 - R_{P2M\_DX}^2 - R_{P2M\_OY}^2)} \quad |$$

Where $\hat{\mathbf{R}}_{\mathbf{P2M\_P}}$ is the Moon vector after the pitch maneuver, R_{P2M_DX} is the X component of the desired Moon vector and R_{P2M_OY} is the Y component of the initial Moon vector. The pitch angle can then be calculated as follows:

$$\Theta_p = \tan^{-1}(R_{P2M\_OX}, R_{P2M\_OY}) - \tan^{-1}(R_{P2M\_PX}, R_{P2M\_PZ}) \quad \text{(Eq 7.19)}$$

where Θ_p is the pitch angle. The roll angle is the calculated in similar fashion, using the desired Moon vector and the vector after the pitch maneuver:

$$\Theta_r = \tan^{-1}(R_{P2M\_DY}, R_{P2M\_DZ}) - \tan^{-1}(R_{P2M\_PY}, R_{P2M\_PZ}) \quad \text{(Eq 7.20)}$$

Note that in both calculations, the form of the arctangent function allows the angles to be computed over the range +/-180 degrees.

Maneuver to Maximize the Y-axis to Nadir Angle

As stated above, the Earth shine on the OCI radiator needs to be minimized during the lunar calibration maneuvers to maintain thermal stability during the calibration measurements. In the nadir orientation, a shield protects the radiator from Earth shine, but at all other orientations the radiator is potentially exposed. Earth shine on radiator is minimized by orienting the spacecraft to maximize the angle between the spacecraft +Y axis, which is normal to the radiator, and the nadir direction; this is equivalent to minimizing the angle between the Y axis and the orbit position vector.

The Y axis lies in the plane defined by the OCI scan; therefore, the minimization described above is accomplished by aligning the OCI scan plane with a plane defined by the Moon vector and the orbit position vector at the time of observation. Since the objective is to calculate a maneuver to the desired orientation, the latter plane is defined in the spacecraft reference frame represented by the matrix **[S]** described above. The calculation of this maneuver is equivalent to the algebraic attitude determination method described in Lerner (1978).

Following this method, the body matrix is determined by orthogonalization of the basis vectors. For the body frame, these are the desired Moon direction, $\hat{\mathbf{R}}_{\mathbf{P2M\_D}}$, and the +Y axis; for the reference frame, they are the initial Moon direction and the orbit vector in the spacecraft frame. Specifically:

$$[\mathbf{M_B}] = [\mathbf{q_B}\ \mathbf{r_B}\ \mathbf{s_B}] \quad \text{(Eq 7.21)}$$

where

$$\mathbf{q_B} = \hat{\mathbf{R}}_{\mathbf{P2M\_D}}\mathbf{s_B} = \hat{\mathbf{R}}_{\mathbf{P2M\_D}} \times \mathbf{Y} \,/\, | \hat{\mathbf{R}}_{\mathbf{P2M\_D}} \times \mathbf{Y} | \quad \text{(Eq 7.22)}$$

$$\mathbf{r_B} = \mathbf{s_B} \times \mathbf{q_B} \quad \text{(Eq 7.23)}$$

Similarly for $[\mathbf{M_R}]$:

$$\mathbf{q_R} = \hat{\mathbf{R}}_{\mathbf{P2M\_O}} \quad \text{(Eq 7.24)}$$

$$\mathbf{s_R} = \hat{\mathbf{R}}_{\mathbf{P2M\_O}} \times \mathbf{P} \,/\, | \hat{\mathbf{R}}_{\mathbf{P2M\_O}} \times \mathbf{P} | \quad \text{(Eq 7.25)}$$

$$\mathbf{r_R} = \mathbf{s_R} \times \mathbf{q} \quad \text{(Eq 7.26)}$$

Finally, since the maneuver can be described by a matrix that represents the transformation between the two frames:

$$[\mathbf{M_B}] = [\mathbf{M_M}]\,[\mathbf{M_R}] \qquad \text{(Eq 7.27)}$$

it follows that:

$$[\mathbf{M_M}] = [\mathbf{M_B}]\,[\mathbf{M_R}]^{-1} \qquad \text{(Eq 7.28)}$$

where $[\mathbf{M_M}]$ is the matrix that represents the desired maneuver.

7.8. Appendix 7.C – Uncertainty in the Lunar Calibration Trend

The uncertainty of the instrument trend determined from the PACE lunar calibration is based on the covariance of the functional fit to the lunar measurements.

The covariance matrix for a linear fit is computed as follows:

$$P = \sigma_m^2 \begin{vmatrix} N & \Sigma x \\ \Sigma x & \Sigma x^2 \end{vmatrix}^{-1} \quad \text{(Eq 7.29)}$$

where σ_m is the uncertainty of a single measurement, N is the number of measurements, and x is the time of each measurement. For this calculation, time scale is expressed in months.

For a 36-month mission with 2 calibrations per month, N = 72, and the resultant covariance is:

$$P = \sigma_m^2 \begin{vmatrix} 72 & 1260 \\ 1260 & 29820 \end{vmatrix}^{-1}$$

$$= \sigma_m^2 \begin{vmatrix} 0.053303 & -0.00225225 \\ -0.00225225 & 0.00012870 \end{vmatrix}$$

The uncertainty in the slope is then computed using P(2,2):

$$\sigma_s = \sigma_m \sqrt{P(2,2)}$$

$$= 0.0113446\ \sigma_m$$

Finally, the uncertainty in the mission-long trend is equal to the product of the slope uncertainty and the time, in this case the number of months:

$$\sigma_T = N\ \sigma_m \sqrt{P(2,2)}$$

$$= 0.4084\ \sigma_m$$

So the uncertainty in the mission-long trend is 40.84% of the individual measurement uncertainty after 36 months. After 24 months, the uncertainty in the trend is 50.04% of the measurement uncertainty, and after 18 months it is 57.82%.

This method can be generalized for a higher-order polynomial. For a cubic fit, the covariance is:

$$P = \sigma_m^2 \begin{vmatrix} N & \Sigma x & \Sigma x^2 & \Sigma x^3 \\ \Sigma x & \Sigma x^2 & \Sigma x^3 & \Sigma x^4 \\ \Sigma x^2 & \Sigma x^3 & \Sigma x^4 & \Sigma x^5 \\ \Sigma x^3 & \Sigma x^4 & \Sigma x^5 & \Sigma x^6 \end{vmatrix}^{-1} \quad \text{(Eq 7.30)}$$

In this case, both the slope and its uncertainty will vary over the mission. To determine the slope uncertainty, we use the derivative of the fitting function. For a cubic polynomial:

$$y = a_0 + a_1 x + a_2 x^2 + a_3 x^3 \quad \text{(Eq 7.31)}$$

the derivative is:

$$y' = a_1 + 2a_2 x + 3a_3 x^2$$

The covariance of the terms (a_1, a_2, a_3) is represented by the lower-right submatrix of the fit covariance:

$$P' = \begin{vmatrix} P_{22} & P_{23} & P_{24} \\ P_{32} & P_{33} & P_{34} \\ P_{42} & P_{43} & P_{44} \end{vmatrix} \quad \text{(Eq 7.32)}$$

The uncertainty of the derivative at each point can be computed from this matrix via covariance analysis. The Jacobian matrix of partial derivatives of the slope w.r.t the fitting coefficients at a point x is just:

$$F(x) = | 1 \quad 2x \quad 3x^2 |$$

Therefore, the Jacobean for N months is:

$$F = \begin{vmatrix} 1 & 0 & 0 \\ 1 & 2 & 3 \\ & . & \\ & . & \\ & . & \\ 1 & 2(N-1) & 3(N-1)^2 \end{vmatrix}$$

The NxN covariance matrix of the slopes over the N months is:

$$P = F\ P'\ F^T \qquad \text{(Eq 7.33)}$$

To compute the total trend uncertainty over the mission, note that the diagonal terms of the covariance matrix represent the variances of the slopes at each point:

$$P_{ii} = \sigma_i^2 \qquad \text{(Eq 7.34)}$$

while the off-diagonal terms represent the correlations between the slope uncertainties:

$$P_{ij} = C_{ij}\ \sigma_i\ \sigma_j$$

where C_{ij} is the correlation between the i^{th} and j^{th} slope uncertainty. Note that P is symmetric, so $C_{ij} = C_{ji}$.

The combined variance for the N slopes is:

$$\sigma_T^2 = \sum \sigma_i^2 + 2\sum\sum C_{ij}\ \sigma_i\ \sigma_j \qquad \text{(Eq 7.34)}$$

which is simply the sum of the terms of P. Therefore:

$$\sigma_T = (\sum\sum P_{ij})^{1/2} \qquad \text{(Eq 7.35)}$$

For missions of 18, 24 and 36 months, the mission trend uncertainty is 1.0733, 0.9221 and 0.7487 times the individual measurement uncertainty, respectively.

Note that the calculation for the linear fit above is equivalent to this method, for constant values of $\sigma_s(x)$. As stated above, this method can readily be extended to higher-order polynomials if needed.

Chapter 8

Ltyp and Lmax Calculations for PACE Ocean Color Instrument

Ziauddin Ahmad, Science Applications International Corporation, Reston, Virginia[7]

Gerhard Meister, NASA Goddard Space Flight Center, Greenbelt, Maryland

Executive Summary

Top of the atmosphere (TOA) Ltyp (typical) and Lmax (maximum) radiance values are needed for the design of the hyperspectral Ocean Color Instrument (OCI). These values can be determined either by using radiative transfer simulations for a realistic model of ocean-atmosphere system, or by using the previously published values of Ltyp for a similar instrument. This paper describes the details of Ltyp calculation by the second method. For Lmax calculations, it is assumed that TOA reflectance would not exceed 110% of the reflectance of a Lambertian perfect reflector, with the exception of SWIR and red bands where lower reflectance (≤ 100%) is assumed. Also, it is assumed that the normalized Ltyp values, defined as Ltyp/F_0 (typical radiance/Thuillier solar irradiance), do not depend on the sensors' band widths. Results for 5-nm band average (from 310 to 2260 nm), and 32 bands, including those reported in *Meister et al.* [2011], are presented in this paper.

8.1. Introduction

This paper describes the Ltyp and Lmax calculations for the PACE Ocean Color Instrument (OCI). Ltyp and Lmax are, respectively, observed spectral radiance and maximum radiance values commonly observed at the top-of-atmosphere (TOA) over the globe. Ltyp, typical spectral radiance expected from clear ocean scenes, and Lmax, maximum measurable spectral radiance (e.g. for highly reflective clouds) are reference signals needed to enable the design studies partaken during the design of the satellite spectroradiometers [*Hu et al.*, 2012].

For remote sensing of the ocean, the OCI will measure the TOA radiances from 350 nm to 900 nm in 5 nm intervals, and at selected wavelengths in SWIR, namely 940, 1250, 1378, 1615, 2130, and 2260 nm [see *Cairns and Ibrahim*, 2018; *Ibrahim and McKinna*, 2018]. As a result, more than 100 Ltyp and Lmax values are needed for OCI design consideration. Ltyp values can be determined by either using radiative transfer simulations for a realistic model of ocean-atmosphere system, or by using the previously published values of Ltyp for a similar instrument. This paper describes the details of Ltyp calculation by the second method. For Lmax, it is assumed that TOA reflectance will not exceed 110% of the reflectance of a perfect Lambertian reflector, except in case of SWIR and red bands where reflectance is assumed to be ≤ 100% (see sections 8.3.1. and 8.3.2)

[8] Cite as: Ahmad, Z., and G. Meister (2018), Ltyp and Lmax calculations for PACE Ocean Color Instrument, in *PACE Technical Report Series, Volume 7: Ocean Color Instrument (OCI) Concept Design Studies (NASA/TM-2018 – 2018-219027/ Vol. 7)*, edited by I. Cetinić, C. R. McClain and P. J. Werdell, NASA Goddard Space Flight Space Center Greenbelt, MD.

8.2. Computational Details for Ltyp Calculations

The OCI Ltyp values reported in *Meister et al.* [2011] were derived from observed MODIS Ltyp values given in Table 8.1.

Table 8.1. Wavelength, band-width, average Solar irradiance and Ltyp values for selected MODIS-Aqua bands [Franz et al., 2006].

no	λ	B_width	F0_avg	Ltyp
	(nm)	(nm)	(W m^{-2})	(W m^{-2} sr^{-1})
1	412	15	1715.1	78.4
2	443	10	1889.2	69.9
3	469	20	2060.3	65.2
4	488	10	1934.8	53.8
5	531	10	1859.1	38.7
6	551	10	1870.2	35
7	555	20	1836.1	32.8
8	645	50	1583.2	16.5
9	667	10	1523.8	14.7
10	678	10	1481.4	13.8
11	748	10	1276.3	8.89
12	859	35	963	4.81
13	869	15	954.1	4.6
14	240	20	455.7	0.89
15	640	35	234.6	0.28
16	2130	50	96.4	0.08

The computation involved normalizing the MODIS Ltyp values by band-averaged solar irradiance, which removed the variation in the solar spectrum from the MODIS data, and resulted in a dataset that could be described by a low order polynomial. A number of polynomials were tried, and it was found that

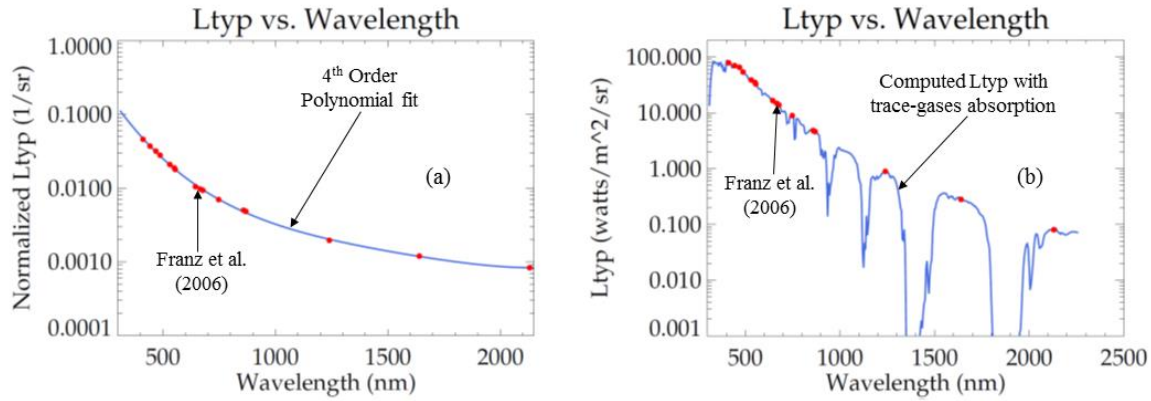

Figure 8.111. (a). The normalized Ltyp values vs. wavelength. The solid line represents a 4th order polynomial fit to MODIS Ltyp values derived by Franz et al. [2006]. Figure 1(b). The absolute Ltyp values vs. wavelength. The structure in the absolute values are due to solar irradiance at the top of the atmosphere. Note: The Ltyp values shown in this graphs include the effect of absorption by trace gases in the atmosphere.

a fourth order polynomial gave a reasonable fit. The coefficients of the fitted polynomial were then used to predict the normalized Ltyp values shown in Figure 8.1(a). The absolute Ltyp values for bands given in Table 8.2 were obtained by multiplying the normalized Ltyp values with the band-averaged solar irradiance values, which are also given in the same table.

Table 8.2. Wavelength, band-width, average solar irradiance (F_0_avg), revised Ltyp and Lmax values for 32 bands including those listed in Meister et al. [2011]. Note that Lmax for red bands and SWIR have been revised (as shown in Table 8.3 and 8.4)

#	λ	B_width	F0_avg	Ltyp_rev	Lmax_rev
	(nm)	(nm)	(W m^{-2} sr^{-1})	(W m^{-2} sr^{-1})	(W m^{-2} sr^{-1})
1	350	15	1019.1	76.77	356.84
2	360	15	1075.6	74.81	376.62
3	385	15	1100.2	63.05	385.21
4	412	15	1715.1	80.44	600.53
5	425	15	1661.6	70.98	581.78
6	443	15	1899.4	71.54	665.06
7	460	15	2064.2	69.26	722.76
8	475	15	2067.2	62.81	723.8
9	490	15	1956.8	53.98	685.16
10	510	15	1898.5	46.21	664.73
11	532	15	1862	39.69	651.98
12	555	15	1836.6	34.26	643.07
13	583	15	1779.6	28.41	623.1
14	617	15	1661	22.18	581.58
15	640	10	1611.9	19.19	564.38
16	655	15	1528.9	16.93	535.33
17	665	10	1531.2	16.17	536.12
18	678	10	1481.4	14.73	518.69
19	710	15	1398.7	12.07	489.75
20	748	10	1276.3	9.4	446.9
21	765	40	1229.2	8.46	430.39
22	820	15	1080	6.06	378.16
23	865	40	955.1	4.61	334.43
24	940	75	823.2	3.16	288.23
25	1245	20	451.7	0.9	158.16
26	1250	30	448.4	0.89	157.01
27	1378	15	364.7	0.6	127.71
28	1615	75	244.8	0.31	85.72
29	1640	40	234.6	0.3	82.16
30	2130	50	96.4	0.09	33.75
31	2135	50	95.6	0.09	33.48
32	2260	35	77	0.07	26.94

It was noted later that the *Meister et al.* [2011] Ltyp values had one problem: some of the bands used in the polynomial-fitting were ozone sensitive and, hence, the extrapolated values for wavelengths shorter than 412 nm were suspect. In addition, Ltyp values were needed at every 5-nm band of the instrument, which included bands that were affected by absorption by trace gases like ozone, oxygen, nitrogen dioxide, carbon dioxide and water vapor. It was apparent that a simple interpolation scheme would not have worked. To resolve the problem, it was decided to first remove the trace gasses absorption effect from the MODIS data, and then normalize the corrected data by the band-averaged solar irradiance at the TOA. This required band-averaged transmission values for the MODIS bands, which were generated using the Lowtran-7 code assuming a sun azimuth and view angle geometry of 30^o and 36^o, respectively.

Next, the corrected normalized Ltyp values, free from trace gases absorptions, were fitted with different orders of polynomial. A fourth order polynomial gave the best fit to the data. The coefficients of the fitted polynomial were then used to predict trace-gas-free normalized Ltyp values from 310 nm to 2260 nm at 5 nm intervals, and for 32 wavelengths including six new wavelengths not given in *Meister et al.* [2011].

To compute the Ltyp values reflecting the effect of absorption by trace-gases in the atmosphere, 5-nm-band-averaged values of transmittance and solar irradiance were determined. For wavelengths greater than 350 nm, the band transmittance computations included trace-gases like ozone, oxygen, nitrogen dioxide, carbon dioxide and water vapor. For wavelengths shorter than 350 nm, the transmittance calculations were only for ozone in the atmosphere. *Bass and Paur* [1984] ozone absorption coefficients and 101.2874 mmol m^{-2} (277 Dobson units) of ozone were used for this purpose. The band-averaged transmission values were determined from Beer's law. These calculations were also repeated for bands given in Table 8.2, where band-widths vary from 10 nm to 50 nm, but mostly they are 15 nm wide.

Finally, the Ltyp values reflecting the effect of trace gases were determined by multiplying the normalized Ltyp values with band-averaged transmittance and solar irradiance values. Here, it should be noted that in these calculations it is assumed that the normalized Ltyp values do not depend on the sensor's band width. Results of this exercise are summarized in Fig. 8.1(b) where 5-nm Ltyp values are plotted against wavelength (solid line). For comparison purposes, the MODIS Ltyp data [Table 8.1] are also shown by red dots.

8.3. Computational Details for Lmax Calculations

The computations of the Lmax values were straightforward. It was assumed that the base of the model atmosphere was a Lambertian surface and its reflectivity was equal to 110% of the perfect reflector, with the exception of red bands and SWIR (see chapters on red bands and swir). Scattering by air molecules and aerosols, as well as absorption by trace gases were ignored making the values conservative or relatively high. The calculations were performed for over-head sun position in the sky. The results for the 32 wavelengths are given in Table 8.2. The 5-nm band average values are shown in Fig. 8.2. Note that the structure in the Lmax values is due to the variation in solar irradiance. Also, note that the range of Lmax/Ltyp values in Table 8.2 is roughly 4.6 to 385, with the high ratios observed in the SWIR especially when revisions presented in next chapters are taken into consideration. Obtaining this range of ratios with adequate quantification (digitization) and SNR performance presents one of many challenges for the OCI design and engineering teams.

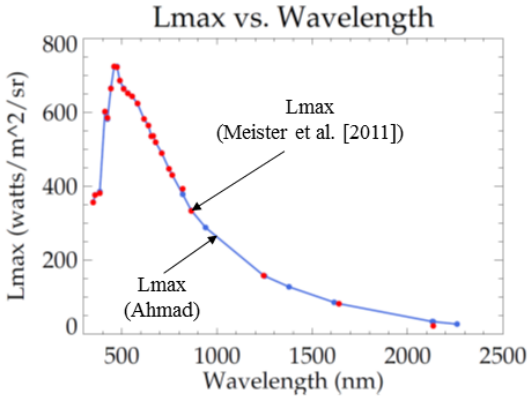

Figure 8.2. Lmax vs. wavelength. The solid line with red dots show Lmax values at the TOA for 32 bands from 350 nm to 2260 nm. The blue dots show Lmax values for 26 bands from 350nm to 2135 nm reported in Meister et al. [2011].

8.3.1. Reduction of SWIR Lmax in February 2018

In February 2018, the vendor for the OCI SWIR bands notified the OCI team that the SWIR Lmax pose a significant challenge to a successful delivery of the SWIR module. For the 1250nm band, a more realistic (but less conservative) maximum reflectivity of 100% (instead of the 110% previously) was used to calculate Lmax. Based on information provided by Brian Cairns, we decided to assume maximum cloud reflectivities of 90% and 62% for the bands at 1615nm and 2260nm, respectively. The 1615nm band has similar absorptions for ice and water, the 2260nm absorption is dominated by ice clouds. Lmax for the 940nm and 2130nm were chosen based on the Lmax suggested by Brian Cairns in his email from June 2017. For 1378nm, the closest equivalent is the cirrus band on VIIRS, so the Lmax of that band is used here. The reduced Lmax values (Lmax_rev2) are shown in Table 8.3 for the SWIR.

Table 8.3. Reduced Lmax for the SWIR bands

Wavelength (nm)	**Bandwidth (nm)**	**Lmax_rev2 (W m^{-2} sr^{-1} μm^{-1})**
940	45	200.53
1038	75	N/A (OCI design choice)
1250	30	142.74
1378	15	77.1
1615	75	70.13
2130	50	21.74
2260	75	15.18

8.3.2. Reduction of Red Spectrograph Lmax in February 2018

In February 2018, test results for the red CCD gain were coming in at the low end of expectation, leading to SNR that were not as high as they could have been. The OCI team determined that by reducing the Lmax for the red spectrograph, the SNR could be increased. For the bands from the red spectrograph

(617nm to 865nm), a more realistic (but less conservative) maximum reflectivity of 100% (instead of the 110% previously) was used to calculate Lmax. The reduced Lmax values (Lmax_rev2) are shown in Table 8.4 for the bands from 617nm to 865nm.

Table 8.4. Reduced Lmax for 617nm to 865nm

Wavelength (nm)	**Bandwidth (nm)**	**Lmax_rev2 (W m^{-2} sr^{-1} μm^{-1})**
617	15	528.71
640	15	513.07
655	15	486.66
665	10	487.38
678	10	471.54
710	15	445.23
748	10	406.27
820	15	343.78
865	40	304.03

Chapter 9

Analysis of PACE OCI Spectral Resolution Considerations

Ryan Vandermeulen, Science Systems and Applications Inc, Lanham, Maryland[9]

Antonio Mannino, NASA Goddard Space Flight Center, Greenbelt, Maryland

Aimee Neeley, Science Systems and Applications Inc, Lanham, Maryland

Jeremy Werdell, NASA Goddard Space Flight Center, Greenbelt, Maryland

Robert Arnone, University of Southern Mississippi, Hattiesburg, Mississippi

Executive Summary

In this study, the optimal spectral resolution for Plankton, Aerosol, Cloud, ocean Ecosystem (PACE) Ocean Color Instrument (OCI) is examined. Requirements for spectral sampling are determined by utilizing a novel statistical technique to quantify the frequency at which spectral patterns occur over a variety of water types and phytoplankton functional types (PFTs). These methods are presented along with results showing that a continuous spectrum of 5 to 7 nm spectral resolution is optimal to resolve the variability across mixed reflectance and absorbance spectra. In addition, the impact of uncertainty on subsequent derivative analysis is assessed, showing that, at 5 nm spectral sampling, a 3% Gaussian noise (signal-to-nose ratio, SNR ~66) addition compromises data quality without smoothing the spectrum, and a 13% noise (SNR ~15) addition compromises data with smoothing. This work additionally appears in Vandermeulen et al. [2017].

9.1. Introduction

Historically, ocean color satellite sensors have increased the number of bio-optical spectral bands with each succeeding mission, e.g., Coastal Zone Color Scanner (3 bands), SeaWiFS (6 bands), and MERIS (9 bands). Since these sensors were approved and designed, much progress has been made with respect to the spectral requirements for future sensors [*IOCCG*, 2012; *Lee et al.*, 2007]. In the planning and design specifications for PACE-OCI, it is noteworthy that higher spectral resolution comes at a cost of reducing the signal-to-noise ratio (SNR) of the instrument, as there is less signal (photons) reaching the detector(s) when shorter spectral intervals are sampled. This can be compensated for by modifying certain engineering parameters in the design of the sensor, but can subsequently have an adverse impact on the quality of satellite retrievals, as well as the cost and complexity of a mission. For example, increased SNR in hyperspectral measurements can be obtained by reducing the spatial resolution (i.e. larger ground sampling footprint) to allow more photons into the sensor and increase the signal, but this can also introduce additional uncertainty as a result of subpixel variation in bio-optical properties [*Lee et al.*, 2012]. Alternatively, reducing the dynamic range of the detector(s) optimizes the sensor's ability to detect a given range of photon densities, but can lead to saturation or non-detection of radiance signals if this

[9] Cite as: Vandermeulen, R., A. Mannino, A. Neeley, J. Werdell, and R. Arnone (2018), Analysis of PACE OCI Spectral Resolution Considerations in *PACE Technical Report Series, Volume 7: Ocean Color Instrument (OCI) Concept Design Studies (NASA/TM-2018 – 2018-219027/ Vol. 7),* edited by I. Cetinić, C. R. McClain and P. J. Werdell, NASA Goddard Space Flight Space Center Greenbelt, MD.

range is too narrow, e.g., the MODIS fluorescence band, and may require multiple gain settings [*Meister et al.*, 2011]. Therefore, it is necessary to quantify the optimal spectral sampling frequency in order to maximize the quality and efficacy of data retrievals. This study tests a new methodology to quantify the optimal spectral resolution and noise thresholds required to discern subtle spectral features that may be important for PFT algorithm development or other applications over a variety of water-types.

9.2. Analysis Methods

9.2.1. Data Collection

Hyperspectral data were collected from multiple sources to simulate a highly idealized environment (phytoplankton absorbance from filter pad-based optical density, OD_f, obtained on various cultures), as well as realistic environments with complex optical features (phytoplankton absorption, a_{ph}, and above water remote sensing reflectance, R_{RS}) from field measurements. These data were the basis for subsequent statistical analysis to help address the optimal spectral resolution at which spectral peaks and valleys can be resolved, as described in section IIB. In order to ensure that the complete characterization of the spectral shape of peaks and valleys, data were collected at the highest available spectral resolutions.

Above-water remote sensing reflectance measurements at < 3 nm spectral resolution (sampled at 1 nm) were taken using Analytical Spectral Device (ASD) FieldSpec^{TM} Spectroradiometers collected over three years (2012–2015) from various locations, including the turbid Mississippi River plume (4 spectra, average chlorophyll-*a* = 6.18 ± 2.58 μg L^{-1}), coastal waters of the Gulf of Mexico/U.S. East Coast (4 spectra, average chlorophyll-*a* = 1.40 ± 0.47 μg L^{-1}), shelf waters from the Gulf of Mexico/U.S. East Coast (4 spectra, average chlorophyll-*a* = 0.59 ± 0.09 μg L^{-1}), the Gulf stream (4 spectra, average chlorophyll-*a* = 0.27 ± 0.09 μg L^{-1}), the Bahamas (4 spectra, average chlorophyll-*a* = 0.19 ± 0.03 μg L^{-1}), and a *Microcystsis* bloom in Lake Erie (1 spectrum, chlorophyll-*a* = 124.23 μg L^{-1}). Vandermeulen et al. [2017] provides detailed information on collection locations, data preparation, and processing.

For phytoplankton absorbance data, four cultures (*Nannochloropsis sp.*, *Thalassiosira weissflogii*, *Emiliania huxleyi*, *Synechococcus sp.*) were grown under simulated sunlight conditions, and filtered onto GF/F filter pads. Vandermeulen et al. [2017] provides details on collection and processing. Blank-corrected filter pad-based optical density OD_f values are utilized for statistical analysis of variability, since the corrections to obtain absolute absorption values would make minimal difference to the spectral shape. We also acquired phytoplankton absorption (a_{ph}) spectra from natural seawater samples in the Yellow Sea/Korean Strait, from the GOCI validation field campaign (2013-09-27 to 2013-10-02) from NASA SeaBASS (https://seabass.gsfc.nasa.gov/) for use as an independent data source to check the consistency of our results.

9.2.2. Statistical Analysis

Variogram analysis is a geo-statistical technique that has been used to determine the optimal frequency of spatial sampling (i.e. spatial resolution) for resolving bio-optical processes in various water types [*Aurin et al.*, 2013; *Bissett et al.*, 2004; *Davis et al.*, 2007; *Yoder et al.*, 1987]. In this study, the use of the empirical variogram is extended to analyze the minima and maxima of the (de-trended) first derivative of spectral data, essentially treating spectral data in the same manner as spatial data. The fundamental concept of the empirical variogram, $\gamma(h)$, is to quantify how data are related (correlated) with "distance":

$$\gamma(h) = \frac{1}{2\left|N(h)\right|}\sum_{N(h)}\left(z_i - z_j\right)^2 \qquad \text{(Eq. 9.1)}$$

where h is spectral distance between locations i and j (e.g., 1 nm), $N(h)$ is the number of all possible pairwise distances (e.g., all instances of 1 nm separation), z_i and z_j are the data values at locations i and j, respectively. The empirical variogram is a measurement of the average squared difference between data separated by distance h, and each average(h) is a point on the variogram (Fig. 9.1(a)). The calculation proceeds for all distances, h = 1 nm, 2 nm… 50 nm. At some point, the variance measured at different distances (spectral resolutions) reaches a maximum, indicating the data are no longer auto-correlated, and this point represents a measurement of the variance of the random field (the sill, σ_n^2, (Fig. 9.1(a)). The range, a, describes the distance at which data are not auto-correlated, and the nugget (c_n, y-intercept) represents the uncertainty, or micro-scale variations in the data, or both [*Matheron*, 1963]. The variogram can be mathematically represented by one of several models depending on the data structure. In this case, the data were best represented by a Gaussian model:

$$g(h) = c_n + \sigma_n^2\left(1 - \exp\left(\frac{-h^2}{a^2}\right)\right) \qquad \text{(Eq. 9.3)}$$

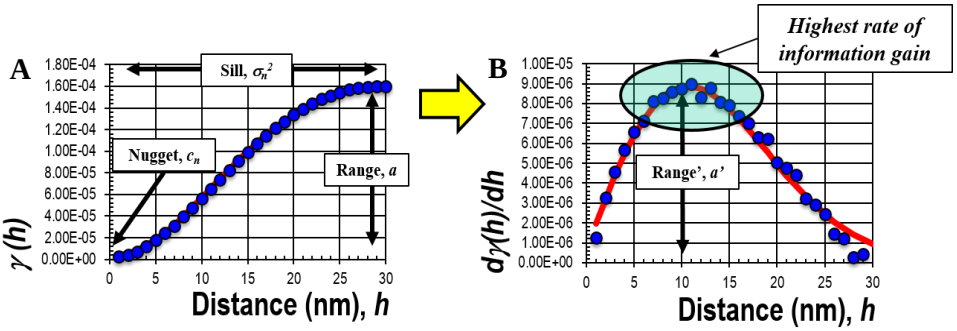

Fig. 9.1. (A) Empirical variogram performed on the first derivative of spectral phytoplankton absorbance data. Note the relative "flattening" of the tail at the origin of the Gaussian curve. This feature is exploited to gain the maximal rate of information gain, as seen in (B). This distance, or spectral resolution, at which $d\gamma(h)/dh$ is maximized is interpreted as the optimal spectral sampling frequency.

Note that the variance decreases significantly as h approaches zero (Fig. 9.1(a)), i.e. the curve flattens out and little information is gained with every nanometer increase in spectral resolution. This "flattening" suggests that the minimum resolution of the spectral data is sufficient to resolve the variability of the underlying patterns. The degree to which this variance changes with every nm increase in resolution will change as a function of the kurtosis of the Gaussian curve. To quantify this, the rate of change in variance, $d\gamma(h)/dh$, can be plotted as a function of spectral resolution, emphasizing the sampling frequency at which more/less information is gained (Fig. 9.1(b)). The maximum value of this plot shows the location of the maximum rate of information gain. Below this point (higher spectral resolution), there is less relative information gained per nanometer of spectral resolution increase, which indicates that increasing the spectral resolution (at the potential cost of reduced SNR) beyond $d\gamma(h)/dh$ *MAX* may not be an optimal sampling design. This maximal value was used to determine the optimal spectral sampling frequency across discrete segments of the UV/visible/NIR spectra.

For each individual spectrum measured, a series of empirical variograms (and subsequent analyses, as described above) were constructed from at least 50 nm discrete segments of data across a spectral range of 375–725 nm. For the phytoplankton absorbance spectra derived from laboratory cultures, these 50 nm windows used to run the statistical analysis were centered and sampled in 25 nm increments (e.g., 375–425 nm, 400–450 nm, 425–475 nm … 675–725 nm), ensuring the entire spectral range of data were covered and slightly oversampled. The R_{RS} variograms were also constructed from 50 nm windows of data, but were sampled at 15 nm increments (e.g., 375–425 nm, 390–440 nm, 405–455 nm … 675–725 nm). The R_{RS} data were sampled at higher incremental frequency due to increased likelihood of overlapping peaks in a mixed natural assemblage. Results are reported in this chapter as the center wavelength of each 50 nm window. Relatively large intervals, $N(h)$, are used for this analysis to ensure that sufficient data points exist to yield robust statistical results. As a general rule of thumb, a minimum of 30 pairs should be examined when calculating empirical variograms, as an increase in data points enhances the accuracy of variogram estimates. The minimum number of pairs that can be examined to yield a reliable variogram estimate is equivalent to half of the maximum distance of the field [*Journel and Huijbregts*, 1978]. In this case, 50 nm is the maximum distance of the field, therefore the information retrieved from variograms is less reliable at resolutions of 25 - 50 nm, and more reliable at 1 – 24 nm. It should be noted that not all variance is resolved at the maximal point of $d\gamma(h)/dh$ that is calculated from each spectrum. Since the value of $\gamma(h)$ at any given point represents the variance at a corresponding spectral resolution, a ratio of this value against the sill (total variance of the random field) represents the relative percentage of total resolved variance at that resolution. This was computed at $\gamma(h)$ points corresponding to the maximal point of $d\gamma(h)/dh$ at each sampling increment in this analysis to quantify how much total variance is resolved at the optimal sampling frequency.

In addition, a sensitivity analysis was performed on the full analyzed spectrum (375–725 nm) of the 21 R_{RS} spectra (converted to normalized water leaving reflectance), in order to assess how much noise can be added to the spectra before the utility of the data is compromised, and thus examine the viability of using derivative-based algorithms with potentially noisy satellite data. The sensitivity analysis is performed by adding 0.25% increments of Gaussian white noise and identifying the noise level at which $\gamma(5\text{nm}) = \gamma(10\text{ nm})$ over the whole spectrum. This is essentially a measure of when 5 nm data is not distinguishable from 10 nm data, therefore a 10 nm continuous spectrum has as much utility as a 5 nm continuous spectrum. This analysis is performed again after performing a Savitsky-Golay smoothing function with a polynomial order of 4 and frame size of 13 (chosen as the closest proxy between 10 and 15 nm smoothing). The Savitsky-Golay filter is frequently used for derivative analysis and was chosen for its capacity to preserve relative minima and maxima inflections in the spectrum [*Xi et al.*, 2015].

9.3. Results

9.3.1. Phytoplankton Absorbance/Absorption

The absorbance from four separate phytoplankton species, including one diatom (*Thalassiosira weissflogii*), one eustigmatophyte (*Nannochloropsis sp.*), one cyanobacteria (*Synechococcus sp.*), one coccolithophore (*Emiliania huxleyi*), and one mixed culture with all four species, encompasses spectral variability scales which include a variety of overlapping pigment peaks, including phycocyanin, phycoerythrobilin, phycoerythrin, chlorophylls, carotenoids, etc. (Fig. 9.2(a)). The optimal spectral sampling frequency was rarely greater than 7 nm spectral resolution for individual or mixed cultures, and was as low as 15 nm spectral resolution (Fig. 9.2(b)). On average, the percent resolved variance at the optimal spectral sampling frequency was 74 ± 3% for *Thalassiosira weissflogii*, 78 ± 6% for *Nannochloropsis sp.*, 72 ± 3% for *Synechococcus sp.*, 72 ± 5% for *Emiliania huxleyi*, and 74 ± 4% for the

mixed assemblage. As a point of reference for comparison, an analysis run on nine natural seawater samples (Fig. 9.2(c)) with higher spectral data intervals (0.2 nm) spanning a spectral range of 400–480 nm and 600–680 nm (areas with highest suggested spectral sampling frequency from Fig. 9.2(b)), yielded an average optimal resolution of 7.0 ± 0.4 nm (90 ± 6% resolved variance) and 6.5 ± 0.3 nm (84 ± 6% resolved variance), respectively.

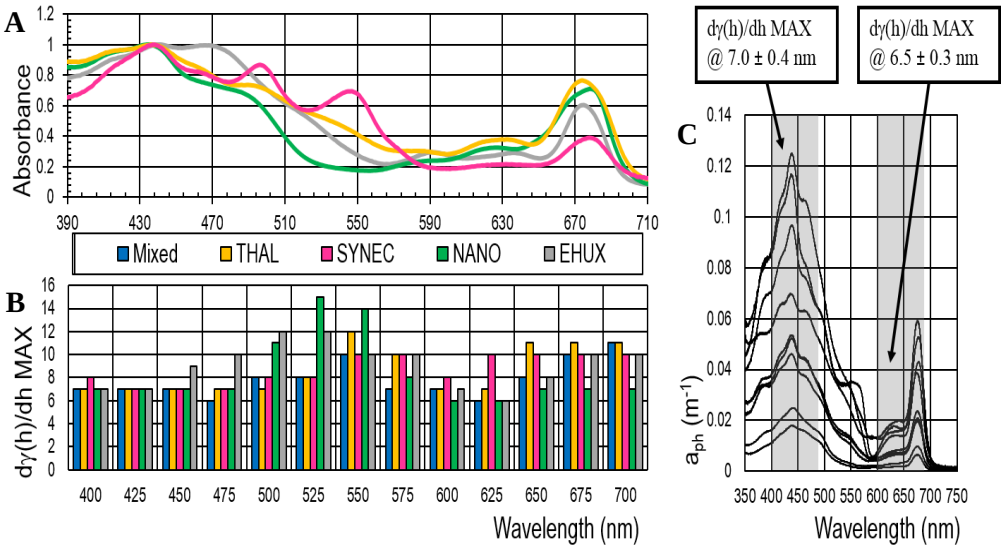

Fig. 9.2. (A) Continuous 1 nm resolution spectra of four species of phytoplankton used in this analysis, Thalassiosira weissflogii (THAL), Synechococcus sp. (SYNEC), Nannochloropsis sp. (NANO), Emiliania huxleyi (EHUX), representing a diverse collection of pigment expressions. (B) The corresponding dγ(h)/dx max in 25 nm increments, indicating the optimal spectral resolution at which the most information is obtained within each increment. Results show most features are resolved between 6–15 nm spectral resolution. (C) Phytoplankton absorption from natural assemblages collected from the Korean Strait, highlighting the areas with the highest frequency of absorptions peaks/inflections. Within these highlighted ranges, the optimal spectral frequency is around 6.5-7.0 nm.

9.3.2. Remote Sensing Reflectance

The analysis of remote sensing reflectance derived from six distinct water types, ranging from turbid freshwater/coastal waters to blue, oligotrophic waters showed that most spectral features were optimally resolved at a spectral resolution of 4–15 nm (Figs. 9.3(a)- 9.4(f)), depending on the location within the spectrum and water type. At the defined spectral resolutions within the figures, this accounts for 60–87% of the total resolved variance. In the case of the turbid monoculture *Microcystis* bloom, most features were resolved with a 6 nm continuous spectrum, with some sloping portions of the spectrum tolerating >12 nm spectral resolution (Fig. 9.3(a)). The coastal and shelf waters along the Gulf of Mexico/U.S. East Coast show a spectral sampling frequency of 5 nm may be required to optimally resolve the spectral features centered around 685 nm (Figs. 9.3(c) and 9.4(d)). The analysis shows that the same regions in the low-signal oligotrophic Gulf Stream and Bahamas water (Figs. 9.3(e) and 9.3(f)), as well as the high-signal *Microcystis* and turbid river plume waters (Figs. 9.3(a) and 9.3(b)) are optimally resolved with a 6 nm semi-continuous spectrum.

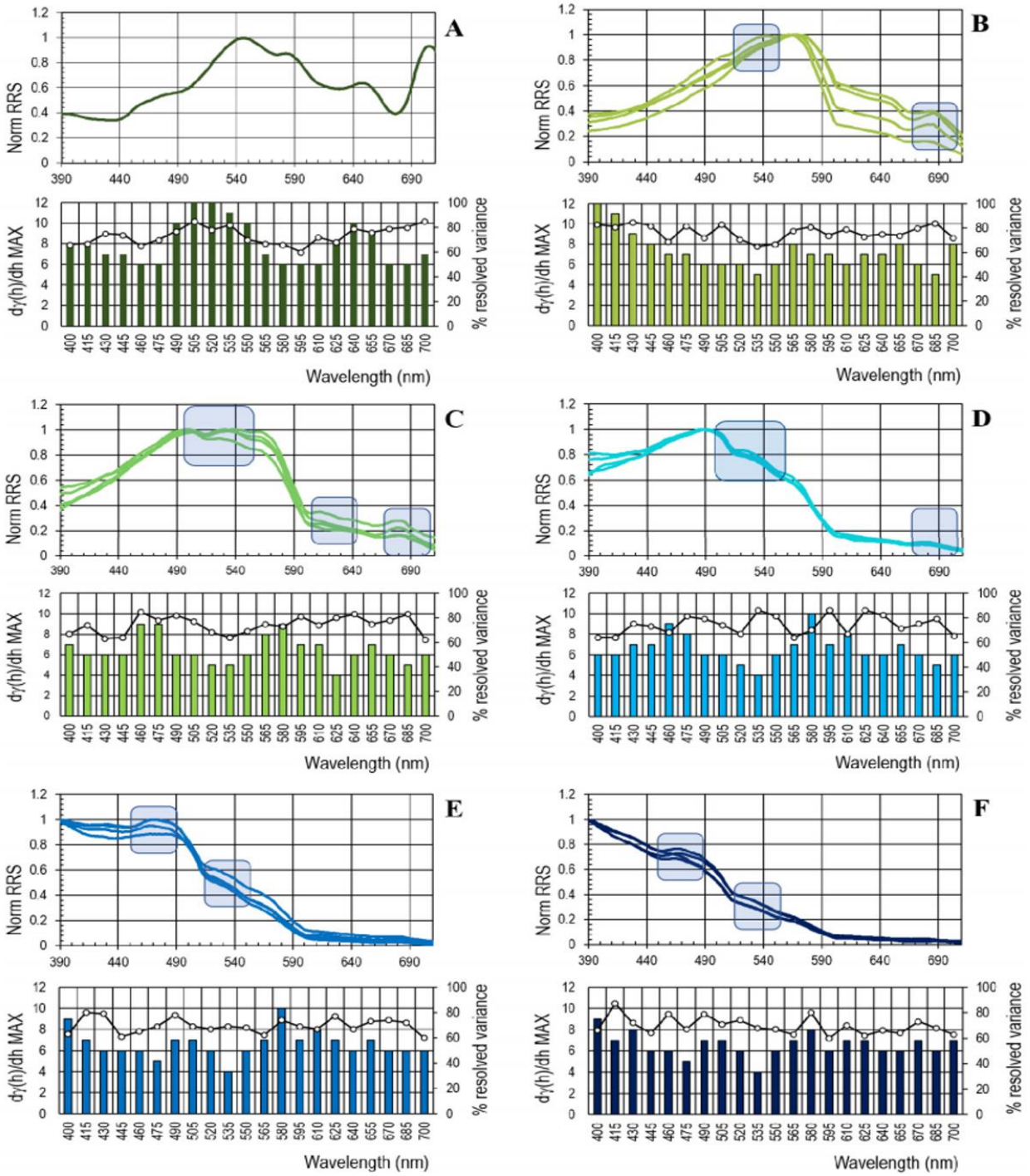

Fig.9.3. Continuous 1 nm spectra and corresponding bar graphs (below) indicating the optimal spectral sampling frequency (dγ(h)/dh maximum; bars) as well as the percent resolved variance (dots + line) at given band centers for varying water types. The blue boxes highlight regions that are optimally resolved at 5 nm or less. Water types: (A) One Microcystis bloom spectrum collected from Lake Erie, MI., (B) Four spectra from the turbid river plume waters of the Gulf of Mexico, (C) Four spectra from green coastal waters in the Gulf of Mexico and U.S. East Coast, (D) Four spectra from the shelf waters in the Gulf of Mexico and U.S. East Coast, (E) Four spectra from the open blue waters of the Gulf Stream along the U.S. East Coast, and (F) Four spectra from clear oligotrophic waters in the Bahamas.

Other persistent features included a region of spectral sensitivity (4 – 5 nm spectral sampling frequency) centered around 535 nm, which was present in all the spectra, besides the *Microcystis* bloom (Figs. 9.3(b)- 9.3(f)). Two other notable features include a region in the coastal green water (Fig. 9.3(c)) centered around 625 nm that suggests an optimal spectral sampling frequency of 4 nm, in addition to a spectral feature centered at 475 nm appearing in the oligotrophic Gulf Stream and Bahamas water (Figs. 9.3(e) and 9.3(f)), which shows an optimal spectral sampling frequency of 5 nm. With a few exceptions, the remainder of the spectral features in all-natural waters typically require less than 10 nm spectral resolution to optimally resolve the underlying spectral features.

9.3.3. Qualitative Analysis of Spectral Subsampling

Here, we qualitatively visualize the impact of spectral subsampling on a remote sensing reflectance spectrum in complex coastal waters. This simple visualization (Fig. 9.4) displays 1 nm data (orange line) with an overlay of corresponding 5 nm weighted bins (gray dots). The 5 nm bin increments are set according to the nominal proposed configuration of OCI (342–587 nm, 585–750 nm), and are subject to change. Highlighted in the zoom windows are some spectrally complex regions, including fluorescence peak (red tint), phycobilin peaks (yellow tint), and a region sensitive to cyanobacteria reflectance and phycoerythrobilin absorption (blue tint).

Results show little information is lost at 5 nm sampling, however, this does not account for potential shifts in spectral peaks (e.g., red fluorescence peak), that may be enhanced with < 2nm spectral subsampling. Visualizing a 10 nm sampling resolution (skipping every other dot), it becomes apparent that, while the absolute location of peaks can often be maintained, subtle peaks that may be important to PFT distinction would be lost in spectral binning.

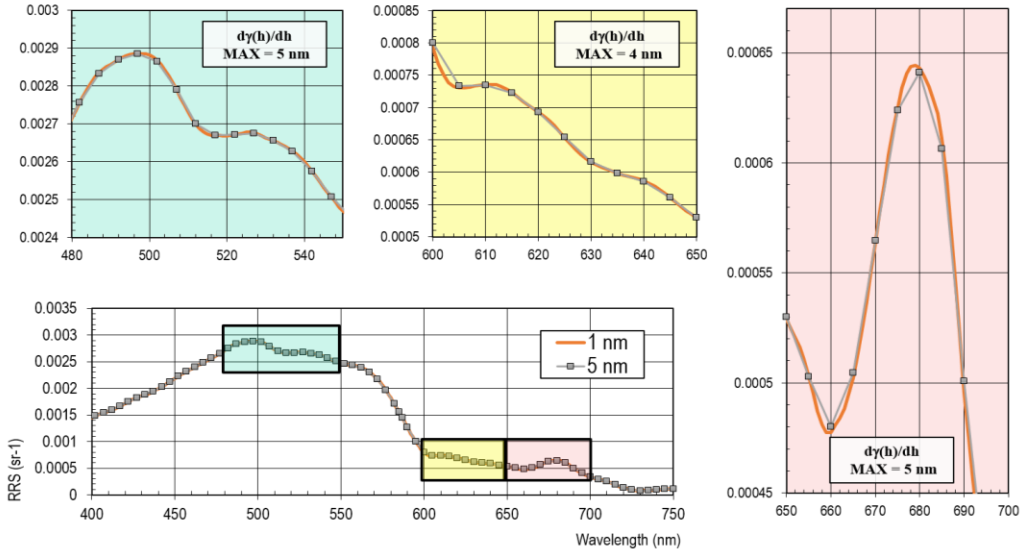

Fig.9.4. A single remote sensing reflectance spectrum taken from coastal waters demonstrates spectral sensitivity on the order of 4-5 nm in certain regions. These regions are highlighted in color-coded boxes, with the corresponding dγ(h)/dh maximum found for each particular spectral region. The orange line represents continuous 1-nm spectral sampling, while the gray dots are the proposed 5 nm weighted bins currently proposed for PACE-OCI.

The spectral range and spectral resolution requirements for PACE still have some degree of flexibility at the current stage of planning. The PACE Ocean Color Instrument (OCI) is projected to nominally

sample at a spectral resolution of 5 nm, with the possibility of 1.25 nm subsampling pre-defined regions at a higher spectral resolution. One key feature of the PACE mission will be the ability to differentiate various PFTs from space, which will require more spectral bands and finer spectral resolution than present ocean color sensors.

9.3.4. Spectral Noise Thresholds

Assuming a 5 nm continuous spectra as a baseline for PACE-OCI, incremental Gaussian noise additions made on all 21 normalized water leaving reflectance spectra show that only ~3% noise could be tolerated before 5 nm (first derivative) data resolves the same amount of variability as 10 nm (first derivative) data (Fig. 9.5(b)) over the entire integrated visible spectrum. For these spectra, the 3% noise addition equated to an SNR of approximately 66. Since it is a common practice to utilize smoothing techniques prior to performing derivative analysis, a 13 nm Savitsky-Golay smoothing function was applied after each increment of noise, bringing the noise threshold up to approximately 13% (Fig. 9.5(c)). Across the entire visible spectrum and across all water types, this equated to an average SNR of approximately 15. Using a 15 nm mean boxcar filter, the threshold was increased to nearly 20% (not shown), however, there were severe aberrations to the original spectrum, including a spectral shift in peaks.

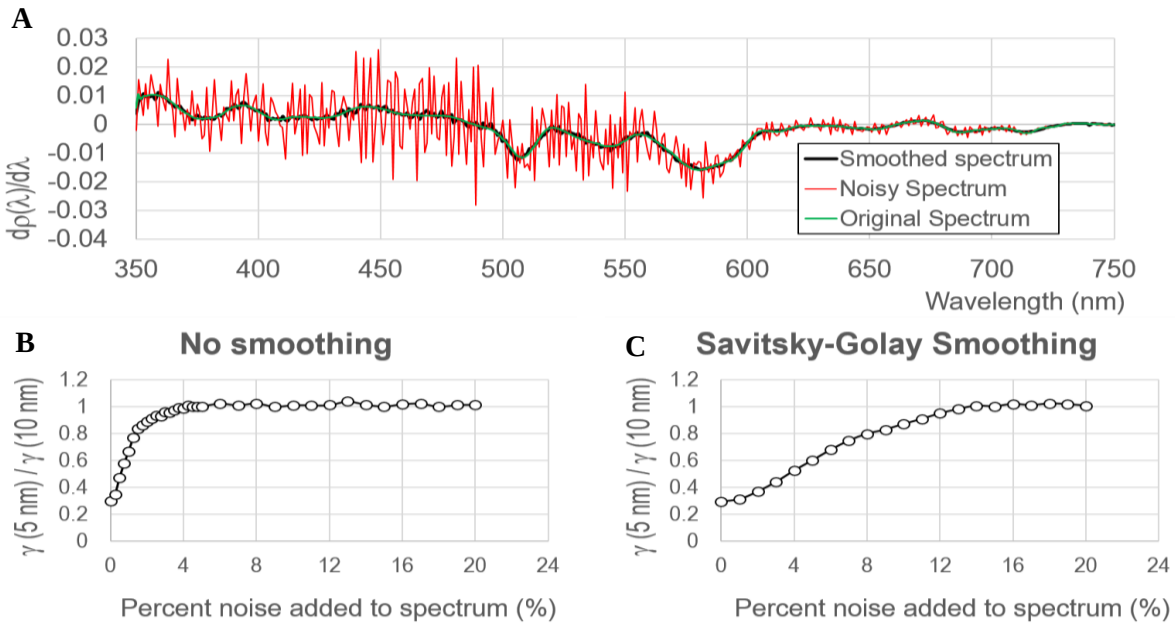

Fig. 9.5. (A) A single differential normalized reflectance spectrum (green line) taken from shelf waters of the Gulf of Mexico (Fig. 9.3(d)), shows aberrations after adding 3% Gaussian noise, with and without smoothing (black and red lines, respectively). Below, the ratio of γ(5 nm) to γ(10 nm) at incremental Gaussian noise additions is calculated for all spectra, indicating the threshold at which the variability of first derivative reflectance data at 5 nm spectral resolution meets or exceeds the variability of first derivative reflectance data at 10 nm spectral resolution, e.g., γ(5 nm)/γ(10 nm) = 1. (B) Without any spectral smoothing, the noise threshold is at ~3%. (C) With a Savitsky-Golay spectral smoothing function, this threshold is extended to 13%.

9.4. Discussion

The principle objective of this research is to evaluate the frequency of spectral sampling required to resolve subtle spectral features contained in hyperspectral data sets, in addition to nominally evaluating the efficacy of expected data product quality based on expected sensor performance. It is recognized that the datasets used for this analysis do not represent an inclusive measure of global ocean environments, however, this does not preclude the significance of results, as the data still represent diverse examples of bio-optical variability that will be detected by future ocean sensors.

It should be understood in the interpretation of results that a first-order derivative transformation of the data increases the sensitivity of the analysis. The original, non-transformed data do not have enough of a signal over narrow spectral windows for the variogram technique to be useful, so the features were exaggerated with the use of a first derivative. This means, at 1 nm spectral sampling, a single peak is transformed into two peaks after the first-derivative, three peaks after the second derivative, etc. creating a higher spectral sampling frequency with every consecutive derivative. Therefore, the spectral sampling frequency obtained from the statistical analysis of the first derivative is relevant to accurately re-constructing the shape of spectral inflections, not just capturing the location of peak maxima/minima. This may not be a high priority for all applications, but is potentially important to resolving spectral features where absorption peaks may overlap closely, especially in waters with mixed phytoplankton community compositions, or, for resolving shifts in spectral peaks. The use of 2nd and 4th derivative analysis can be used to further accentuate these peaks, however, the application of the empirical variogram technique to higher order derivatives would yield frequency information required for the hyperbolic reconstruction of the absolute spectral shape of a high order differential spectra, an application which may be excessive when considering the optimization of sensor design.

Additionally, in examining these results, it is noteworthy that there is some inherent limitation associated with the absolute resolution of the radiometric instrumentation to be able to detect narrow spectral features. While a 3 nm (or wider) bandwidth sampled at 1 nm could feasibly retrieve a signal from a 1 nm wide spectral feature (if the signal is strong enough), it is possible that such a feature would not be incorporated into the variogram analysis. Regardless, each variogram analysis consistently showed an increase in resolved variance as a function of increased the spectral resolution, down to the 1 nm sampling frequency (Fig. 9.1(a)). In other words, while the ASD sensor may measure at a larger spectral bandwidth than the absolute width of a given feature, the variogram still shows a reduction in variance (gain in spectral information) at 1 nm relative to 3 nm sampling intervals. However, this analysis is not intended to examine the exact resolution required to detect all spectral features present, per say, it is otherwise designed as a method to determine the optimal spectral resolution. The variograms are cast over a wide spectral window (50+ nm), examining the rate at which the highest amount of information is gained, on average, over this spectral window. Even with multiple 1 nm features present, for instance, the variogram would not likely display 1 nm as the optimal spectral resolution. There is some corroboration that 1 nm spectral features are not ubiquitous, as the laboratory-based absorbance measurements (absolute resolution 1 nm or less) did not show features present at 1 nm among multiple PFTs (Fig. 9.2(a)), however, absorbance is only one dimension of a multi-faceted in situ or satellite-based reflectance measurement. Finally, we note that other derivative analysis in the literature specifically aimed at extracting information on PFTs and pigments [*Isada et al.*, 2015; *Torrecilla et al.*, 2011] have utilized a 9 nm smoothing and band separation function to yield positive distinction of PFTs and/or pigments, therefore, the resolution and smoothing functions used in this study are likely relevant to these applications.

Based on this interpretation, several of the natural water spectra show that there are instances at which 5-6 nm spectral resolution may be required in order to fully resolve the various inflections within the spectra, such as around the chlorophyll fluorescence peak (~680 nm) in the reflectance data (Figs. 9.3(b)-9.3(d)). While a relatively broad peak (~20 nm wide), a sampling frequency of 10 nm would only enable the capture of the relative magnitude of the peak, and makes a critical assumption that this peak location is static. However, fluorescence peaks have been known to shift by several nanometers, especially in waters with high concentrations of chlorophyll. This suggests that in some instances, an even finer spectral resolution than 5 nm could be useful to detect the true maxima of the fluorescence peak. In contrast, the absorbance data from the laboratory cultures do not include fluorescence and exhibit much broader absorption peaks in the red (650 – 700 nm) that are optimally resolved with 10 nm resolution, with the exception of the chlorophyll absorption peak seen in the Nannochloropsis culture, which may require a slightly higher sampling frequency (~7 nm) compared to other cultures in order to characterize the slightly irregular shaped peak (Fig. 9.2).

Elsewhere in the absorption and reflectance data, there are several instances of spectral variance on the order of 4-6 nm, such as around 625 nm, where multiple overlapping peaks and concentrations of chlorophylls-a,b,c are present over a broad spectral range, or around 425 – 500 nm, where multiple chlorophyll, photo-protective, and carotenoid pigment absorption peaks overlap [*Wright et al.*, 2005]. There are also regions in the spectra which exhibit high spectral variance, but which are not traditionally recognized as significant to ocean color. For instance, a high amount of spectral variance centered at ~535 nm (510 – 560 nm) was common to most all reflectance spectra. While this is a region of strong phycoerythrobilin pigment absorption as well as cyanobacteria reflectance, it is unlikely ubiquitous in all the water types sampled. Since the nature of the variogram analysis requires large spectral windows (at least 50 nm window at 1 nm spectral resolution) to gain enough signal, there are likely a combination of spectral features spanning this window that are integrated into the results. This is supported by observations by Torrecilla et al. [2011] showing that the 495 – 540 nm window has been recognized as a distinctly useful spectral region for discriminating phytoplankton pigment assemblages in open ocean waters. While the analysis is highly sensitive to spectral variability, the exact locations of these inflections within the 50 nm spectral window are more difficult to pinpoint with variograms, and are better resolved with studies examining zero-intercepts of the first and second derivative [*Isada et al.*, 2015; *Lee et al.*, 2007; *Wolanin et al.*, 2016].

Results derived from independent analysis specifically aimed to determine the spectral resolution required for PFT and/or phytoplankton pigment distinction are generally in line with the suggested optimal resolutions which are concluded from this study (5 – 7 nm), however, as previously mentioned, there is some discrepancy in the literature among specific recommendations for spectral resolutions. For instance, results from Roelke et al. [1999] suggest a slightly higher spectral resolution than presented in this study, showing that the distinction of chlorophyll-a and chlorophyll-b peaks in green algae composite absorption data begin to deteriorate at 5 nm and 7 nm spectral resolutions, respectively. *Wolanin et al.* [2016] focused on the distinction of three specific PFTs, and showed a small improvement of results when increasing from 10 nm to 5 nm continuous spectral resolution, and even less improvement when increasing from 5 nm to 1 nm spectral resolution. By contrast, Lee et al. [2007] used 1st and 2nd derivative analysis to suggest 17 strategically placed bands based on the highest frequency of peak occurrences on over 400 spectra, however, this is optimized for the detection of the most frequently occurring peaks, and can change with variability of the datasets, potentially neglecting the detection of signal at the cost of reducing redundancy. The focus of this study is not to assign attribution of individual peak signals or detect specific PFTs, per say, but to present an unbiased methodology to detect the frequency of spectral inflections across any region of the electromagnetic spectrum, regardless of the

source of the signal. The adaptive nature of continuous hyperspectral data enables users to determine which bands are most important for specific applications, but it is imperative to first ensure that these spectral features are being detected with a reasonable SNR that will enable viable retrievals of downstream product applications. As suggested by Wolanin et al. [2016], some redundancy in spectral information can increase the adaptability of data across multiple algorithms and water types.

The afore mentioned sensitivity of the empirical variogram analysis to variability makes it a useful tool to additionally quantify the impacts of noise on spectral signatures. This analysis showed that data viability for derivative analysis is compromised when only ~3% noise is introduced (SNR ~66), however, this was significantly alleviated by smoothing the spectrum, which is a common treatment for derivative analysis. This finding is in line with a previous study of SNR in which an analysis of 2,500 absorption spectra containing mixed concentrations of *Prorocentrum minimum* and other algae showed that an SNR of ~34 was sufficient to properly distinguish and classify P. minimum as a dinoflagellate (≥ 80% chlorophyll contribution) using 4th derivative analysis [*Roelke et al.*, 1999]. Various methods of smoothing can be implemented to reduce the possibility of leveling spectral features [*Tsai and Philpot*, 1998] beyond that used in this experiment, and may be useful for further reducing instrument noise effects.

The PACE OCI is projected to nominally sample at a spectral resolution of 5 nm, and with careful smoothing procedures, the current design for the PACE OCI should provide useful hyperspectral derivative data for use in PFT algorithm development and improved ocean color products. It should be noted, however, that this analysis is focused on the resolution required to detect ocean-specific features from in situ and laboratory data, but does not take into account very narrow spectral features introduced from vibrational Raman scattering and Fraunhofer Lines [*Wolanin et al.*, 2015] or other spectral features that a satellite sensor will be subject to at the top of the atmosphere, such as absorbing gases [*Tzortziou et al.*, 2014], which can introduce uncertainty in retrievals and may require higher spectral resolution to correct for.

9.5. Recommendation

This study aimed to quantify the optimal spectral resolution and signal to noise thresholds required to discern subtle spectral features across various water types and phytoplankton functional groups. The results indicate that a continuous 5 nm spectrum with less than 13% uncertainty in the ocean signal is optimal in the resolution of ocean color variability from in situ derived remote sensing reflectance, with some regions of the spectrum potentially benefiting from enhanced spectral subsampling which would account for spectral shifts in peak maxima (e.g., chlorophyll fluorescence). At a 5 nm continuous spectral sampling frequency, the signal to noise ratio of the sensor will likely be the ultimate limiting factor for distinguishing fine scale peaks, but may be mitigated with various statistical smoothing techniques.

References

Aculinin, A. (2006), Variability of total column ozone content measured at Chisinau site, Republic of Moldova, *Moldavian Journal of the Physical Sciences*, *5*(2).

Ahmad, Z., B. A. Franz, C. R. McClain, E. J. Kwiatkowska, J. Werdell, E. P. Shettle, and B. N. Holben (2010), New aerosol models for the retrieval of aerosol optical thickness and normalized water-leaving radiances from the SeaWiFS and MODIS sensors over coastal regions and open oceans, *Appl. Opt.*, *49*(29), 5545-5560, doi:10.1364/AO.49.005545.

Ancellet, G., and F. Ravetta (2005), Analysis and validation of ozone variability observed by lidar during the ESCOMPTE-2001 campaign, *Atmospheric Research*, *74*(1-4), 435-459.

Antoine, D., J. M. André, and A. Morel (1996), Oceanic primary production: 2. Estimation at global scale from satellite (coastal zone color scanner) chlorophyll, *Global Biogeochem. Cycles*, *10*(1), 57-69.

Aurin, D., A. Mannino, and B. Franz (2013), Spatially resolving ocean color and sediment dispersion in river plumes, coastal systems, and continental shelf waters, *Remote Sens. Environ.*, *137*(Supplement C), 212-225, doi:https://doi.org/10.1016/j.rse.2013.06.018.

Ayukai, T., and D. Miller (1998), Phytoplankton biomass, production and grazing mortality in Exmouth Gulf, a shallow embayment on the arid, tropical coast of Western Australia, *Journal of Experimental Marine Biology and Ecology*, *225*(2), 239-251, doi:http://dx.doi.org/10.1016/S0022-0981(97)00226-8.

Bailey, S. W., B. A. Franz, and P. J. Werdell (2010), Estimation of near-infrared water-leaving reflectance for satellite ocean color data processing, *Optics express*, *18*(7), 7521-7527.

Barnes, P. Y., E. A. Early, and A. C. Parr (1998), Spectral reflectance NIST Special Publication 250-48, edited, US Department of Commerce, NIST.

Bass, A., and R. Paur (1984), Ultraviolet absorption cross-section of ozone: measurements, results and error analysis, paper presented at Proceedings, Quadriennal Ozone Symposium, Halkidiki, Greece.

Behrenfeld, M. J. (2010), Abandoning Sverdrup's Critical Depth Hypothesis on phytoplankton blooms, *Ecology*, *91*(4), 977-989, doi:10.1890/09-1207.1.

Behrenfeld, M. J., E. Boss, D. A. Siegel, and D. M. Shea (2005), Carbon-based ocean productivity and phytoplankton physiology from space, *Global Biogeochem. Cycles*, *19*(1), GB1006, doi:10.1029/2004GB002299.

Behrenfeld, M. J., and E. S. Boss (2014), Resurrecting the ecological underpinnings of ocean plankton blooms, *Annual Review of Marine Science*, *6*, 167-194.

Behrenfeld, M. J., and E. S. Boss (2018), Student's tutorial on bloom hypotheses in the context of phytoplankton annual cycles, *Global Change Biol.*, *24*(1), 55-77.

Behrenfeld, M. J., S. C. Doney, I. Lima, E. S. Boss, and D. A. Siegel (2013), Annual cycles of ecological disturbance and recovery underlying the subarctic Atlantic spring plankton bloom, *Global Biogeochem. Cycles*, *27*(2), 526-540.

Behrenfeld, M. J., and P. G. Falkowski (1997a), A consumer's guide to phytoplankton primary productivity models, *Limnol. Oceanogr.*, *42*(7), 1479-1491.

Behrenfeld, M. J., and P. G. Falkowski (1997b), Photosynthetic rates derived from satellite-based chlorophyll concentration, *Limnol. Oceanogr.*, *42*(1), 1-20, doi:10.4319/lo.1997.42.1.0001.

Behrenfeld, M. J., Y. Hu, R. T. O'Malley, E. S. Boss, C. A. Hostetler, D. A. Siegel, J. L. Sarmiento, J. Schulien, J. W. Hair, and X. Lu (2017), Annual boom–bust cycles of polar phytoplankton biomass revealed by space-based lidar, *Nature Geoscience*, *10*(2), 118.

Behrenfeld, M. J., and A. J. Milligan (2013), Photophysiological expressions of iron stress in phytoplankton, *Ann Rev Mar Sci*, *5*, 217-246, doi:10.1146/annurev-marine-121211-172356.

Behrenfeld, M. J., R. T. O'Malley, E. S. Boss, T. K. Westberry, J. R. Graff, K. H. Halsey, A. J. Milligan, D. A. Siegel, and M. B. Brown (2016), Revaluating ocean warming impacts on global phytoplankton, *Nature Climate Change*, *6*, 323, doi:10.1038/nclimate2838

Behrenfeld, M. J., et al. (2009), Satellite-detected fluorescence reveals global physiology of ocean phytoplankton, *Biogeosciences*, *6*(5), 779-794, doi:10.5194/bg-6-779-2009.

Behrenfeld, M. J., K. Worthington, R. M. Sherrell, F. P. Chavez, P. Strutton, M. McPhaden, and D. M. Shea (2006), Controls on tropical Pacific Ocean productivity revealed through nutrient stress diagnostics, *Nature*, *442*(7106), 1025-1028, doi:10.1038/nature05083.

Bhartia, P., and G. Wellemeyer (2002), TOMS V8 total ozone algorithm in OMI algorithm theoretical basis document: OMI ozone products*Rep.*, Tech. Rep. 2, edited by: Bhartia, PK, NASA Goddard Space Flight Center, Greenbelt, MD, USA.

Bissett, P., R. Arnone, C. Davis, T. Dickey, D. Dye, D. D. Kohler, and R. W. Gould (2004), From meters to kilometers, *Oceanography*, *17*(2), 32-34.

Blackwell, S. M., M. A. Moline, A. Schaffner, T. Garrison, and G. Chang (2008), Sub-kilometer length scales in coastal waters, *Continental Shelf Research*, *28*(2), 215-226, doi:http://dx.doi.org/10.1016/j.csr.2007.07.009.

Boyd, P. W., et al. (2007), Mesoscale iron enrichment experiments 1993-2005: synthesis and future directions, *Science*, *315*(5812), 612-617, doi:10.1126/science.1131669.

Bricaud, A., A. Morel, M. Babin, K. Allali, and H. Claustre (1998), Variations of light absorption by suspended particles with chlorophyll a concentration in oceanic (case 1) waters: Analysis and implications for bio-optical models, *Journal of Geophysical Research-Oceans*, *103*(C13), 31033-31044.

Cairns, B., and A. Ibrahim (2018), Analysis of PACE OCI SWIR Bands, in *PACE Technical Report Series, Volume 7: Ocean Color Instrument (OCI) Concept Design Studies (NASA/TM-2018 – 2018-219027/ Vol. 7)*, edited by I. Cetinić, C. R. McClain and P. J. Werdell, NASA Goddard Space Flight Space Center Greenbelt, MD.

National Research Council (2011), *Assessing the requirements for sustained ocean color research and operations*, The National Academies Press, Washington DC.

Cox, C., and W. Munk (1954), Measurement of the Roughness of the Sea Surface from Photographs of the Sun's Glitter, *J. Opt. Soc. Am.*, *44*(11), 838-850, doi:10.1364/JOSA.44.000838.

Davis, C. O., M. Kavanaugh, R. Letelier, W. P. Bissett, and D. Kohler (2007), Spatial and spectral resolution considerations for imaging coastal waters, paper presented at Optical Engineering + Applications, SPIE.

Delwart, S., and L. Bourg (2013), MERIS calibrations: 10 years, paper presented at Earth Observing Systems XVIII, International Society for Optics and Photonics.

Eplee Jr, R. E., F. S. Patt, R. A. Barnes, and C. R. McClain (2007), SeaWiFS long-term solar diffuser reflectance and sensor noise analyses, *Appl. Opt.*, *46*(5), 762-773.

Eplee, R. E., G. Meister, F. S. Patt, R. A. Barnes, S. W. Bailey, B. A. Franz, and C. R. McClain (2012), On-orbit calibration of SeaWiFS, *Appl. Opt.*, *51*(36), 8702-8730, doi:10.1364/AO.51.008702.

Eplee, R. E., K. R. Turpie, G. Meister, F. S. Patt, B. A. Franz, and S. W. Bailey (2015), On-orbit calibration of the Suomi National Polar-Orbiting Partnership Visible Infrared Imaging Radiometer Suite for ocean color applications, *Appl. Opt.*, *54*(8), 1984-2006, doi:10.1364/AO.54.001984.

Feng, L., and C. Hu (2016), Cloud adjacency effects on top-of-atmosphere radiance and ocean color data products: A statistical assessment, *Remote Sens. Environ.*, *174*, 301-313, doi:http://dx.doi.org/10.1016/j.rse.2015.12.020.

Franz, B., and E. Karaköylü (2016), Estimating uncertainty in the retrieval of water-leaving reflectance from spaceborne ocean color sensors: effect of instrument noise, paper presented at Ocean Optics XXIII, Victoria, Canada.

Franz, B. A., S. W. Bailey, N. Kuring, and P. J. Werdell (2015), Ocean color measurements with the Operational Land Imager on Landsat-8: implementation and evaluation in SeaDAS, *J. Appl. Remote Sens.*, *9*(1), 096070-096070, doi:10.1117/1.JRS.9.096070.

Franz, B. A., and E. M. Karaköylü (2018), PACE OCI Signal to Noise Performance Requirement: Assessment and Verification Approach for Ocean Color Science, in *PACE Technical Report Series, Volume 6: Data Product Requirements and Error Budgets (NASA/TM-2018 – 2018-219027/ Vol. 6)*, edited by I. Cetinić, C. R. McClain and P. J. Werdell, NASA Goddard Space Flight Space Center Greenbelt, MD.

Franz, B. A., P. J. Werdell, G. Meister, E. J. Kwiatkowska, S. W. Bailey, Z. Ahmad, and C. R. McClain (2006), MODIS land bands for ocean remote sensing applications, paper presented at Proc. Ocean Optics XVIII, Montreal, Canada.

Frouin, R., P.-Y. Deschamps, and F. Steinmetz (2009), Environmental effects in ocean color remote sensing, paper presented at Proc. SPIE.

Garver, S. A., and D. A. Siegel (1997), Inherent optical property inversion of ocean color spectra and its biogeochemical interpretation .1. Time series from the Sargasso Sea, *Journal of Geophysical Research-Oceans*, *102*(C8), 18607-18625.

Geider, R. J. (1987), Light and temperature-dependence of the carbon to chlorophyll-a ratio in microalgae and cyanobacteria - implications for physiology and growth of phytoplankton, *New Phytol.*, *106*(1), 1-34, doi:10.1111/j.1469-8137.1987.tb04788.x.

Gerace, A. D., J. R. Schott, and R. Nevins (2013), Increased potential to monitor water quality in the near-shore environment with Landsat's next-generation satellite, *J. Appl. Remote Sens.*, *7*(1), 073558-073558, doi:10.1117/1.JRS.7.073558.

Gordon, H. R. (1979), Diffuse reflectance of the ocean: the theory of its augmentation by chlorophyll a fluorescence at 685 nm, *Appl. Opt.*, *18*(8), 1161-1166, doi:10.1364/AO.18.001161.

Gordon, H. R., and M. Wang (1994), Retrieval of water-leaving radiance and aerosol optical thickness over the oceans with SeaWiFS: a preliminary algorithm, *Appl. Opt.*, *33*(3), 443-452, doi:10.1364/AO.33.000443.

Graff, J. R., T. K. Westberry, A. J. Milligan, M. B. Brown, G. Dall'Olmo, V. van Dongen-Vogels, K. M. Reifel, and M. J. Behrenfeld (2015), Analytical phytoplankton carbon measurements spanning diverse ecosystems, *Deep Sea Res Part 1 Oceanogr Res Pap.*, *102*, 16-25.

Hair, J., et al. (2015), Combined Atmospheric and Ocean Profiling from an Airborne High Spectral Resolution Lidar, in *27th International Laser Radar Conference*, edited, New York.

Hair, J. W., C. A. Hostetler, A. L. Cook, D. B. Harper, R. A. Ferrare, T. L. Mack, W. Welch, L. R. Izquierdo, and F. E. Hovis (2008), Airborne high spectral resolution lidar for profiling aerosol optical properties, *Appl. Opt.*, *47*(36), 6734-6752.

Halsey, K. H., and B. M. Jones (2015), Phytoplankton strategies for photosynthetic energy allocation, *Ann Rev Mar Sci*, *7*, 265-297, doi:10.1146/annurev-marine-010814-015813.

Halsey, K. H., A. J. Milligan, and M. J. Behrenfeld (2010), Physiological optimization underlies growth rate-independent chlorophyll-specific gross and net primary production, *Photosynth Res*, *103*(2), 125-137, doi:10.1007/s11120-009-9526-z.

Halsey, K. H., A. J. Milligan, and M. J. Behrenfeld (2014), Contrasting strategies of photosynthetic energy utilization drive lifestyle strategies in ecologically important picoeukaryotes, *Metabolites*, *4*(2), 260-280, doi:10.3390/metabo4020260.

Halsey, K. H., R. T. O'Malley, J. R. Graff, A. J. Milligan, and M. J. Behrenfeld (2013), A common partitioning strategy for photosynthetic products in evolutionarily distinct phytoplankton species, *New Phytol*, *198*(4), 1030-1038, doi:10.1111/nph.12209.

Harrison, A., and C. Coombes (1988), An opaque cloud cover model of sky short wavelength radiance, *Solar Energy*, *41*(4), 387-392.

Heaney, J., L. Kauder, and S. Freese (2015), The irradiation testing of UV enhanced silver mirror coatings*Rep.*, NASA Goddard Space Flight Center, Greenbelt, MD.

Hu, C., L. Feng, Z. Lee, C. O. Davis, A. Mannino, C. R. McClain, and B. A. Franz (2012), Dynamic range and sensitivity requirements of satellite ocean color sensors: learning from the past, *Appl. Opt.*, *51*(25), 6045-6062, doi:10.1364/AO.51.006045.

Huot, Y., C. A. Brown, and J. J. Cullen (2005), New algorithms for MODIS sun-induced chlorophyll fluorescence and a comparison with present data products, *Limnology and Oceanography-Methods, 3*, 108-130.

Ibrahim, A., B. Franz, Z. Ahmad, R. Healy, K. Knobelspiesse, B.-C. Gao, C. Proctor, and P.-W. Zhai (2018), Atmospheric correction for hyperspectral ocean color retrieval with application to the Hyperspectral Imager for the Coastal Ocean (HICO), *Remote Sens. Environ.*, *204*, 60-75, doi:https://doi.org/10.1016/j.rse.2017.10.041.

Ibrahim, A., and L. I. W. McKinna (2018), Project Science Analyses Supporting the Addition of a PACE OCI 1038 nm Band, in *PACE Technical Report Series, Volume 7: Ocean Color Instrument (OCI) Concept Design Studies (NASA/TM-2018 – 2018-219027/ Vol. 7)*, edited by I. Cetinić, C. R. McClain and P. J. Werdell, NASA Goddard Space Flight Space Center Greenbelt, MD.

IOCCG (2012), Mission Requirements for Future Ocean-Colour Sensors, Mission Requirements for Future Ocean-Colour Sensors*Rep.*, 98 pp, IOCCG, Dartmouth, Canada.

IOCCG (2013), In-flight Calibration of Satellite Ocean-Colour Sensors*Rep.*, International Ocean-Colour Coordinating Group, Dartmouth, Canada.

Isada, T., T. Hirawake, T. Kobayashi, Y. Nosaka, M. Natsuike, I. Imai, K. Suzuki, and S.-I. Saitoh (2015), Hyperspectral optical discrimination of phytoplankton community structure in Funka Bay and its implications for ocean color remote sensing of diatoms, *Remote Sens. Environ.*, *159*, 134-151.

Jaross, G. (2017), Excerpt from OMPS ATBD, provided in email by Glen Jaross, edited.

Johnson, J. E., R. H. Gammon, J. Larsen, T. S. Bates, S. J. Oltmans, and J. C. Farmer (1990), Ozone in the marine boundary layer over the Pacific and Indian Oceans: Latitudinal gradients and diurnal cycles, *Journal of Geophysical Research: Atmospheres*, *95*(D8), 11847-11856.

Journel, A. G., and C. J. Huijbregts (1978), *Mining geostatistics*, Academic press.

Kemp, W. M., et al. (2005), Eutrophication of Chesapeake Bay: historical trends and ecological interactions, *Mar. Ecol. Prog. Series*, *303*, 1-29.

Keppel-Aleks, G., P. Wennberg, and T. Schneider (2011), Sources of variations in total column carbon dioxide, *Atmospheric Chemistry and Physics*, *11*(8), 3581-3593.

Kieffer, H. H., and T. C. Stone (2005), The Spectral Irradiance of the Moon, *The Astronomical Journal*, *129*(6), 2887.

Knaeps, E., A. I. Dogliotti, D. Raymaekers, K. Ruddick, and S. Sterckx (2012), In situ evidence of non-zero reflectance in the OLCI 1020 nm band for a turbid estuary, *Remote Sens. Environ.*, *120*, 133-144, doi:http://doi.org/10.1016/j.rse.2011.07.025.

Knaeps, E., K. G. Ruddick, D. Doxaran, A. I. Dogliotti, B. Nechad, D. Raymaekers, and S. Sterckx (2015), A SWIR based algorithm to retrieve total suspended matter in extremely turbid waters, *Remote Sens. Environ.*, *168*, 66-79, doi:http://doi.org/10.1016/j.rse.2015.06.022.

Kouvarakis, G., M. Vrekoussis, N. Mihalopoulos, K. Kourtidis, B. Rappenglueck, E. Gerasopoulos, and C. Zerefos (2002), Spatial and temporal variability of tropospheric ozone (O3) in the boundary layer above the Aegean Sea (eastern Mediterranean), *Journal of Geophysical Research: Atmospheres*, *107*(D18).

Kutser, T. (2004), Quantitative detection of chlorophyll in cyanobacterial blooms by satellite remote sensing, *Limnol. Oceanogr.*, *49*(6), 2179-2189.

Laws, E. A., and T. Bannister (1980), Nutrient-and light-limited growth of Thalassiosira fluviatilis in continuous culture, with implications for phytoplankton growth in the ocean1, *Limnol. Oceanogr.*, *25*(3), 457-473.

Lee, Z., K. Carder, R. Arnone, and M. He (2007), Determination of primary spectral bands for remote sensing of aquatic environments, *Sensors*, *7*(12), 3428-3441, doi:10.3390/s7123428.

Lee, Z., C. Hu, R. Arnone, and Z. Liu (2012), Impact of sub-pixel variations on ocean color remote sensing products, *Opt. Express*, *20*(19), 20844-20854, doi:10.1364/OE.20.020844.

Lee, Z. P., K. L. Carder, and R. A. Arnone (2002), Deriving inherent optical properties from water color: a multiband quasi-analytical algorithm for optically deep waters, *Appl. Opt.*, *41*(27), 5755-5772, doi:10.1364/AO.41.005755.

Lubin, D., and J. E. Frederick (1990), Column ozone measurements from Palmer Station, Antarctica: Variations during the austral springs of 1988 and 1989, *Journal of Geophysical Research: Atmospheres*, *95*(D9), 13883-13889.

Macey, A. I., T. Ryan-Keogh, S. Richier, C. M. Moore, and T. S. Bibby (2014), Photosynthetic protein stoichiometry and photophysiology in the high latitude North Atlantic, *Limnol. Oceanogr.*, *59*(6), 1853-1864, doi:doi:10.4319/lo.2014.59.6.1853.

Mackas, D. L. (1984), Spatial autocorrelation of plankton community composition in a continental shelf ecosystem, *Limnology and Oceanography*, *29*(3), 451-471.

Maritorena, S., D. A. Siegel, and A. R. Peterson (2002), Optimization of a semianalytical ocean color model for global-scale applications, *Appl. Opt.*, *41*(15), 2705-2714, doi:10.1364/AO.41.002705.

Matheron, G. (1963), Principles of geostatistics, *Economic geology*, *58*(8), 1246-1266.

McKinna, L. I. W., P. J. Werdell, and C. W. Proctor (2016), Implementation of an analytical Raman scattering correction for satellite ocean-color processing, *Opt. Express*, *24*(14), A1123-A1137.

Meister, G., and C. R. McClain (2010), Point-spread function of the ocean color bands of the Moderate Resolution Imaging Spectroradiometer on Aqua, *Appl. Optics*, *49*(32), 6276-6285.

Meister, G., C. R. McClain, Z. Ahmad, S. W. Bailey, R. A. Barnes, S. Brown, R. E. Eplee, B. Franz, A. Holmes, and W. B. Monosmith (2011), Requirements for an advanced ocean radiometer*Rep.*

Miller, R., M. Twardowski, C. Moore, and C. Casagrande (2003), The Dolphin: Technology to support remote sensing bio-optical algorithm development and applications, *Backscatter*, *14*(2), 8-12.

Mobley, C. D. (1994), *Light and water : radiative transfer in natural waters*, Academic Press, San Diego.

Mobley, C. D., and L. K. Sundman (2012), HYDROLIGHT 5.1 Technical Documentation*Rep.*, 110 pp, Sequoia Scientific Inc., Bellevue, WA.

Mobley, C. D., J. Werdell, B. Franz, Z. Ahmad, and S. Bailey (2016), Atmospheric Correction for Satellite Ocean Color Radiometry, *NASA/TM Rep. NASA/TM–2016-217551*, 73 pp, NASA, Greenbelt.

Morel, A. (1974), Optical properties of pure water and pure sea water, in *Optical Aspects of Oceanography*, edited by N. G. Jerlov and E. Steeman-Nielsen, pp. 1-24, Academic Press, New York.

Morel, A. (1991), Light and marine photosynthesis - a spectral model with geochemical and climatological implications, *Prog. Oceanogr.*, *26*(3), 263-306, doi:10.1016/0079-6611(91)90004-6.

Morel, A., D. Antoine, and B. Gentili (2002), Bidirectional reflectance of oceanic waters: accounting for Raman emission and varying particle scattering phase function, *Appl. Opt.*, *41*(30), 6289-6306.

Morel, A., and S. Maritorena (2001), Bio-optical properties of oceanic waters: A reappraisal, *Journal of Geophysical Research-Oceans*, *106*(C4), 7163-7180, doi:10.1029/2000JC000319.

Moses, W. J., S. G. Ackleson, J. W. Hair, C. A. Hostetler, and W. D. Miller (2016), Spatial scales of optical variability in the coastal ocean: Implications for remote sensing and in situ sampling, *Journal of Geophysical Research: Oceans*, n/a-n/a, doi:10.1002/2016JC011767.

Mount, G., R. Sanders, A. Schmeltekopf, and S. Solomon (1987), Visible spectroscopy at Mcmurdo Station, Antarctica: 1. Overview and daily variations of NO2 and O3, Austral Spring, 1986, *Journal of Geophysical Research: Atmospheres*, *92*(D7), 8320-8328.

Mueller, J. L. (2000), SeaWiFS algorithm for the diffuse attenuation coefficient, K (490), using water-leaving radiances at 490 and 555 nm, *SeaWiFS postlaunch calibration and validation analyses, part*, *3*(11), 24-27.

Nair, P. R., L. M. David, I. Girach, and K. S. George (2011), Ozone in the marine boundary layer of Bay of Bengal during post-winter period: Spatial pattern and role of meteorology, *Atmos. Environ.*, *45*(27), 4671-4681.

O'Reilly, J. E., S. Maritorena, B. G. Mitchell, D. A. Siegel, K. L. Carder, S. A. Garver, M. Kahru, and C. McClain (1998), Ocean color chlorophyll algorithms for SeaWiFS, *Journal of Geophysical Research: Oceans (1978–2012)*, *103*(C11), 24937-24953.

Oltmans, S. J. (1981), Surface ozone measurements in clean air, *Journal of Geophysical Research: Oceans*, *86*(C2), 1174-1180.

Pahlevan, N., Z. Lee, J. Wei, C. Schaff, J. Schott, and A. Berk (2014), On-orbit radiometric characterization of OLI (Landsat-8) for applications in aquatic remote sensing, *Remote Sensing of Environment*, *154*, 272–284.

Pahlevan, N., J.-C. Roger, and Z. Ahmad (2017), Revisiting short-wave-infrared (SWIR) bands for atmospheric correction in coastal waters, *Opt. Express*, *25*(6), 6015-6035, doi:10.1364/OE.25.006015.

Pahlevan, N., and J. R. Schott (2013), Leveraging EO-1 to Evaluate Capability of New Generation of Landsat Sensors for Coastal/Inland Water Studies, *Selected Topics in Applied Earth Observations and Remote Sensing, IEEE Journal of*, *6*(2), 360-374, doi:10.1109/JSTARS.2012.2235174.

Platt, T., C. Caverhill, and S. Sathyendranath (1991), Basin-scale estimates of oceanic primary production by remote sensing: The North Atlantic, *Journal of Geophysical Research: Oceans*, *96*(C8), 15147-15159.

Platt, T., and S. Sathyendranath (1988), Oceanic primary production: estimation by remote sensing at local and regional scales, *Science*, *241*(4873), 1613-1620.

Pope, R. M., and E. S. Fry (1997), Absorption spectrum (380-700 nm) of pure water .2. Integrating cavity measurements, *Appl. Opt.*, *36*(33), 8710-8723.

Pritchard, D. W. (1956), The dynamic structure of a coastal plain estuary, *J. Mar. Res*, *42*, 15-33.

Pritchard, D. W. (1967), Observations of circulation in coastal plain estuaries, in *Estuaries*, edited by G. H. Lauff, pp. 37-44, American Association for the Advancement of Science, Washington, DC.

Rahman, A. F., J. A. Gamon, D. A. Sims, and M. Schmidts (2003), Optimum pixel size for hyperspectral studies of ecosystem function in southern California chaparral and grassland, *Remote Sens. Environ.*, *84*(2), 192-207.

Roelke, D., C. Kennedy, and A. Weidemann (1999), Use of discriminant and fourth-derivative analyses with high-resolution absorption spectra for phytoplankton research: Limitations at varied signal-to-noise ratio and spectral resolution, *Gulf Mex. Sci.*, *17*(2), 75-86.

Rothman, L. S., I. E. Gordon, Y. Babikov, A. Barbe, D. C. Benner, P. F. Bernath, M. Birk, L. Bizzocchi, V. Boudon, and L. R. Brown (2013), The HITRAN2012 molecular spectroscopic database, *J. Quant. Spectrosc. Radiat. Transfer*, *130*, 4-50.

Ruddick, K., and Q. Vanhellemont (2015), Use of the new OLCI and SLSTR bands for atmospheric correction over turbid coastal and inland waters, paper presented at Sentinel-3 for Science Workshop, Venice-Lido, Italy, 2-5 June 2015 ESA Special Publication SP-734.

Schrader, P. S., A. J. Milligan, and M. J. Behrenfeld (2011), Surplus photosynthetic antennae complexes underlie diagnostics of iron limitation in a cyanobacterium, *PLoS ONE*, *6*(4), e18753, doi:10.1371/journal.pone.0018753.

Siegel, D. A., S. Maritorena, N. B. Nelson, D. Hansell, and M. Lorenzi-Kayser (2002), Global distribution and dynamics of colored dissolved and detrital organic materials, *Journal of Geophysical Research: Oceans*, *107*(C12), doi:10.1029/2001JC000965.

Smith, R. C., and K. S. Baker (1981), Optical properties of the clearest natural waters (200-800 nm), *Appl. Opt.*, *20*(2), 177-184, doi:10.1364/AO.20.000177.

Suggett, D. J., C. M. Moore, A. E. Hickman, and R. J. Geider (2009), Interpretation of fast repetition rate (FRR) fluorescence: signatures of phytoplankton community structure versus physiological state, *Mar. Ecol.-Prog. Ser.*, *376*, 1-19, doi:10.3354/meps07830.

Sun, J. Q., X. Xiong, W. L. Barnes, and B. Guenther (2007), MODIS Reflective Solar Bands On-Orbit Lunar Calibration, *IEEE Transactions on Geoscience and Remote Sensing*, *45*(7), 2383-2393, doi:10.1109/TGRS.2007.896541.

Team, P. S. D. (2018), Pre-Aerosol, Clouds, and ocean Ecosystem (PACE) Mission Science Definition Team Report*Rep.*, NASA Goddard Space Flight Center, Greenbelt, MD.

Thuillier, G., M. Hersé, T. Foujols, W. Peetermans, D. Gillotay, P. Simon, and H. Mandel (2003), The solar spectral irradiance from 200 to 2400 nm as measured by the SOLSPEC spectrometer from the ATLAS and EURECA missions, *Sol. Phys.*, *214*(1), 1-22.

Torrecilla, E., D. Stramski, R. A. Reynolds, E. Millán-Núñez, and J. Piera (2011), Cluster analysis of hyperspectral optical data for discriminating phytoplankton pigment assemblages in the open ocean, *Remote Sens. Environ.*, *115*(10), 2578-2593.

Tsai, F., and W. Philpot (1998), Derivative analysis of hyperspectral data, *Remote Sens. Environ.*, *66*(1), 41-51.

Twardowski, M. S., H. Claustre, S. A. Freeman, D. Stramski, and Y. Huot (2007a), Optical backscattering properties of the 'clearest' natural waters, *Biogeosciences*, *4*, 1041-1058.

Twardowski, M. S., M. R. Lewis, A. H. Barnard, and J. R. V. Zaneveld (2007b), In-water instrumentation and platforms for ocean color remote sensing applications, in *Remote Sensing of Coastal Aquatic Environments*, edited, pp. 69-100, Springer.

Tzortziou, M., J. R. Herman, Z. Ahmad, C. P. Loughner, N. Abuhassan, and A. Cede (2014), Atmospheric NO2 dynamics and impact on ocean color retrievals in urban nearshore regions, *Journal of Geophysical Research: Oceans*, *119*(6), 3834-3854.

Tzortziou, M., J. R. Herman, A. Cede, and N. Abuhassan (2012), High precision, absolute total column ozone measurements from the Pandora spectrometer system: Comparisons with data from a Brewer double monochromator and Aura OMI, *Journal of Geophysical Research: Atmospheres*, *117*(D16).

Vandermeulen, R. A., A. Mannino, A. Neeley, J. Werdell, and R. Arnone (2017), Determining the optimal spectral sampling frequency and uncertainty thresholds for hyperspectral remote sensing of ocean color, *Opt. Express*, *25*(16), A785-A797.

Vanhellemont, Q., and K. Ruddick (2014), Turbid wakes associated with offshore wind turbines observed with Landsat 8, *Remote Sens. Environ.*, *145*, 105-115.

Wagner, S., T. Hewison, T. Stone, S. Lachérade, B. Fougnie, and X. Xiong (2015), A summary of the joint GSICS–CEOS/IVOS lunar calibration workshop: moving towards intercalibration using the Moon as a transfer target, paper presented at Sensors, Systems, and Next-Generation Satellites XIX, International Society for Optics and Photonics.

Wang, M., and W. Shi (2007), The NIR-SWIR combined atmospheric correction approach for MODIS ocean color data processing, *Opt. Express*, *15*(24), 15722-15733, doi:10.1364/OE.15.015722.

Wang, M., S. Son, and W. Shi (2009), Evaluation of MODIS SWIR and NIR-SWIR atmospheric correction algorithms using SeaBASS data, *Remote Sens. Environ.*, *113*(3), 635-644, doi:https://doi.org/10.1016/j.rse.2008.11.005.

Washburn, L., B. M. Emery, B. H. Jones, and D. G. Ondercin (1998), Eddy stirring and phytoplankton patchiness in the subarctic North Atlantic in late summer, *Deep Sea Research Part I: Oceanographic Research Papers*, *45*(9), 1411-1439.

Wellemeyer, C. G., P. K. Bhartia, S. L. Taylor, W. Qin, and C. Ahn (2004), Version 8 Total Ozone Mapping Spectrometer (TOMS) algorithm, paper presented at Proceedings of the XX Quadrennial Ozone Symposium.

Werdell, P. J. (2018), PACE Ocean Color Science Data Product Requirements, in *PACE Technical Report Series, Volume 6: Data Product Requirements and Error Budgets (NASA/TM-2018 – 2018-219027/ Vol. 6)*, edited by I. Cetinić, C. R. McClain and P. J. Werdell, NASA Goddard Space Flight Space Center Greenbelt, MD.

Werdell, P. J., B. A. Franz, and S. W. Bailey (2010), Evaluation of shortwave infrared atmospheric correction for ocean color remote sensing of Chesapeake Bay, *Remote Sens. Environ.*, *114*(10), 2238-2247, doi:10.1016/j.rse.2010.04.027.

Werdell, P. J., B. A. Franz, S. W. Bailey, G. C. Feldman, E. Boss, V. E. Brando, M. Dowell, T. Hirata, S. J. Lavender, and Z. Lee (2013), Generalized ocean color inversion model for retrieving marine inherent optical properties, *Appl. Opt.*, *52*(10), 2019-2037.

Westberry, T., M. J. Behrenfeld, D. A. Siegel, and E. Boss (2008), Carbon-based primary productivity modeling with vertically resolved photoacclimation, *Global Biogeochem. Cycles*, *22*(2), doi:10.1029/2007GB003078.

Westberry, T. K., and M. J. Behrenfeld (2014), Oceanic Net Primary Production, in *Biophysical Applications of Satellite Remote Sensing*, edited by H. J., Springer, Berlin, Heidelberg.

Westberry, T. K., E. Boss, and Z. Lee (2013), Influence of Raman scattering on ocean color inversion models, *Appl. Opt.*, *52*(22), 5552-5561, doi:10.1364/AO.52.005552.

Wolanin, A., V. Rozanov, T. Dinter, S. Noël, M. Vountas, J. Burrows, and A. Bracher (2015), Global retrieval of marine and terrestrial chlorophyll fluorescence at its red peak using hyperspectral top of atmosphere radiance measurements: Feasibility study and first results, *Remote Sens. Environ.*, *166*, 243-261.

Wolanin, A., M. A. Soppa, and A. Bracher (2016), Investigation of spectral band requirements for improving retrievals of phytoplankton functional types, *Remote Sensing*, *8*(10), 871.

Woodward, R. H., R. A. Barnes, C. R. McClain, W. E. Esaias, W. L. Barnes, and A. Mecherikunnel (1993), SeaWiFS Technical Report Series: Modeling of the SeaWiFS Solar and Lunar Observations*Rep.*, 26 pp, NASA Goddard Space Flight Center, Greenbelt, Maryland.

Worden, J., A. Turner, A. Bloom, S. Kulawik, J. Liu, M. Lee, R. Weidner, K. Bowman, C. Frankenberg, and R. Parker (2015), Quantifying lower tropospheric methane concentrations using GOSAT near-IR and TES thermal IR measurements.

Wright, S., S. Jeffrey, and R. Mantoura (2005), *Phytoplankton pigments in oceanography: guidelines to modern methods*, Unesco Pub.

Xi, H., M. Hieronymi, R. Röttgers, H. Krasemann, and Z. Qiu (2015), Hyperspectral Differentiation of Phytoplankton Taxonomic Groups: A Comparison between Using Remote Sensing Reflectance and Absorption Spectra, *Remote Sensing*, *7*(11), 14781.

Xiong, X., J. Sun, J. Fulbright, Z. Wang, and J. J. Butler (2016), Lunar Calibration and Performance for S-NPP VIIRS Reflective Solar Bands, *IEEE Transactions on Geoscience and Remote Sensing*, *54*(2), 1052-1061, doi:10.1109/TGRS.2015.2473665.

Xiong, X. J., A. Angal, J. Sun, T. J. Choi, and E. Johnson (2014), On-orbit performance of MODIS solar diffuser stability monitor, *Journal of Applied Remote Sensing*, *8*(1), 083514.

Yoder, J. A., C. R. McClain, J. O. Blanton, and L. Y. Oey (1987), Spatial scales in CZCS-chlorophyll imagery of the southeastern US continental shelf, *Limnol. Oceanogr.*, 929-941.

Previous Volumes in This Series

Volume 1 *April 2018*	ACE Ocean Working Group recommendations and instrument requirements for an advanced ocean ecology mission
Volume 2 *May 2018*	Pre-Aerosol, Clouds, and ocean Ecosystem (PACE) Mission Science Definition Team Report
Volume 3 *October 2018*	Polarimetry in the PACE mission: Science Team consensus document
Volume 4 *October 2018*	Cloud retrievals in the PACE mission: Science Team consensus document
Volume 5 *December 2018*	Mission Formulation Studies
Volume 6 *December 2018*	Data Product Requirements and Error Budgets